

# **Interaction between the LINE1 retrotransposon and the hepatitis C virus**

**Dissertation**

submitted to the

Department of Chemistry

Faculty of Mathematics, Informatics and Natural Science

University of Hamburg

In fulfillment of the requirements

for the degree of

Doctor of Natural Science (Dr. rer. nat.)

by

Anja Schöbel

Hamburg, 2019

Reviewer: Prof. Dr. rer. nat. Eva Herker

Prof. Dr. rer. nat. Chris Meier

Oral defence: March 01, 2019

# Content

Publications and presentations .....	1
Abbreviations .....	4
Abstract .....	9
Zusammenfassung .....	10
1 Introduction .....	12
1.1 Hepatitis C virus .....	12
1.2 HCV infection and disease progression .....	12
1.3 HCV treatment .....	12
1.4 HCV epidemiology and classification .....	13
1.5 Structure of HCV particles .....	14
1.6 HCV life cycle .....	15
1.6.1 HCV entry .....	16
1.6.2 Genome organization and translation .....	17
1.6.3 HCV RNA replication .....	21
1.6.4 Assembly and release of HCV particles .....	22
1.7 LDs as HCV assembly sites .....	23
1.8 Host RNA-binding proteins in HCV replication .....	24
1.9 Transposable elements .....	25
1.9.1 Transposable elements in the human genome .....	25
1.9.1.1 DNA transposons .....	26
1.9.1.2 Retrotransposons .....	26
1.10 LINE1 .....	30
1.10.1 Organization of the human LINE1 retroelement .....	30
1.10.1.1 Structure and function of LINE1 encoded proteins .....	31
1.10.2 LINE1 retrotransposition .....	34

1.10.3	LINE1 expression and activity .....	36
1.10.4	Host mechanisms to control LINE1 retrotransposition .....	36
1.10.5	LINE1 retrotransposition and diseases .....	37
1.10.5.1	Single-gene diseases caused by LINE1 retrotransposition .....	37
1.10.5.2	LINE1 and cancer .....	38
1.10.5.3	LINE1 and viral infections.....	38
2	Aim of the thesis.....	40
3	Results .....	41
3.1	HCV infection changes LINE1 expression levels and L1ORF1p localization.....	41
3.1.1	HCV infection increases LINE1 expression .....	41
3.1.2	L1ORF1p is enriched in LD fractions of HCV-infected cells .....	43
3.1.3	L1ORF1p re-localizes to LDs in HCV-infected cells.....	45
3.1.4	L1ORF1p recruitment to LDs is independent of HCV RNA replication .....	48
3.1.5	HCV core induces the recruitment of L1ORF1p to LDs .....	49
3.1.5.1	HCV core expression enriches the L1ORF1p interacting proteins PABPC1 and MOV-10 in LD fractions.....	53
3.2	L1ORF1p interacts with HCV core and the viral genome.....	54
3.2.1	HCV core interacts with L1ORF1p in an RNA-dependent manner.....	54
3.2.2	RNA-binding capacity of L1ORF1p is important for its re-localization to LDs...	57
3.2.3	HCV RNA co-precipitates with L1ORF1p .....	58
3.3	HCV RNA as template for L1ORF2p-reverse transcriptase activity.....	59
3.4	L1ORF1p overexpression does not affect HCV RNA replication.....	63
3.5	Overexpression of full-length LINE1 affects HCV replication .....	65
3.6	LINE1 retrotransposition frequency is lower in HCV-infected cells.....	67
4	Discussion.....	70

4.1	HCV infection increases LINE1 expression level and redistributes L1ORF1p to LDs.	70
4.2	HCV core interacts with RNP components in an RNA-dependent manner and induces their redistribution to HCV assembly sites.	71
4.3	HCV RNA is part of LINE1 RNPs, but not reversely transcribed by L1ORF2p	73
4.4	L1ORF1p is not involved in HCV RNA replication.	74
4.5	HCV infection decreases LINE1 retrotransposition frequency.	75
4.6	Conclusion and working model.	78
5	Material	80
5.1	Bacteria	80
5.2	Eukaryotic cell lines	80
5.3	Solvents and buffers	81
5.3.1	Lysis buffer	81
5.3.2	SDS PAGE and western blotting	82
5.3.3	Agarose gel electrophoresis	82
5.3.4	DNA and protein ladder	82
5.3.5	LD isolation buffer	83
5.3.6	LEAP assay buffer	83
5.3.7	Solutions for immunofluorescence staining and microscopy	84
5.4	Inhibitors	84
5.5	Enzymes	84
5.6	Kits	85
5.7	Plasmids	86
5.8	Oligonucleotides	89
5.9	Antibodies and dyes	91
5.10	Consumables	93

5.11	Chemicals .....	94
5.12	Devices .....	97
5.13	Software .....	98
6	Methods .....	99
6.1	Molecular biological methods .....	99
6.1.1	Cultivation of bacteria .....	99
6.1.2	Plasmid isolation .....	99
6.1.3	Glycerol stocks .....	99
6.1.4	Cloning .....	99
6.1.4.1	Polymerase chain reaction (PCR) .....	99
6.1.4.2	Overlap extension PCR .....	99
6.1.4.3	Restriction endonuclease digestion .....	102
6.1.4.4	Ligation .....	103
6.1.4.5	Ligation independent cloning .....	103
6.1.4.6	Bacterial transformation .....	103
6.1.4.7	Sequencing .....	104
6.1.5	Phenol-chloroform extraction .....	104
6.1.6	HCV RNA <i>in vitro</i> transcription .....	104
6.2	Cell culture techniques .....	105
6.2.1	Cell culture .....	105
6.2.2	Thawing and freezing of eukaryotic cells .....	105
6.2.3	Electroporation of cells with <i>in vitro</i> transcribed HCV RNA .....	105
6.2.4	Generation of HCV stocks .....	105
6.2.5	Titration of HCV stocks (TCID <sub>50</sub> ) .....	106
6.2.6	Production of lentiviral pseudoparticles and lentiviral transduction .....	106

6.2.7	Transfection of Huh7 and Huh7.5 cells using FuGENE .....	107
6.2.8	Flow cytometry .....	107
6.2.9	LINE1 retrotransposition reporter assay .....	107
6.2.9.1	LINE1 retrotransposition in ABA-treated Huh7.5 cells .....	107
6.2.9.2	LINE1 retrotransposition in HCV-infected Huh7.5 cells.....	107
6.2.10	Immunofluorescence and LD staining for confocal microscopy .....	108
6.2.11	LD Isolation .....	108
6.2.12	RNP isolation and LINE1 element amplification protocol (LEAP).....	109
6.2.12.1	Transfection of Huh7 cells and RNP isolation.....	109
6.2.12.2	LEAP assay .....	110
6.3	Biochemical methods .....	111
6.3.1	Cell lysates.....	111
6.3.2	SDS-PAGE and western blot analysis.....	112
6.3.3	Co-immunoprecipitation .....	112
6.3.3.1	Co-immunoprecipitation to determine HCV RNA copies in HA-L1ORF1p-precipitated samples.....	112
6.3.3.2	Co-immunoprecipitation with RNase A treatment to investigate RNA dependent interactions.....	113
6.3.3.3	Co-immunoprecipitation of FLAG-tagged viral proteins with RNase A treatment to investigate RNA dependent interactions.....	113
6.4	RNA isolation .....	113
6.5	cDNA synthesis.....	114
6.6	Quantitative real time PCR (qRT-PCR) .....	114
6.6.1	HCV standard for qRT-PCR .....	115
6.7	Luciferase assays to analyze HCV replication in LINE1-overexpressing cells .....	115
6.7.1	HCV RNA replication in HA-L1ORF1p-overexpressing cells.....	115

6.7.2	HCV replication in LINE1-overexpressing cells.....	116
6.8	Secreted embryonic alkaline phosphatase (SEAP) assay .....	116
6.9	Statistical analysis.....	117
7	References.....	118
8	Appendix .....	140
8.1	List of figures.....	140
8.2	List of tables .....	140
8.4	Toxicity of chemicals .....	142
8.5	Danksagung .....	155
8.6	Correctness of the English Language.....	156
8.7	Eidesstattliche Versicherung .....	157



## Publications and presentations

### Publications

During the dissertation, the author participated in the following publications:

Lunemann S, **Schöbel A**, Kah J, Fittje P, Hölzemer A, Langeneckert AE, Hess LU, Poch T, Martrus G, Garcia-Beltran WF, Körner C, Ziegler AE, Richert L, Oldhafer KJ, Schulze Zur Wiesch J, Schramm C, Dandri M, Herker E, Altfeld M. (2018) Interactions Between KIR3DS1 and HLA-F Activate Natural Killer Cells to Control HCV Replication in Cell Culture. *Gastroenterology* 155 (5)

**Schöbel A**, Rösch K, Herker E. (2018) Functional innate immunity restricts Hepatitis C Virus infection in induced pluripotent stem cell-derived hepatocytes. *Sci. Rep.* 8 (1)

Rösch K, Kwiatkowski M, Hofmann S, **Schöbel A**, Grüttner C, Wurlitzer M, Schlüter H, Herker E. (2016) Quantitative Lipid Droplet Proteome Analysis Identifies Annexin A3 as a Cofactor for HCV Particle Production. *Cell Rep.* 16 (12)

Allweiss L, Gass S, Giersch K, Groth A, Kah J, Volz T, Rapp G, **Schöbel A**, Lohse AW, Polywka S, Pischke S, Herker E, Dandri M, Lütgehetmann M. (2016) Human liver chimeric mice as a new model of chronic hepatitis E virus infection and preclinical drug evaluation. *J. Hepatol.* 64 (5)

## Presentations

The author presented at the following conferences. Presentations containing parts of this thesis are marked with an asterisk

- 10/2018 \* Anja Schöbel, Gerald G. Schumann, and Eva Herker  
**Interaction between the LINE1 Retrotransposon and the Hepatitis C Virus**  
*Joint Scientific Retreat, Heinrich Pette Institute, Hamburg, Germany (poster)*
- 10/2018 \* Anja Schöbel, Gerald G. Schumann, and Eva Herker  
**Interaction between the LINE1 Retrotransposon and the Hepatitis C Virus**  
*25<sup>th</sup> International Symposium on Hepatitis C Virus and Related Viruses, Dublin, Ireland (poster) (poster prize)*
- 03/2018 \* Anja Schöbel, Gerald G. Schumann, and Eva Herker  
**Interaction between the LINE1 Retrotransposon and the Hepatitis C Virus**  
*28th Annual Meeting of the Society for Virology, Würzburg, Germany (oral presentation)*
- 11/2017 \* Anja Schöbel, Gerald G. Schumann, and Eva Herker  
**Interaction between the LINE1 Retrotransposon and the Hepatitis C Virus**  
*16<sup>th</sup> Workshop "Cell Biology of Viral infections", German Society for Virology; Schöntal, Germany (oral presentation)*
- 10/2017 \* Anja Schöbel, Gerald G. Schumann, and Eva Herker  
**Interaction between the LINE1 Retrotransposon and the Hepatitis C Virus**  
*Joint Scientific Retreat, Heinrich Pette Institute, Hamburg, Germany (oral presentation) (presentation prize)*
- 03/2017 Anja Schöbel, Kathrin Rösch and Eva Herker  
**An Induced Pluripotent Stem Cell-derived Model to Study Hepatitis C Virus-Host Interactions**  
*27th Annual Meeting of the Society for Virology, Marburg, Germany (poster)*
- 11/2016 \* Anja Schöbel, Gerald G. Schumann, and Eva Herker  
**Interaction between the LINE1 Retrotransposon and the Hepatitis C Virus**  
*15<sup>th</sup> Workshop "Cell Biology of Viral infections", German Society for Virology; Schöntal, Germany (oral presentation)*
- 11/2016 \* Anja Schöbel, Gerald G. Schumann, and Eva Herker  
**Interaction between the LINE1 Retrotransposon and the Hepatitis C Virus**  
*Joint Scientific Retreat, Heinrich Pette Institute, Hamburg, Germany (poster)*

- 11/2016 \* Anja Schöbel, Gerald G. Schumann, and Eva Herker  
**Interaction between the LINE1 Retrotransposon and the Hepatitis C Virus**  
*HPI Young Scientist Retreat, Seevetal, Germany (poster)*
- 10/2016 Anja Schöbel, Kathrin Rösch and Eva Herker  
**An Induced Pluripotent Stem Cell-derived Model to Study Hepatitis C Virus-Host Interactions**  
*6th European Congress of Virology, Hamburg, Germany (poster)*
- 10/2015 Anja Schöbel, Kathrin Rösch and Eva Herker  
**Studying Innate Immunity in an iPSC-derived Hepatocyte-Model**  
*Joint Scientific Retreat, Heinrich Pette Institute, Hamburg, Germany (oral presentation)*

### Scholarships

- 12/2017– Completion fellowship University of Hamburg
- 11/2018

## Abbreviations

°C	degree celsius
μF	microfarrad
μg	microgram
μl	microliter
μM	micromolar
3' OH	3' hydroxyl group
∞	infinite
aa	amino acid
ABA	abacavir
ADAR1	adenosine deaminases acting on RNA 1
APC	adenomatosis polyposis coli
apo	apolipoprotein
APOBEC3	apolipoprotein B mRNA editing enzyme, catalytic polypeptide-like 3
as	antisense
ATP	adenosine triphosphate
BRCA I/II	breast cancer I/II
BSA	bovine serum albumin
BSD	blasticidin S deaminase
BSL	biosafety level
BV421	brilliant violet 421
CD81	cluster of differentiation 81
cDNA	complementary DNA
CLDN1	claudin-1
CLSM	confocal laser scanning microscope
Con1 SGR	Con1 subgenomic replicon
CpG island	deoxycytidine deoxyguanosine rich sequence
Cry	cryptic domain
CTD	C-terminal domain
d	day
D	domain
DAA	direct acting antivirals
DDX	DEAD box RNA helicase
DGAT	diacylglycerol O-acyltransferase
DMD	dystrophin
DMSO	dimethyl sulfoxide
DMV	double membrane vesicles

## Abbreviations

---

DNA	deoxyribonucleic acid
dpe	days post electroporation
dpi	days post infection
DTT	1,4-dithiothreitol
EF1a	eukaryotic translation elongation factor 1 alpha 1
EGFP	enhanced green fluorescent protein
EGFR	epidermal growth factor receptor
Env	envelope
ER	endoplasmic reticulum
ESCRT	endosomal sorting complex required for transport
FCS	fetal calf serum
FLuc	firefly luciferase
FVIII	factor VIII
fw	forward
Gag	group specific antigen
GLuc	gaussia luciferase
gp	guinea pig
gt	goat
gt	genotype
h	hours
HBS	hepes buffered saline
HBV	hepatitis B virus
HCC	hepatocellular carcinoma
HCV	hepatitis C virus
HEK	human embryonic kidney
HERV	human endogenous retrovirus
hESCs	human embryonic stem cells
HIV-1	human immunodeficiency virus 1
HNRNP	heterogeneous ribonucleoprotein
HRP	horseradish peroxidase
HSPG	heparansulfat proteoglycans
Huh	human hepatoma
HygB	hygromycin B
IF	immunofluorescence
IGF2BP1	insulin-like growth factor-II mRNA-binding protein 1
IP	immunoprecipitation
iPSCs	Induced pluripotent stem cells
IRES	internal ribosomal entry site

## Abbreviations

---

ISGs	interferon stimulated genes
JFH1	japanese fulminant hepatitis 1
kb	kilo basepair
kDa	kilodalton
L1ORF1p	LINE1 open reading frame 1
L1ORF2p	LINE1 open reading frame 2
LD	lipid droplet
LDLR	low-density lipoprotein receptor
LEAP	LINE1 element amplification protocol
LIC	ligation independent cloning
LINE	long interspersed nuclear element
LTR	long terminal repeats
LV	lentivirus
LVP	lipoviroparticle
M	mol/l
M	marker
MCC	Manders' colocalization coefficient
<i>MCC</i>	mutated in colorectal cancers
mg	milligram
min	minutes
mKO2	monomeric kusabira orange 2
ml	milliliter
mM	millimolar
mm	millimeter
MMV	multi membrane vesicles
MOI	multiplicity of infection
MOV-10	Moloney leukemia virus 10 homolog
mRNA	messenger RNA
ms	mouse
mut	mutant
MW	membranous web
Neo <sup>R</sup>	neomycin resistance
NF1	neurofibromin 1
NLS	nuclear localization sequence
nm	nanometer
NPC1L1	Niemann-Pick C1 like1
NRTI	nucleoside analog reverse-transcriptase inhibitor
NS	non-structural

## Abbreviations

---

nt	nucleotide
o/n	overnight
OCLN	occludin
ORF	open reading frame
PABPC1	polyA binding protein cytoplasmic 1
PBS	phosphate buffered saline
PCC	Pearson's correlation coefficient
PCR	polymerase chain reaction
PEG	polyethylene glycol
PEG-IFN $\alpha$	pegylated interferon alpha
PFA	paraformaldehyde
PIC	protease inhibitor cocktail
PLIN	perilipin
PMSF	phenylmethylsulfonyl fluoride
Pol	polymerase
polyA	polyadenylation
polyU	polyuridine
Prt	protease
qRT	quantitative real time
rb	rabbit
RC	retrotransposition competent
RdRp	RNA-dependent RNA polymerase
rev	reverse
RFP	red fluorescent protein
RIG-I	retinoic acid inducible gene 1
RLU	relative light units
RNA	ribonucleic acid
RNA Pol II	RNA polymerase II promoter
RNP	ribonucleoprotein particle
ROI	region of interest
rpm	revolutions per minute
RRM	RNA recognition motif
rRNA	ribosomal ribonucleic acid
RT	reverse transcriptase
rt	room temperature
s	seconds
SA	splice acceptor
SAMHD1	SAM and HD domain containing protein 1

## Abbreviations

---

scRNA	small cytoplasmic RNA
SD	splice donor
SDS	sodium dodecyl sulfate
SDS-PAGE	sodium dodecyl sulfate polyacrylamide gel electrophoresis
SEAP	secreted embryonic alkaline phosphatase
SEM	standard error of the mean
SG	stress granula
SINE	short interspersed nuclear element
SINE-R	short interspersed element of retroviral origin
snRNA	small nuclear RNA
SPP	signal peptide peptidase
SRBI	scavenger receptor B1
SV40 polyA	simian virus 40 polyA signal
SVA	SINE-VNTR-Alu
SVR	sustained virological responder
t	transduction/transfection
TCID <sub>50</sub>	50% tissue culture infective dose
TE	transposable elements
TG	triglycerides
T <sub>m</sub>	melting temperature
TRPT	target-site primed reverse transcription
TSD	target-site duplication
Ub	ubiquitin promoter
UTR	untranslated region
UV	ultraviolet
V	volt
v/v	volume per volume
VLDL	very low-density lipoprotein
VLP	virus-like particle
VNTR	variable number of terminal repeats
w/v	weight per volume
WB	western blot
wt	wildtype
x g	times gravity
YB-1	Y-box binding protein 1
ZAP	zinc finger antiviral protein



## Abstract

Nearly half of the human DNA consists of transposons, which are mobile genetic elements that can change their position within the genome. To date, the retrotransposon long interspersed nuclear element 1 (LINE1) is the only active element in the human genome. LINE1 encodes three open reading frames (ORFs) of different functions: the RNA-binding protein ORF1p (L1ORF1p), the reverse transcriptase and endonuclease ORF2p (L1ORF2p), and the small antisense ORF0 of yet undefined function. LINE1 retrotransposition has been associated with a variety of genetic mutations and hypomethylation of LINE1 promoter regions has lately been proposed as prognostic marker for malignant tumors. Little is known about a potential role of LINE1 in viral infections and disease progression. The hepatitis C virus (HCV) is closely tied to the hepatic lipid metabolism and virion assembly takes place at lipid droplets (LDs). A recent study reported profound changes in the LD proteome of HCV-infected Huh7.5 hepatoma cells, indicating that HCV changes the LD protein composition in favor of viral replication (Rosch et al., 2016). In the respective study, L1ORF1p was exclusively found in LD fractions of HCV-infected cells. Following up on this result, the interplay between LINE1 and HCV was investigated in this thesis. HCV infection *in vitro* modestly but significantly increased LINE1 expression at 6 days post infection. Further, a strong and stable redistribution of L1ORF1p to LDs was observed in HCV-infected cells. Individual expression of the LD-associated viral proteins HCV core and NS5A revealed that L1ORF1p recruitment depends on HCV core trafficking to LDs. Along with L1ORF1p, its interaction partners PABPC1 and MOV-10 were enriched in LD fractions. L1ORF1p, PABPC1, and MOV-10 interacted with HCV core but not NS5A in an RNA-dependent manner, indicating that HCV core is part of a ribonucleoprotein particle (RNP) and redistributes it to HCV assembly sites. Supporting this idea, a putative L1ORF1p RNA-binding mutant was found at LDs to a lesser extent and the HCV RNA was enriched in HA-L1ORF1p immunoprecipitation samples. HCV RNA was found in isolated LINE1 RNPs but was not identified as template for reverse transcription by L1ORF2p. Overexpression of L1ORF1p did not affect HCV RNA replication, but a role in HCV infection remains to be elucidated. In this context, preliminary data suggested a decrease of HCV replication in full-length LINE1-overexpressing cells. To evaluate if HCV infection affects LINE1 retrotransposition, a retrotransposition reporter assay was used. LINE1 activity was significantly decreased in HCV-infected cells compared to uninfected cells, suggesting that HCV infection might alter cellular factors important for retrotransposition. Moreover, the interaction with HCV core might sequester L1ORF1p at LDs, thereby preventing LINE1 RNP formation and decreasing retrotransposition. Taken together, this work confirms and extends previous studies describing the interaction and redistribution of RNA-binding proteins to LDs dependent on the HCV core protein and provides insight to the interplay of LINE1 and HCV.

## Zusammenfassung

Fast die Hälfte der menschlichen DNA besteht aus Transposons, mobilen genetischen Elementen, die ihre Position im Genom verändern können. Gegenwärtig ist das *long interspersed nuclear element 1* (LINE1) das einzig bekannte aktive Element im menschlichen Genom. LINE1 codiert drei offene Leserahmen (ORFs) mit unterschiedlichen Funktionen: das RNA-Bindeprotein ORF1p (L1ORF1p), die reverse Transkriptase und Endonuclease ORF2p (L1ORF2p) und das *antisense* orientierte ORF0-Protein mit bisher unbekannter Funktion. LINE1-Retrotransposition wurde mit verschiedenen genetischen Mutationen in Verbindung gebracht, und die Hypomethylierung der LINE1 Promotorregionen wird als prognostischer Marker für maligne Tumoren diskutiert. Bisher ist wenig über eine mögliche Rolle von LINE1 in Virusinfektionen bekannt. Der Lebenszyklus des Hepatitis-C-Virus (HCV) ist eng mit dem Lipidmetabolismus der Leberzellen verknüpft und die Assemblierung neuer Viruspartikel erfolgt an *lipid droplets* (LDs). In einer kürzlich veröffentlichten Proteomstudie zur Analyse der LD-Proteinkomposition während einer HCV-Infektion wurde L1ORF1p ausschließlich in LD-Fractionen von HCV-infizierten Huh7.5 Hepatomazellen identifiziert (Rosch et al., 2016). Im Rahmen dieser Dissertation wurde eine mögliche Interaktion zwischen HCV und LINE1 mit Fokus auf L1ORF1p untersucht. Eine leichte, aber signifikante Erhöhung der LINE1-Expression konnte sechs Tage nach HCV-Infektion *in vitro* detektiert werden. Ferner wurde in HCV-infizierten Zellen eine stabile Relokalisierung von L1ORF1p zu LDs beobachtet. Die Expression einzelner LD-assoziiierter Virusproteine, HCV-Core und NS5A, zeigte, dass L1ORF1p abhängig von HCV-Core zu LDs rekrutiert wird. Zusammen mit L1ORF1p waren die L1ORF1p-Interaktionspartner PABPC1 und MOV-10 in LD-Fractionen angereichert. L1ORF1p, PABPC1 und MOV-10 interagierten RNA-abhängig mit HCV-Core, jedoch nicht mit NS5A. Dies lässt den Schluss zu, dass HCV-Core in infizierten Zellen Teil eines Ribonukleoprotein-Partikels (RNP) ist und diesen zu HCV-Assemblierungsstellen rekrutiert. Übereinstimmend mit dieser Hypothese konnte eine geringere Anreicherung einer mutmaßlichen L1ORF1p-RNA-Bindemutante in LD-Fractionen beobachtet werden. Zusätzlich war die HCV RNA in HA-L1ORF1p-Präzipitationsproben angereichert. HCV RNA war ebenfalls in isolierten LINE1-RNPs nachweisbar, kann jedoch nicht durch das L1ORF2p-Protein revers transkribiert werden. Die Überexpression von L1ORF1p hatte keinen Einfluss auf die HCV RNA Replikation, eine mögliche Rolle in der HCV-Infektion ist allerdings noch nicht vollständig geklärt. In diesem Zusammenhang zeigten vorläufige Experimente eine geringere HCV-Replikation in Zellen, die ein vollständiges LINE1-Element überexprimieren. Um zu beurteilen, ob eine HCV-Infektion die LINE1-Retrotransposition beeinflusst, wurde ein Retrotranspositions-Reporter-Assay verwendet. Die LINE1-Aktivität war in HCV-infizierten Zellen im Vergleich zu nicht infizierten Zellen signifikant verringert. Dies deutet darauf hin, dass eine HCV-Infektion möglicherweise zelluläre Faktoren verändert, die für die Retrotransposition wichtig sind. Darüber hinaus könnte die Interaktion zwischen L1ORF1p und HCV-Core die Assemblierung von L1ORF1p in LINE1-RNPs verhindern und dadurch die

Retrotransposition verringern. Zusammenfassend bestätigt diese Arbeit frühere Studien, die eine Interaktion von RNA-Bindeproteinen mit HCV Core und die daraus resultierende Relokalisierung zu LDs beschreiben. Darüber hinaus wurden vielversprechende Einblicke in die LINE1-Biologie während einer HCV-Infektion *in vitro* gewonnen.

# 1 Introduction

## 1.1 Hepatitis C virus

Worldwide, chronic hepatitis C virus (HCV) infection affects 115 million people with 71 million people (~1%) of the world's population suffering from chronic viraemic infections (Gower et al., 2014; WHO, 2017). Left untreated, a high percentage of patients with chronic HCV infection develop severe liver comorbidities, e.g. steatosis, cirrhosis, or hepatocellular carcinoma (HCC), leading to approximately 0.4 million HCV-related deaths per year (WHO, 2017). For this reason, chronic HCV infection is still one of the major causes of liver transplantations. In 2015, an estimated number of 1.75 million new HCV infections occurred (WHO, 2017), and in the US, increasing rates of acute infections in the last decade were connected to the expanding opioid epidemic (Zibbell et al., 2018).

## 1.2 HCV infection and disease progression

HCV is a bloodborne virus that is mainly transmitted by contaminated blood products and needle sharing between intravenous drug users. Less frequent transmission routes are the infection of a new-born from an HCV-positive mother as well as sexual contact (reviewed in Thursz and Fontanet, 2014). HCV causes acute as well as chronic infections. The first 6 months of infection are considered acute and are mostly asymptomatic (reviewed in Hajarizadeh et al., 2013). A recent meta-analysis has shown that 36% of infected individuals can spontaneously clear HCV infection within 12 months post infection. This is dependent on sex, behavioral and demographic circumstances as well as on genetic factors. The strongest genetic association was observed for polymorphisms in the *IL28B* (*IFNL3*) gene that encodes for interferon  $\lambda 3$  (Aisyah et al., 2018). Further, HCV genotypes are cleared differentially (Lehmann et al., 2004). However, most HCV-positive patients develop a chronic HCV infection with severe liver pathologies. During disease progression, 16% of the patients develop cirrhosis after 20 years and progression to HCC is observed in 2-8% (Thein et al., 2008; Trinchet et al., 2007).

## 1.3 HCV treatment

Until 2011, HCV-infected patients were treated with a combination of PEGylated interferon  $\alpha$  (PEG-IFN $\alpha$ ) and the antiviral drug ribavirin, leading to a sustained virological response (SVR) in 50% of the patients (reviewed in Webster et al., 2015). However, treatment success was dependent on several factors. Patients with pre-elevated levels of interferon-stimulated genes (ISGs) responded less to PEG-IFN $\alpha$  treatment and, in line with spontaneous viral clearance, polymorphisms in *IL28B* correlated with SVR (Chen et al., 2005; Ge et al., 2009; Suppiah et al., 2009; Tanaka et al., 2009). Further, IFN therapy had severe side effects (reviewed in Manns et al., 2006). The development of novel direct acting antivirals (DAAs) led to a broader spectrum of therapy options. DAAs are effective in  $\geq 90\%$  of treated patients (reviewed in Webster et al., 2015) and are divided into four classes: nucleoside/nucleotide

and non-nucleotide NS5B polymerase inhibitors, inhibitors of NS5A, and NS3-4A protease inhibitors. Different DAA combinations, with and without ribavirin, are recommended for therapy depending on the HCV genotype and present comorbidities (EASL, 2018). A protective HCV vaccine has not been developed yet.

#### 1.4 HCV epidemiology and classification

HCV belongs to the genus *Hepacivirus* (14 species), one of four genera within the *Flaviviridae* family. The other three genera are *Flavivirus* (53 species), *Pestivirus* (11 species), and *Pegivirus* (4 species) (ICTV, 2017). HCV is the only member of the *Hepacivirus* C species and is restricted to humans and chimpanzees. The positive single stranded RNA virus was first described in 1989 (Choo et al., 1989). Today, seven major HCV genotypes (1-7) with several subtypes are described (Simmonds et al., 2005; Smith et al., 2014). The genotypes show a nucleotide sequence variance of ~30-35% and subtype sequences are also highly variable within the individual genotypes. With 46.2%, genotype 1 shows the highest global prevalence, followed by genotype 3 with 30.1%. The genotypes 2, 4, and 6 account for 9.1%, 8.3%, and 5.4% of HCV infections, respectively. A very low prevalence is described for genotype 5 with less than 1% (Messina et al., 2015). Only one infection of genotype 7 has been described worldwide (Murphy et al., 2007) (Figure 1).

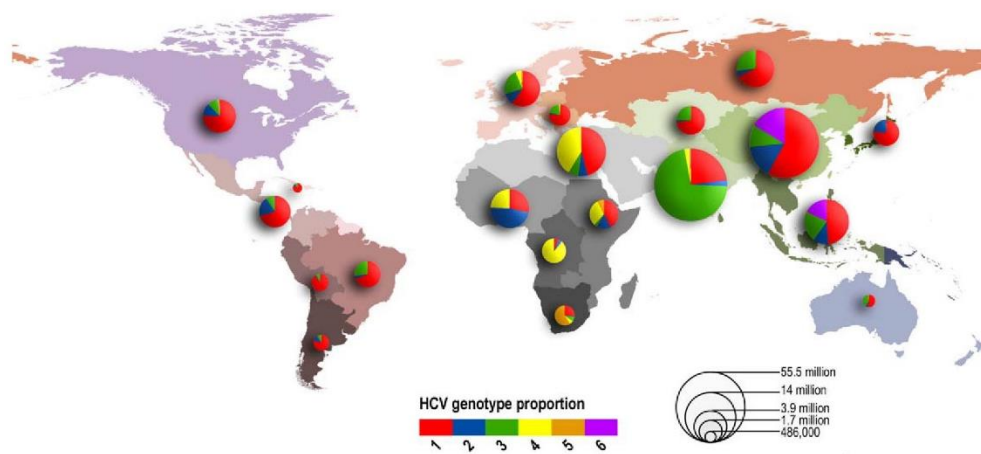


**Figure 1: Global prevalence of HCV genotypes 1-6.**

The size of the pie chart correlates with the number of infected individuals in the respective geographical area (modified from Messina et al., 2015).

## 1.5 Structure of HCV particles

HCV is an enveloped virus with a diameter of 40–100 nm. Ultrastructural analysis revealed pleiomorphic particles with a dense core surrounded by a membrane bilayer (Catanese et al., 2013; Gastaminza et al., 2010) (Figure 2 A). In contrast to other *Flaviviridae* members, HCV is characterized by a low buoyant density resulting from the association of HCV virions with lipoproteins (mainly LDL and VLDL) to form a so-called lipoviroparticle (LVPs) (Andre et al., 2002; reviewed in Lindenbach and Rice, 2013). In density gradients of primary isolates, the majority of HCV RNA was found in low-density fractions (<1.08 g/mL) that contained a high amount of triglycerides and the apolipoproteins E (apoE) and B-100 (apoB) (Nielsen et al., 2006; Nielsen et al., 2008). Additionally, apoA-I and apoC are described as components of LVPs (reviewed in Lindenbach, 2013). A low density directly correlates with a high specific infectivity of HCV (Lindenbach et al., 2006) and apoE is an essential host factor for HCV replication (Chang et al., 2007). Nevertheless, the exact interaction between HCV and lipoproteins is not known. Currently, two models are proposed: in a two-particle model, the lipoprotein and the virion exist as individual particles that undergo a transient or stable interaction. In the second model, viral particles possibly form a hybrid together with lipoproteins that share one membrane (single-particle model) (reviewed in Lindenbach, 2013) (Figure 2 C). Apart from apolipoproteins, a variety of host proteins was identified in purified HCV particles, indicating a close virus-host interaction in particle assembly (Lussignol et al., 2016).

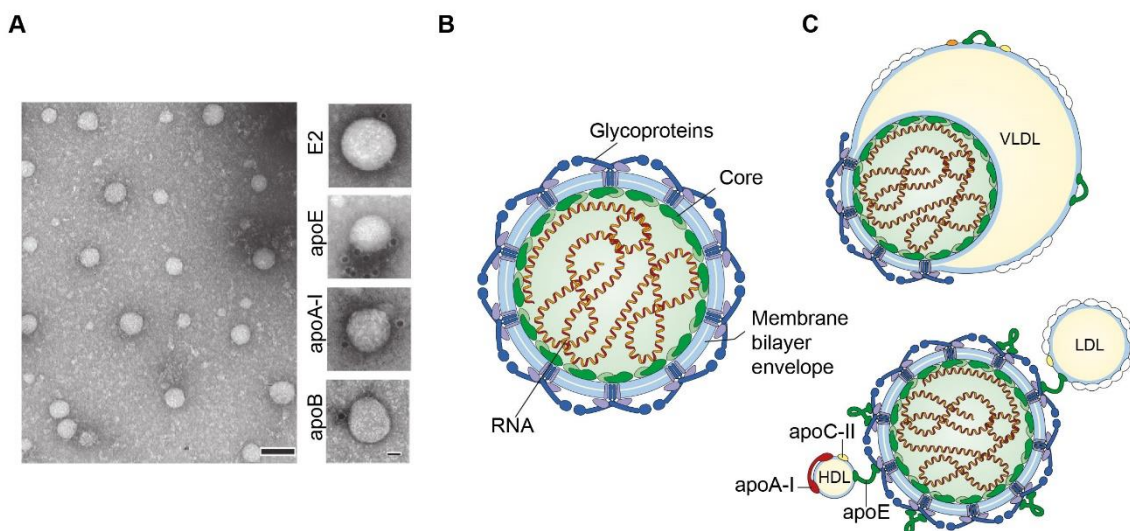


**Figure 2: Morphology of the HCV particle.**

(A) Electron microscopic visualization of HCV particles derived from primary human hepatocytes (human fetal liver cells, HFLCs). Right panel shows immunolabelling with the respective antibody. Scale bars: left = 100 nm; right = 20 nm. (B) Schematic representation of an HCV virion. (C) Hypothetical hybrid model of the mature lipoviroparticle. HCV particles are assumed to either fuse with lipoproteins (single-particle model) or undergo a transient or stable interaction (two-particle model) (A = (modified from Catanese et al., 2013); B = (modified from Lindenbach and Rice, 2013)).

## 1.6 HCV life cycle

HCV replication is a multistep process, involving a complex interplay of viral and cellular factors. The narrow HCV species tropism is defined by several host factors, such as the tight junction protein occluding (OCLN) and the cluster of differentiation 81 (CD81) (Ploss et al., 2009). In addition, HCV is strictly tissue specific as it only infects hepatocytes. Again, this is based on the requirement of several liver-specific factors for viral replication, such as the apolipoprotein E (apoE) and the microRNA 122 (miR-122) (Chang et al., 2007; Da Costa et al., 2012; Jopling et al., 2005). Figure 3 illustrates the main steps of the viral life cycle (reviewed in Herker and Ott, 2012).

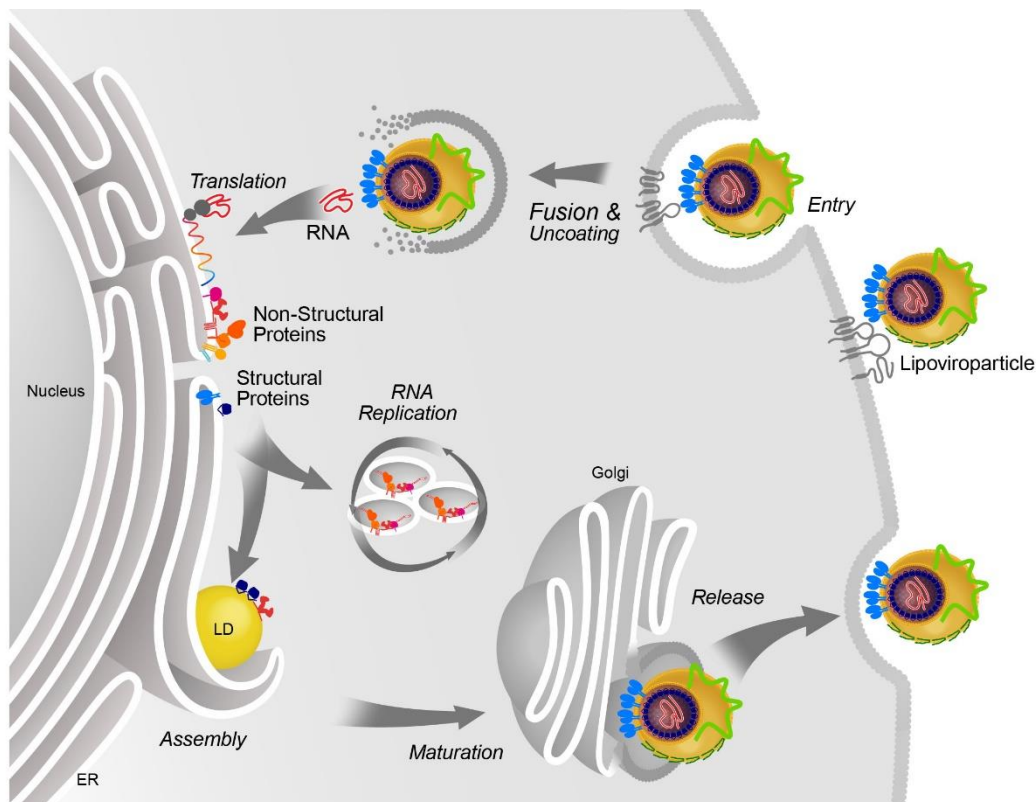


**Figure 3: The HCV life cycle.**

After initial attachment to several surface receptors, the virus enters the cell via clathrin-mediated endocytosis. Fusion of the viral envelope with the endosomal membrane leads to uncoating of the viral genome. The positive single stranded RNA genome is translated into a single precursor polypeptide at the ER that is further processed into ten viral proteins. RNA replication takes place in distinct membrane rearrangements and LDs serve as assembly sites for new virions. The virus matures upon association with lipoproteins to form a characteristic lipoviroparticle and egresses from the cell via the secretory pathway (Illustration kindly provided by Eva Herker (modified from Herker and Ott, 2012)).



### 1.6.1 HCV entry

Like many other viruses, HCV enters the host cell *via* clathrin-mediated endocytosis (Blanchard et al., 2006). For HCV, this multistep process requires a variety of different receptors. Initially, the virus attaches to the host cell by an interaction between the E2 envelope protein and heparansulfat proteoglycans (HSPG) as well as the low-density lipoprotein receptor (LDLR) on the surface of the hepatocyte (Barth et al., 2003; Barth et al., 2006; Germi et al., 2002) (Figure 4).

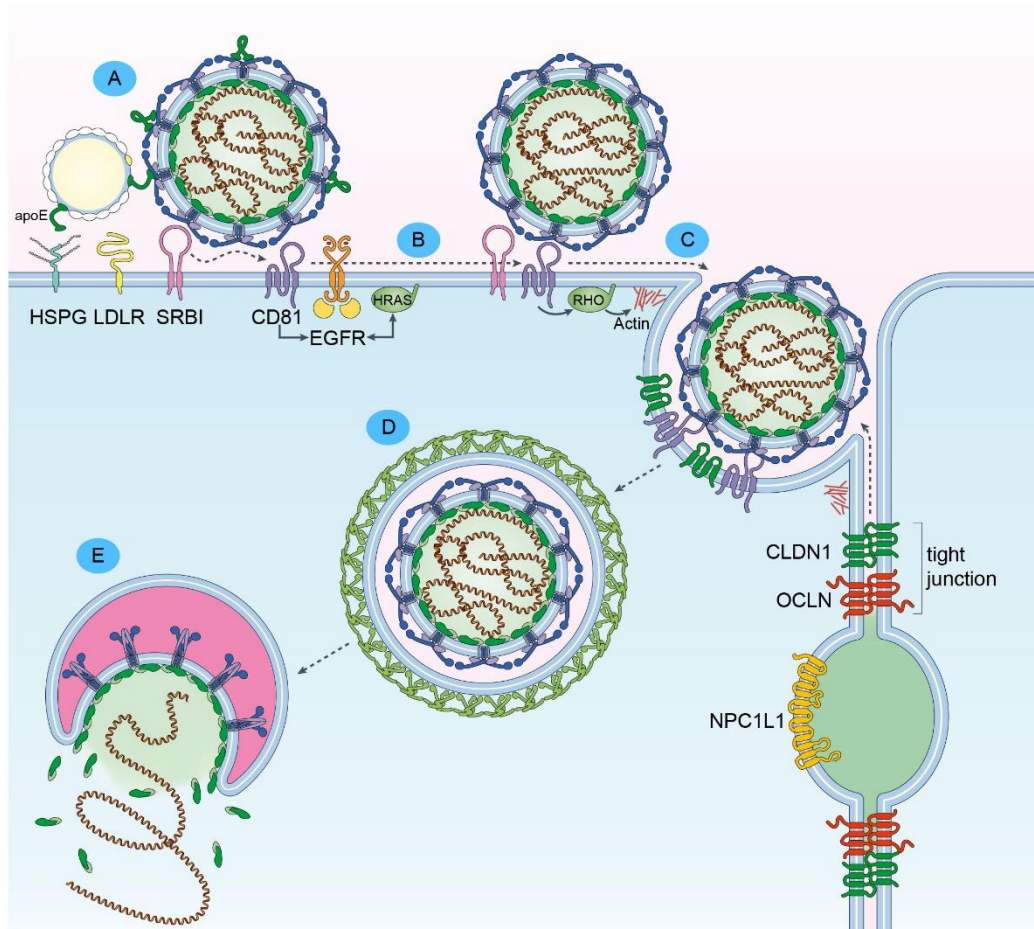


**Figure 4: HCV entry.**

The first step in the HCV entry process is the attachment of the virus to several receptors on the hepatocyte surface (HSPG, LDLR and SRBI). The interaction with SRBI exposes E2 to CD81 (A). The E2-CD81 interaction includes intracellular signaling cascades via EGFR/HRAS and RHO GTPases (B), leading to the lateral diffusion and interaction of CD81 with the tight junction protein CLDN1 (C). After clathrin-mediated endocytosis (D), low pH-mediated fusion of the viral envelope and the early endosome leads to the release of the HCV RNA to the cytoplasm (E) (HSPG = heparansulfat proteoglycans; LDLR = low-density lipoprotein receptor; SRBI = scavenger receptor B1; EGFR = epidermal growth factor receptor) (modified from Lindenbach and Rice, 2013).



In addition to E2, the interaction of apoE, present in lipoviroparticles, with HSPGs contributes to the surface binding of HCV (Jiang et al., 2012). The third surface receptor that is involved in the initial virus-cell surface interaction is the scavenger receptor B1 (SRBI) (Scarselli et al., 2002). Multimodal functions for SRBI have been described: first, the interaction of SRBI with apoE promotes HCV attachment to the cell. This is followed by an interaction with E2 that mediates and enhances viral entry. Likely, binding to SRBI leads to changes in the lipoprotein composition of the viral particle, leading to the exposure of E2 to the tetraspanin CD81 (Dao Thi et al., 2012). The E2-CD81 interaction activates cellular signaling pathways that involve the epidermal growth factor receptor (EGFR), the HRAS GTPase and members of the RHO GTPase family (Brazzoli et al., 2008; Lupberger et al., 2011; Zona et al., 2013). Lateral diffusion of CD81 at the cellular membrane is induced, subsequently leading to the complexation of CD81 with the tight junction protein claudin-1 (CLDN1). This interaction primes internalization of HCV via clathrin-mediated endocytosis (Harris et al., 2010). A second tight junction protein that is essential for the late stages of HCV entry is occludin (OCLN) (Ploss et al., 2009). OCLN has been described to act downstream of the CD81-CLDN1 complex, however its exact function is not known to date (Sourisseau et al., 2013). Recently, the cholesterol transporter Niemann-Pick C1 like-1 (NPC1L1) was identified as a novel entry factor for HCV, involved in post binding steps (Sainz et al., 2012). Following internalization, HCV particles are found in early endosomes (Meertens et al., 2006). In order to release the viral genome into the cytoplasm, HCV particles fuse with the endosomal membrane in a process that requires low pH (Bartosch et al., 2003; Meertens et al., 2006; Tscherne et al., 2006).

### **1.6.2 Genome organization and translation**

The single stranded HCV RNA genome is ~9600 bp in length and encodes for a single open reading frame (ORF) of approximately 3000 amino acids (aa) (reviewed in Moradpour et al., 2007). The ORF is framed by untranslated regions (UTRs) at the 5' and 3' end (Figure 5). The 3' UTR features three distinct segments: a variable region, a poly (U/UC) tract and the terminal 3'X region (X-tail), a highly conserved sequence of 98 nt that putatively forms three stem-loop structures (SL1-3). The 3' X region is essential for efficient RNA replication, partly due to an interaction with a stem-loop structure in the coding region of the viral polymerase NS5B (5BSL3.2) (Friebe and Bartenschlager, 2002; Friebe et al., 2005; Yi and Lemon, 2003). The 5' UTR contains an internal ribosomal entry site (IRES) that facilitates cap-independent translation of the viral genome (Wang et al., 1993). In addition, two binding motifs for the liver-specific microRNA 122 (miR-122) are located in the 5' UTR (Jopling et al., 2008). Binding of miR-122 to the 5' UTR is crucial for HCV RNA replication, as it protects the viral genome from degradation (Jopling et al., 2005; Sedano and Sarnow, 2014). IRES-mediated translation at the endoplasmic reticulum (ER) gives rise to a single precursor polyprotein that is co- and posttranslationally cleaved into the ten viral proteins in a concerted

process by cellular and viral proteases (Figure 5). Proteolytic processing of the structural proteins (core, E1, and E2) at the N-terminus is performed by the signal peptidase, that also cleaves the non-structural protein p7 from the precursor. Maturation of the core protein additionally requires cleavage by the signal peptide peptidase (SPP) (McLauchlan et al., 2002). All non-structural proteins (except for p7) are cleaved by the HCV-encoded proteases NS2 and NS3-4A. The junction between NS2 and NS3 is cleaved by the NS2 autoprotease and NS3-4A processes the remaining downstream proteins (reviewed in Moradpour et al., 2007).

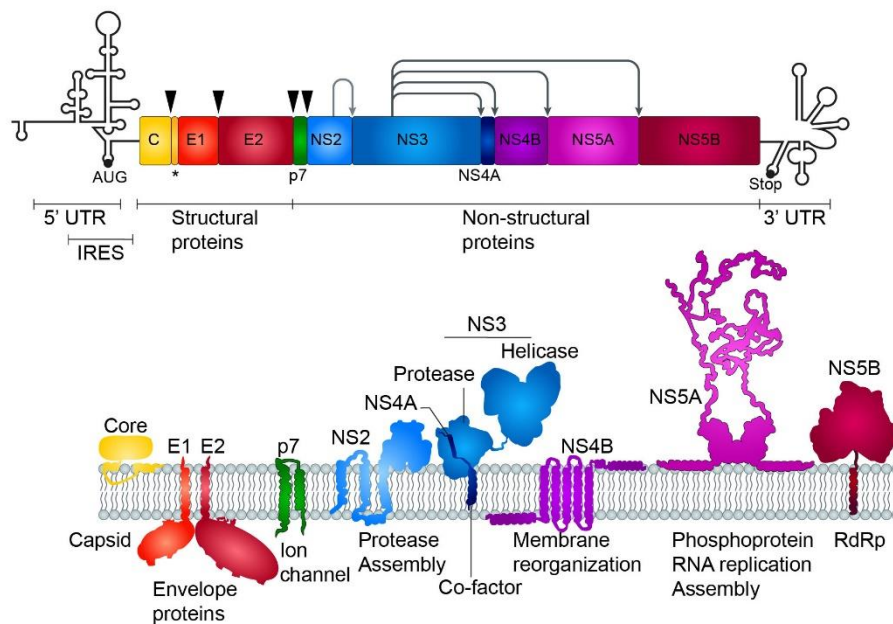


**Figure 5: HCV genome and viral proteins.**

The HCV genome is a positive single stranded RNA of ~9.6 kb. One single ORF of ~3000 amino acids is flanked by untranslated regions (UTRs). IRES-mediated translation gives rise to a precursor polyprotein that is co- and posttranslationally cleaved by cellular and viral proteases. The structural proteins core, E1, and E2, as well as the p7-NS2 junction are cleaved by a cellular signal peptidase, indicated by black arrowheads. An asterisk marks the position of the second proteolytic cleavage of the core protein by the signal peptide peptidase. All non-structural proteins are processed by the viral proteases: NS2 cleaves the NS2-NS3 junction, whereas NS3-4A processes all remaining downstream proteins (RdRp = RNA-dependent RNA polymerase) (modified from Neufeldt et al., 2018).

**Structural proteins:** Three structural proteins, the capsid protein core and the glycoproteins E1 and E2 are encoded in the HCV genome. All of them are structural components of the viral particle.

**Core:** The HCV capsid protein core is a highly basic protein of 191 aa and its main function with respect to viral replication is the encapsidation of the HCV genome during particle assembly (reviewed in McLauchlan, 2000). Its sequence is highly conserved between the different HCV genotypes (Bukh et al., 1994). Core is the first protein to be processed from the precursor polyprotein and in its immature form (molecular weight = 23 kDa) it consists of

three distinct domains (D1-D3). The 117 aa N-terminal D1 domain possesses RNA-binding properties (Santolini et al., 1994; Shimoike et al., 1999) and is likely important for encapsidation, as it is required for capsid assembly in a cell-free system (Klein et al., 2005; Majeau et al., 2004). D2 comprises ~50 aa and consists of two amphipathic helices which facilitate the association of core with cellular membranes (Boulant et al., 2006; Boulant et al., 2005). In this context, D2 is essential for the association of core and lipid droplets (LDs) and disruption of this interaction abolishes viral particle production (Boulant et al., 2006; Miyanari et al., 2007; Shavinskaya et al., 2007). The C-terminal D3 of 20 aa is highly hydrophobic and acts as signal peptide for E1 at the ER (Santolini et al., 1994). D3 is cleaved from the immature core by SPP (McLauchlan et al., 2002), a process that is critical to produce infectious viral particles (Targett-Adams et al., 2008). The mature core protein (21 kDa) is an  $\alpha$ -helical dimer (Boulant et al., 2005). Besides encapsidation, the core protein displays different functions during HCV replication, e.g. recruiting the non-structural proteins and the replication complex to the assembly sites at LDs (Miyanari et al., 2007). Relating to its RNA-binding ability, a nucleic acid chaperone function for core has been proposed; however, the exact role of this property in viral replication is not known yet (Cristofari et al., 2004; Ivanyi-Nagy et al., 2006). Core protein expression alters several metabolic processes. Therefore, it has been associated with the development of steatosis (Moriya et al., 1997; Perlemuter et al., 2002), induction of oxidative stress (Moriya et al., 2001; Okuda et al., 2002) and cancerogenesis (Moriya et al., 1998; Tanaka et al., 2008) in HCV-related liver pathologies.

**E1 and E2:** The glycoproteins E1 (35 kDa) and E2 (72 kDa) are essential for viral particle assembly due to their function as viral envelope proteins. Both possess a short C-terminal transmembrane domain that is co-translationally inserted into the ER membrane, and a large N-terminal ectodomain that faces the ER lumen (reviewed in Voisset and Dubuisson, 2004). E1 and E2 are posttranslationally N-glycosylated at their ectodomains and form a heterodimer (Deleersnyder et al., 1997; Op De Beeck et al., 2004). The transmembrane domains are required for ER retention and necessary for the dimerization of E1 and E2 (Cocquerel et al., 1998; Op De Beeck et al., 2000). The E1/E2 dimer also plays a role in viral entry by interaction with different HCV receptors (Barth et al., 2003; Barth et al., 2006; Germi et al., 2002; Op De Beeck et al., 2004).

**Non-structural proteins:** HCV encodes for seven non-structural (NS) proteins that play different roles in RNA replication and particle assembly.

**p7:** p7 is the smallest protein encoded in the viral genome with a molecular weight of 7 kDa. It is characterized by two transmembrane domains that are connected *via* a positively charged loop that faces the cytoplasm (Carrere-Kremer et al., 2002). p7 assembles into oligomeric complexes, forming a pore that functions as an ion channel (also known as viroporin) (Clarke et al., 2006; Luik et al., 2009). While p7 is dispensable for HCV RNA replication, it is crucial for infectious particle production, most likely due to the concerted action with other viral proteins (reviewed in Steinmann and Pietschmann, 2010).

**NS2:** The cysteine protease NS2 is a 21 kDa polytropic membrane protein with three putative transmembrane domains, though its exact transmembrane structure is not clear (Yamaga and Ou, 2002). Recently, it has been demonstrated that the protease domain itself is involved in membrane association (Lange et al., 2014). The carboxyterminal protease domain of NS2 dimerizes (Lorenz et al., 2006) and, together with the serine protease function of NS3, cleaves the NS2-NS3 junction upon polyprotein processing (Grakoui et al., 1993). Like p7, NS2 is not required for RNA replication but essential for HCV assembly and has been shown to interact with other viral proteins during this process, e.g. p7 and E2 (Jones et al., 2007; Popescu et al., 2011).

**NS3-4A:** NS3 is a bifunctional protein of 70 kDa that contains an N-terminal serine protease domain and a C-terminal NTPase/RNA helicase. Both functions require the interaction with its cofactor NS4A, a 6 kDa peptide that enhances the enzymatic activity of NS3. Additionally, NS4A anchors NS3 to the membrane via an N-terminal  $\alpha$ -helix (Brass et al., 2008). The NS3-4A complex is responsible for the cleavage of all remaining proteins in the HCV polyprotein downstream of NS2 (NS3-NS5B) (Failla et al., 1994). In addition to its requirement for viral replication, NS3-4A cleaves important adaptor proteins of the cell intrinsic immunity, such as the mitochondrial antiviral signaling protein (MAVS) and the TLR3 adaptor TRIF, contributing to HCV immune evasion (Li et al., 2005b; Li et al., 2005c; Meylan et al., 2005; reviewed in Morikawa et al., 2011).

**NS4B:** The integral membrane protein NS4B (27 kDa) has two amphipathic  $\alpha$ -helices at each terminus and a central stretch of four putative transmembrane domains (Gouttenoire et al., 2009; Lundin et al., 2003). The expression of NS4B induces rearrangements of intracellular membranes, termed the membranous web, that are assumed to be the site of viral RNA replication (Egger et al., 2002; Gosert et al., 2003). Although little is known about secondary functions, transcomplementation experiments revealed a role for NS4B in viral particle assembly (Jones et al., 2009).

**NS5A:** NS5A is a membrane-associated protein that exists in two stages: the basal phosphorylated form (56 kDa) and the hyperphosphorylated form (58 kDa). Membrane interactions of NS5A are facilitated by an N-terminal  $\alpha$ -helix (Brass et al., 2002; Penin et al., 2004) that precedes three distinct domains (D1–D3) (Tellinghuisen et al., 2004). The N-terminal D1 contains a zinc binding motif and together with D2 it is mainly involved in RNA replication (Romero-Brey et al., 2012). In this context, NS5A-D1 is essential for the formation of double membrane vesicles (DMVs). Biochemical and structural analysis suggest that NS5A is an RNA-binding protein and this function is located in D1 (Huang et al., 2005; Tellinghuisen et al., 2005). The C-terminal D3 and localization of NS5A to LDs is essential for HCV assembly (Appel et al., 2008; Masaki et al., 2008; Miyanari et al., 2007; reviewed in Moradpour and Penin, 2013).

**NS5B:** The last protein that is released from the HCV polyprotein is the RNA-dependent RNA polymerase NS5B, a tail-anchored protein of 68 kDa (Schmidt-Mende et al., 2001). A short aa stretch at the C-terminus anchors the enzyme at the ER membrane; this interaction is required for efficient RNA replication in cell culture (Moradpour et al., 2004). NS5B has three subdomains, termed palm, finger and thumb (Bressanelli et al., 1999). Interactions between the finger and thumb domain lead to the formation of a characteristic encircled active site (Lesburg et al., 1999). During RNA replication, NS5B synthesizes a negative strand intermediate of the HCV RNA that is used as a template for the synthesis of new positive strand RNA (reviewed in Lohmann, 2013).

### 1.6.3 HCV RNA replication

HCV RNA replication takes place in rearranged membrane structures termed the membranous web (MW) (Egger et al., 2002; Gosert et al., 2003). In the HCV life cycle, membranous web formation is induced after translation and polyprotein processing, though expression of NS4B is sufficient to induce membrane malformations. Predominantly, the MW consists of single, double, and multi membrane vesicles (DMVs and MMVs) that harbor active RNA replication, likely derived from ER membranes (Paul et al., 2013; Romero-Brey et al., 2012). Blocking several lipid transfer proteins resulted in decreased HCV RNA replication and inhibition of the cholesterol transporter NPC1 additionally disrupted MW structures (Stoeck et al., 2018). Several other proteins of the lipid metabolism are connected to MW integrity and efficient RNA replication, e.g. the oxysterol-binding protein (OSBP) and the lipid kinase PI4KIII $\alpha$  (Reiss et al., 2011; Wang et al., 2014). Expression of the non-structural proteins NS3-NS5B is sufficient for RNA replication (Lohmann et al., 1999). The key protein is the viral polymerase NS5B, facilitating *de novo* synthesis of positive strand RNA genomes *via* a negative strand RNA intermediate. This process is highly error prone with  $\sim 10^{-3}$  mismatches per site, contributing to high mutation rates and drug resistance of several HCV strains (Powdrill et al., 2011). Besides the polymerase activity of NS5B, a series of other viral

and host factors is required for efficient RNA replication, among them the presence of *cis* acting replication elements (CREs) within the HCV genome (reviewed in Lohmann, 2013).

#### **1.6.4 Assembly and release of HCV particles**

The late stages of the HCV life cycle, particle assembly and release respectively, are least understood. Following RNA replication, the newly synthesized HCV genome is encapsidated, progeny virions bud into the ER lumen and maturation and release is connected to the secretory pathway (Figure 6). A prerequisite for efficient particle assembly is the localization of the mature core protein to LDs, the putative HCV assembly sites (Boulant et al., 2006; Miyanari et al., 2007; Shavinskaya et al., 2007). Trafficking of core to LDs depends on the activity of the MAP-kinase regulated cytosolic phospholipase A2 (cPLA2) (Menzel et al., 2012) as well as on the diacylglycerol-O-acyltransferase 1 (DGAT1) (Herker et al., 2010). Other NS-proteins and the viral replication complexes are recruited to LDs by the core protein (Miyanari et al., 2007). Recruitment of NS5A to LDs and its interaction with core are key steps in infectious particle production (Appel et al., 2008; Camus et al., 2013; Masaki et al., 2008). Here, NS5A is important for the association of core with the HCV RNA, likely enhancing nucleocapsid formation (Masaki et al., 2008). The transfer of core to the ER budding sites and nascent virion formation is facilitated by the NS-proteins. NS2 plays a key role by interacting with a several other viral proteins (Jirasko et al., 2010). The interaction of NS2 and p7 leads to a complex of NS2/p7 with the E1/E2 dimer. This complex is subsequently recruited to ER areas adjacent to LDs (Popescu et al., 2011). Further, NS2/NS3-4A interaction was shown to be essential to retrieve core from LDs to the budding sites (Counihan et al., 2011). HCV particles obtain their membrane envelope by budding into the ER lumen. This process has been connected to the endosomal sorting complex required for transport (ESCRT) pathway (Ariumi et al., 2011b; Corless et al., 2010). During maturation, E1 and E2 undergo posttranslational glycosylation (Vieyres et al., 2010). As intracellular HCV particles have a higher density compared to secreted particles, association with lipoproteins for lipovirion formation is a key aspect of HCV maturation (Gastaminza et al., 2006). Further, inhibition of VLDL synthesis reduces HCV particle production (Gastaminza et al., 2008). All together, this indicates that HCV shares the route of lipoprotein secretion to exit the cell.

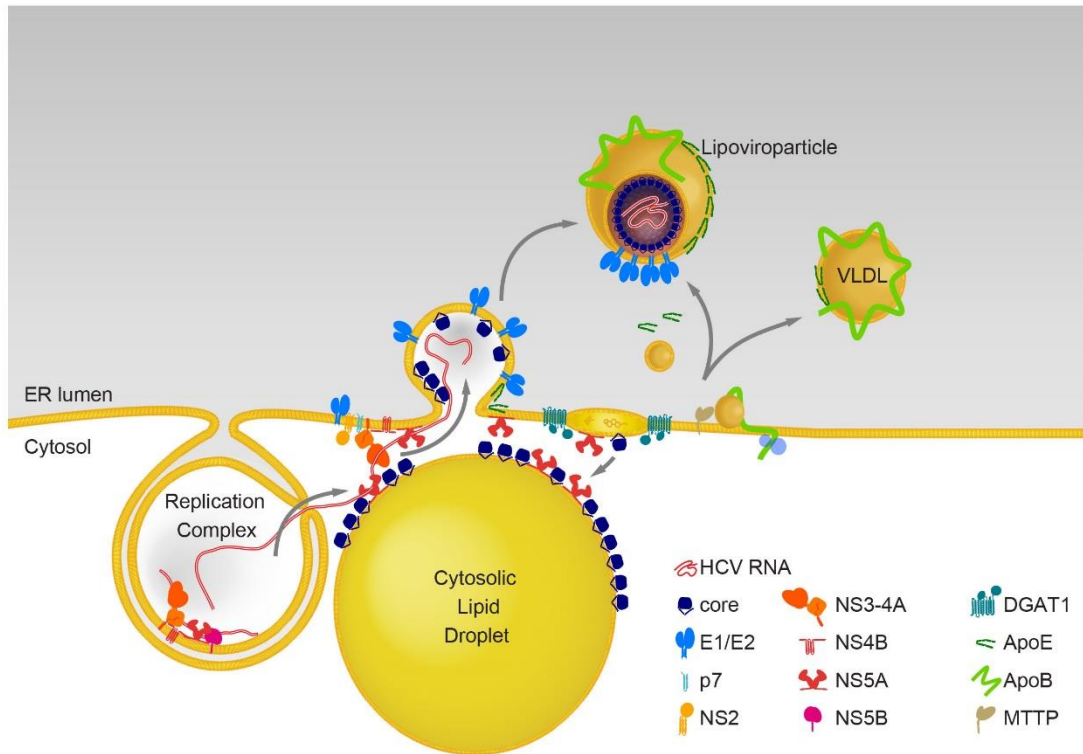


**Figure 6: Assembly and maturation of HCV particles.**

In HCV-infected cells, the core protein localizes to LDs thereby recruiting the replication complex to adjacent sites at the ER. NS5A interacts with core, likely facilitating the interaction of core and HCV RNA during encapsidation. In a concerted process, the interaction of NS2 with p7 and NS3-4A retrieves core from LDs to the sites of nucleocapsid formation. The NS2/p7 complex also recruits the E1/E2 dimer. During maturation, the nascent virions associate with lipoproteins, forming a lipovirion that leaves the cell *via* the secretory pathway (Illustration kindly provided by Eva Herker).

### 1.7 LDs as HCV assembly sites

LDs are cytosolic organelles that are ubiquitously found in eukaryotic cells. Their predominant function is the storage of neutral lipids, such as triglycerides (TGs) as energy resource for cellular processes. Further, they provide components for membrane formation. LDs consist of a dense core of neutral lipids (TGs and sterol esters) that are surrounded by a phospholipid monolayer (Tauchi-Sato et al., 2002). Several proteins are found on the LD surface, including members of the perilipin family, DGAT2, and Rab18 (reviewed in Farese and Walther, 2009). Depending on the cell type, LDs vary in size with a range from 100–200 nm up to 100 µm in white adipocytes (reviewed in Walther and Farese, 2012). HCV infection is connected to LDs and LD biology in different ways. Roughly 50% of chronic HCV patients develop steatosis caused by the accumulation of LDs (Adinolfi et al., 2001) and this phenotype has been connected to the alteration of the LD turnover by the core protein in transgenic mice (Harris et al., 2011). During HCV replication, the core protein traffics to LDs (Miyanari et al., 2007). This process depends on DGAT1, a protein that catalyzes the final step in the triglyceride synthesis (Herker et al., 2010). Further, NS-proteins and HCV RNA

are found adjacent to LDs and nascent virions bud into the ER at LD-adjacent sites, making LDs the putative HCV assembly sites (Miyanari et al., 2007; Roingeard et al., 2008). In addition to viral proteins, different host proteins have been found to localize to LDs in HCV-infected cells, many of them involved in viral replication (Ariumi et al., 2011a; Chatel-Chaix et al., 2013; Chatel-Chaix et al., 2011; Lim et al., 2016). Recently, a proteomic approach identified profound changes in the LD proteome in HCV-infected cells, indicating that HCV changes the LD proteome in favor of productive replication (Rosch et al., 2016).

### **1.8 Host RNA-binding proteins in HCV replication**

During HCV infection, a complex interaction between viral and host proteins is established. On one hand, antiviral factors try to control the infection; on the other hand, HCV modulates plenty of host proteins to promote viral replication. Both groups comprise several RNA-binding proteins that are involved in different steps of the HCV life cycle. Some RNA-binding proteins, e.g. the insulin-like growth factor-II mRNA-binding protein 1 (IGF2BP1) or the heterogeneous ribonucleoprotein D (HNRNPD), are involved in HCV translation (Paek et al., 2008; Weinlich et al., 2009). Two members of the DEAD box RNA helicase family, DDX3 and DDX6, have been shown to be important for HCV replication and to interact with the core protein. Downregulation of DDX6 led to a decrease in virus production and DDX3 knockdown decreased HCV RNA and viral titers (Ariumi et al., 2007; Jangra et al., 2010; Randall et al., 2007). Further, binding of DDX3 to the HCV 3' UTR led to the activation of IKK- $\alpha$ , a crucial host factor for assembly that stimulates lipogenesis in infected cells (Li et al., 2013a). DDX3 and DDX6 are both found in ribonucleoprotein particles (RNPs) that are associated with P-bodies and stress granula. Upon infection, both are redistributed to LDs together with other stress granula components such as G3BP1 or the polyA binding protein PABPC1 (Ariumi et al., 2011a). PABPC1 and other stress granula proteins are also required for efficient HCV replication (Ariumi et al., 2011a; Rosch et al., 2016). In an NS3-4A interaction screen, the Y-box binding protein 1 (YB-1) was identified as a regulator between RNA replication and particle production, as downregulation decreases RNA replication but increases viral particle production (Chatel-Chaix et al., 2011). YB-1 re-localized to LDs in HCV-infected cells and additionally recruited interacting proteins, which all displayed a similar phenotype upon downregulation. Therefore, a YB-1 ribonucleoprotein complex was described, regulating an NS3-dependent step in HCV particle production (Chatel-Chaix et al., 2013). During the late stages of the HCV life cycle, the heterogeneous ribonucleoprotein K (HNRNPK), also found at assembly sites, has been described as a restriction factor for HCV that suppresses viral particle production (Poenisch et al., 2015). In summary, RNA-binding proteins have multiple roles during different steps of HCV infection.



## 1.9 Transposable elements

Transposable elements (TEs), also known as transposons or “jumping genes”, are pieces of nucleic acid with the ability to change their position within the DNA. They were first discovered in *zea mays* and described as “controlling elements” by Barbara McClintock (McClintock, 1950). Today, it is known that TEs exist in the genome of almost all analyzed prokaryotic and eukaryotic organisms, except for the *bacillus subtilis* laboratory strain 168 (Kunst et al., 1997) and the protozoan parasite *plasmodium falciparum* (Gardner et al., 2002). The proportion of the genome that is covered by TEs varies inter- and intraspecifically, e.g. with 37.5% found in mice, 12–16% in the model organism *C. elegans*, and less than 10% in different yeast strains (Bleykasten-Grosshans et al., 2013; Laricchia et al., 2017; Waterston et al., 2002). According to their mode of transposition, eukaryotic TEs were initially divided into two major classes, I and II (Finnegan, 1989): class I elements (retrotransposons) use a “copy and paste” mechanism via an RNA intermediate. On the contrary, class II elements (DNA transposons) mobilize via “cut and paste”. These classes contain many TE subfamilies and show a variable abundance within and across the genome of different species (Deininger et al., 1992; reviewed in Feschotte and Pritham, 2007; Malik et al., 1999; Smit et al., 1995; reviewed in Sotero-Caio et al., 2017). Since the historical classification, updates of the classification system have been attempted, grouping TEs based on different characteristics (Kapitonov and Jurka, 2008; Wicker et al., 2007).

### 1.9.1 Transposable elements in the human genome

The initial sequencing of the human genome in 2001 revealed that about 45% of the DNA consists of TEs of different classes (Figure 7) (Lander et al., 2001). Recently, *de novo* search algorithms described that even more than 60% are repetitive sequences, likely derived from TEs (de Koning et al., 2011). Although almost all human TEs except for the long interspersed nuclear element 1 (LINE1) are inactive today (reviewed in Mills et al., 2007), they probably had an enormous impact on genetic diversity and genome evolution (reviewed in Cordaux and Batzer, 2009; reviewed in Kazazian, 2004).

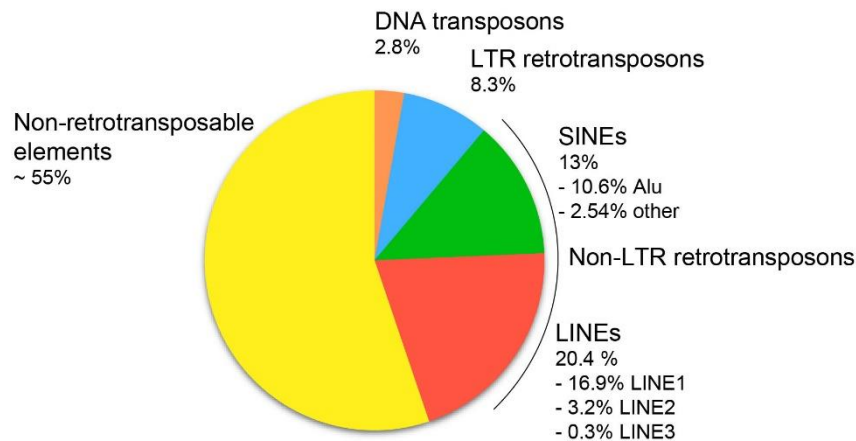


**Figure 7: Abundance of retroelements in the human genome.**

Nearly half of the human genome sequence (~ 45%) is composed of transposable elements with the majority being derived from non-LTR retrotransposons (LINEs and SINEs). LTR retrotransposons represent 8% of human DNA, whereas DNA transposons are the minority with approximately 3% (LINEs = Long interspersed nuclear elements; SINEs = Short interspersed nuclear elements) (Lander et al., 2001).

### 1.9.1.1 DNA transposons

With a total frequency of 3%, DNA transposons represent the smallest group of TEs in the human genome (Lander et al., 2001). They were first described to be part of the human DNA more than 20 years ago and currently 125 different families have been identified (Pace and Feschotte, 2007; Smit and Riggs, 1996). Mainly, they encode for a transposase that is flanked by inverted terminal repeats (Figure 8), allowing them to autonomously excise and reintegrate into the genome ("cut and paste"). Also, non-autonomous derivatives of those elements can exist (reviewed in Feschotte and Pritham, 2007). However, DNA transposons in humans have been inactive for the past 37 million years (Lander et al., 2001; Pace and Feschotte, 2007).

### 1.9.1.2 Retrotransposons

In contrast to class II transposons, class I elements or retrotransposons use an RNA intermediate for their mobilization ("copy and paste"), leading to the duplication of the element in the genome. Briefly, a functional reverse transcriptase encoded by autonomous retrotransposons is required for this mechanism. The mRNA transcript of the element is used as template for reverse transcription and the synthesized complementary DNA (cDNA) is reintegrated into the genome (Boeke et al., 1985). Their integration sites are typically flanked by target-site duplications (TSDs) (Lander et al., 2001). Based on the presence (retrovirus-like elements, LTR retrotransposons) or the lack of long-terminal-repeats (LINE-like elements, Non-LTR retrotransposons), retrotransposons were further subdivided into two subclasses (see below) (Finnegan, 1992).

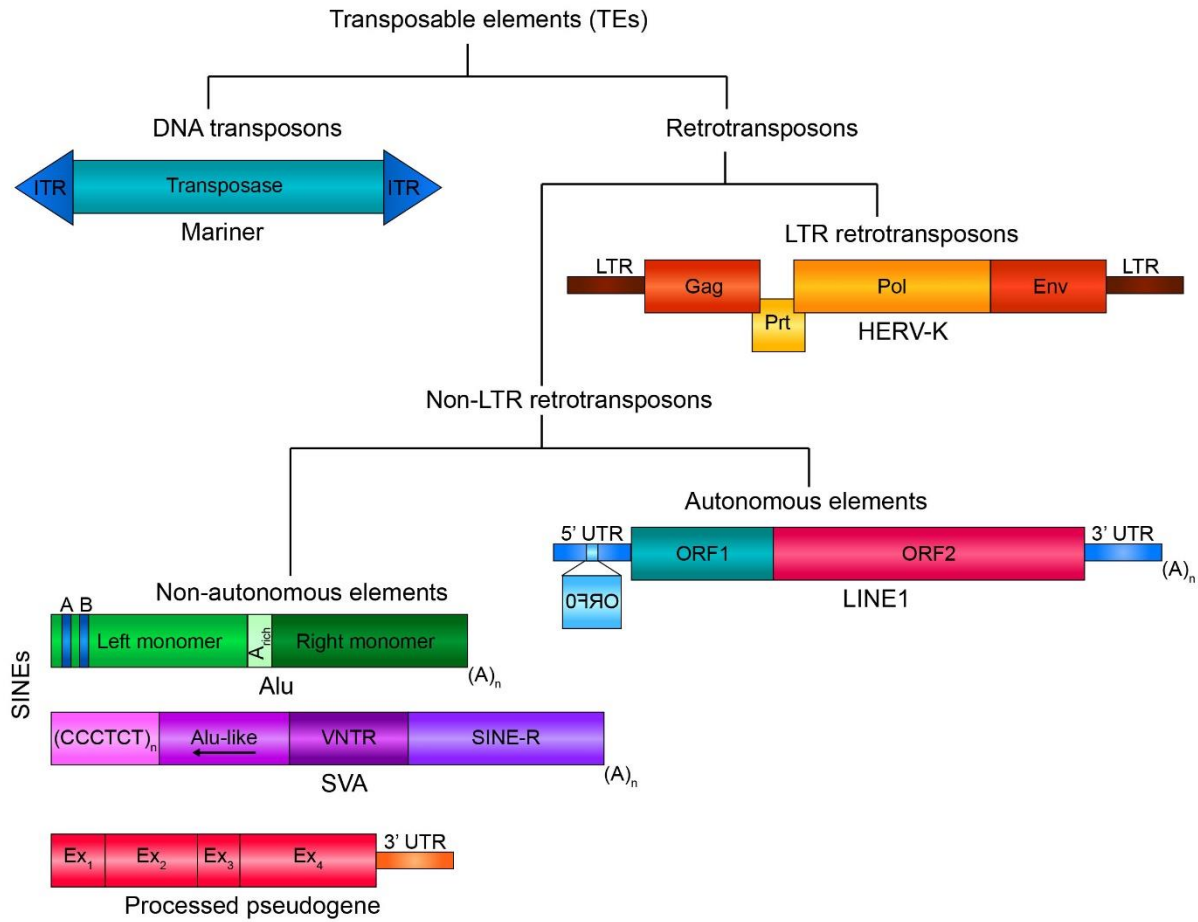


**Figure 8: Transposable elements in the human genome.**

Classification of transposable elements present in the human genome with one representative element depicted for each group. DNA transposons like the Mariner element encode their transposase and are flanked by inverted terminal repeats (ITRs). Retrotransposons are further grouped by the presence or absence of long-terminal repeats (LTR). LTR retrotransposons are endogenous retroviruses, that are theoretically autonomous but dysfunctional (e.g. human endogenous retrovirus type K (HERV-K)). Non-LTR retrotransposons are divided into autonomous and non-autonomous elements that require the activity of an autonomous element to mobilize. LINE1 is the only retroelement that is still active in the human genome, but can *trans* mobilize other elements such as SINEs (Dewannieux et al., 2003). Processed pseudogenes are cellular mRNAs that are integrated by LINE1 (Esnault et al., 2000; Wei et al., 2001). (Gag = group specific antigen; Prt = protease; Pol = polymerase; Env = envelope protein (non-functional); ORF = open reading frame; UTR = untranslated region; A and B in the Alu element = A and B box RNA polymerase III promoter; SVA = SINE-R/VNTR/Alu; VNTR = variable number of terminal repeats; (A)<sub>n</sub> symbolizes a polyA tail; Ex = exon) (reviewed in Beck et al., 2011; reviewed in Goodier and Kazazian, 2008).

**LTR retrotransposons:** Human LTR retrotransposons, mainly human endogenous retroviruses (HERVs) and their related elements, comprise 8% of the human DNA (Lander et al., 2001). They are likely derived from the ancient integration of retroviruses into germ line cells and are still structurally and functionally similar. A variety of different HERV-families has been identified (reviewed in Mayer and Meese, 2005). Flanked by LTRs, those elements encode for at least two genes related to the retroviral core protein (*gag*) and the polymerase

(*pol*). Some HERVs additionally encode an *env*-like ORF (reviewed in Bannert and Kurth, 2006) (see Figure 8); however, mutations and deletions prevent the re-formation of infectious particles. Although inactive in the human genome, their retrotransposition mechanism is assumed to have characteristics of the retroviral life cycle, as formation of virus-like particles (VLPs) by endogenous HERV-K has been described in early studies of germ cell tumors (Lower et al., 1984; reviewed in Lower et al., 1996). Recently, sequence comparison of the genome sequence of individual human beings described different integration sites for HERV-K family members in the past two million years (Wildschutte et al., 2016) and the identification of a functional *env* protein from one HERV-K family member increases evidence that HERVs remain active in the human genome (Dewannieux et al., 2005). Further, the envelope protein of HERV-W, also known as syncytin, is primarily expressed in the placenta and has been shown to induce syncytia formation *in vitro*, thus suggesting a role in human placenta development (Blond et al., 2000; Mi et al., 2000).

**Non-LTR retrotransposons:** Class I elements from the group of non-LTR retrotransposons account for one third of the human genome (Lander et al., 2001). Based on the presence or absence of an ORF encoding for a reverse transcriptase, they are divided into autonomous and non-autonomous elements (Wicker et al., 2007). Whereas autonomous elements mobilize themselves, a non-autonomous element requires the activity of an autonomous element to duplicate within the genome (reviewed in Ostertag and Kazazian, 2001).

**Autonomous non-LTR retrotransposons:** In humans, the family of long interspersed nuclear elements (LINEs) is the predominant group of retroelements: 21% of the genome is covered by three members of the LINE family (LINE1, LINE2, and LINE3): LINE2 elements encode for 3.2%, whereas LINE3 elements only cover 0.3% of the DNA; both elements are no longer active (Lander et al., 2001). With 17%, LINE1 represents most of the LINE family and is the only autonomous element that is still active in humans. Its activity and correlating mutagenic potential have first been discovered by an insertion to the *Factor VIII* gene in two individual haemophilia A patients (Kazazian et al., 1988).

**Non-autonomous LTR retrotransposons:** Due to the lack of a self-encoded reverse transcriptase, the retrotransposition of non-autonomous elements depend on the activity of an autonomous retroelement. In humans, three different groups of such elements, all dependent on LINE1 activity, are known: the short interspersed nuclear elements (SINEs), the SINE-VNTR-Alu elements (SVAs) and processed pseudogenes that result from the reverse transcription of cellular mRNAs (Figure 8) (Dewannieux et al., 2003; Esnault et al., 2000; Hancks et al., 2011; Raiz et al., 2012; Wei et al., 2001).

**SINEs:** 13% of the human genome consists of SINEs, non-coding repetitive sequences shorter than 500 bp in length (reviewed in Batzer and Deininger, 2002). Members of the Alu family, named after the *AluI* restriction site that is commonly present within their sequence

(Houck et al., 1979), are the most abundant repetitive sequence in the human genome with  $1.5 \times 10^6$  copies (Lander et al., 2001). In contrast to the tRNA-derived SINE families present in the human genome (Mammalian-wide interspersed repeat, MIR and MIR3) (Jurka et al., 1995; Lander et al., 2001; Smit and Riggs, 1995), Alu elements are evolutionary derived from the small 7SL RNA (Ullu and Tschudi, 1984) and consist of two monomers divided by an adenosine-rich sequence with a total length of ~300 bp, ending with a polyA tract (reviewed Batzer and Deininger, 2002) (Figure 8). Their transcription is driven by RNA Polymerase III from a bipartite promoter in the left monomer (Fuhrman et al., 1981; Paoletta et al., 1983). Sequence analysis revealed that SINE repetitions are mainly found in GC-rich regions and introns compared to other retroelements (Medstrand et al., 2002). Whereas MIR SINEs are fixed, identification of a *de novo* insertion of Alu into the *NF1* gene of a patient with neurofibromatosis type 1 in 1991 suggested that Alus are still active in the human genome (Wallace et al., 1991). Recently, *in vitro* experiments confirmed that Alu mobilization is driven by the LINE1 retrotransposition machinery (Dewannieux et al., 2003). Up to date, an increasing amount of Alu insertions causing single-gene diseases has been described (reviewed in Hancks and Kazazian, 2016).

**SVA elements:** The SVA element is formed by the combination of sequences derived from other retrotransposons (Ostertag et al., 2003; Shen et al., 1994). Numerous hexameric repeats at the 5' end are followed by an antisense-orientated Alu-like sequence and a variable number of terminal repeats (VNTR). Downstream, a short interspersed element of retroviral origin (SINE-R) (Ono et al., 1987) is located, terminated by a polyA tract (Figure 8). Compared to LINEs and SINEs, the number of SVAs present in the human genome is drastically lower with approximately 2700 copies (Lander et al., 2001; Wang et al., 2005). Although non-autonomous, SVA activity was reported to cause mutations by integration, most likely by *trans* mobilization by LINE1 (Hancks et al., 2011; Ostertag et al., 2003; Raiz et al., 2012; Rohrer et al., 1999). In an evolutionary context, the hominid-specific SVA represents the youngest group of active retroelements (Ostertag et al., 2003; Wang et al., 2005).

**Processed pseudogenes:** In 1982, the identification of elements in the human genome that share sequence homology with known genes but lack functional characteristics, such as introns and a promoter sequence, led to the description of so-called “processed genes”, today also known as “processed pseudogenes” (Figure 8) (Hollis et al., 1982). Here, the model of mRNA as transcript for reverse transcription and reintegration of the cDNA was already described, as reintegrated sequences additionally carried a polyA sequence. Evidence that retrotransposition was the cause for pseudogene formation *in vitro* piled up (Maestre et al., 1995) and recently, experiments confirmed that pseudogenes originate from reverse transcription of cellular mRNAs and reintegration of the respective cDNAs by LINE1 (Esnault et al., 2000; Wei et al., 2001). In humans, ~8,000 copies of processed pseudogenes

were identified (Zhang et al., 2003). Another LINE1-mediated mechanism by which encoding genes are retrotransposed is termed 3' transduction: due to its rather weak polyA signal, mRNA transcription of LINE1 continues at the 3' end and produces a chimeric mRNA with the adjacent gene, which is subsequently used as a template for reverse transcription (Holmes et al., 1994; Moran et al., 1999).

### **1.10 LINE1**

The clade of LINE1 retrotransposons is the predominant group of non-LTR retrotransposon in the mammalian genome. Nevertheless, LINE1 family members encoding for functional ORFs are only described in humans and mice (Loeb et al., 1986; Scott et al., 1987). Early studies identified repeated sequences in the genome of higher eukaryotes (Britten and Kohne, 1968) and in 1980, a 6.4 kb element in the 3' UTR of the  $\beta$ -globulin gene was repeatedly found in the DNA library of the human genome, marking the first description of long interspersed repeated segments (Adams et al., 1980; reviewed in Singer, 1982). Sequence analysis revealed  $5 \times 10^5$  copies of LINE1 that are, in contrast to Alu, concentrated in AT-rich regions of the DNA (Lander et al., 2001; Medstrand et al., 2002). A comparison of LINE1 integration sites in individuals revealed that there is an average difference of 285 LINE1 integrations between any two analyzed human beings (Ewing and Kazazian, 2010). While the majority of LINE1 elements is inactive as a consequence of 5' truncations, mutations, or rearrangements (Lander et al., 2001), an estimated number of 30–100 full-length elements from different families is still mobile (termed “hot” or retrotransposition competent LINE1 (RC-LINE1) (Brouha et al., 2003; Sassaman et al., 1997). Additionally, a sequencing study of six individual human genomes revealed differences in the frequency of active LINE1 elements in individuals from different geographic populations (Beck et al., 2010).

#### **1.10.1 Organization of the human LINE1 retroelement**

Full-length LINE1 retrotransposons are about 6 kb in size. Two ORFs encoding for L1ORF1p and L1ORF2p, are flanked by a ~900 bp 5' and a ~200 bp 3' UTR that contains a polyadenylation signal and ends in a polyA tract (Figure 9). The ORFs are separated by a short intergenic region that contains at least two stop codons (Dombroski et al., 1991; Scott et al., 1987). Transcription of the bicistronic LINE1 mRNA is driven by an RNA polymerase II promoter in the ~900 bp 5' UTR, that additionally contains an antisense promoter and a third ORF (ORF0) (Denli et al., 2015; Speek, 2001; Swergold, 1990). Characteristically, LINE1 integrations are flanked by target-site duplications (TSDs) of various length (Moran et al., 1996; Szak et al., 2002).

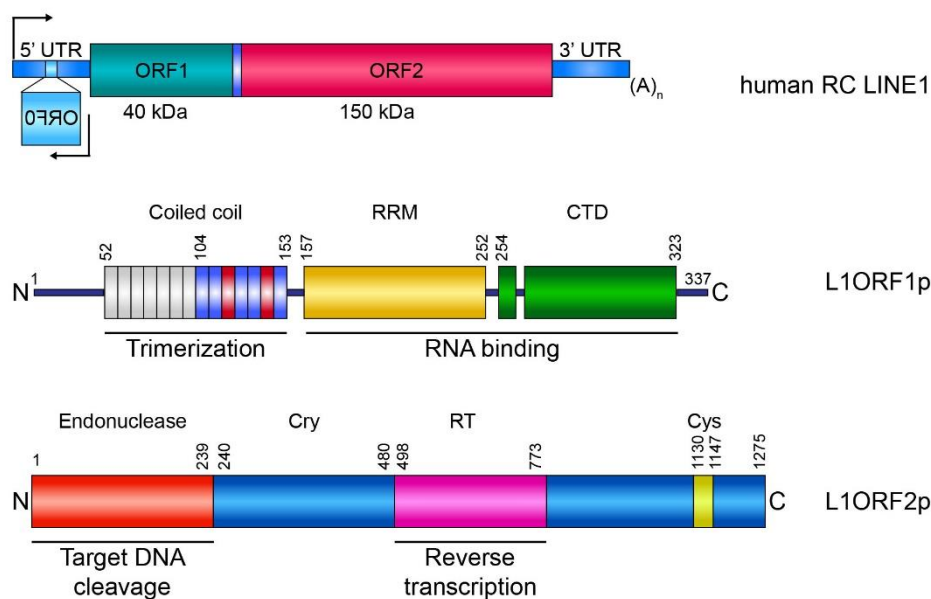


**Figure 9: Schematic representation of LINE1 and its encoded proteins L1ORF1p and L1ORF2p.**

A retrotransposition competent LINE1 is ~6 kb in length. Two of the three ORFs, ORF1 and ORF2, are flanked by UTRs. A polymerase II promoter is located in the 5' UTR. The N-terminal ORF1 encodes for the 40 kDa RNA-binding protein L1ORF1p that is separated from the second ORF by a short intergenic region. ORF2 encodes for the 150 kDa enzyme L1ORF2p, that has an endonuclease as well as a reverse transcriptase function. The 3' UTR comprises ~200 bp with a weak polyA signal and terminates in a polyA tract. The antisense ORF in the 5' UTR, ORF0, encodes a recently identified protein of unknown function. Arrows indicate promoter regions (Denli et al., 2015; Dombroski et al., 1991; Scott et al., 1987; Speek, 2001; Swergold, 1990). L1ORF1p consists of three distinct domains: an N-terminal coiled-coil domain that is required for trimerization, a central RNA recognition motif (RRM) and a C-terminal domain (CTD). The coiled coil domain consists of heptad repeats. Unconserved repeats are depicted in grey; heptads that are essential for trimerization are colored in blue, the red marked regions contain a trimerization RxxxxE motif. The RRM and CTD are both involved in RNA binding (modified from Khazina et al., 2011). L1ORF2p has an N-terminal endonuclease domain required for genomic DNA cleavage. A cryptic domain (Cry) is followed by the reverse transcriptase (RT) (Dombroski et al., 1994; Feng et al., 1996; Mathias et al., 1991). A conserved cysteine-rich repeat is located in the C-terminal part (Moran et al., 1996).

#### 1.10.1.1 Structure and function of LINE1 encoded proteins

The first open reading frame, ORF1, encodes for a ~40 kDa protein (L1ORF1p) with RNA-binding capacity that forms flexible homotrimers and displays an RNA-binding function (Hohjoh and Singer, 1996; Khazina and Weichenrieder, 2009). Early on, it was described that L1ORF1p forms ribonucleoprotein particles (RNPs) containing LINE1 mRNA within the cells and that the stability of this complex is RNA-dependent (Hohjoh and Singer, 1996; Hohjoh and Singer, 1997). The monomeric L1ORF1p is composed of three distinct domains: An N-terminal coiled-coil domain, a central RNA recognition motif (RRM), and a C-terminal domain (CTD) (Figure 9) (Hohjoh and Singer, 1996; Khazina and Weichenrieder, 2009). The coiled-coil domain facilitates trimerization of L1ORF1p and mostly consists of hydrophobic  $\alpha$ -helical heptad repeats, interrupted by two ion-binding hydrophilic heptad sequences (Khazina

et al., 2011; Khazina and Weichenrieder, 2009). Additionally, RhxxxE motifs were identified that have been linked to the trimerization of proteins before (Kammerer et al., 2005). Although highly variable, a putative leucine zipper motif was identified in the N-terminal domain and the sequence preceding the coiled-coil domain with positive charged residues close to the N-terminus is crucial for retrotransposition (Holmes et al., 1992; Khazina and Weichenrieder, 2018). L1ORF1p binds single stranded nucleic acids with a strong preference for its own encoding transcripts (Callahan et al., 2012; Esnault et al., 2000; Khazina and Weichenrieder, 2009; Wei et al., 2001). Both, the RRM and the CTD are responsible for RNA binding (Khazina and Weichenrieder, 2009). Mutant studies of the CTD have shown that RNA binding of L1ORF1p is crucial for ribonucleoprotein particle (RNP) formation and disruption decreases or abolishes retrotransposition (Kulpa and Moran, 2005). In addition to RNA binding, the mouse L1ORF1p functions as a nucleic acid chaperone and this function is necessary for retrotransposition (Martin and Bushman, 2001; Martin et al., 2005). Analogous mutants of the human L1ORF1p also displayed reduced retrotransposition, suggesting a functional role for L1ORF1p downstream of the RNP assembly (Kulpa and Moran, 2005). Further, a potential nucleic acid chaperone function was underlined by exclusive binding of the human L1ORF1p to single stranded but not double stranded nucleic acids and polymeric complexes of purified L1ORF1p facilitated melting of mismatched DNA duplexes (Callahan et al., 2012; Khazina and Weichenrieder, 2009). LINE1 mobilization *in vitro* requires expression of L1ORF1p, as deletion of L1ORF1p or mutations of three conserved amino acid residues in the CTD prevent LINE1 retrotransposition (Kulpa and Moran, 2005; Moran et al., 1996). In contrast, *trans* mobilization of Alu only requires L1ORF2p (Dewannieux et al., 2003). Mass spectrometry followed by sequence analysis revealed 22 putative or actual phosphorylation sites for L1ORF1p, six of them are highly conserved target or docking sites for the proline-directed protein kinase (PDPK). Mutations in the PDPK motifs severely decreased or abolished LINE1 retrotransposition, suggesting that L1ORF1p phosphorylation is required for LINE1 activity (Cook et al., 2015). Even though L1ORF1p has a remarkably unique domain composition, its tertiary and quaternary protein structure is comparable to nucleoprotein and membrane fusion protein structures of the influenza A virus (Khazina et al., 2011; Khazina and Weichenrieder, 2009; Khazina and Weichenrieder, 2018). In a recent study, an N-terminally truncated mutant of L1ORF1p was found to be associated with liposomes in a floatation assay, suggesting a possible interaction with membranes (Schneider et al., 2013). L1ORF1p is predominantly localized in cytoplasm, however, in overexpression studies a partial colocalization with nucleoli was reported as well (Goodier et al., 2004; Hohjoh and Singer, 1996). Immunofluorescence studies revealed a localization to distinct foci distributed throughout the cytoplasm that were identified as stress granula (SG) (Goodier et al., 2007). Induction of SGs or similar distinct structures seems to be specific to L1ORF1p, as expression of L1ORF2p alone does not induce foci formation (Doucet et al., 2010). Proteomic studies mapping the interactome of a tagged L1ORF1p expressed from a full-



length LINE1 exposed a high number of interactors, many of them involved in RNA binding or processing (Goodier et al., 2013; Moldovan and Moran, 2015; Taylor et al., 2013). In addition, a variety of these interacting proteins was found to colocalize to the cytoplasmic foci observed for overexpressed L1ORF1p, and co-immunoprecipitation revealed that most interactions are RNA-dependent, indicating that also host proteins are part of the LINE1 RNPs (Goodier et al., 2013). Yet, the exact role of L1ORF1p in retrotransposition remains to be elucidated.

The second ORF encodes for L1ORF2p, a 150 kDa protein with endonuclease as well as reverse transcriptase activity (Figure 9) (Dombroski et al., 1994; Feng et al., 1996; Mathias et al., 1991). Additionally, the C-terminal domain harbors a cysteine-rich region that is essential for retrotransposition activity (Moran et al., 1996). In contrast to L1ORF1p, L1ORF2p expression is much lower and several studies describe an unconventional translation model for L1ORF2p from the bicistronic LINE1 mRNA in which L1ORF2p translation takes place by a termination/re-initiation mechanism that is still not fully solved, but seems to be IRES-independent (Alisch et al., 2006; Dmitriev et al., 2007; McMillan and Singer, 1993). The endonuclease encoded in L1ORF2p preferentially cleaves DNA at a specific AT-rich target sequence that maps the integration sites observed for LINE1 in human genome sequences (Cost and Boeke, 1998; Feng et al., 1996; Jurka, 1997). L1ORF2p also assembles with L1ORF1p and the LINE1 mRNA into RNPs, as reverse transcriptase activity was detected in isolated RNPs from LINE1-overexpressing cells (Kulpa and Moran, 2005; Kulpa and Moran, 2006). This was further confirmed by microscopic analysis, showing colocalization of overexpressed L1ORF1p and L1ORF2p together with probed LINE1 mRNA (Doucet et al., 2010). It is widely assumed that far more L1ORF1p is present in the RNP compared to L1ORF2p, but exact numbers are controversial (Taylor et al., 2013). L1ORF2p also exhibits a strong *cis* preference for its encoding transcript, but still can use other mRNAs in *trans* for reverse transcription (Dewannieux et al., 2003; Esnault et al., 2000; Kulpa and Moran, 2006; Wei et al., 2001). Additionally, reverse transcription is independent of the presence of L1ORF1p, indicating that L1ORF2p can assemble with RNA on its own (Doucet et al., 2010). Still, both proteins are required for LINE1 retrotransposition *in vitro* (Moran et al., 1996).

Three years ago, a primate-specific third ORF of ~7 kDa was discovered (ORF0), located in antisense orientation in the 5' UTR (Denli et al., 2015). Expression of a GFP-tagged fusion protein revealed predominant localization in the nucleus adjacent to PML nuclear bodies. Although its exact function has not yet been described, overexpression of ORF0 enhances LINE1 mobility *in vitro*.

### 1.10.2 LINE1 retrotransposition

As described for the retrotransposon class, RC-LINE1 elements mobilize *via* an RNA intermediate (reviewed in Babushok and Kazazian, 2007). Retrotransposition starts with the transcription of the LINE1 mRNA, followed by translation into the encoded proteins L1ORF1p and L1ORF2p (Figure 10). After formation of the LINE1 RNP (Doucet et al., 2010; Hohjoh and Singer, 1996; Kulpa and Moran, 2005), this complex shuttles back to the nucleus, but the mechanism behind this is still unknown. While some studies report retrotransposition in nondividing cells (Kubo et al., 2006; Macia et al., 2017), others describe that cell division is required for LINE1 activity (Shi et al., 2007; Xie et al., 2013). Recently, it was reported that the LINE RNP localizes to the nucleus directly after mitosis (Mita et al., 2018). Whereas L1ORF1p is exported from the nucleus in an exportin 1 (CRM1) involving mechanism, L1ORF2p stays in the nucleus and is recruited to chromatin in the S phase of the cell cycle. Noteworthy, L1ORF2p was shown to interact with proteins of the replication fork and interaction with one of these proteins, the proliferating cell nuclear antigen (PCNA), is required for retrotransposition (Taylor et al., 2013). Additionally, LINE1 retrotransposition peaks in the S phase in this *in vitro* system, showing a cell cycle dependency (Mita et al., 2018). The endonuclease encoded by L1ORF2p nicks the genomic DNA at a specific AT-rich target sequence, giving rise to a free terminal 3' hydroxyl group (3' OH) that is used as a primer for reverse transcription. This process, termed "target-site primed reverse transcription" (TRPT) has first been described for the LINE-like element R2Bm from the silkworm *Bombyx mori* (Luan et al., 1993) and was later verified for the human LINE1 element *in vitro* (Cost and Boeke, 1998; Cost et al., 2002; Feng et al., 1996). Pre-existing free 3' OH ends can serve as primer for reverse transcription as well, likely explaining LINE1-mediated integration differing from the characteristic insertion sites of LINE1 (Cost et al., 2002). It is believed that at the beginning of TRPT, a T-rich stretch comprising the 3' OH end is generated to which the polyA tail of the LINE1 mRNA is binding and biochemical studies have revealed that a stretch of four T nucleotides is sufficient to prime reverse transcription (Feng et al., 1996; Monot et al., 2013). The presence of a 3' polyA tail or tract is required for *cis* and *trans* retrotransposition by the LINE1 machinery (Doucet et al., 2015). The generated cDNA is reintegrated into the genome in a yet unknown mechanism, but based on experimental evidence from the R2 element a model was proposed in which two L1ORF2p subunits are present. One subunit nicks the first strand and primes reverse transcription while the second subunit performs second strand cleavage and synthesis (Christensen and Eickbush, 2005). A hallmark of LINE1 insertion sites is the generation of target-site duplications (Lander et al., 2001).

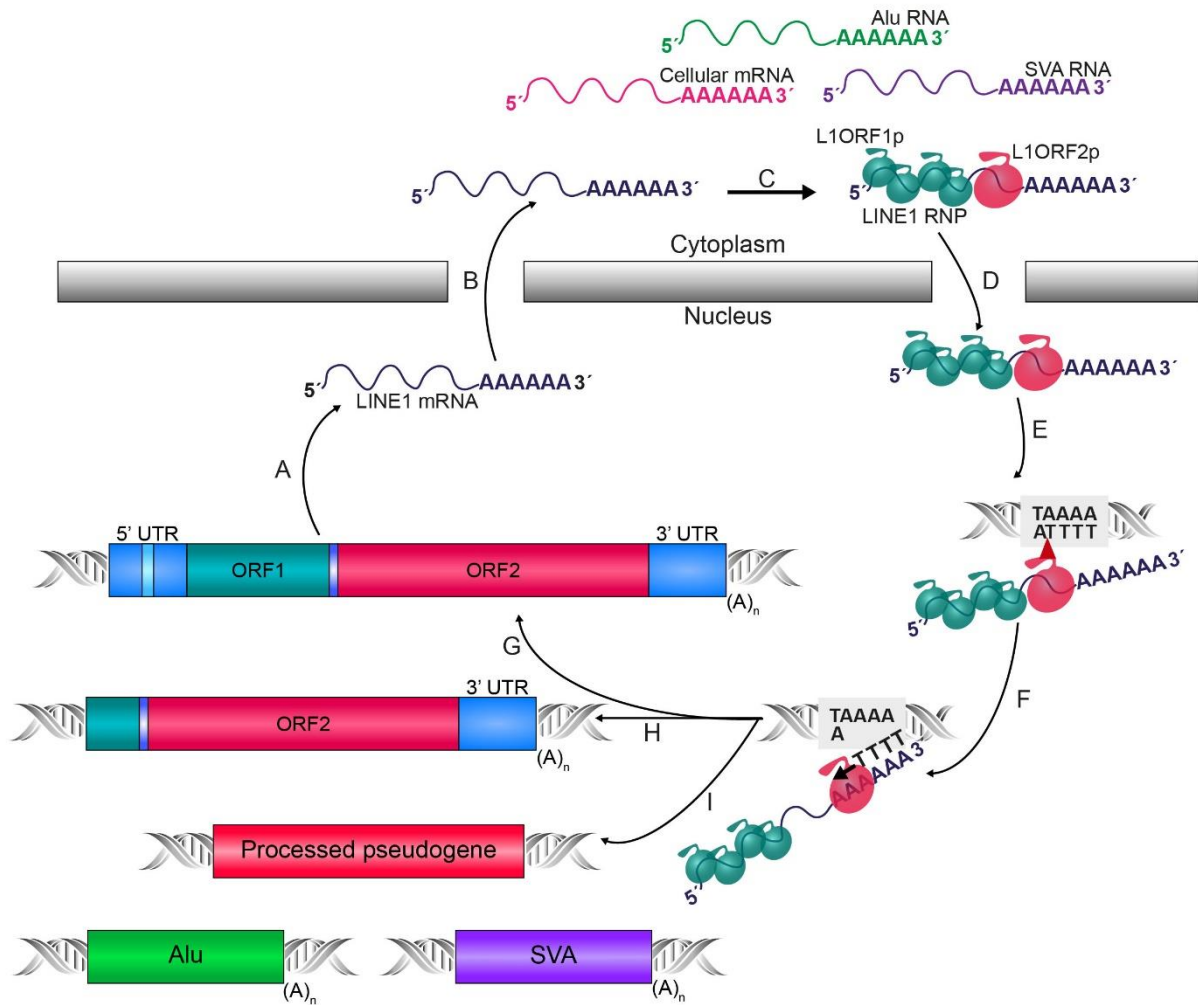


**Figure 10: LINE1 retrotransposition cycle.**

LINE1 retrotransposition starts with transcription (A) and translation (B) of the LINE1 mRNA into L1ORF1p and L1ORF2p. Both proteins assemble with their mRNA to form a ribonucleoprotein particle (LINE1 RNP, (C)). The RNP shuttles to the nucleus in a yet unexplained mechanism (D) and the endonuclease encoded in L1ORF2p nicks the genomic DNA at a specific target site (E). The generated 3' OH end is used to prime reverse transcription (target site primed reverse transcription, TRPT) (F). The synthesized cDNA is reintegrated to the genome; in case of complete reverse transcription, reintegration creates a new RC-LINE1 (G). Most reverse transcription processes are prematurely terminated, leading to 5' truncated defective elements (H). Despite their *cis* preference, LINE1 proteins can also associate with RNAs of non-autonomous retrotransposons (Alu, SVA) or cellular mRNAs (resulting in processed pseudogenes) and facilitate their mobilization in *trans* (I) (reviewed in Beck et al., 2011; Cost and Boeke, 1998; Cost et al., 2002; Dewannieux et al., 2003; Doucet et al., 2010; Doucet et al., 2015; Esnault et al., 2000; Feng et al., 1996; Grimaldi et al., 1984; Hohjoh and Singer, 1996; Kulpa and Moran, 2005; Lander et al., 2001; Moran et al., 1996).

Despite its strong *cis* preference, non-autonomous elements (SINEs, SVA) as well as cellular mRNAs hijack the LINE1 machinery for mobilization (Dewannieux et al., 2003; Doucet et al., 2015; Esnault et al., 2000). More than 99% of LINE1 insertions in the human genome are 5' truncated and *in vitro* experiments confirmed 5' truncation as a characteristic of *de novo* LINE1 integration (Grimaldi et al., 1984; Lander et al., 2001; Moran et al., 1996).

### 1.10.3 LINE1 expression and activity

As endogenous LINE1 activity is not instantly traceable, studies on the frequency of LINE1 retrotransposition are mainly based on a reporter system, allowing to track *de novo* events by marker genes which are only expressed if a full round of retrotransposition is completed (Freeman et al., 1994; Heidmann et al., 1988; Moran et al., 1996; Ostertag et al., 2000). Whereas LINE1 expression is suppressed in most somatic cells, *de novo* retrotransposition of LINE1 was thought to mainly take place in germ line cells and during embryonic development, as it was shown in transgenic mice (Kano et al., 2009; Ostertag et al., 2002). However, the possibility of somatic insertions was already discussed (Babushok et al., 2006). LINE1 is expressed and active in human embryonic stem cells (hESCs) (Garcia-Perez et al., 2007) and *in vitro* reprogramming of human somatic cells into induced pluripotent stem cells (iPSCs) led to an upregulation in LINE1 expression and retrotransposition, providing further evidence of LINE1 activity during embryonic development (Friedli et al., 2014; Klawitter et al., 2016; Wissing et al., 2012). Further, a genetic insertion of LINE1 into the *CHM* gene of a male patient suffering from x-linked choroideremia, that was also detected in germ line and somatic cells of the mother, suggested retrotransposition occurred during the mother's embryonic development (van den Hurk et al., 2007). To date, estimated numbers for *de novo* LINE1 insertions vary between one in ~100 and one in > 200 new-born children (Ewing and Kazazian, 2010; Huang et al., 2010; Kazazian, 1999). *Trans* mobilization of Alu elements is found in one out 20 newborns (Cordaux et al., 2006; Xing et al., 2009). Evidence that LINE1 retrotransposition was not restricted to germ cells arose in the last decade, as human neural progenitor cells (NPCs) support retrotransposition *in vitro* (Coufal et al., 2009). Sequencing analysis further proofed that LINE1 insertions are increased in tissue isolates from the brain compared to other tissues or reference sequences, implicating a role for LINE1 activity in the creation of genetic mosaics, especially in the brain (Baillie et al., 2011) (reviewed in Erwin et al., 2014). As most *in vitro* studies on LINE1 activity are conducted in immortalized or cancer cell lines such as HeLa cells, retrotransposition is also supported in cancer cells (Dewannieux et al., 2003; Kulpa and Moran, 2005; Kulpa and Moran, 2006; Moran et al., 1996; Ostertag et al., 2000).

### 1.10.4 Host mechanisms to control LINE1 retrotransposition

Since reintegration of transposable elements, especially into gene-coding regions can cause genomic instability and severe mutations, several mechanisms for suppression of LINE1 activity have evolved (reviewed in Ariumi, 2016). Epigenetically, the expression of LINE1 is controlled by methylation of CpG islands within the 5' end of the element (Hata and Sakaki, 1997; Thayer et al., 1993). These experimental data were further confirmed by the observation that LINE1 is often hypomethylated in malignant tissues (Chalitchagorn et al., 2004; Florl et al., 1999; Florl et al., 2004; Gao et al., 2014). Additionally, packaging of LINE1 encoding regions into heterochromatin leads to transcriptional inactivation (Castro-Diaz et al.,

2014; Van Meter et al., 2014). On a post-transcriptional level, RNA interference (RNAi) is involved in the degradation of LINE1 mRNA transcripts, thereby preventing translation (Hamdorf et al., 2015; Heras et al., 2013; Soifer et al., 2005; Yang and Kazazian, 2006). Activation of innate immune pathways and the interferon response are involved in the cell intrinsic defense against a variety of pathogens. Several interferon stimulated genes (ISGs) have been reported to restrict LINE1 activity: treatment with type I interferon decreased retrotransposition frequencies *in vitro* in a dose-dependent manner and overexpression of a variety of ISGs including ISG20, the putative RNA helicase Moloney leukemia virus 10 homolog (MOV-10), myxovirus resistance 2 (MX2) and the zinc finger antiviral protein (ZAP) had similar effects (Goodier et al., 2012; Goodier et al., 2013; Goodier et al., 2015; Moldovan and Moran, 2015). Some inhibitors of retrotransposition, such as ZAP and MOV-10 were additionally found to colocalize with L1ORF1p in cytoplasmic foci and interacted with L1ORF1p in an RNA-dependent manner (Choi et al., 2018; Goodier et al., 2013; Goodier et al., 2015; Li et al., 2013b; Moldovan and Moran, 2015). Recently, the adenosine deaminases acting on RNA 1 (ADAR1) protein was identified to assemble with LINE1 RNPs and to negatively regulate LINE1 retrotransposition (Orecchini et al., 2017). Proteins of the apolipoprotein B mRNA editing enzyme, catalytic polypeptide-like 3 (APOBEC3) family, known to be involved in the control of retroviral infections (reviewed in Willems and Gillet, 2015) restrict LINE1 *cis* and *trans* mobilization in cell culture retrotransposition assays of human embryonic stem cells and widely used cell lines, but the exact mechanism remains to be defined (Bogerd et al., 2006; Muckenfuss et al., 2006; Stenglein and Harris, 2006; Wissing et al., 2011). Another protein of the antiviral response, the SAM and HD domain containing protein 1 (SAMHD1) has been described to inhibit LINE1 retrotransposition in several studies. However, the exact mechanism remains controversial (Herrmann et al., 2018; Hu et al., 2015; Zhao et al., 2013). Overall, control of LINE1-mediated retrotransposition by diverse antiviral factors supports the idea of retroelements as “genomic parasites” that must be controlled to protect genomic integrity.

### **1.10.5 LINE1 retrotransposition and diseases**

#### **1.10.5.1 Single-gene diseases caused by LINE1 retrotransposition**

LINE1-mediated *cis* and *trans* mobilization and subsequent integration into coding regions of the genome can severely alter the function and expression of the respective gene product. The first concrete evidence of diseases resulting from LINE1 retrotransposition arose in 1988 when the insertion of LINE1 into the *Factor VIII* gene was discovered to be the cause for haemophilia A (Kazazian et al., 1988). Currently, 124 cases of single-gene diseases caused by LINE1 activity have been described (reviewed in Hancks and Kazazian, 2016). These mutations are distributed on different chromosomes, vary in length and are the result of different mechanisms by which LINE1 retrotransposition can alter the genome. Most of the *de novo* events are insertions, but deletional mutations have been reported as well (Mine et

al., 2007; Okubo et al., 2007; Udaka et al., 2007). Whereas a high percentage of *de novo* retrotransposition is linked to tumor development, other diseases such as neurocutaneous disorders, haemophilia and Duchenne muscular dystrophy (DMD) can also result from LINE1-mediated mutations (reviewed in Ganguly et al., 2003; Green et al., 2008; Hancks and Kazazian, 2016; Holmes et al., 1994; Kazazian et al., 1988; Sukarova et al., 2001; Wimmer et al., 2011). Examples are shown in table 1.

**Table 1: Single-gene diseases caused by LINE1 retrotransposition.**

(modified from Hancks and Kazazian, 2016)

Insertion	Gene	Disease	Reference
Alu	<i>FVIII</i>	Haemophilia A	(Ganguly et al., 2003; Green et al., 2008; Sukarova et al., 2001)
LINE1	<i>FVIII</i>	Haemophilia A	(Kazazian et al., 1988)
Alu	<i>BRCA1 / BRCA2</i>	Hereditary breast cancer	(Qian et al., 2017; Teugels et al., 2005)
Alu/LINE1	<i>NF1</i>	Neurofibromatosis type 1	(Wimmer et al., 2011)
LINE1	<i>APC</i>	Colon cancer	(Miki et al., 1992)
LINE1	<i>DMD</i>	Duchenne muscular dystrophy	(Holmes et al., 1994)
LINE1	<i>MCC</i>	Hepatocellular carcinoma	(Shukla et al., 2013)

#### 1.10.5.2 LINE1 and cancer

In addition to tumor formation resulting from e.g. the insertion of LINE1 into a tumor suppressor gene (Shukla et al., 2013), hypomethylation of the LINE1 promoter region has been reported as a feature of different cancer malignancies that often correlates with poorer survival rates (Antelo et al., 2012; Gao et al., 2014; Lou et al., 2014; Zhu et al., 2014). Further, L1ORF1p was highly expressed in tumor sections but not in the corresponding healthy tissue (Rodic et al., 2014). L1ORF2p also showed increased expression levels in cancer cell lines and tumor sections (De Luca et al., 2016) and inhibition or downregulation of L1ORF2p decreased cell growth of tumor derived cell lines *in vitro*, suggesting a role of LINE1 expression in tumor-promotion (Sciamanna et al., 2005). However, if the differential activation and expression of LINE1 is cause or consequence of cancer formation is yet not fully understood.

#### 1.10.5.3 LINE1 and viral infections

In the context of viral infections and disease progression, little is known about LINE1 expression and activity. Increased LINE1 retrotransposition frequency and LINE1 cDNA accumulation was observed in HIV-1-infected cells *in vitro* (Jones et al., 2013). This increase

was dependent on the presence of the HIV protein *vif*, a known inhibitor of the LINE1 repressor APOBEC3C. On the contrary, a decrease of LINE1 mobility in HIV-infected cells as a result of HIV-1 *vpr* mediated inhibition of the L1ORF2p reverse transcriptase was described (Kawano et al., 2018). Here, L1ORF1p was also found incorporated into HIV-1 virions. Regarding reverse transcription of exogenous viruses by L1ORF2p, sequence homologues of the N-protein of bornaviruses, non-retroviral negative single stranded RNA viruses, were discovered in the human genome, likely derived from active *trans* mobilization by LINE1 (Horie et al., 2010). Further evidence on integration of non-retroviruses emerged when a study on chronically infected HCV patients reported the presence of HCV sequences in the genome of four individuals (Zemer et al., 2008). Here, the HCV sequence was present in a larger DNA fragment, highlighting integration into the genome, possibly as a result of retrotransposon activity. Chronic HCV infection is still listed as a leading course for the development of hepatocellular carcinoma (HCC) (reviewed in Bandiera et al., 2016). LINE1-mediated integrations into the tumor suppressor gene *mutated in colorectal cancers* (MCC), promoting tumor formation by activating the  $\beta$ -catenin/Wnt pathway, were discovered in HCV or HBV-related HCC (Shukla et al., 2013), indicating that the viral infection alters LINE1 activity. Additionally, hypomethylation of LINE1 promoter regions and elevated expression levels in HCC resections from chronic HBV patients have been linked to poorer overall survival (Gao et al., 2014). Transcriptome sequencing of HBV-positive cell lines revealed a chimeric RNA of LINE1 and the hepatitis B X protein (HBX) that promotes tumor formation in mice (Lau et al., 2014). This hybrid transcript was also detected in ~23% of HCC samples from chronic HBV patients. How exactly LINE1 activity is altered in HBV and HCV infections and if this is cause or consequence of HCC formation remains to be elucidated. So far, it is discussed if the interference of HBV and HCV with the innate immunity results in the activation of LINE1 (reviewed in Honda, 2016).

## 2 Aim of the thesis

LINE1 remains the only active retrotransposon in the human genome and its activity has been connected to several single gene diseases. Except for two studies on retrotransposition in HIV-1 infected cells (Jones et al., 2013; Kawano et al., 2018), little is known about LINE1 in context of viral infections and its contribution to disease progression. Assembly of new HCV particles is associated with LDs and recently, changes of the LD protein composition were reported in HCV-infected cells (Rosch et al., 2016). In this context, the ORF1 protein of LINE1 (L1ORF1p) was identified at LDs upon HCV infection. Therefore, the aim of this thesis was to investigate the mechanism of L1ORF1p enrichment at HCV assembly sites and a putative interaction with viral components. As other RNA-associated proteins have been described to localize to LDs in HCV-infected cells comprising pro- or antiviral functions, a role for L1ORF1p and full-length LINE1 in HCV replication was also addressed. Further, it was sought to evaluate if HCV infection alters LINE1 retrotransposition. LINE1 is also capable of *trans* mobilizing other RNA transcripts. Thus, this study aimed on investigating if HCV RNA serves as template for L1ORF2p reverse transcription, thereby possibly being integrated into the genome.



### 3 Results

#### 3.1 HCV infection changes LINE1 expression levels and L1ORF1p localization

##### 3.1.1 HCV infection increases LINE1 expression

In a previous study aimed at investigating changes of the LD proteome upon HCV infection by mass spectrometry, the ORF1 protein of LINE1 was exclusively identified in LD fractions of HCV-infected cells (Rosch et al., 2016). To address if LINE1 expression is initially changed by HCV infection *in vitro*, a time course experiment was performed (Figure 11 A). Both, L1ORF1p and L1ORF2p are expressed from one bicistronic LINE1 mRNA; however, due to truncation mutations, different levels of truncated mRNAs might be present. Therefore, mRNA levels were determined by quantitative real-time PCR (qRT-PCR) using primer pairs located either in the L1ORF1p or L1ORF2p coding sequence. Additionally, protein levels of L1ORF1p and L1ORF2p were analyzed. Huh7.5 cells were infected with a Jc1 reporter strain carrying an enhanced green fluorescent protein (EGFP) in a duplicated NS5AB cleavage site (Jc1<sup>NS5AB-EGFP</sup>) to monitor infection rates via flow cytometry at the respective time points (Figure 11 B) (Webster et al., 2013). One day and 3 or 5 days post infection, cells were seeded in 6 well plates and harvested at 3, 6 and 9 days post infection. For harvest at day 9, twice the number of infected cells was seeded to exclude major growth differences due to infection. Compared to uninfected cells harvested at the same time, HCV-infected cells displayed a modest, transient elevation of LINE1 mRNA levels with both primer pairs with a significant increase at 6 days post infection (Figure 11 C). L1ORF1p protein levels were elevated in HCV-infected cells compared to uninfected cells, shown by western blot analysis (Figure 11 D). Quantification of the western blot bands confirmed an increased expression of L1ORF1p upon HCV infection, starting at 3 days post infection with significantly higher levels at 6 days post infection (Figure 11 E). In contrast to its mRNA levels, L1ORF1p protein levels remained elevated at 9 days post infection. L1ORF2p protein levels in HCV-infected cells also appeared to increase early post infection, but did not show a steady increase compared to L1ORF1p (Figure 11 D). However, high variances in the expression levels were observed in the individual experiments and due to technical issues and its low expression level compared to L1ORF1p, L1ORF2p was only detectable in three out of seven experiments.

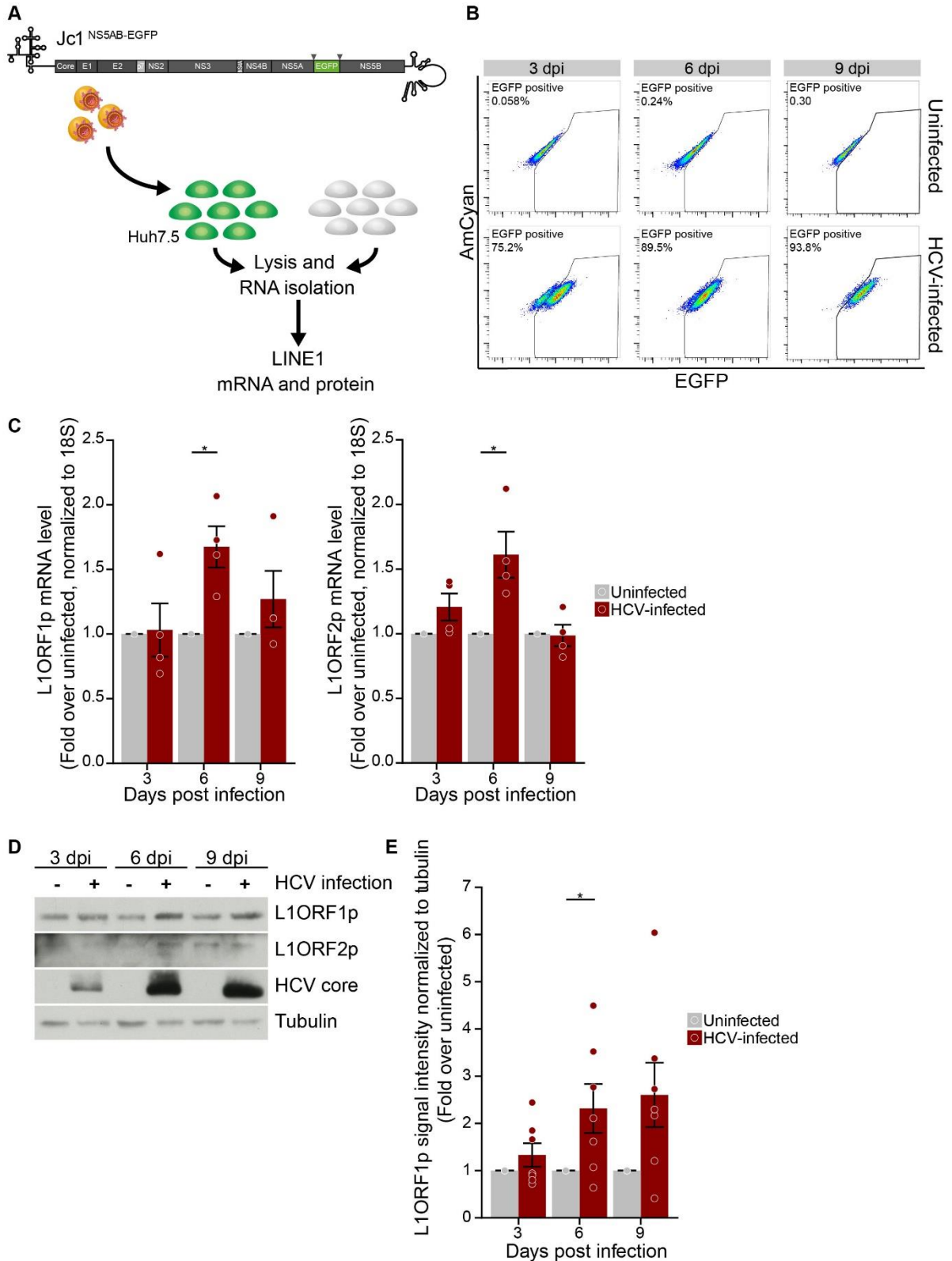


**Figure 11: LINE1 mRNA and protein levels increase in HCV-infected cells.**

(A) Huh7.5 cells were infected with Jc1<sup>NS5AB-EGFP</sup> (MOI = 0.2) and cells were lysed in NP-40 lysis buffer at 3, 6, and 9 days post infection (dpi). Total RNA was isolated from lysates and mRNA and protein

expression of L1ORF1p and L1ORF2p was compared to uninfected cells harvested at the same time. (B) Infection rates were determined by flow cytometry at the indicated time points. Shown is one representative experiment. (C) LINE1 mRNA expression was determined by qRT-PCR using specific primers in the L1ORF1p and L1ORF2p coding region. Shown is the fold induction of HCV-infected over uninfected cells normalized to *18S rRNA* at the indicated time points; dots represent values of the individual experiments (Mean  $\pm$  SEM,  $n = 4$ ;  $*p \leq 0.05$ ). (D) Representative western blot of L1ORF1p and L1ORF2p protein expression using specific antibodies. HCV infection was confirmed by detection of HCV core; tubulin served as loading control. (E) Densitometric quantification of L1ORF1p western blot bands. Shown is the signal intensity normalized to the signal intensity of tubulin as fold over uninfected cells; dots represent values of the individual experiments. Quantification was performed using the densitometric quantification function of Fiji (Mean  $\pm$  SEM,  $n = 7$ ;  $*p \leq 0.05$ ).

### 3.1.2 L1ORF1p is enriched in LD fractions of HCV-infected cells

To verify the enrichment of L1ORF1p in LD fractions of HCV-infected cells that was observed in the mass spectrometry analysis of the above-mentioned study (Rosch et al., 2016), LDs were isolated from uninfected and HCV-infected Huh7.5 cells and L1ORF1p levels were analyzed by western blotting (Figure 12 A). For HCV infection, EGFP-based reporter strains were used to assess the infection rate by flow cytometry (Figure 12 B). Cells were infected with Jc1<sup>NS5AB-EGFP</sup> and, in parallel to uninfected cells, seeded in 150 mm cell culture dishes at a density of  $5 \times 10^6$  cells 2 days prior to isolation. Cells were harvested at 9 days post infection and LDs were isolated *via* sucrose density centrifugation (Figure 12 C, “HCV-infected”). In a second approach, cells were infected with a Jc1 EGFP reporter strain that additionally encodes for a blasticidin resistance gene (Jc1<sup>NS5AB-EGFP-BSD</sup>). Selection for infected cells with 10  $\mu$ g/ml blasticidin was started 3 days post infection and cells were selected for a minimum of 21 days before LDs were isolated (Figure 2 B, C, “long-term HCV-infected”). Note that upon selection, the long-term HCV-infected cells lost the EGFP expression, presumably due to mutations, as they were still viable under selective pressure (Figure 12 B, right panel). Again, L1ORF1p levels were elevated in HCV-infected cells (Figure 2 C, input), confirming the time course experiment (3.1.1). L1ORF1p was detectable in LD fractions isolated at 9 or more than 21 days post infection, whereas no L1ORF1p was present at LDs from uninfected cells (Figure 12 B). LDs from long-term infected cells showed a stronger signal for L1ORF1p compared to the HCV-infected sample, but this might be due to a slight difference in protein amount loaded, as the loading control PLIN2 is also slightly stronger in the long-term infected sample.

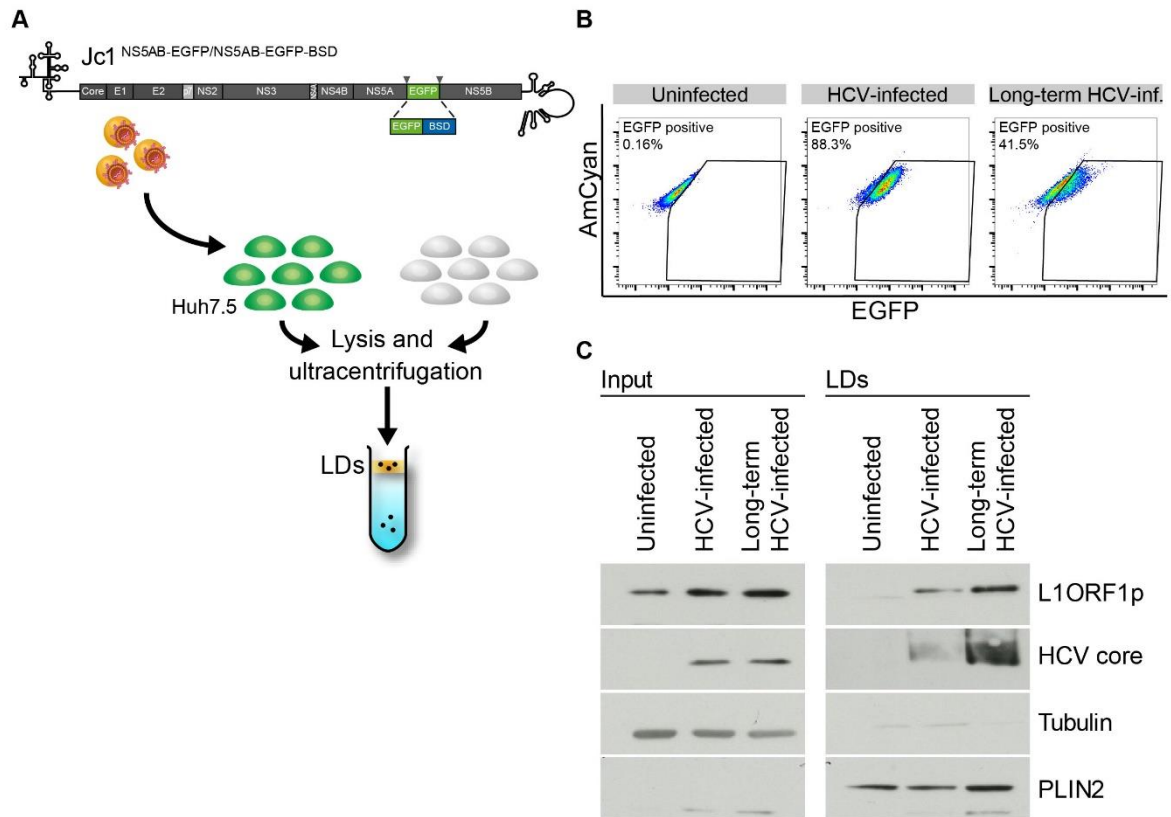


**Figure 12: HCV infection induces the recruitment of L1ORF1p to lipid-rich fractions.**

Western blot analysis of LDs isolated from HCV-infected and uninfected cells. (A) Experimental set-up. Huh7.5 cells were infected with Jc1<sup>NS5AB-EGFP</sup> (MOI = 0.02) for 9 days ("HCV-infected") or using a Jc1<sup>NS5AB-EGFP-BSD</sup> strain for selection of HCV-infected cells for more than 3 weeks ("long-term HCV-infected") prior to LD isolation by sucrose density centrifugation. (B) The rate of HCV-infected cells at the day of LD isolation was determined by flow cytometry. Shown is one representative analysis. (C) LD fractions were analyzed for L1ORF1p by western blotting. Detection of HCV core served as infection control. Equal loading of lysates (input) was verified by tubulin detection; enrichment and equal loading of LDs was verified by PLIN2 as marker protein. Shown is one representative experiment out of three for Jc1<sup>NS5AB-EGFP</sup> and two for Jc1<sup>NS5AB-EGFP-BSD</sup>.

### 3.1.3 L1ORF1p re-localizes to LDs in HCV-infected cells

In order to visualize the differing subcellular localization of L1ORF1p in HCV-infected and uninfected cells, immunofluorescence staining (IF) was performed and analyzed by confocal microscopy. For all IF staining experiments, Huh7 cells were used instead of Huh7.5 cells, as they display a superior flat morphology similar to Huh7-Lunet cells that is more suitable for microscopic analysis (Shavinskaya et al., 2007). Here, cells were either infected with Jc1<sup>wt</sup> or JFH1<sup>wt</sup>. The strains were chosen based on the different subcellular distribution pattern of the HCV capsid protein core: while the core protein of JFH1 mainly localizes to LDs forming ring-like structures, Jc1-infected cells secrete more virions and often harbour less core with a more punctate pattern at LDs (Shavinskaya et al., 2007). HCV-infected or uninfected cells were seeded onto cover slips placed in a 6 well plate at 6 days post infection at a density of  $8 \times 10^4$  cells/well and transfected with a plasmid encoding an HA-tagged L1ORF1p (HA-L1ORF1p) the following day. The overexpression approach was used as the immunofluorescence staining of endogenous L1ORF1p did not work well. Cells were fixed at 9 days post infection and 2 days post transfection, and stained with antibodies for HCV core and HA. BODIPY493/503 was used to visualize LDs and confocal microscopy was performed. In uninfected cells, HA-L1ORF1p was distributed throughout the cytoplasm with a partially punctuate staining pattern (Figure 13 A, left panel). In line with the enrichment of endogenous L1ORF1p in LD fractions from HCV-infected cells (see 3.1.2, Figure 12 C), HA-L1ORF1p was strongly re-localized to LDs in JFH1-infected cells (Figure 13 A, right panel). A comparable pattern was observed in Jc1-infected cells, although the phenotype was less strong (Figure 13 A, middle panel), possibly resulting from the different distribution pattern and different protein levels of Jc1 and JFH1 core. To quantify the colocalization of HA-L1ORF1p and LDs, the Pearson's correlation coefficient (PCC) and the Manders' colocalization coefficients (MCC) were calculated using the Coloc2 function of Fiji (Figure 13 B). Colocalization quantification according to the MCC calculates the fraction of fluorescence signal from each channel that overlaps with the signal from the second channel (Manders et al., 1993). Values range between 0 and 1; 0 reflects no overlap and values of 1 indicate a total overlap of the signal from one channel with the second channel. The PCC measures the correlation between the intensity values of two different fluorescence signals. A value of 1 represents a perfect linear correlation between two signal intensities, a value of -1 describes a perfectly linear, but inverse correlation between the two signals. Values around 0 represent non-correlating signal intensities (reviewed in Dunn et al., 2011). According to the MCC, a significantly higher proportion of the HA-L1ORF1p signal overlapped with the LD signal in JFH1-infected cells compared to uninfected cells (M1). Colocalization of HA-L1ORF1p and LDs in Jc1-infected cells was also increased but displayed a higher variance than JFH1. Analysis of the overlap of the LD signal with the HA-L1ORF1p signal resulted in much higher values for the MCC (M2). While colocalization of LDs with HA-L1ORF1p was again significantly higher in JFH1-infected cells, no difference was observed between Jc1-infected

and uninfected cells. Hence, JFH1-infected cells also showed a higher degree of colocalization of LDs and HA-L1ORF1p compared to Jc1-infected cells. Calculation of the PCC resulted in a negative mean value for uninfected cells, describing an inverse relation of the signal intensities for HA-L1ORF1p and LDs (no colocalization). In contrast, PCC mean values of the infected cells were significantly higher (Figure 13 B, right panel), indicating a partial colocalization of HA-L1ORF1p and LDs. In line with the MCC, the degree of colocalization was greater in JFH1-infected cells compared to cells infected with Jc1. Based on the observation that HA-L1ORF1p distribution resembled the pattern of the HCV core protein localized at LDs, colocalization analysis was also performed for HA-L1ORF1p and HCV core (Figure 13 C). No difference was observed between the overlap of HA-L1ORF1p and core of Jc1 and JFH1 (M1), whereas a significantly higher proportion of the JFH1-core fluorescence overlapped with HA-L1ORF1p compared to Jc1 (M2). Nevertheless, calculation of the PCC revealed a slight inverse relation of HCV core and HA-L1ORF1p signal intensities, indicating that both proteins only partially colocalize. Taken together, HCV infection initially increases L1ORF1p and L1ORF2p expression *in vitro* and induces re-localization of L1ORF1p to LDs.

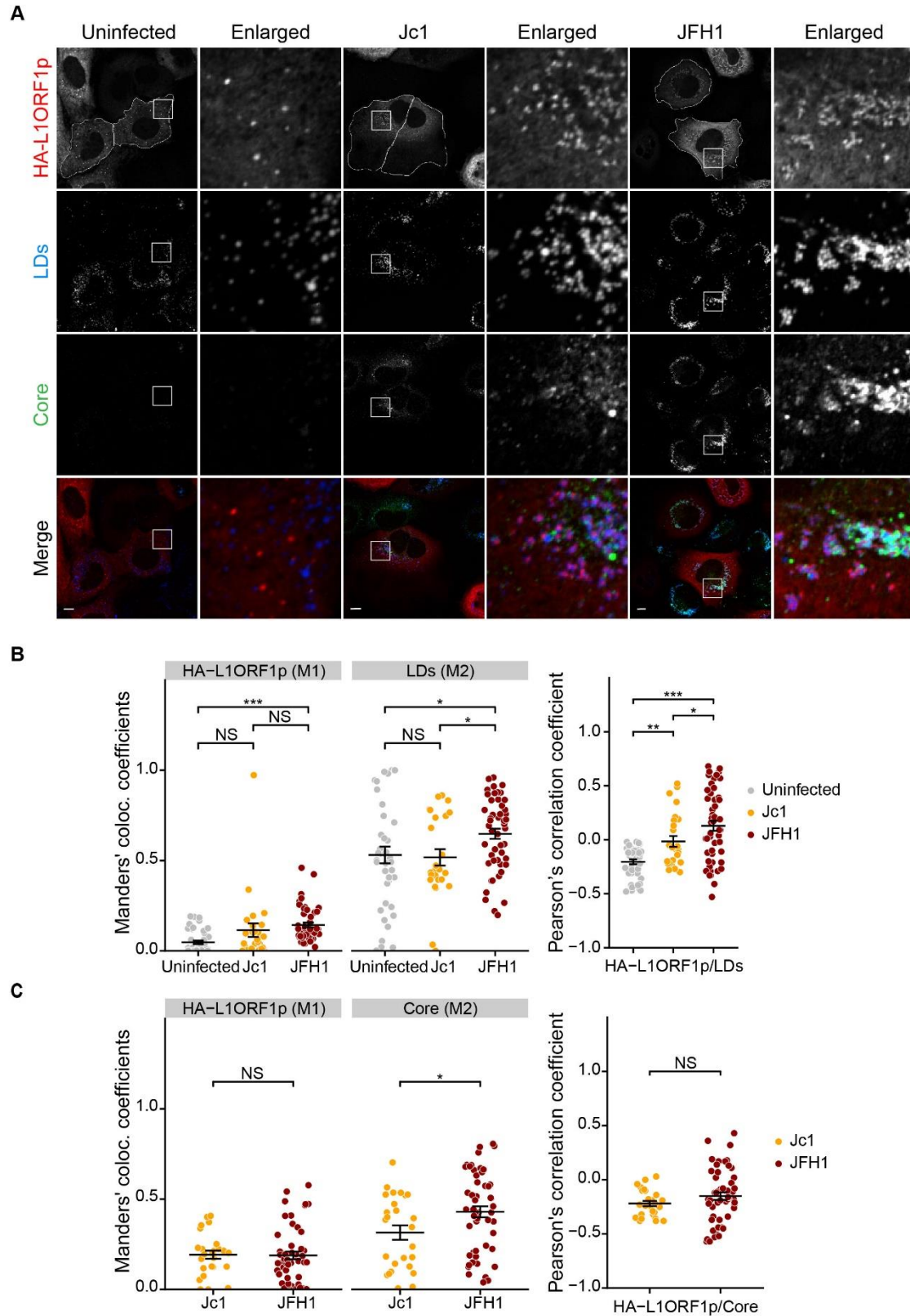


**Figure 13: Re-localization of L1ORF1p to LDs in HCV-infected cells.**

Confocal microscopy analysis of subcellular L1ORF1p localization in HCV-infected cells. (A) Huh7 cells were infected with Jc1<sup>wt</sup> (MOI = 0.03) or JFH1<sup>wt</sup> (MOI = 0.02), followed by transfection with an HA-tagged L1ORF1p (HA-L1ORF1p). Cells were fixed at 9 days post infection and 2 days post transfection and stained with antibodies against HA and HCV core. BODIPY493/503 was used to stain LDs. Uninfected cells were treated equally. The white square marks the enlarged area depicted on the

right of the respective image. Scale bars 10  $\mu$ m. (B) Colocalization of HA-L1ORF1p and LDs in cells from (A) was quantified by calculation of the Manders' colocalization coefficients and the Pearson's correlation coefficient using the Coloc2 function of Fiji. (C) Colocalization analysis of HA-L1ORF1p and HCV core was performed as described for (B). Cells from two independent experiments were analyzed (n = 42 (Control), 26 (Jc1), 52 (JFH1); NS = not significant; \* $p \leq 0.05$ ; \*\* $p \leq 0.01$ ; \*\*\* $p \leq 0.001$ ).

### 3.1.4 L1ORF1p recruitment to LDs is independent of HCV RNA replication

Active replication of the HCV RNA genome without formation of infectious particles is sufficient to induce changes in the host cell that are important for the viral life cycle such as the formation of the membranous web (Gosert et al., 2003). To this end, the recruitment of L1ORF1p to LDs was investigated in cells harboring the subgenomic replicon Con1 (SGR) (Choi et al., 2004). This bicistronic RNA expresses the non-structural proteins NS3-NS5B together with a neomycin resistance gene, but lacks the viral structural proteins, therefore active RNA replication occurs, but no infectious particles are produced. One day post electroporation with the SGR RNA, Huh7.5 cells were selected with 1 mg/ml G418 for 3 weeks prior to LD isolation (Figure 14 A).

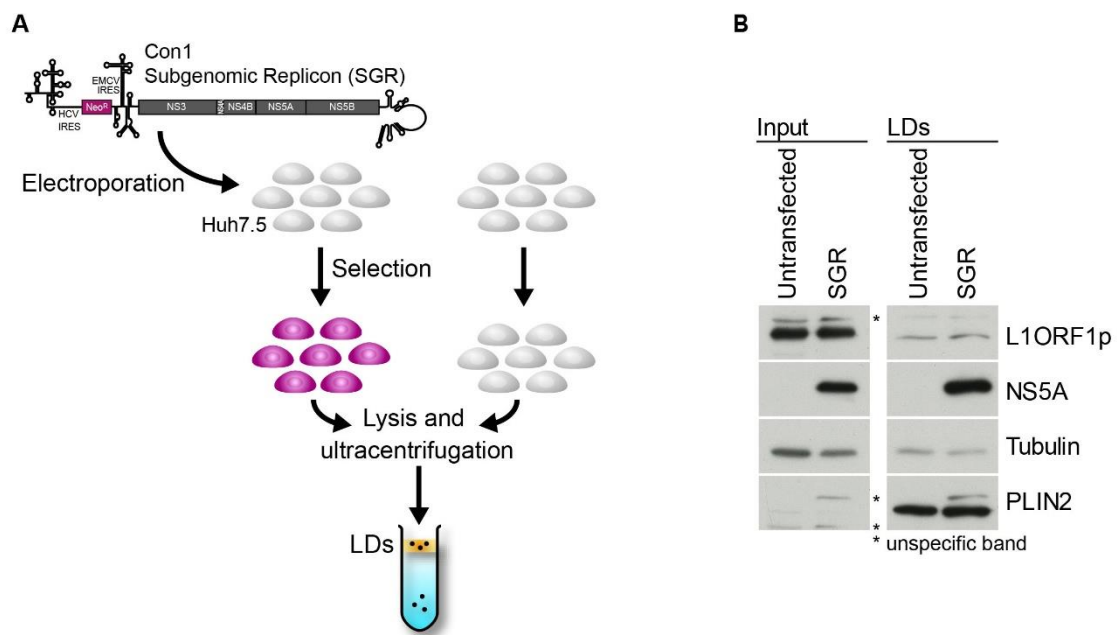


**Figure 14: HCV RNA replication does not induce L1ORF1p-enrichment at LDs.**

LD isolation from Huh7.5 cells harboring the Con1 SGR or untransfected cells. (A) Scheme of the experimental set up. Cells were electroporated with Con1 SGR RNA, selected with 1 mg/ml G418 for active RNA replication and LDs were isolated parallel to untransfected cells. (B) L1ORF1p presence in LD fractions was analyzed by western blotting. NS5A served as control for the SGR. Equal loading and enrichment of LDs was verified by PLIN2; tubulin served as loading control for the lysate (input). Asterisks mark unspecific bands. Shown is one representative western blot (n = 3).

L1ORF1p was barely detectable in western blot analysis of LD fractions isolated from SGR and untransfected control cells (Figure 14 B), indicating that the recruitment of L1ORF1p to LDs is independent of active HCV RNA replication. Further, this suggests that trafficking of



L1ORF1p to LDs is not linked to the localization of NS5A to the LD surface or to the expression of any of the other non-structural proteins encoded in the SGR.

### **3.1.5 HCV core induces the recruitment of L1ORF1p to LDs**

As L1ORF1p enrichment at LDs was independent of HCV RNA replication and in this context of expression of the viral non-structural proteins NS3-NS5B, it seemed likely that one of the structural proteins, namely the envelope proteins E1 and E2 or the capsid protein core, the non-structural proteins p7 or NS2, or intact particle assembly was responsible for the observed phenotype. For this reason, Huh7.5 cells were first electroporated with *in vitro* transcribed RNA of a replicon strain that encodes all viral proteins, but lacks part of E1 and E2, thereby abolishing HCV particle production (Jc1ΔE1E2<sup>NS5AB-EGFP</sup>) (Figure 15 A). Cells were seeded in 150 mm dishes directly after transfection with  $8 \times 10^6$  cells/dish and LDs were isolated 3 days post electroporation. Here, L1ORF1p was solely detectable in LD fractions from replicon cells and not in the untransfected control, indicating that the presence of HCV core, p7 or NS2, and not HCV particle assembly, is linked to the recruitment of L1ORF1p to LDs (Figure 15 B). Besides NS5A, HCV core also localizes to the surface of LDs when expressed individually (Camus et al., 2013). To investigate if the expression of HCV core alone can induce re-localization of L1ORF1p to LDs, an overexpression of HCV core of two different genotypes (gt) was introduced to Huh7.5 cells using lentiviral particles (FLAG-core of gt2a or untagged HCV core of gt1b); control cells were transduced with a corresponding empty vector. Transduced cells were seeded in 150 mm cell culture dishes at a density of  $5 \times 10^6$  cells 3 days prior to isolation and LDs were isolated at 5 days post transduction. Western blot analysis confirmed an enrichment of L1ORF1p in LD fractions from HCV core-overexpressing cells independent of the HCV genotype, whereas less or no L1ORF1p was detectable in fractions of the empty vector (Figure 15 C, D). In line with the results from the SGR-harboring cells (3.1.4), overexpression of NS5A-FLAG (gt2a) did not induce recruitment of L1ORF1p to LDs (Figure 15 C).

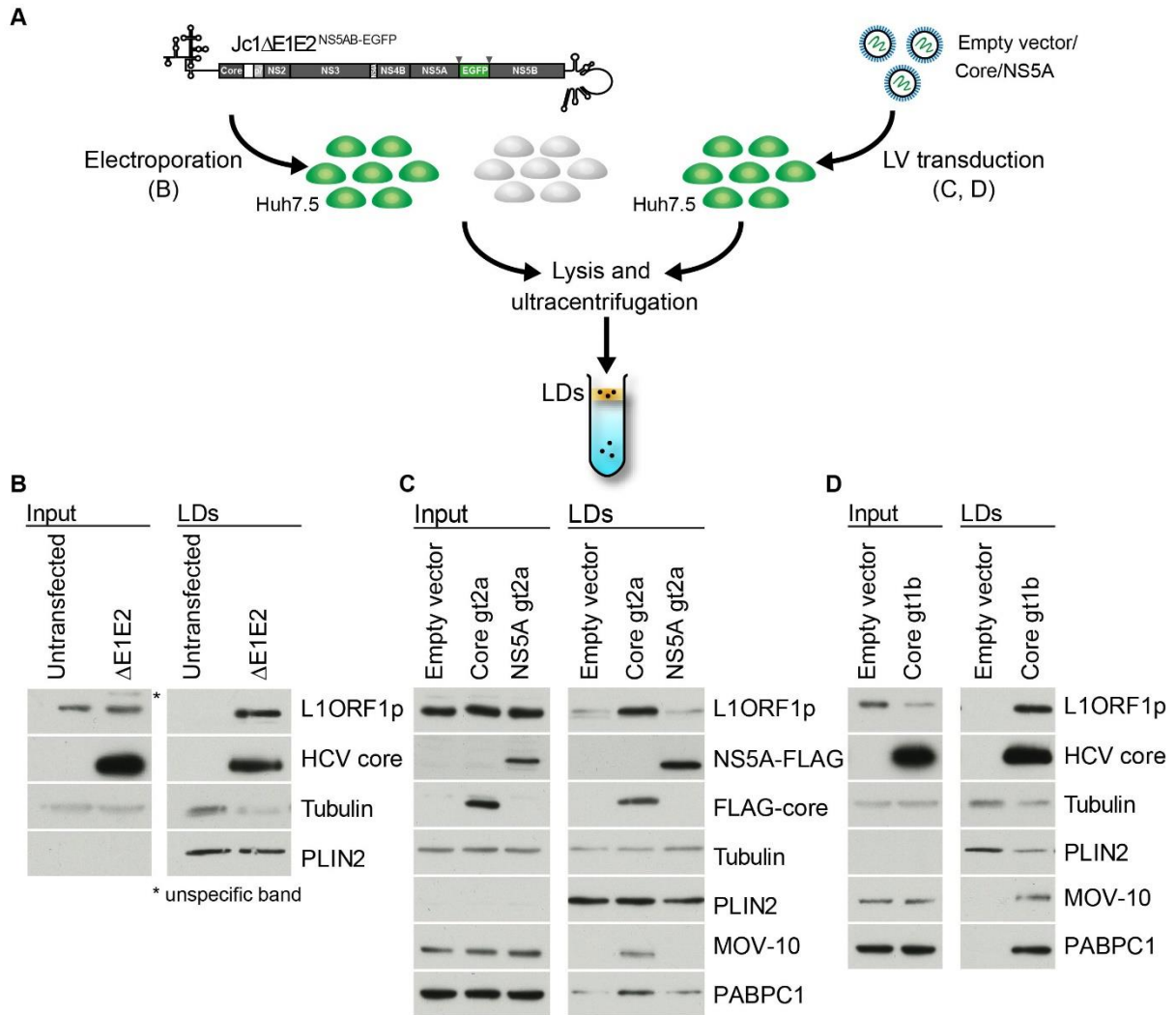


**Figure 15: HCV core re-localizes L1ORF1p to LDs.**

(A) Scheme of the experimental set up. Huh7.5 cells were electroporated with Jc1ΔE1E2<sup>NS5AB-EGFP</sup> RNA or HCV core or NS5A overexpression was introduced by lentiviral transduction before LDs were isolated. (B) LD fractions from Jc1ΔE1E2<sup>NS5AB-EGFP</sup>-harboring and untransfected cells were analyzed for the presence of L1ORF1p by western blotting (n = 1). Asterisks mark unspecific bands. Successful transfection was verified by detection of the HCV core protein. (C, D) Western blot analysis of L1ORF1p in LD fractions isolated from cells overexpressing either FLAG-core or NS5A-FLAG of the HCV gt2a (C) or core from the gt1b (D). Transduction with an empty vector served as control. Expression of the FLAG-tagged viral proteins was confirmed using a FLAG-specific antibody, HCV core from gt1b was detected using a core-specific antibody. Shown is one representative western blot (n = 3 for FLAG-core; n = 1 for NS5A-FLAG; n = 3 for HCV core gt1b). For two out of three experiments, membranes were also probed with specific antibodies for the L1ORF1p-interacting proteins PABPC1 and MOV-10. Equal loading and enrichment of LDs was verified by PLIN2 detection; tubulin served as loading control for the lysate (input).

Next, the re-localization of L1ORF1p to LDs in HCV core-overexpressing cells was analyzed by microscopy. Here, Huh7 cells were co-transfected with equal amounts of the HA-L1ORF1p expression plasmid and a plasmid for HCV core expression (JFH1 core, gt2a), fixed 2 days post transfection and stained with antibodies for HCV core and HA. LDs were visualized with BODIPY493/503 and cells were analyzed by confocal microscopy. As a control, cells were transfected with the HA-L1ORF1p plasmid only. Without HCV core present, the same cytoplasmic distribution pattern as in the uninfected cells was observed (Figure 16 A, left panel; see 3.1.3, Figure 13 A for comparison). In contrast, HA-L1ORF1p was mainly localized at LDs in HCV core-overexpressing cells, sometimes forming ring-like structures surrounding the droplets (Figure 16 A, right panel). Quantification of the colocalization using MCC revealed a significantly higher overlap for HA-L1ORF1p and LD signal intensities in cells expressing the HCV core protein compared to HA-L1ORF1p expression only (Figure 16 B). The same result was observed for the PCC, confirming that HA-L1ORF1p is recruited to LDs in HCV core-overexpressing cells. In line with the colocalization analysis of the HCV-infected cells, the proportion of HCV core overlapping with the signal for HA-L1ORF1p (M2) was higher than the overlap of the HA-L1ORF1p with the HCV core signal intensity (M1), likely because the HA-L1ORF1p signal is also still detectable throughout the cytoplasm (Figure 16 C). The PCC was slightly increased compared to the infected cells, but still the mean value was around 0, indicating that HCV core and HA-L1ORF1p are both present at LDs but only show a partial colocalization. Taken together, these data suggest that re-localization of L1ORF1p to LDs is facilitated by HCV core and that this phenotype is independent of the expression of other viral proteins, HCV RNA replication, or formation of viral particles.

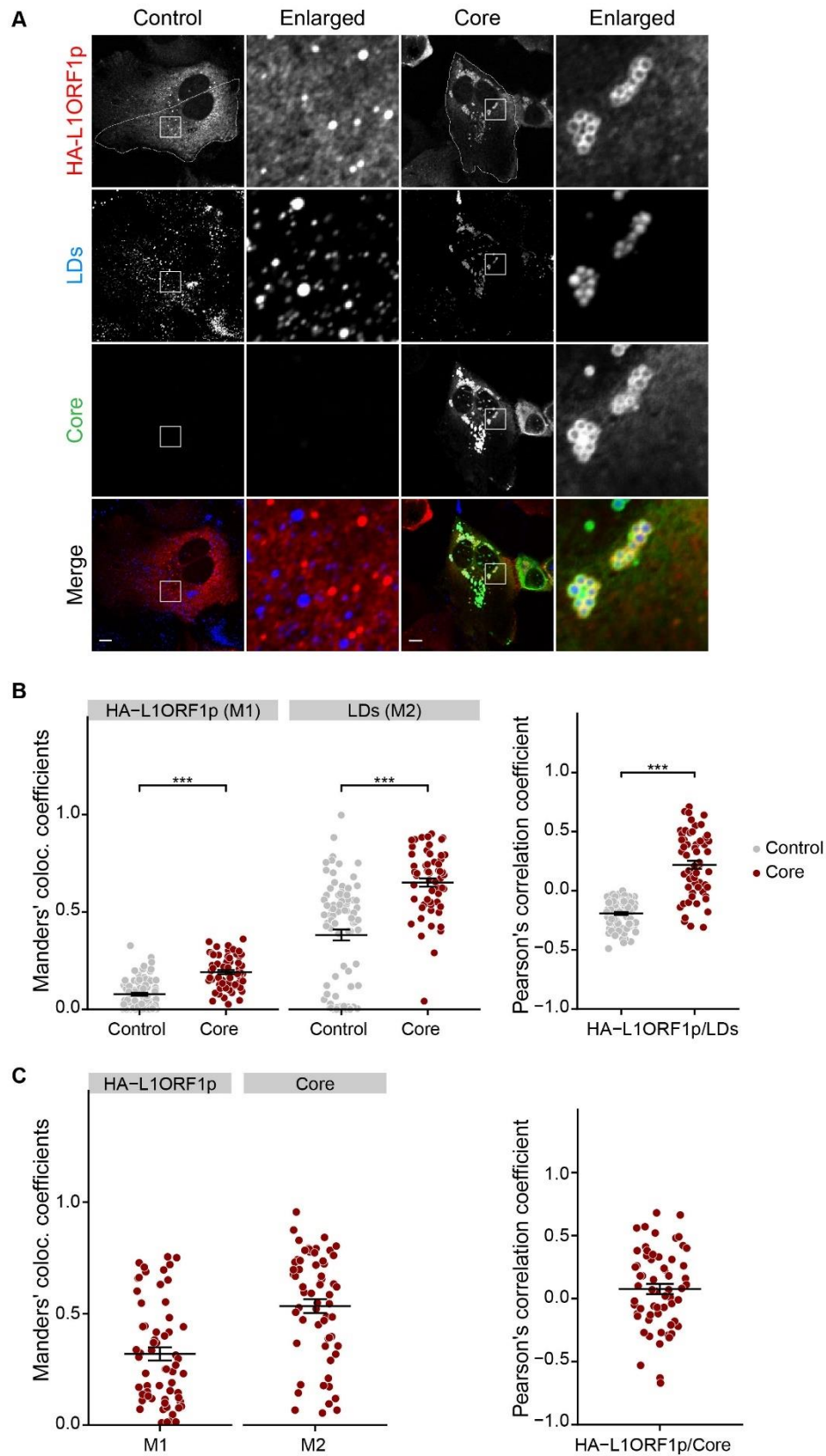


**Figure 16: Expression of HCV core is sufficient to re-localize L1ORF1p to LDs.**

Immunofluorescence microscopy of cells overexpressing HCV core and HA-L1ORF1p. (A) Huh7 cells were co-transfected with an HCV core and an HA-L1ORF1p overexpression plasmid and compared to

cells expressing HA-L1ORF1p only. Cells were fixed 2 days post transfection and stained with antibodies against HCV core and HA. BODIPY493/503 was used to stain LDs and cells were analyzed by confocal microscopy. The white square marks the enlarged area depicted on the right of the respective image. Scale bars 10  $\mu$ m. (B) Quantification of the colocalization of HA-L1ORF1p and LDs in cells from (A) by calculation of the Manders' colocalization coefficients and the Pearson's correlation coefficient. (C) Quantification of the colocalization of HA-L1ORF1p and HCV core in cells from (A) by calculation of the Manders' colocalization coefficients and the Pearson's correlation coefficient. Cells from three independent experiments were analyzed and quantification was performed using the Coloc2 function of Fiji (n = 91 (Control), 61 (Core); \*\*\* $p \leq 0.001$ ).

### **3.1.5.1 HCV core expression enriches the L1ORF1p interacting proteins PABPC1 and MOV-10 in LD fractions**

In 2013, a proteomic study was conducted mapping interaction partners of L1ORF1p (Goodier et al., 2013). As it is likely that some of these interactors are recruited to LDs upon HCV infection as well, the identified L1ORF1p interactors were compared to proteins that were found enriched or depleted in LD fractions of HCV-infected cells compared to uninfected cells (Rosch et al., 2016) (Figure 17). In total, 25 proteins were commonly identified in both screens, mostly involved in RNA binding or regulation. As the polyadenylate-binding protein 1 (PABPC1) has already been described to re-localize to LDs in JFH1-infected cells (Ariumi et al., 2011a) and its interactor L1ORF1p is recruited to LDs by HCV core, it is likely that PABPC1 also traffics to LDs in an HCV core-dependent manner. Therefore, LD fractions from HCV core-overexpressing cells (see 3.1.5) were also analyzed by western blotting for the presence of PABPC1. Indeed, PABPC1 was enriched in LD fractions when HCV core was expressed, again independent of the genotype that was used (Figure 15 C and D). Concordant with the phenotype for L1ORF1p, overexpression of NS5A did not result in re-localization of PABPC1 to LDs (Figure 15 C). The same phenotype was observed for the putative helicase MOV-10, a described inhibitor of LINE1 retrotransposition and part of the LINE1 RNP (Goodier et al., 2012). This observation suggests that HCV core does not only recruit L1ORF1p alone, but rather a group of proteins with RNA-binding affinity to LDs.

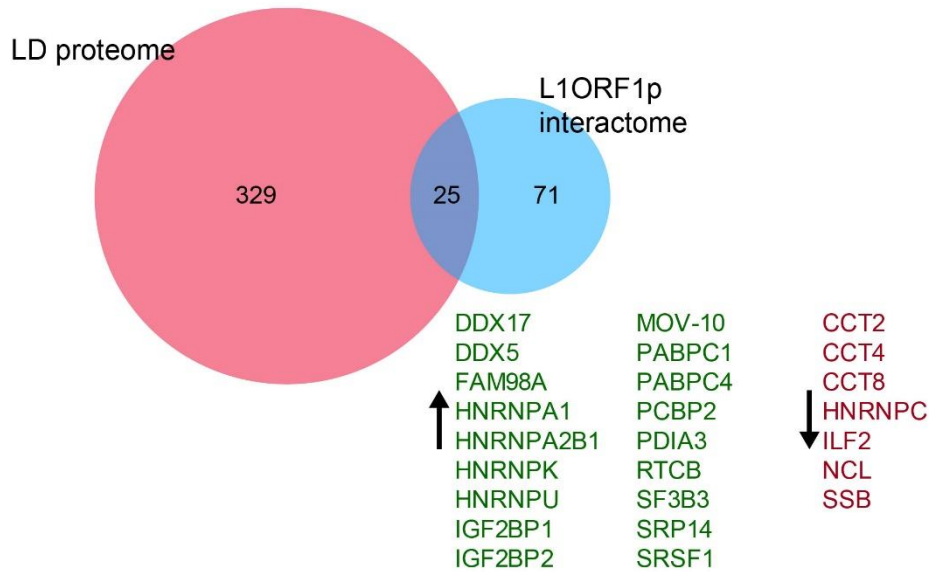


**Figure 17: Comparison of LD-associated proteins and L1ORF1p interactors.**

Venn Diagram of proteins identified in LD fractions of HCV-infected and uninfected Huh7.5 cells (Rosch et al., 2016) and the L1ORF1p interactome (Goodier et al., 2013). Of the 25 overlapping proteins, 18 were found enriched at LDs in HCV-infected cells (represented in green) and 7 were found to be decreased (represented in red).

### 3.2 L1ORF1p interacts with HCV core and the viral genome

#### 3.2.1 HCV core interacts with L1ORF1p in an RNA-dependent manner

Given the distinct role of HCV core in the re-localization of L1ORF1p, co-immunoprecipitation experiments were performed to investigate a direct interaction between the two proteins. First, Huh7.5 cells infected with Jc1<sup>NS5AB-EGFP</sup> or uninfected cells were seeded in 100 mm cell culture dishes and transfected with the HA-L1ORF1p expression plasmid the following day. Cells were lysed at 2 days post transfection and 9 days post infection and lysates were subjected to HA-specific immunoprecipitation followed by western blot analysis. Notably, HCV core and L1ORF1p both display RNA-binding capacities (Hohjoh and Singer, 1996; Khazina et al., 2011; Santolini et al., 1994; Shimoike et al., 1999), therefore a putative RNA-based interaction was addressed by incubating the lysates with or without RNase A prior to co-immunoprecipitation. HCV core was detected in the HA-L1ORF1p-precipitated samples from HCV-infected cells and, to a lesser extent also in the RNase A-treated sample from the same lysate, indicating an interaction of HA-L1ORF1p and HCV core that is RNA-dependent (Figure 18 B). As described before, PABPC1 and MOV-10 showed an RNA-based interaction with HA-L1ORF1p (Goodier et al., 2013) that was not affected by HCV infection (Figure 18 B). RNase A digestion was confirmed by agarose gel electrophoresis (Figure 18 C).

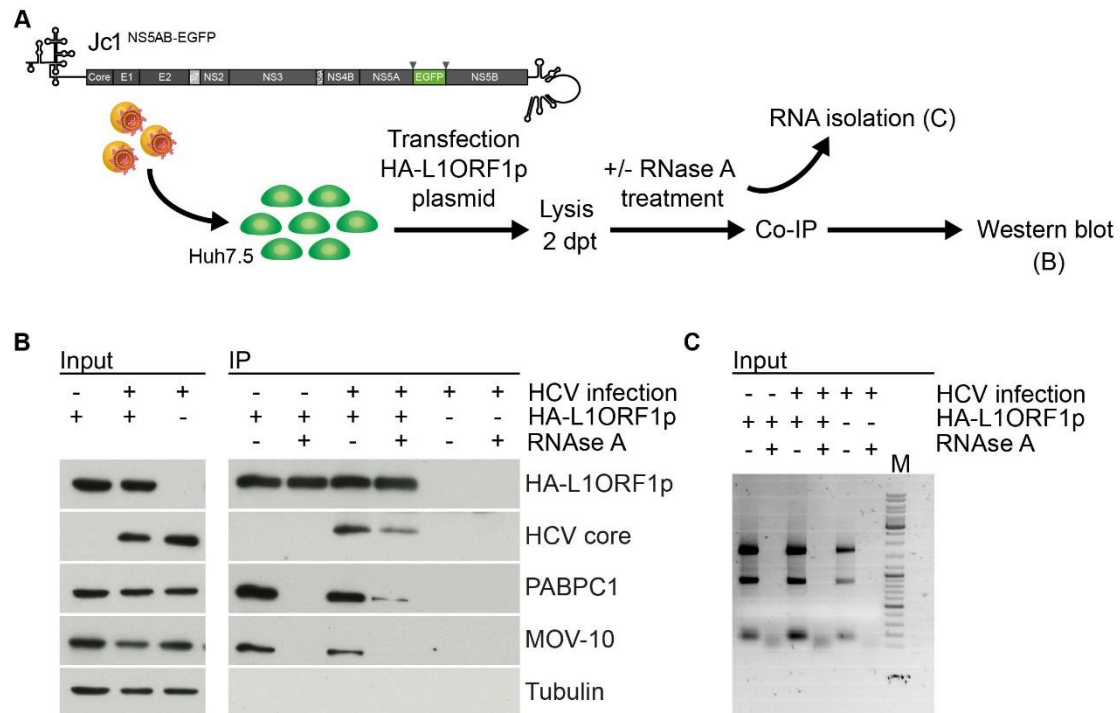


**Figure 18: RNA-dependent interaction between HA-L1ORF1p and HCV core.**

Co-immunoprecipitation of HA-L1ORF1p and HCV core from HCV-infected cells. (A) Scheme of the experimental set up. Huh7.5 cells infected with Jc1<sup>NS5AB-EGFP</sup> (MOI = 0.2) and uninfected cells were transfected with the HA-L1ORF1p expression plasmid and lysed in NP-40 lysis buffer at 9 days post infection and 2 days post transfection. Infected cells lacking HA-L1ORF1p expression served as background control. Two samples of each lysate were prepared: one was treated with RNase A and one was treated with an RNase inhibitor (RNaseOUT). After treatment, a portion of each lysate was removed for RNA isolation before HA-specific immunoprecipitation was performed. (B) Western blot analysis of HCV core, PABPC1, and MOV-10 in lysates (input) and co-immunoprecipitated samples (IP). Expression and precipitation of HA-L1ORF1p was detected using an HA-specific antibody. Tubulin served as loading control. Shown is one representative western blot (n = 2–3). (C) Agarose gel electrophoresis of RNA isolated from lysates to confirm successful RNase A treatment. Samples were analyzed on a 1% agarose gel, nucleic acids were stained with ethidium bromide and visualized by UV light. M = GeneRuler DNA Ladder Mix.

To confirm the interaction between endogenous L1ORF1p and HCV core, Huh7.5 cells were transduced with lentivirus particles for the overexpression of a FLAG-tagged HCV core protein (gt2a or gt1b), FLAG-tagged NS5A (gt2a) or an empty vector as control. Three days post transduction, cells were lysed, incubated with or without RNase A and subjected to FLAG-specific immunoprecipitation. Western blot analysis verified an RNA-dependent interaction of L1ORF1p and HCV core independent of the genotype (Figure 19 B and C) and no interaction between L1ORF1p and NS5A-FLAG (Figure 19 B). Moreover, PABPC1 and MOV-10 were found to co-precipitate with the gt2a HCV core protein (Figure 19 B). Due to high background of the MOV-10 antibody, only PABPC1 was detected in co-precipitated samples from the gt1b HCV core protein (Figure 19 C). These results indicate that L1ORF1p interacts with HCV core and that this interaction is partly facilitated by the concomitant



binding of cellular RNAs. The presence of PABPC1 and MOV-10 suggests that HCV core is part of a larger protein-RNA complex.

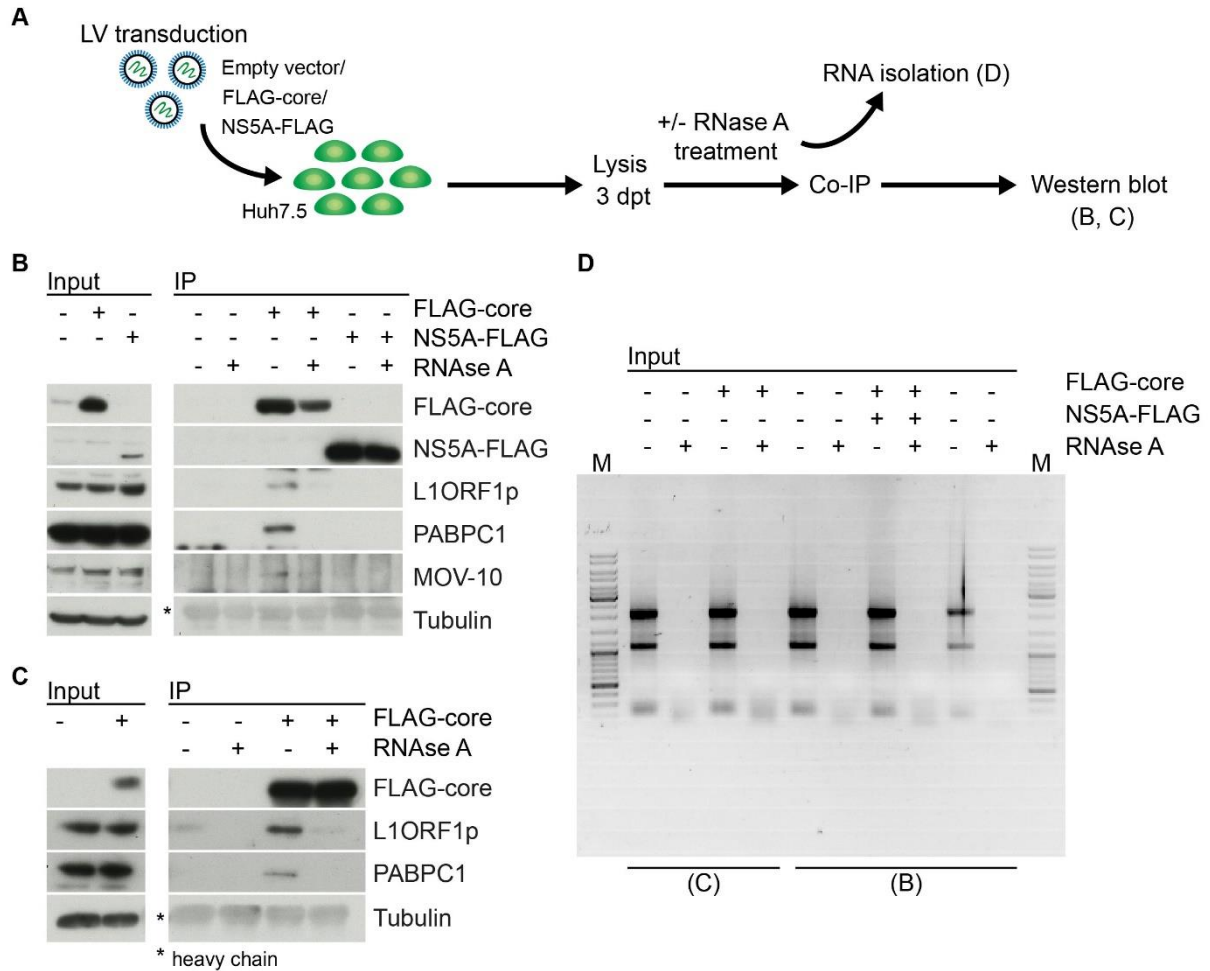


**Figure 19: Endogenous L1ORF1p interacts with HCV core but not NS5A.**

Co-immunoprecipitation of FLAG-tagged HCV proteins and endogenous L1ORF1p. (A) Scheme of the experimental set up. Overexpression of FLAG-tagged HCV core (gt1b or 2a) and NS5A (gt2a) in Huh7.5 cells was achieved by lentiviral transduction; an empty vector was used as control. Three days post transduction, cells were lysed in NP-40 lysis buffer. Two samples of each lysate were prepared: one was treated with RNase A and one was incubated with an RNase inhibitor (RNaseOUT). After treatment, a portion of each lysate was taken for RNA isolation, before FLAG-specific immunoprecipitation was performed. (B) The presence of L1ORF1p, PABPC1, and MOV-10 in lysates (input) and co-immunoprecipitated samples (IP) of cells expressing gt2a FLAG-core or NS5A-FLAG was analyzed by western blotting using specific antibodies. Expression and precipitation of FLAG-tagged viral proteins was detected using a FLAG-specific antibody. Tubulin served as loading control. Shown is one representative western blot (n = 3; n = 1 for PABPC1 and MOV10). (C) Lysates (input) and co-immunoprecipitated samples (IP) of cells expressing gt1b FLAG-core were analyzed by western blotting as described for (B) (n = 2; n = 1 for PABPC1). Asterisk marks the antibody heavy chain. (D) Successful RNase A treatment was confirmed by agarose gel electrophoresis. Samples were analyzed on a 1% agarose gel, nucleic acids were stained with ethidium bromide and visualized by UV light. M = GeneRuler DNA Ladder Mix.



### 3.2.2 RNA-binding capacity of L1ORF1p is important for its re-localization to LDs

Even though the interaction of HCV core and L1ORF1p is RNA-dependent, this interaction is not necessarily a requirement for the recruitment of L1ORF1p to LDs. To address if RNA binding of L1ORF1p is crucial for its re-localization in presence of HCV core, the localization of a L1ORF1p mutant (RR261-262AA) with decreased RNA-binding ability (Khazina and Weichenrieder, 2009; Kulpa and Moran, 2005) in HCV core-overexpressing cells was analyzed (Figure 20). HA-L1ORF1p wt or the 261-262AA mutant was overexpressed in Huh7.5 cells using lentiviral vectors. Three days post transduction, the cells were additionally inoculated with lentivirus for the overexpression of HCV core protein. The double-transduced cells were seeded in 150 mm cell culture dishes at a density of approx.  $5 \times 10^6$  cells 3 days prior to harvest. LDs were isolated at 8 and 5 days post transduction and LD fractions were analyzed by western blotting (Figure 20 B). Compared to the wildtype protein, the mutant was less enriched in LD fractions, indicating that the re-localization of L1ORF1p by HCV core is at least in part dependent on a functional RNA-binding ability of the protein.

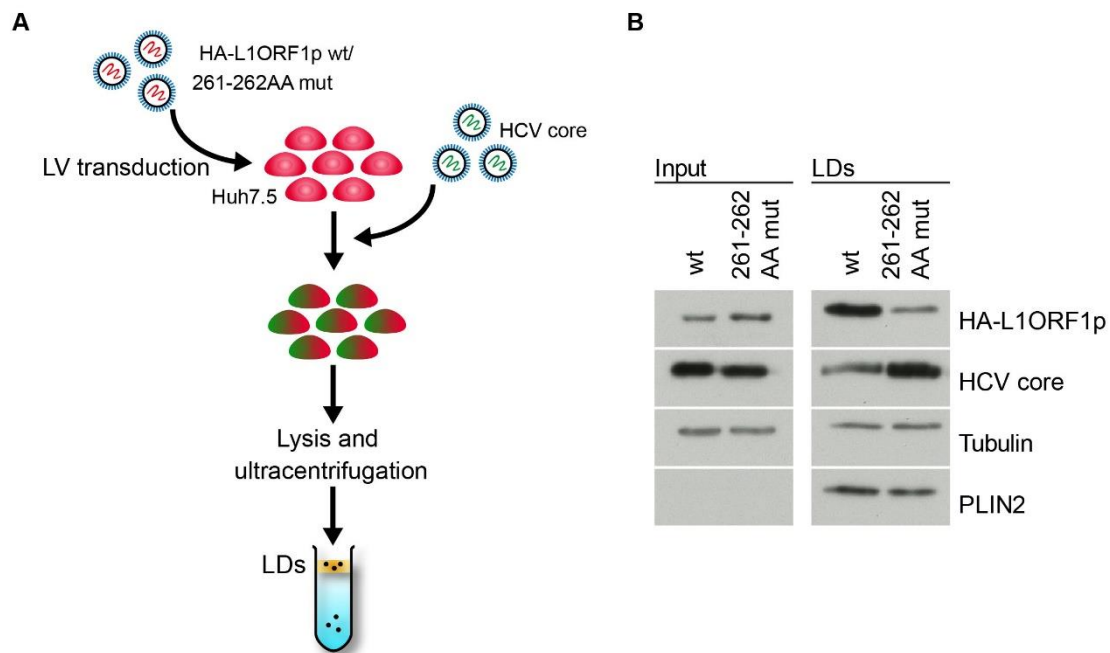


**Figure 20: Re-localization of L1ORF1p to LDs is partially dependent on its RNA-binding capacity.**

Comparison of the localization of HA-L1ORF1p wildtype and its RNA-binding mutant to LDs. (A) Scheme of the experimental set up. Three days post transduction with lentiviral particles encoding HA-L1ORF1p (wt) or a putative RNA-binding mutant (261-262AA mut), Huh7.5 cells were additionally transduced with lentiviral particles for the expression of HCV core (gt1b). LDs were isolated 5 days after HCV core expression was introduced. (B) Western blot analysis of LD fractions. Membranes were probed with antibodies for HA and HCV core to determine expression and localization of the proteins. Equal loading was verified by tubulin for the lysate (input) and PLIN2 as a marker for the LD fraction. Shown is one representative experiment (n = 2).

### 3.2.3 HCV RNA co-precipitates with L1ORF1p

It is known that L1ORF1p preferably binds to its encoding mRNA in *cis*; nevertheless, binding to other cellular mRNAs in *trans* has been reported (Goodier et al., 2013; Kulpa and Moran, 2006; Wei et al., 2001). To analyze if L1ORF1p binds the HCV genome, Jc1<sup>NS5AB-EGFP</sup>-infected Huh7.5 cells were transfected with the HA-L1ORF1p expression plasmid, lysed 2 days post transfection and samples were subjected to HA-specific immunoprecipitation that was confirmed by western blotting (Figure 21 A). Subsequently, 1/2 to 2/3 of the beads were resuspended in Trizol, total RNA was isolated and reversely transcribed into cDNA. Of note, as only a small proportion of the precipitated sample was taken for western blot analysis, the HCV core protein was not detectable in the IP (Figure 21 A compared to Figure 18 B).

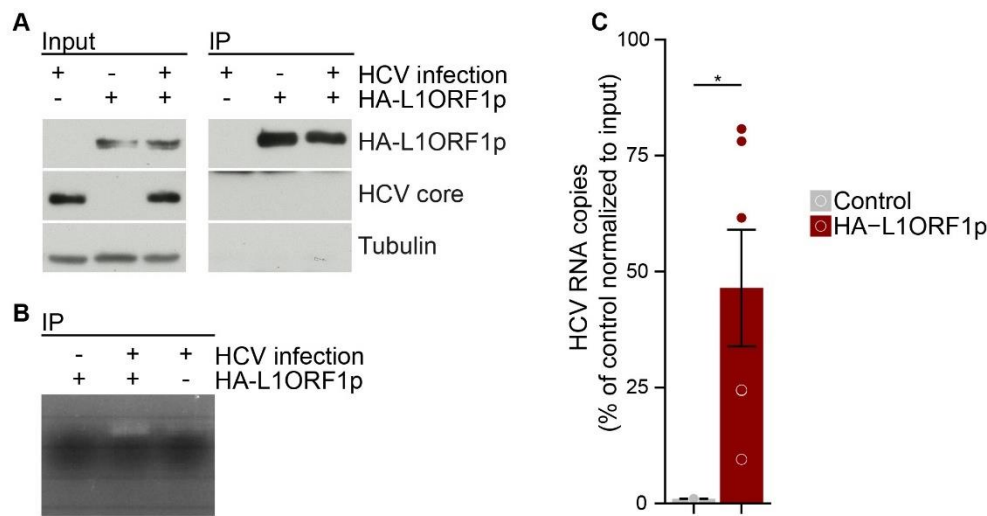


**Figure 21: HCV RNA is enriched in co-IP fractions of HA-L1ORF1p.**

Detection of the HCV genome in HA-L1ORF1p-precipitated samples. Huh7.5 cells infected with Jc1<sup>NS5AB-EGFP</sup> and uninfected cells were transfected with the HA-L1ORF1p overexpression plasmid and lysed in NP-40 lysis buffer 2 days post transfection. Lysates were subjected to HA-specific immunoprecipitation. Infected cells without HA-L1ORF1p expression served as background control. (A) Expression and co-immunoprecipitation of HA-L1ORF1p was confirmed by western blotting. Detection of HCV core served as infection control. Equal loading was verified by tubulin detection. Shown is one representative western blot. (B) RNA was isolated from equal amounts of the bead precipitate of each sample after co-immunoprecipitation and reversely transcribed into cDNA. HCV cDNA was amplified using an HCV-specific primer pair, and PCR products were analyzed on a 2% agarose gel, stained with ethidium bromide and visualized by UV-light. Shown is one representative experiment (n = 3). (C) HCV RNA copies were measured by qRT-PCR and RNA copy numbers were calculated. Shown are the copy numbers per immunoprecipitation (IP) as percent of the background control normalized to the HCV copy number in the input (Mean  $\pm$  SEM, n = 6; \* $p$   $\leq$  0.05).

PCR analysis of the cDNA revealed an enrichment of HCV RNA in HA-L1ORF1p-precipitated samples (Figure 21 B). Additionally, RNA was isolated from the lysates (input) and HCV RNA copy numbers were determined by qRT-PCR (Figure 21 C). HCV RNA copies were significantly enriched in HA-L1ORF1p-precipitated samples compared to the untransfected Jc1<sup>NS5AB-EGFP</sup> background control, indicating that the viral genome is either bound by

L1ORF1p itself or is part of an RNA-protein-complex that is co-precipitated with either HCV core or L1ORF1p (see 3.2.1).

### 3.3 HCV RNA as template for L1ORF2p-reverse transcriptase activity

As the HCV genome was significantly enriched in co-immunoprecipitation samples of HA-L1ORF1p, an incorporation of the viral RNA into the LINE1 RNP is presumably possible. To this end, Huh7 cells were transfected with plasmids encoding a retrotransposition competent LINE1 (pDK101) or an L1ORF2p reverse transcriptase mutant (pDK135; RT-, D702A) (Kulpa and Moran, 2005). Selection with 200 µg/ml hygromycin was started 3 days post transfection and carried out for 4–6 days. Six days post selection, either HCV-infected or uninfected Huh7 cells were added to the transfected cells and cultured without selective pressure for 3–4 days to allow HCV infection. The selected cells grew in dense foci and in an initial experiment, infection with cell-free virus stock was not successful. However, HCV infection by cell-to-cell transmission is much more efficient than infection with cell-free virus (Timpe et al., 2008); therefore, the addition of infected cells was used to infect the selected cells *via* transmission from cells harboring an already established HCV infection. Re-selection for transfected cells was applied for a minimum of 5 days before cells were lysed and LINE1 RNPs were isolated by ultracentrifugation using a sucrose cushion (Kulpa and Moran, 2006). Uninfected and HCV-infected cells lacking LINE1 overexpression were used as negative control. Expression of LINE1 was confirmed by western blotting, using a T7 specific antibody that recognizes the T7-tagged L1ORF1p (Figure 22 B). Detection of HCV core confirmed infection of the transfected cells, however, the signal was barely detectable indicating a lower infection of the transfected cells compared to the untransfected control. To verify the presence of LINE1 mRNA and HCV RNA in the isolated RNPs, RNA was isolated from equal protein amounts of RNP fractions followed by reverse transcription into cDNA using SuperScript III reverse transcriptase. For reverse transcription of LINE1 mRNA and the HCV - strand, a polyT-rich primer was used, binding to the polyA tail of LINE1 or a polyA-rich region in the 5' UTR of the HCV replication intermediate. For the HCV + strand, a polyA-rich primer was used, binding to a polyU-stretch in the 3' UTR of the viral genome. Both RT-primer contained a linker sequence, allowing PCR amplification *via* the linker and a target-specific sense primer. PCR products were analyzed by agarose gel electrophoresis. In the LINE1-overexpressing cells, a distinct band was detectable for the LINE1-specific PCR that was absent in the untransfected control (Figure 22 C). No clear PCR amplificate was detectable for the HCV - strand; for the + strand genome, a distinct band was present in all HCV-infected samples (Figure 22 D). Concordant with the detection of the HCV core protein (Figure 22 B), the HCV genome was also detectable in the untransfected control sample of the isolated RNPs, indicating that those viral components are not exclusively enriched in RNPs isolated from LINE1-overexpressing cells. Based on this result, no distinct conclusion about the incorporation of the viral genome to LINE1 RNPs generated from the overexpressed LINE1 was possible.

The detection of HCV core and the viral genome in RNP isolations from untransfected cells might result from an incorporation in LINE1 RNPs formed by the endogenously expressed L1ORF1p and L1ORF2p which are not detected by the T7 antibody used for western blot analysis. Compared to the untransfected control cells, less HCV core and HCV + strand RNA was detected in LINE1-overexpressing cells (Figure 22 B, D). Of note, LINE1-overexpressing cells divided less and showed signs of stress, either from constant hygromycin selection or from LINE1 overexpression. This might lead to lower infection rates, explaining the lower levels of HCV core and HCV RNA. On the other hand, the overexpression of LINE1 could directly affect the HCV life cycle, inhibiting HCV replication.

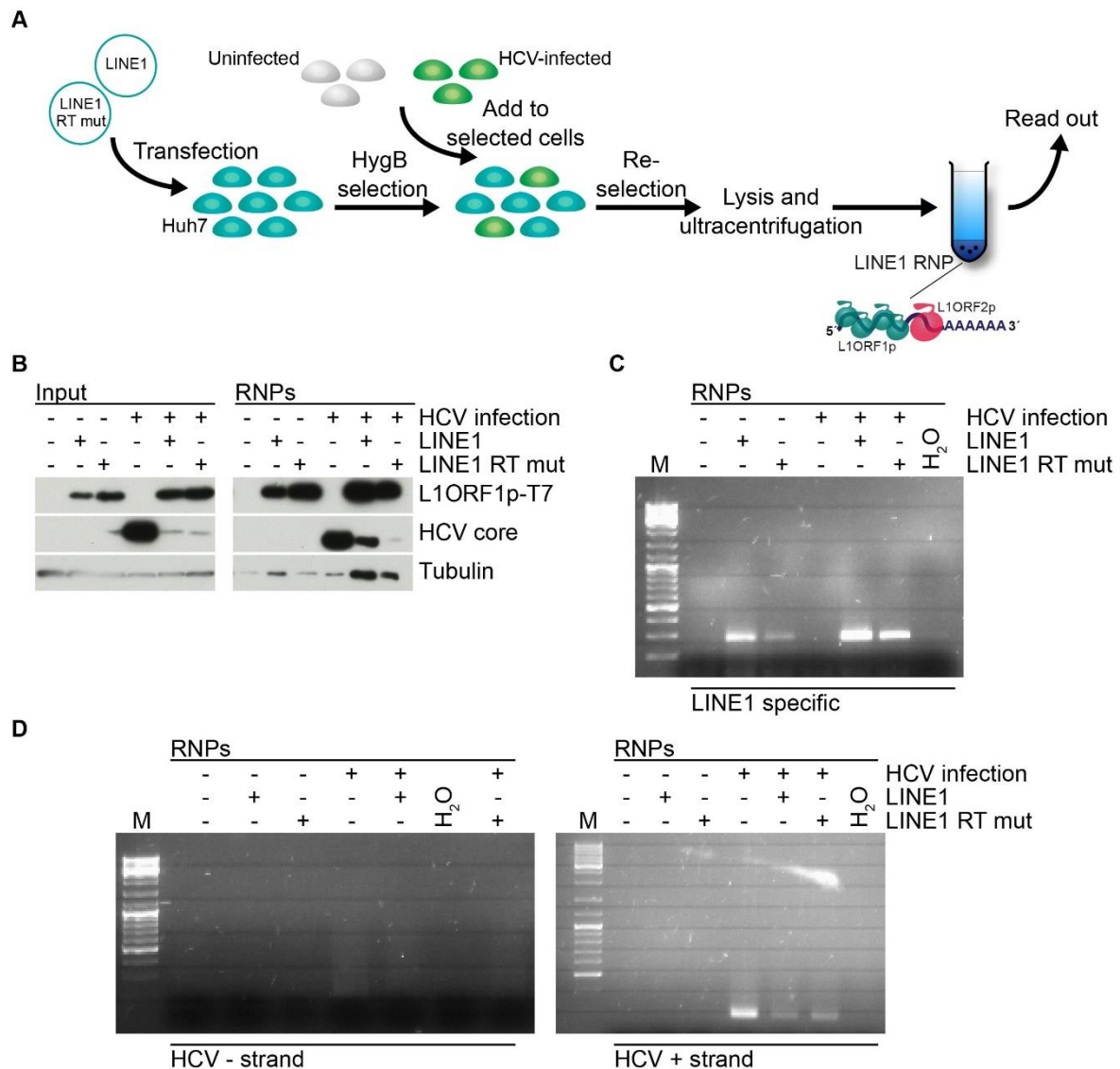
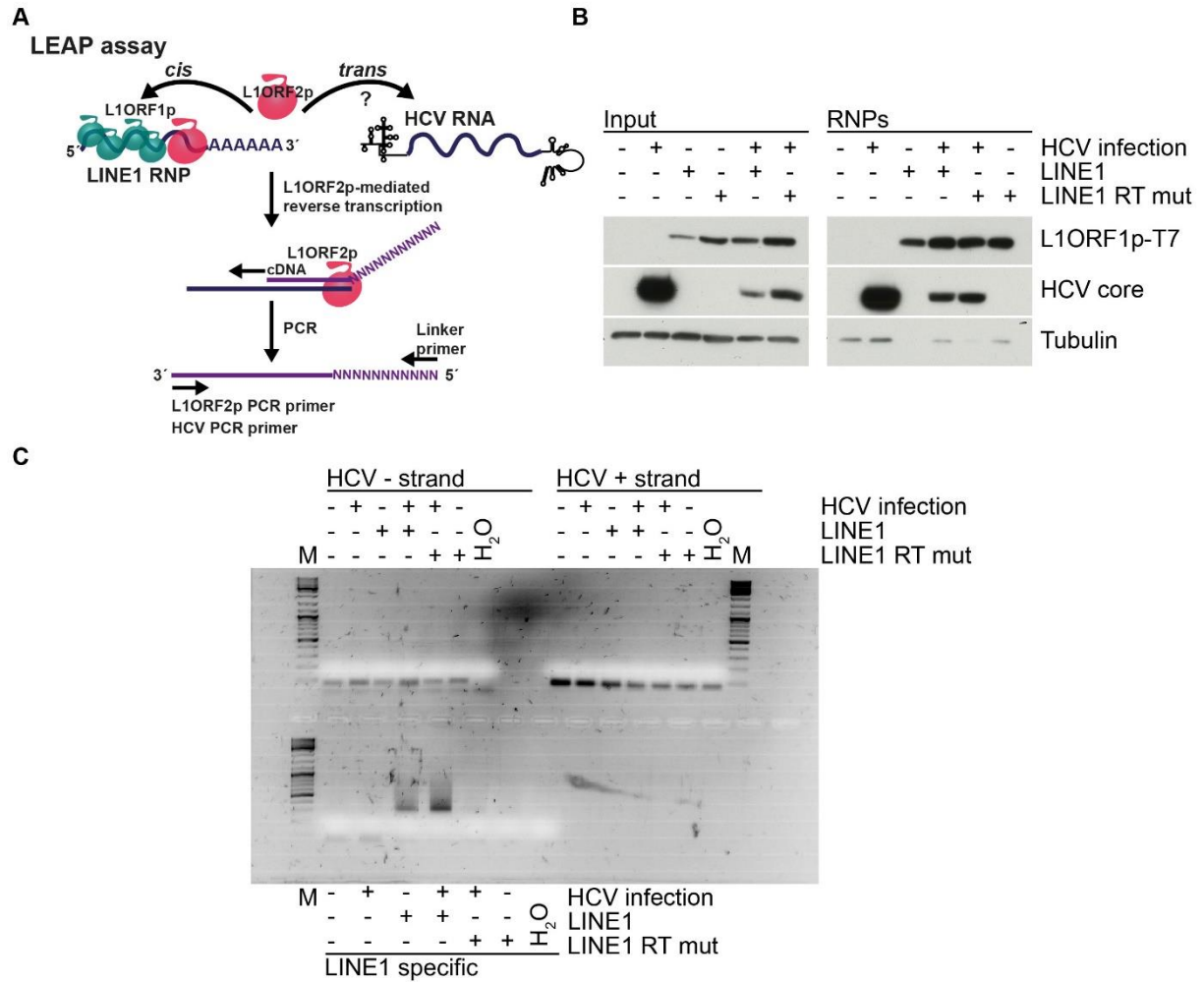


**Figure 22: Presence of HCV RNA in LINE1 RNPs.**

(A) Isolation of LINE1 RNPs. Huh7 cells were transfected with a plasmid for the overexpression of LINE1 (pDK101) or the LINE1 RT mut (pDK135) and selected with hygromycin B. For infection, HCV-infected Huh7 cells were seeded to the selected population and re-selection was performed after 3 days until cells were harvested. Transfected cells mixed with uninfected cells served as control. RNPs were isolated from lysates *via* ultracentrifugation on a sucrose cushion. Untransfected cells served as negative control. (B) Expression of LINE1 and enrichment of RNPs was confirmed by western blotting

using a T7-specific antibody detecting the T7-tagged L1ORF1p. Membranes were also probed for HCV core to verify infection. Tubulin served as loading control. (C, D) RNA was isolated from RNPs and subjected to reverse transcription using SuperScript III with a polyT-rich primer that binds to the 3' polyA tail of LINE1 or to the polyA stretch in the 5' UTR of the HCV – strand. For reverse transcription of the HCV + strand, a polyA-rich primer was used to allow binding to the polyU-rich region in the 3' UTR. A linker region at the end of the primer allows amplification of the generated cDNA together with a target-specific sense primer (modified from (Kulpa and Moran, 2006)). (C) Agarose gel electrophoresis of LINE1-specific PCR products (D) Agarose gel electrophoresis of HCV-specific PCR products. 35 µl of each PCR reaction were loaded to a 2% agarose gel; nucleic acids were detected by ethidium bromide staining under UV light. M = GeneRuler DNA Ladder Mix (n = 1).

Although LINE1 has a strong *cis* preference, other RNAs can serve as template for reverse transcription by L1ORF2p (Kulpa and Moran, 2006). Additionally, LINE1 can mobilize other retroelements such as Alu by using their transcript as template for cDNA synthesis (Dewannieux et al., 2003). In a modified L1 element amplification protocol (LEAP), a biochemical assay to detect L1ORF2p reverse transcriptase activity *in vitro* (Kulpa and Moran, 2006), it was addressed if HCV RNA can serve as a template for reverse transcription by L1ORF2p. Transfection and infection of Huh7 cells for RNP isolation were performed as described above. Enrichment of LINE1 RNPs and expression of LINE1 were confirmed by western blotting; detection of HCV core served as control for infection (Figure 23 B). The LEAP reaction was performed using a strand specific LEAP primer for the HCV + strand RNA; the LINE1 LEAP primer was used for the antisense replication intermediate of HCV, as it contains a polyA stretch in its 5' UTR providing a putative binding sequence for the primer. For amplification of the cDNA product, a conventional PCR was performed. The PCR product was analyzed *via* agarose gel electrophoresis (Figure 23 C). Neither for the HCV + strand, nor the – strand amplification was detectable, indicating that no cDNA transcript of the viral RNA was generated by L1ORF2p. The LINE1 specific PCR showed a strong band with the expected size (~300 bp), confirming that the LEAP reaction was successful. Thus, the lack of a 3'polyA tail in the HCV RNA, which is required for efficient L1ORF2p binding and reverse transcription (Doucet et al., 2015) or the strong *cis* preference of LINE1 might prevent the viral genome from reverse transcription.





### 3.4 L1ORF1p overexpression does not affect HCV RNA replication

As LINE1 is present in approximately  $5 \times 10^5$  copies per cellular genome (Lander et al., 2001), knockdown of LINE-1 is technically challenging, if not unachievable. To this end, overexpression of L1ORF1p was used to study a putative role of LINE1 in the HCV life cycle. First, effects of L1ORF1p overexpression on HCV RNA replication were investigated by using a Jc1ΔE1E2 replicon that carries a firefly luciferase as a reporter in a duplicated NS5AB cleavage site (Jc1ΔE1E2<sup>NS5AB-FLuc</sup>).

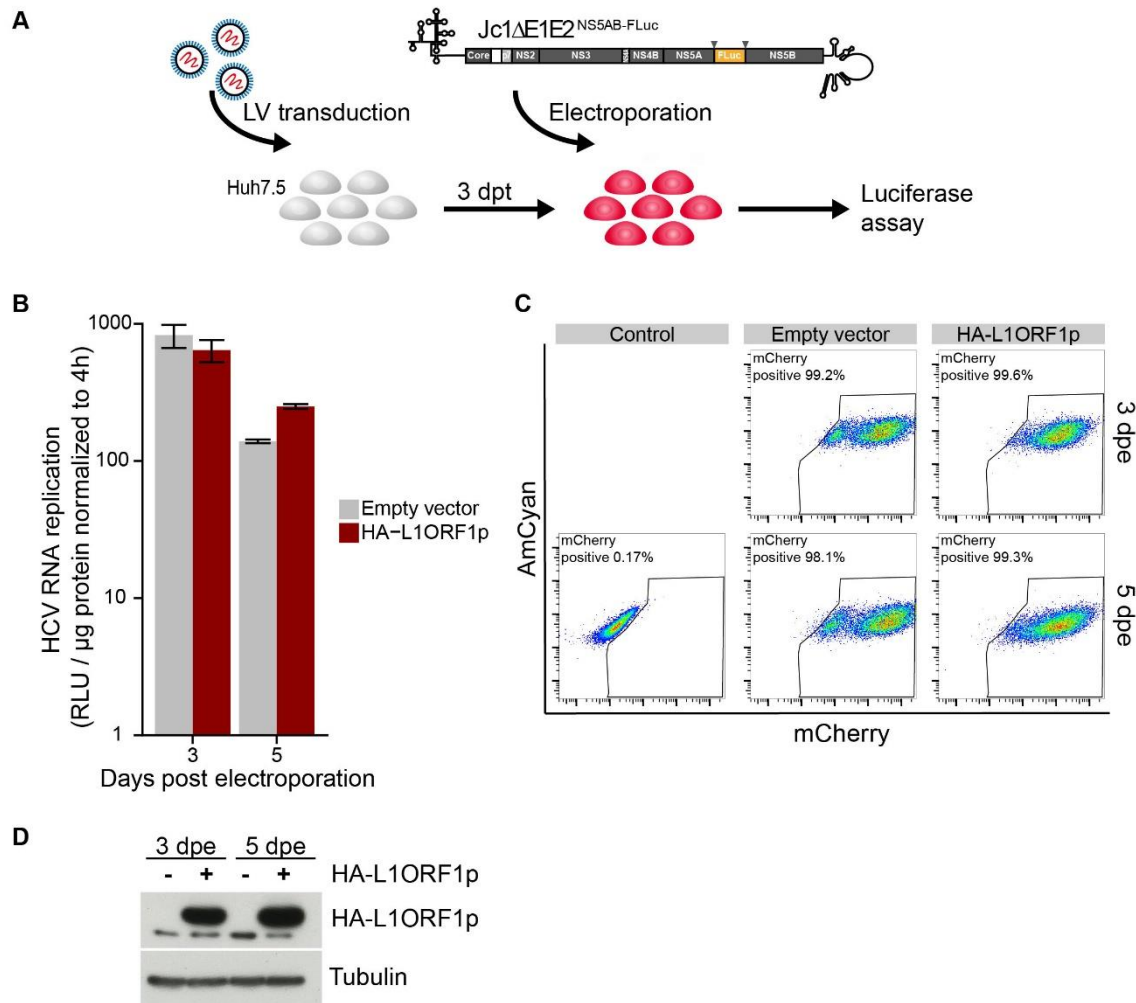


**Figure 24: Pre-established HA-L1ORF1p overexpression does not affect HCV RNA replication.**

(A) Scheme of the experimental set up. For determination of HCV RNA replication, Huh7.5 cells were transduced for HA-L1ORF1p overexpression or with an empty vector 3 days prior to electroporation with Jc1ΔE1E2<sup>NS5AB-FLuc</sup> replicon RNA. Cells were lysed 4 hours (hpe) and 3 and 5 days post electroporation (dpe). (B) Firefly luciferase activity (RLU, relative light units) was measured at the indicated time points. RLU was normalized to the protein level and the 4 hour time point (Mean ± SEM, n = 2). (C) Transduction rates were determined by flow cytometry at the indicated time points. (D) Overexpression of HA-L1ORF1p was confirmed by western blotting. Tubulin served as loading control. Shown is one representative experiment.

In a first experiment, Huh7.5 cells were transduced with lentiviral particles for HA-L1ORF1p expression or an empty vector, both carrying mCherry as a marker, and electroporated with *in vitro* transcribed replicon RNA 3 days post transduction when overexpression was already established (Figure 24 A). Cells were lysed 3 and 5 days post electroporation and HCV RNA replication was determined by measuring the luciferase activity (Figure 24 B). No alterations in HCV RNA replication in HA-L1ORF1p-overexpressing cells were detectable. Successful transduction was measured by flow cytometry (Figure 24 C) and overexpression of HA-L1ORF1p was confirmed by western blotting (Figure 24 D). In a second approach, Huh7.5 cells were first electroporated with *in vitro* transcribed Jc1ΔE1E2<sup>NS5AB-FLuc</sup> RNA, seeded at equal densities and transduced with HA-L1ORF1p-lentivirus or the empty vector 4 hours post electroporation to eliminate variations from different electroporation efficacies (Figure 25). Again, HCV RNA replication in HA-L1ORF1p-overexpressing cells was similar to control cells at the indicated time points, suggesting that L1ORF1p overexpression does not affect HCV RNA replication (Figure 25 B).

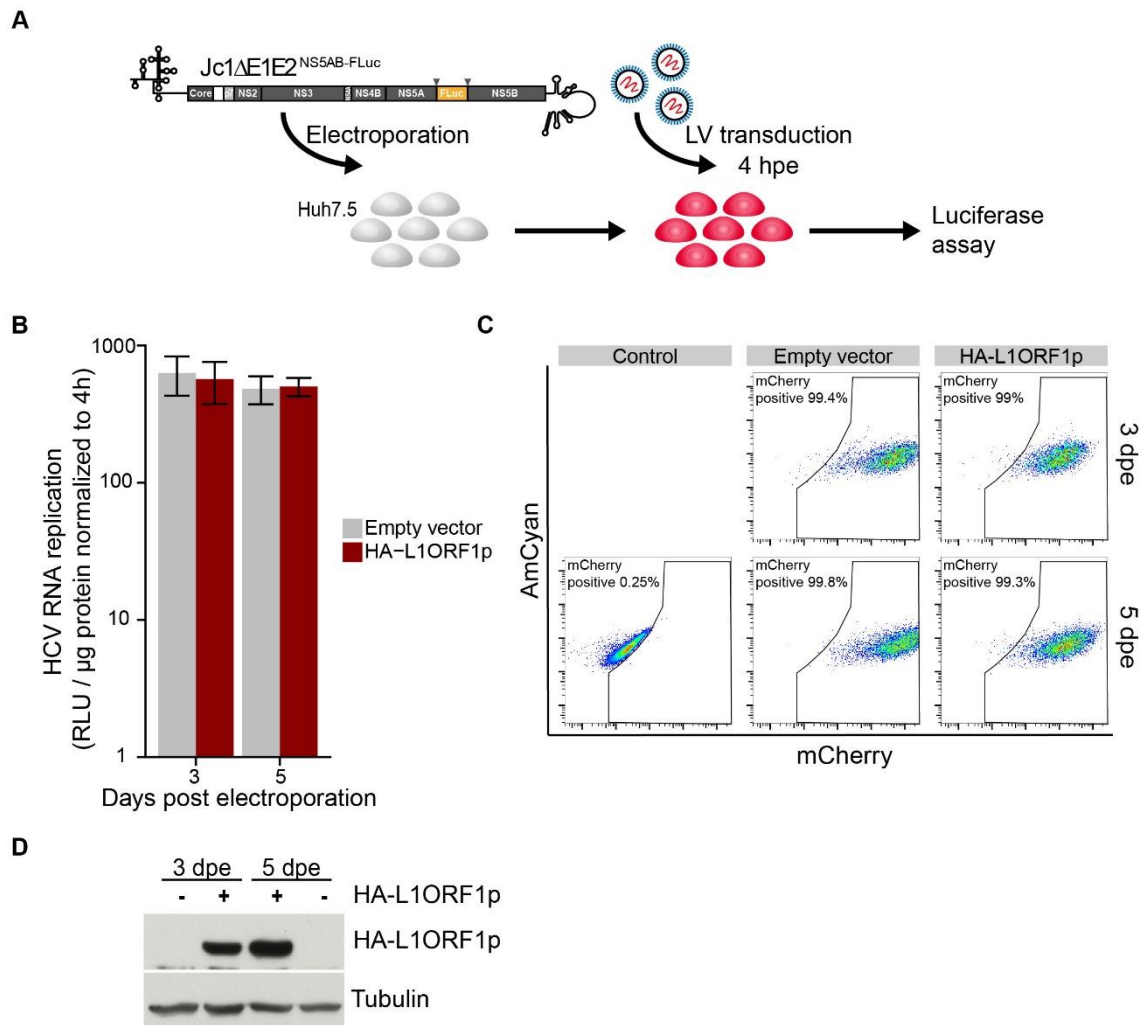


**Figure 25: HCV RNA replication is not altered by HA-L1ORF1p overexpression.**

(A) Scheme of the experimental set up. For determination of HCV RNA replication, Huh7.5 cells were electroporated with Jc1ΔE1E2<sup>NS5AB-FLuc</sup> replicon RNA and transduction for HA-L1ORF1p



overexpression or the empty vector was performed 4 hours post electroporation (hpe). Cells were lysed 4 hours and 3 and 5 days post electroporation (dpe). (B) Firefly luciferase activity (RLU, relative light units) was measured at the indicated time points. RLU was normalized to the protein level and the 4 hour time point (Mean  $\pm$  SEM,  $n = 2$ ). (C) Transduction rates were determined by flow cytometry at the indicated time points. (D) Overexpression of HA-L1ORF1p was determined by western blotting. Tubulin served as loading control. Shown is one representative experiment.

### 3.5 Overexpression of full-length LINE1 affects HCV replication

Despite the fact that only L1ORF1p and not L1ORF2p was identified at LDs of HCV-infected cells (Rosch et al., 2016), influencing the HCV life cycle might still require the full-length LINE1 and even depend on its retrotransposition activity. Therefore, Huh7 cells were seeded and transfected with plasmids encoding a retrotransposition competent LINE1 (pDK101), an L1ORF2p reverse transcriptase mutant (pDK135; RT-, D702A) (Kulpa and Moran, 2005), or an empty vector (pCEP4) in duplicates the following day. All plasmids contained a hygromycin B resistance gene and selection with 200  $\mu$ g/ml hygromycin B was started 3 days post transfection for a total of 9 days. Next, cells were infected with a Jc1 reporter strain carrying a gaussia luciferase and a modified P2A ribosomal skipping site between p7 and NS2 (Jc1<sup>p7-GLuc-2A-NS2</sup>) (Marukian et al., 2008; Schobel et al., 2018). The gaussia luciferase is secreted from the cell and allows tracking of viral replication in the same cell population over time by collecting the supernatant. To preclude that changes in cell viability by overexpression of LINE1 and transfection differences affect the outcome of the experiment, the cells were transduced beforehand with lentiviral particles for the expression of a secreted embryonic alkaline phosphatase (SEAP) that is constantly secreted to the supernatant. Measurement of the SEAP activity allows normalization of the gaussia luciferase activity (RLU). Supernatants were collected, and media was changed every second day. To prevent loss of LINE1 overexpression, cells were kept under selective pressure. Gaussia luciferase activity as a measure of viral replication as well as the SEAP activity were determined at the indicated time points (Figure 26 B, C). As a control for SEAP lentivirus transduction, an EGFP expressing vector was used and cells were transfected and infected parallel as described. Analysis of the SEAP activity revealed slightly lower values for LINE1-overexpressing cells compared to the cells harboring the empty vector, indicating slower cell growth or lower transfection rates resulting in fewer cells that were resistant to hygromycin selection (Figure 26 C). Overexpression of LINE1 in EGFP control cells decreased viral replication about 10 fold (Figure 26 B, left panel). The same result was observed for the LINE1 RT mutant, indicating that this effect is independent of active LINE1 retrotransposition. To include growth differences, the luciferase activity was normalized to protein levels of the final time point (lysates were prepared 14 days post infection). For comparison, the same normalization was performed on the SEAP expressing cells, but no effect of LINE1 on viral replication was detected (Figure 26 B, right panel), even though expression of the active LINE1 was higher compared to the EGFP control cells (Figure 26 D). However, comparison

of the duplicates in LINE1-overexpressing cells revealed a high variance in gaussia luciferase activity compared to the EGFP control cells, likely contributing to the different results. Additionally, overexpression and secretion of SEAP might influence the secretory pathway, thereby affecting the secretion of mature HCV particles and/or the gaussia luciferase, explaining the different results.

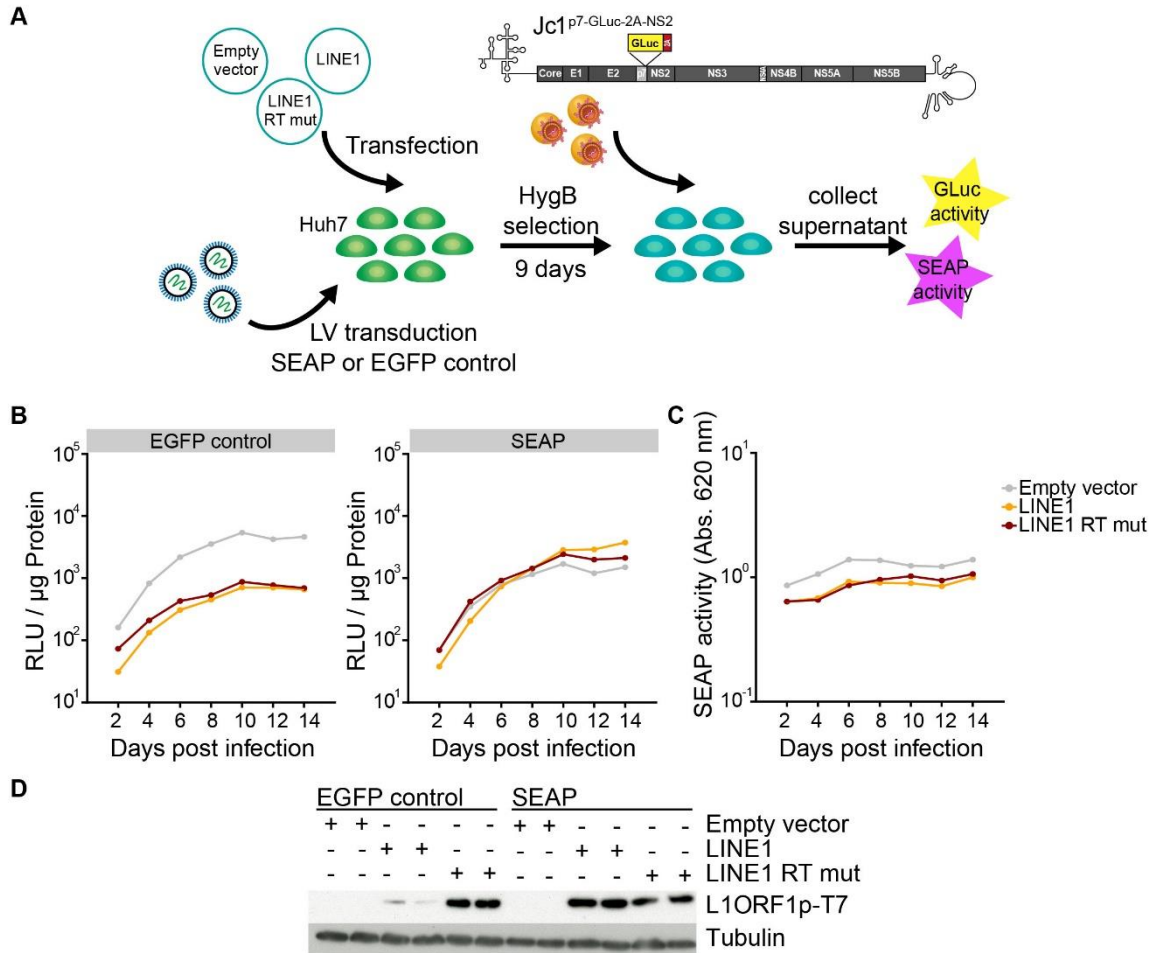


**Figure 26: Effect of LINE1 overexpression on HCV replication.**

(A) Scheme of the experimental set up. Three days prior to transfection, Huh7 cells were transduced with lentiviral particles for SEAP expression or EGFP control. Cells were seeded equally and transfected with a retrotransposition competent LINE1 (pDK101; LINE1), the RT inactive ORF2p mutant (pDK135, LINE1 RT mut) or an empty vector in duplicates. Transfected cells were selected with 200 µg/ml hygromycin B for 9 days and cells were infected with equal volumina of Jc1<sup>p7-GLuc-2A-NS2</sup> stock. Supernatants were harvested every second day for a period of 14 days and HCV replication was measured by determination of gaussia luciferase activity. SEAP activity was determined from the respective samples. Cells were lysed at 14 days post infection for protein extraction. (B) Gaussia luciferase assay of HCV-infected EGFP control and SEAP-Huh7 cells. Gaussia luciferase activity (RLU) was measured at the indicated time points. RLU was normalized to protein of the 14 days time point. (C) SEAP activity in cell culture supernatants of LINE1-overexpressing or control cells. (D) Expression of the T7-tagged L1ORF1p was analyzed by western blotting. Tubulin served as loading control (n = 1).

### 3.6 LINE1 retrotransposition frequency is lower in HCV-infected cells

Although little is known about the biology of LINE1 retrotransposition in viral infections, it was recently described that HIV-1 infection increases the LINE1 retrotransposition frequency *in vitro* (Jones et al., 2013). To study if HCV infection impacts LINE1 activity, a fluorescence-based retrotransposition assay was used (Ostertag et al., 2000; Wissing et al., 2011). This assay is based on a plasmid for expression of a retrotransposition competent LINE1 element (LRE3), containing an inverted EGFP in its 3' UTR under the control of an additional promoter. The EGFP itself is disrupted by an intron, preventing expression of a functional protein from the plasmid. During transcription and mRNA processing, the intron is spliced out and after reverse transcription and integration of the LINE1 reporter cDNA, the EGFP is expressed, reflecting active retrotransposition (Figure 27 A). In an initial experiment, cells transfected with the retrotransposition reporter were treated with the nucleoside analogue reverse transcriptase inhibitor (NRTI) abacavir (ABA) to verify the retrotransposition positive population, as the percentage of EGFP-positive cells was extremely low. ABA-treatment reduced the number of EGFP-positive cells by 60%, confirming that the reporter assay was functional (Figure 27 B, C). To identify the HCV positive population, Huh7.5 cells were infected with a Jc1 reporter strain encoding for a mKusabira-Orange2 (mKO2) fluorescence reporter between a duplicated NS5AB cleavage site (Jc1<sup>NS5AB-mKO2</sup>) (Webster et al., 2013), seeded in 6 well plates 1 day post infection and transfected with the retrotransposition reporter or transfection control plasmid containing the EGFP without the intron the following day. Uninfected cells were treated equally (Figure 27 D). Cells were harvested at 6 days post transfection/8 days post infection and analyzed *via* flow cytometry (Figure 27 E–G). In a second approach, cells were transfected 7 days and analyzed 13 days post infection to assess if timing of infection differentially influences LINE1 retrotransposition activity (Figure 27 E–G). Compared to uninfected cells, the percentage of EGFP-positive cells was significantly lower at 8 days post infection, whereas transfection efficacy was similar (Figure 27 G, left panel). This effect was even more pronounced in the HCV-infected population at 13 days post infection, displaying a decrease in EGFP-positive cells of about 80% compared to uninfected cells; however, transfection efficacy was significantly reduced by 20% as well (Figure 27 G, right panel). Additionally, cells transfected at the later stage of HCV-infection grew less than the uninfected control; this might at least partly contribute to the difference in transfection and retrotransposition observed at 13 days post infection. In conclusion, HCV infection impairs LINE1 retrotransposition frequency *in vitro*, indicating an interplay of HCV and LINE1 that negatively affects LINE1 activity.

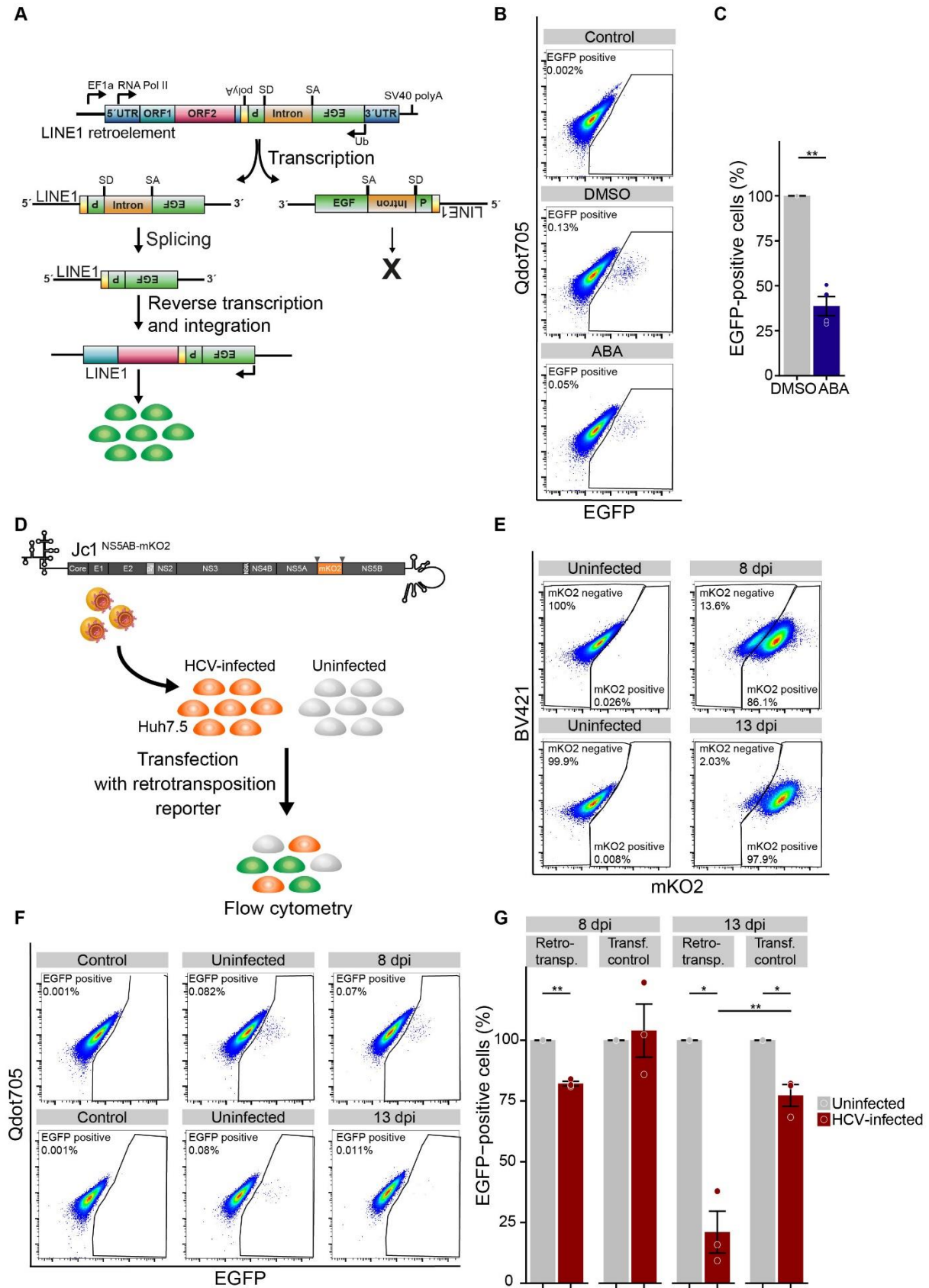


**Figure 27: HCV infection decreases LINE1 retrotransposition frequency.**

Retrotransposition reporter assay in HCV-infected and uninfected cells. (A) EGFP-based LINE1 retrotransposition reporter. In addition to its own promoter located in the 5' UTR (RNA polymerase II

promoter, RNA Pol II), LINE1 expression from the reporter plasmid is driven by an EF1 $\alpha$ -promoter (EF1 $\alpha$ ). An inverted EGFP under the control of an antisense ubiquitin promoter (Ub) is integrated into the 3' UTR and an intron in the EGFP prevents expression of an intact protein. During transcription and mRNA processing, only the intron in the correct orientation is spliced; after reverse transcription of the LINE1 reporter mRNA and reintegration into the genomic DNA, the EGFP is expressed from the Ub promoter. Therefore, only cells in which retrotransposition was completed express EGFP (Ostertag et al., 2000; Wissing et al., 2011). (B) Flow cytometry analysis of retrotransposition frequency in presence or absence of the NRTI abacavir (ABA). Shown is one representative experiment. (C) Quantification of active retrotransposition in presence or absence of ABA. Shown is the percentage of EGFP-positive cells normalized to DMSO-treated control cells (Mean  $\pm$  SEM,  $n = 4$ ;  $*p \leq 0.05$ ). (D) Huh7.5 cells were infected with Jc1<sup>NS5AB-mKO2</sup> (MOI = 0.005) and transfected with the LINE1 EGFP reporter plasmid either 2 or 7 days post infection. The same plasmid, but without the intron in the EGFP served as transfection control. Cells were fixed and analyzed by flow cytometry at 8 (8 dpi) or 13 (13 dpi) days post infection and 6 days post transfection. (E) Infection rates were determined by mKO2 expression *via* flow cytometry. Shown is one representative experiment for each time point. (F) Representative flow cytometry plots of retrotransposition events in HCV-infected and uninfected cells. (G) Flow cytometry analysis of EGFP-positive cells/retrotransposition events. Shown is the percentage of EGFP-positive cells normalized to uninfected cells (Mean  $\pm$  SEM,  $n = 3$ ;  $*p \leq 0.05$ ;  $**p \leq 0.01$ ).

## 4 Discussion

The establishment of a productive HCV infection requires a complex interplay of host and viral factors and a variety of cellular pathways are hijacked by the virus. Recently, a proteomic study identified profound changes in the LD proteome of HCV-infected Huh7.5 cells, suggesting that HCV modifies the LD protein composition in favor of efficient replication (Rosch et al., 2016). In this proteome analysis, the RNA-binding protein ORF1p (L1ORF1p) of the non-LTR retrotransposon LINE1 was exclusively identified at LDs in HCV-infected cells. As L1ORF1p has not been described in the context of HCV infection before, this study focused on a possible interaction between LINE1, especially L1ORF1p, and HCV *in vitro*.

### 4.1 HCV infection increases LINE1 expression level and redistributes L1ORF1p to LDs

Primarily, an increased LINE1 expression has been observed in cancerogenic malignancies and LINE1 hypomethylation has lately been proposed as a prognostic marker for several cancers (Antelo et al., 2012; De Luca et al., 2016; Gao et al., 2014; Lou et al., 2014; Rodic et al., 2014). Only few data exist on LINE1 expression in viral infections. Jones *et al.* described a transient increase of LINE1 transcripts in primary CD4<sup>+</sup> T cells early after HIV-1 infection, preceding the accumulation of extrachromosomal LINE1 cDNA in HIV-1-infected cells (Jones et al., 2013). Likewise, HCV infection of Huh7.5 cells led to a modest transient increase of LINE1 transcripts (detected with primers located in L1ORF1p and L1ORF2p) compared to uninfected cells at 6 days post infection. Concomitantly, L1ORF1p protein level increased in HCV-infected cells and remained elevated at 9 days post infection. Regarding LINE1 hypomethylation, a positive correlation to the presence of oxidative stress has been reported (Patchsung et al., 2012). Further, oxidative stress has been described to increase LINE1 transcripts and L1ORF1p protein levels *in vitro* (Giorgi et al., 2011; Whongsiri et al., 2018). HCV infection and individual expression of HCV proteins, especially core and NS5A have been described to induce oxidative stress as well as nitrosative stress (Garcia-Mediavilla et al., 2005; Ivanov et al., 2011). Thus, an increase of LINE1 expression might result from HCV-induced oxidative stress.

Detailed analysis of isolated LDs confirmed that L1ORF1p was enriched in LD fractions of HCV-infected but not uninfected Huh7.5 cells. This redistribution was stable, as it was observed at 9 days as well as  $\geq 21$  days post infection. L1ORF1p predominantly localizes to cytoplasmic foci containing other RNA-associated proteins as well as markers of stress granula (Doucet et al., 2010; Goodier et al., 2013; Goodier et al., 2007). The same distribution was observed in Huh7 cells overexpressing an HA-tagged L1ORF1p (HA-L1ORF1p). In line with the results of the LD isolation, microscopic analysis revealed the re-localization of HA-L1ORF1p to LDs in HCV-infected cells. This phenotype was observed using the JFH1<sup>wt</sup> as well as the Jc1<sup>wt</sup> strain. Jc1 replicates to higher titers in cell culture

whereas JFH1 is characterized by a higher accumulation of HCV core at LDs (Pietschmann et al., 2006; Shavinskaya et al., 2007). Correspondingly, a stronger colocalization between HA-L1ORF1p and LDs or HCV core was observed in JFH1-infected cells compared to Jc1. The re-localization of host proteins to LDs in HCV-infected cells has been observed in preceding studies (Ariumi et al., 2011a; Chatel-Chaix et al., 2013; Chatel-Chaix et al., 2011; Poenisch et al., 2015; Rosch et al., 2016). Interestingly, many of these proteins also possess RNA-binding properties and were described to play a role in HCV replication, indicating a functional relevance for RNA-binding proteins in close proximity to LDs. *Chatel-Chaix et al.* described the Y-box-binding protein-1 (YB-1) as a proviral factor re-localizing to LDs. This redistribution was dependent on the presence of HCV core (Chatel-Chaix et al., 2011). Further, the DEAD-box helicase DDX3 re-localizes to LDs in an HCV core dependent manner (Angus et al., 2010). In line with this, L1ORF1p was not present in LD fractions from cells harboring the subgenomic replicon (SGR). Replication of a Jc1 $\Delta$ E1E2 strain, a virus with a partial deletion of the envelope proteins, led to the recruitment of L1ORF1p to LDs, suggesting that L1ORF1p redistribution might be also be connected to the the capsid protein core or efficient capsid formation.

#### **4.2 HCV core interacts with RNP components in an RNA-dependent manner and induces their redistribution to HCV assembly sites**

During HCV replication, the HCV core protein and the non-structural protein NS5A localize to LDs, the putative HCV assembly sites (Appel et al., 2008; Boulant et al., 2006; Miyanari et al., 2007; Shavinskaya et al., 2007). In addition, both proteins traffic to LDs when individually expressed (Camus et al., 2013). In the presented study, the overexpression of HCV core but not NS5A recruited L1ORF1p to LD fractions. Microscopic analysis confirmed a strong re-localization of HA-L1ORF1p to LDs in HCV core-overexpressing cells, sometimes even forming ring-like structures surrounding the droplets. Similar patterns of host proteins at LDs were already described by *Ariumi et al.*, showing ring-like shapes of the poly A binding protein PABPC1 and the DEAD box helicases DDX3 and DDX6 in JFH1-infected cells (Ariumi et al., 2011a). As mentioned above, the majority of host proteins identified at LDs in HCV-infected cells is connected to RNA binding or found in RNPs (Ariumi et al., 2011a; Chatel-Chaix et al., 2013; Chatel-Chaix et al., 2011; Rosch et al., 2016). Noteworthy, *Chatel-Chaix et al.* described an interaction between individual proteins that are localized to LDs, suggesting the redistribution of protein complexes and RNP components rather than single proteins (Chatel-Chaix et al., 2013). Several studies have reported an RNA-dependent interaction and colocalization of L1ORF1p with other RNA associated proteins (Goodier et al., 2013; Goodier et al., 2015; Moldovan and Moran, 2015). A comparative analysis of the L1ORF1p interactome described by *Goodier et al.* and the LD proteome data from *Rosch et al.* revealed 25 commonly identified proteins (Goodier et al., 2013; Rosch et al., 2016). 18 of

the identified proteins were enriched at LDs in HCV-infected cells, suggesting the redistribution of L1ORF1p-interacting complexes rather than L1ORF1p alone. Concordant with this assumption, the L1ORF1p interaction partners PABPC1 and MOV-10 were also enriched in LD fractions of HCV core-overexpressing cells. *Ariumi* and colleagues hypothesized that HCV infection disrupts cellular P-bodies and redistributes the components to the HCV assembly sites in parallel to stress granula formation (Ariumi et al., 2011a). In the presented thesis, HCV core expression alone induced the enrichment of the stress granula associated protein PABPC1 in LD fractions, indicating a dynamic redistribution that depends on core-trafficking to LDs. RNPs are characteristically composed of proteins and RNA. Early on, it was shown that the stability of LINE1 RNPs depends on the L1ORF1p-RNA interaction (Hohjoh and Singer, 1996; Hohjoh and Singer, 1997; Kulpa and Moran, 2005). Further, many proteins that localize with L1ORF1p to cytoplasmic foci interact with L1ORF1p in an RNA-dependent manner (Goodier et al., 2013; Goodier et al., 2007; Moldovan and Moran, 2015). Concomitantly, co-immunoprecipitation of HA-L1ORF1p from HCV-infected cells revealed an interaction between the HCV core protein and L1ORF1p that was abolished upon RNase A treatment. Besides the core protein, NS5A is capable of RNA binding (Huang et al., 2005). Individual expression and co-immunoprecipitation of FLAG-tagged HCV core (gt2a and gt1b) confirmed the RNA-dependent interaction with L1ORF1p. In contrast, no L1ORF1p/NS5A-FLAG (gt2a) interaction was observed. Whereas *Shimoike et al.* described a specific binding of HCV core to the 5' UTR of the HCV genome, others described an unspecific interaction with the hepatitis B mRNA and low affinity binding to cellular tRNAs as well as to the HCV antisense RNA (Fan et al., 1999; Santolini et al., 1994; Shimoike et al., 1999). NS5A has been shown to bind the 3' UTR of the sense and antisense HCV RNA with a high affinity for polyU tracts (Huang et al., 2005). Noteworthy, L1ORF1p and HCV core also interacted in the absence of HCV RNA, indicating that cellular RNAs bridge this interaction. In co-immunoprecipitates of LINE1 RNPs, *Goodier et al.* identified several snRNAs (small nuclear RNAs) as well as scRNAs (small cytoplasmic RNAs) (Goodier et al., 2013). Both species have conserved secondary structures (reviewed in Kowalski and Krude, 2015; reviewed in Will and Luhrmann, 2011). HCV core has been described to bind highly structured tRNA (Fan et al., 1999); thus, the interaction of L1ORF1p and HCV core might result from a shared binding preference for similar RNA species that is not owned by NS5A. Possibly, NS5A only binds weakly or not at all to cellular RNAs, explaining the lacking interaction with L1ORF1p. However, specific evidence of HCV core binding to cellular RNAs is missing. Consistent with the idea of an RNP complex that HCV core is part of, the L1ORF1p interaction partners PABPC1 and MOV-10 were identified in co-immunoprecipitation fractions of overexpressed FLAG-core but not NS5A-FLAG. Again, the interaction of HCV core with both proteins was disrupted upon RNase A treatment. Of note, MOV-10 was only detected in FLAG-core precipitates of gt2a. This was rather due to the high background caused by the MOV-10 antibody than a genotype-specific effect. The co-precipitation of PABPC1 and MOV-10



indicates that L1ORF1p and HCV core are not directly interacting but simply part of the same RNP. For a putative L1ORF1p RNA-binding mutant (RR261-262AA) (Khazina and Weichenrieder, 2009; Kulpa and Moran, 2005) a decreased re-localization to LDs compared to the wildtype was observed in HCV core-overexpressing cells. An impaired RNA binding of L1ORF1p likely decreases the interaction with HCV core, thereby reducing the redistribution to LDs. As mentioned above, the stability of LINE1 RNPs is dependent on protein-RNA interaction and RNA-binding mutants of L1ORF1p affect LINE1 RNP formation and retrotransposition (Kulpa and Moran, 2005; Moran et al., 1996). As only L1ORF1p but not L1ORF2p was identified at LDs of HCV-infected cells (Rosch et al., 2016), it is likely that not the intact LINE1 RNP is recruited to LDs, but only unassembled L1ORF1p. *Goodier et al.* reported slight changes of foci morphology in RR261-262AA expressing cells; it is not unlikely that the loss of RNA binding changes the composition of the L1ORF1p-containing foci, thereby disrupting interactions which are important for the redistribution of L1ORF1p to LDs (Goodier et al., 2007). However, a decreased protein stability of the RR261-262AA mutant has been reported, possibly also accounting for the decreased re-localization (Kulpa and Moran, 2005).

#### **4.3 HCV RNA is part of LINE1 RNPs, but not reversely transcribed by L1ORF2p**

In a process called *trans* mobilization, non-LINE1 RNA serves as templates for L1ORF2p-reverse transcription (L1ORF2p-RT) and the cDNA is re-integrated into the genome (Dewannieux et al., 2003; Esnault et al., 2000; Kulpa and Moran, 2006; Wei et al., 2001). Although L1ORF1p has a strong *cis* preference for its own transcript, other RNAs have been found in LINE1 RNPs (Goodier et al., 2013; Kulpa and Moran, 2006). qRT-PCR analysis of HA-L1ORF1p precipitation fractions revealed a significant enrichment of HCV RNA compared to the background control, indicating that the viral genome can be bound by L1ORF1p. Admittedly, it is not possible to conclude if L1ORF1p directly binds to HCV RNA or if, together with the core protein, it is part of an RNP and bound by other components. Although HCV RNA was detected in LINE1 RNPs isolated from cells overexpressing a full-length LINE1, a specific assay for detection of L1ORF2p-RT activity did not yield in HCV specific cDNA. Due to the strong *cis* preference of LINE1, reverse transcription of HCV RNA by L1ORF2p might require an excess of viral RNA within the LINE1 RNP that is not given. Additionally, less HCV core protein was detected in LINE1-overexpressing cells compared to untransfected cells, indicating a low infection rate possibly contributing to the negative result. Priming of L1ORF2p reverse transcription requires a polyA tail that is missing in the HCV RNA (Doucet et al., 2015). The positive strand HCV RNA comprises a polyU-rich stretch within its conserved 3' UTR, resulting in a polyA-rich region in the negative strand replication intermediate. However, the positive strand is present in excess (Keum et al., 2012) and almost no HCV negative strand specific cDNA was detected in isolated LINE1 RNPs. Thus,

too little negative strand RNA might be available. The first integration of endogenous non-retroviral RNA viruses was reported by *Horie et al.*, connecting integration of the non-retroviral bornavirus to LINE1 activity (Horie et al., 2010). In contrast to HCV, bornaviruses are replicating within the nucleus, the site of L1ORF2p-RT activity (Briese et al., 1992; Cost et al., 2002). Recently, it has been proposed that L1ORF1p is exported from the nucleus prior to reverse transcription and a L1ORF2p LINE1 mRNA particle is completing LINE1 retrotransposition (Mita et al., 2018). Thus, the presence of the bornavirus genome in the nucleus might provide a higher chance of reverse transcription by L1ORF2p compared to HCV. *In vitro*, binding of four T nucleotides to the LINE1 poly A tail was sufficient to prime reverse transcription (Monot et al., 2013). Within the HCV positive strand genome, several short stretches of 4–5 A nucleotides are present. However, if they are sufficient to prime reverse transcription of the HCV genome remains to be elucidated.

#### 4.4 L1ORF1p is not involved in HCV RNA replication

In addition to its RNA-binding function, L1ORF1p displays nucleic acid chaperone activity (Callahan et al., 2012; Khazina and Weichenrieder, 2009; Kulpa and Moran, 2005; Martin and Bushman, 2001; Martin et al., 2005); thus, it might be involved in structural rearrangements of the HCV RNA. In this study, a stable overexpression of HA-L1ORF1p did not affect HCV RNA replication of a Jc1ΔE1E2<sup>NS5AB-FLuc</sup> reporter strain at any time point. Likewise, *Kawano et al.* reported that L1ORF1p overexpression did not affect HIV-1 transcription or nuclear export, though it is found incorporated into HIV-1 virions (Kawano et al., 2018). As the HA-tagged L1ORF1p displayed the same phenotype as the endogenous L1ORF1p, this result was not due to a lack of interaction or redistribution. Certainly, L1ORF1p enrichment at LDs might be an unspecific process, as several L1ORF1p interactors, like YB-1 or PABPC1 are recruited to LDs in HCV-infected cells (Ariumi et al., 2011a; Chatel-Chaix et al., 2013; Chatel-Chaix et al., 2011; Goodier et al., 2013). On the other hand, L1ORF1p might be involved in the late steps of assembly and virus production, which were not addressed with the Jc1ΔE1E2<sup>NS5AB-FLuc</sup> reporter strain, e.g. capsid assembly or envelopment. However, the gold standard to determine a pro- or antiviral effect of a host protein still is the downregulation of the respective factor. Due to the high LINE1 copy number ( $5 \times 10^5$ /genome (Lander et al., 2001)) and the frequent mutation rate, the establishment of a sufficient knockdown is difficult, but might be required to definitively assess a potential role for LINE1 in the HCV life cycle. Whereas individual expression of L1ORF1p did not affect HCV RNA replication, overexpression of a full-length LINE1 decreased HCV replication of a Jc1<sup>p7-GLuc-2A-NS2</sup> reporter strain about 1 log compared to the empty vector control, indicating that viral spreading might be impaired. Another possible explanation for this result is that not L1ORF1p but L1ORF2p or their combined expression possibly affects HCV replication. Further, the use of a replicon (Jc1ΔE1E2<sup>NS5AB-FLuc</sup>) vs. a full-length (Jc1<sup>p7-GLuc-2A-NS2</sup>) virus might contribute to the different outcome. Interestingly, this was

independent of the L1ORF2p reverse transcriptase activity, as the LINE1 RT negative mutant decreased HCV replication similar to the wildtype. As the expression of the RT negative mutant was stronger than wildtype expression but HCV replication was comparable, it is likely that other factors within the experimental set up influence HCV replication. LINE1 expression and individual expression of L1ORF2p have been shown to decrease cell viability and to induce senescence (Wallace et al., 2008), thereby likely decreasing HCV replication. Initially, this assay was tested with cells stably expressing a secreted embryonic alkaline phosphatase (SEAP) to monitor cell growth. Here, LINE1-overexpressing cells showed slightly lower SEAP activity compared to the control cells, indicating a minor growth defect. Surprisingly, SEAP cells did not show any differences in HCV replication between LINE1 overexpression and the empty vector control, but the luciferase activity was very low. Secretion of the gaussia luciferase can be affected by ER stress (Badr et al., 2007). High levels of SEAP expression and secretion possibly causes ER stress, thereby interfering with the secretion of the gaussia luciferase. Taken together, this experimental system still has to be optimized to analyze a potential role for LINE1 in the HCV life cycle.

#### **4.5 HCV infection decreases LINE1 retrotransposition frequency**

To investigate if HCV infection influences LINE1 mobility, the retrotransposition frequency in HCV-infected and uninfected cells was compared using a fluorescence-based reporter system for LINE1 retrotransposition. Here, LINE1 activity was significantly reduced in HCV-infected cells at 8 and 13 days post infection. As described above, HCV infection initially increased L1ORF1p protein level. Recently, it was reported that exogenously expressed full-length and truncated L1ORF1p can suppress LINE1 retrotransposition in *trans* (Sokolowski et al., 2017). Hence, the increased L1ORF1p protein expression might contribute to the lower retrotransposition frequency observed in HCV-infected cells. However, L1ORF1p expression levels showed a high variance between the individual experiments. Therefore, it is unlikely that the *trans* inhibitory effect is the major cause for the observed phenotype. Compared to cells analyzed at 8 days post infection, retrotransposition was even lower at 13 days post infection. Concomitant with progressive infection, the cells displayed a slower proliferation that was even more pronounced in cells that were transfected with the retrotransposition reporter plasmid. This is in line with previous studies connecting HCV infection to slower proliferation and cell cycle arrest *in vitro* (Kannan et al., 2011; Walters et al., 2009). Treatment with cell cycle inhibitors arresting cells in the M (nocodazole) or at the transit of G1/S phase (thymidine; mimosine) led to a significant decrease of LINE1 retrotransposition *in vitro*. Further, a peak of retrotransposition events was observed in the S phase (Mita et al., 2018). Thus, a decreased cell proliferation and reduced S phase transition caused by HCV infection might partially contribute to the observed reduction in LINE1 retrotransposition and explain the differences between the different time points post infection. HCV replication as well as LINE1 activity involve different cellular processes. Endosomal sorting complex

required for transport (ESCRT) complexes are involved in a variety of cellular processes, including not only endosomal trafficking but also autophagy, cytokinesis, and viral budding (reviewed in Henne et al., 2011). In the late stages of the HCV life cycle, budding, assembly and release of progeny HCV particles has been connected to the ESCRT pathway (Ariumi et al., 2011b; Barouch-Bentov et al., 2016; Corless et al., 2010). Recently, ESCRT was identified as a crucial factor for effective LINE1 retrotransposition (Horn et al., 2017). Here, speculative models were proposed in which LINE1 might induce membrane budding to form maturation sites for RNPs or uses the ESCRT pathway for membrane-associated transit to the nucleus. HCV replication might excessively engage the ESCRT machinery, thereby decreasing LINE1 retrotransposition in HCV-infected cells. So far, L1ORF1p and HCV proteins differ in their direct ESCRT interaction partners. Knockdown experiments of the known ESCRT components in yeast have shown a decreased retrotransposition of the *Zorro3* element, a *candida albicans* homologue of the human LINE1 (Horn et al., 2017). Among the required proteins were the yeast homologues of Hrs and CHMP4b, two ESCRT components that are required for HCV replication. CHMP4b interacts with HCV core and Hrs with NS2 and NS5A (Ariumi et al., 2011b; Barouch-Bentov et al., 2016). Supposed that, similar to the yeast proteins, CHMP4b and Hrs are required for LINE1 activity, interaction with the viral proteins might inhibit retrotransposition. However, this is highly speculative as the role of Hrs and CHMP4b for human LINE1 remains to be elucidated. Another cellular process involved in HCV replication is autophagy. Several studies have reported that autophagosome formation is induced in HCV-infected and replicon-containing cells and is required for efficient HCV RNA replication (Ait-Goughoulte et al., 2008; Dreux et al., 2009; Huang et al., 2013; Mizui et al., 2010; Sir et al., 2008; Wang et al., 2017; Wang et al., 2015). Whereas some studies showed an induction of autophagy (Huang et al., 2013; Wang et al., 2015), others only report an increased autophagosome formation without enhanced degradation (Sir et al., 2008). Regarding LINE1 retrotransposition, the knockdown of the autophagy-associated proteins ATG5 and p62 increased LINE1 and Alu mobilization and LINE1 RNA as well as L1ORF1p were described to localize to autophagosomes. Further, bafilomycin treatment lead to an increased level of LINE1 RNA, suggesting that retrotransposition is partly controlled by autophagy (Guo et al., 2014). Autophagy induction in HCV-infected cells might contribute to sequestration of LINE1 RNA in autophagosomes, hindering the formation of LINE1 RNPs and thereby reducing retrotransposition. Referring to complete autophagy induction upon HCV-infection (Huang et al., 2013; Wang et al., 2015), the decrease of LINE1 retrotransposition might also result from an increased degradation of LINE1 RNA. p62 decrease as a marker for autophagy was described at 48 h as well as 5 days post infection; this is somehow contradicting the observed increase of LINE1 mRNA at 6 days post infection. However, both studies used JFH1 strains for infection, whereas Jc1 was used for the time course experiment within this study. Both strains replicate to different titers in cell culture (Pietschmann et al., 2006) and might differently induce autophagy. The

interaction of L1ORF1p with HCV core and its re-localization to LDs might protect the protein from lysosomal degradation *via* autophagy.

A prerequisite for efficient retrotransposition is the assembly of LINE1 RNPs composed of L1ORF1p, L1ORF2p, and LINE1 RNA (Kulpa and Moran, 2005). Upon HCV infection, endogenous L1ORF1p is re-localized and kept at LDs. As this phenotype is also observed for overexpressed L1ORF1p (HA-L1ORF1p), it is likely that L1ORF1p expressed from the retrotransposition reporter is similarly re-localized. Sequestration of L1ORF1p at LDs could prevent RNP assembly, thus leading to a decreased retrotransposition frequency in HCV-infected cells. Additionally, the redistribution of RNA-binding and RNP-associated proteins to LDs in HCV-infected cells has been described in several studies (Ariumi et al., 2011a; Chatel-Chaix et al., 2013; Chatel-Chaix et al., 2011; Rosch et al., 2016). Among them are known interactors of L1ORF1p, e.g. LARP-1, DDX17, YB-1, PABPC1 and MOV-10 (Goodier et al., 2012; Goodier et al., 2013; Goodier et al., 2015; Moldovan and Moran, 2015). The MOV-10 helicase is one of the most potent LINE1 inhibitors known to date (Goodier et al., 2012; Li et al., 2013b). Although MOV-10 is usually found together with L1ORF1p in cytoplasmic foci, already controlling retrotransposition (Goodier et al., 2012; Goodier et al., 2013), the redistribution to LDs might change spatial interactions, thereby increasing its suppressive effect. Apart from a possible spatial inhibition, HCV infection might upregulate LINE1 restriction factors. Many of the known cellular LINE1 inhibitors are interferon stimulated genes (ISGs) that play a role in antiviral immunity (Goodier et al., 2015; Herrmann et al., 2018; Hu et al., 2015; Moldovan and Moran, 2015; Zhao et al., 2013). The Huh7.5 cell line used in this study has several defects in antiviral sensing and is characterized by an overall low innate immune response (Li et al., 2005a; Sumpter et al., 2005; Wang et al., 2009). Therefore, a strong upregulation of an antiviral response gene that controls LINE1 retrotransposition is rather unlikely. However, HCV certainly changes the cellular expression as well as the metabolic profile *in vitro* (Hofmann et al., 2018; Jacobs et al., 2005), possibly inducing a LINE1 restriction factor. In conclusion, HCV infection modulates a variety of host cell factors that might, individually or in a concerted process, cause the decrease in LINE1 retrotransposition frequency in HCV-infected cells.

#### 4.6 Conclusion and working model

In summary, the data presented suggest that HCV infection increases LINE1 expression levels, possibly through induction of cell stress. Moreover, L1ORF1p and its interactors PABPC1 and MOV-10 are redistributed from cytoplasmic foci to HCV assembly sites by HCV core. As other known interactors of L1ORF1p have been described to localize to LDs upon HCV infection as well (Ariumi et al., 2011a; Chatel-Chaix et al., 2013; Chatel-Chaix et al., 2011; Rosch et al., 2016), it can be assumed that HCV core assembles with L1ORF1p into RNPs, e.g. stress granula, and recruits them to LDs. The RNA-dependent interaction of L1ORF1p, PABPC1, and MOV-10 with HCV core and the enrichment of HCV RNA in co-immunoprecipitates of L1ORF1p support this conclusion. The HCV core-dependent redistribution of L1ORF1p and its potential sequestration at LDs might be the cause for the significant reduction of LINE1 retrotransposition frequency observed in HCV-infected cells. Further, HCV infection likely activates different cellular pathways that have been previously shown to suppress LINE1 activity, but the exact mechanism remains to be elucidated. Whereas *trans* mobilization of cellular mRNAs has been described for LINE (Dewannieux et al., 2003), no experimental evidence for HCV RNA as a template for L1ORF2p reverse transcription was obtained. Despite the re-localization of L1ORF1p in HCV-infected cells, overexpression of L1ORF1p did not affect HCV RNA replication. However, other RNA-binding proteins that localize to LDs in HCV-infection, e.g. LARP-1 and YB-1 (Chatel-Chaix et al., 2013; Chatel-Chaix et al., 2011) have been shown to be involved in HCV particle production. Thus, a role of L1ORF1p in HCV replication is possible and would be best assessed upon knockdown conditions.

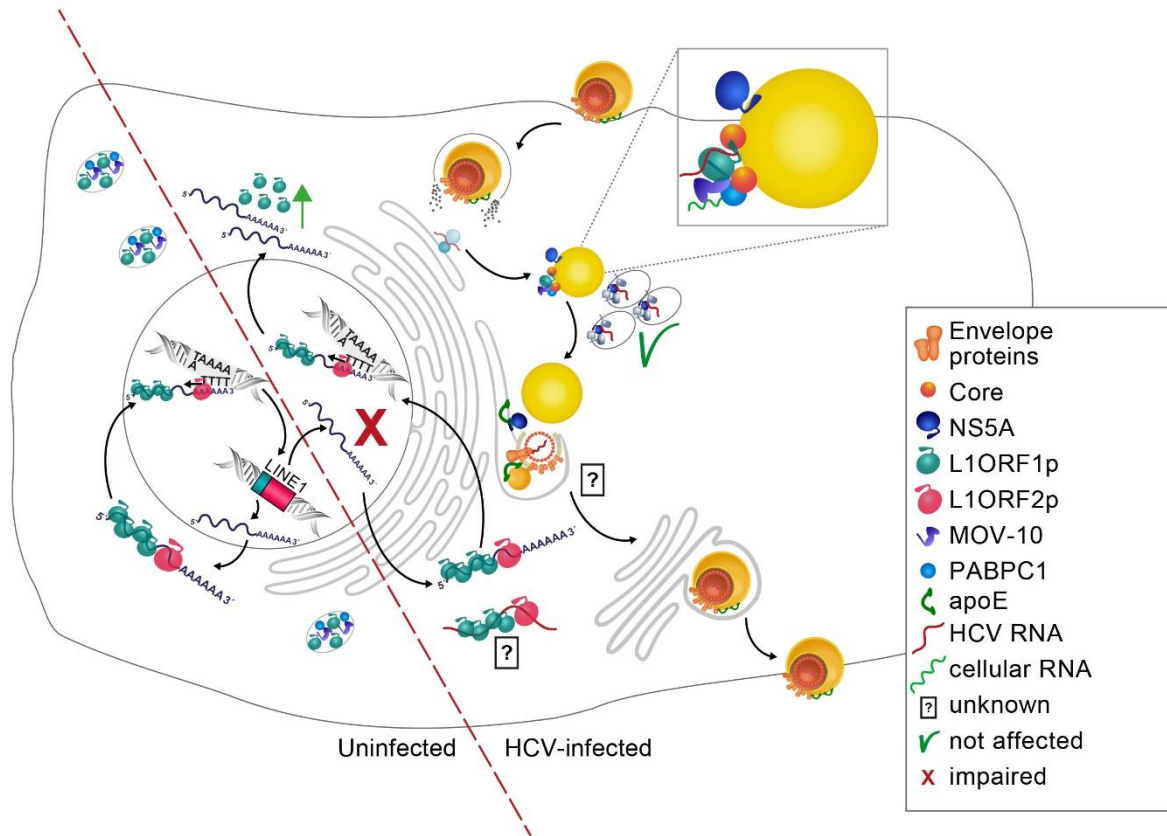


**Figure 28: Interplay of LINE1 and HCV.**

In uninfected cells, L1ORF1p is found in cytoplasmic foci together with PABPC1, MOV-10, and other RNA-associated proteins. Upon HCV infection, LINE1 expression is increased and L1ORF1p is redistributed to LDs in an HCV core-dependent manner. The interaction of both proteins is facilitated by cellular RNAs and required for efficient L1ORF1p re-localization. Together with L1ORF1p, PABPC1 and MOV-10 traffic to HCV assembly sites, likely forming a ribonucleoprotein particle in which the HCV RNA is incorporated as well. L1ORF1p does not influence HCV RNA replication but a potential function in the full viral life cycle remains to be further investigated. LINE1 retrotransposes at lower frequencies in HCV-infected cells compared to uninfected cells, but mechanistic details still need to be elucidated. If the HCV genome can serve as template for reverse transcription, thereby being integrated into the genome remains to be clarified.

## 5 Material

### 5.1 Bacteria

**Table 2: Bacterial strains.**

Name	Genotype	Company
DH5 $\alpha$	F- $\Phi$ 80/ <i>lacZ</i> $\Delta$ M15 $\Delta$ ( <i>lacZYA-argF</i> ) U169 <i>recA1 endA1 hsdR17</i> ( $r_k^-$ , $m_k^+$ ) <i>phoA</i> <i>supE44 thi-1 gyrA96 relA1 <math>\lambda^-</math></i>	Thermo Fisher Scientific, Darmstadt

**Table 3: Media for bacterial culture.**

Name	Components	Quantity
LB medium	Yeast extract	5 g
	Trypton	10 g
	NaCl	10 g
	5 M NaOH	200 $\mu$ l
	dH <sub>2</sub> O	ad 1 l

LB media was autoclaved and cooled to approximately 60 °C before 100  $\mu$ g/ml ampicillin or 50  $\mu$ g/ml kanamycin was added. For preparation of LB agar plates, 15 g/l agar (biological grade) were added prior to autoclaving. LB agar was cooled to approximately 60 °C before antibiotics were added. Plates were prepared under sterile conditions and stored at 4 °C.

### 5.2 Eukaryotic cell lines

**HEK 293T:** HEK 293T is a human embryonic kidney cell line stably expressing a mutant version of the SV40 large T antigen. Thus, the replication of plasmids carrying the SV40 origin of replication is supported (DuBridge et al., 1987). HEK293T cells were obtained from the American Type Culture Collection (ATCC).

**Huh7 and Huh7-derivates:** The human hepatoma cell line Huh7 was established from cells isolated from a hepatocellular carcinoma (Nakabayashi et al., 1982). The Huh7.5 sub-cell line originates from Huh7 cells harboring an HCV replicon followed by cure with IFN $\alpha$  treatment (Blight et al., 2002). Both cell lines are permissive for HCV infection *in vitro* and support viral replication. Huh7.5.1 cells, characterized by fast kinetics of HCV infection, are derived from the Huh7.5 cell line (Zhong et al., 2005). Huh7.5 and Huh7.5.1 cells show a higher permissiveness for HCV compared to the parental Huh7 cell line. This is partly due to a point mutation in the antiviral pattern recognition receptor *retinoic-acid-inducible gene-1* (RIG-I) (Sumpter et al., 2005). Huh7 cells were kindly provided by Ralf Bartenschlager. Charles M. Rice kindly provided Huh7.5 cells and Huh7.5.1 cells were obtained from Apath, LLC.



**Huh7.5-RFP-NLS-IPS:** Huh7.5 cells were transduced with lentiviral particles to stably induce the expression of a fluorescence-based reporter to visually monitor HCV infection *in vitro* (Jones et al., 2010). A red fluorescent protein (RFP) is fused to a nuclear localization signal (NLS) and parts of the *mitochondrial antiviral signaling protein* MAVS (also known as IPS or Cardiff or VISA). In naïve cells, the RFP signal localizes to mitochondria. In HCV-infected cells, IPS/MAVS is cleaved by the HCV NS3-4A protease and the RFP translocates to the nucleus, allowing to distinguish between HCV-infected and uninfected cells.

**Table 4: Cell culture media, buffers, and supplements.**

Name	Components
DMEM	Dulbecco's Modified Eagle Medium (high glucose, no glutamine), 10% (v/v) fetal bovine calf serum (FCS), 1% (v/v) GlutaMAX, 1% (v/v) penicillin/streptomycin
Freezing medium	90% (v/v) FCS, 10% (v/v) DMSO
2x HEPES buffered saline (HBS)	275 mM NaCl, 10 mM KCl, 1.4 mM Na <sub>2</sub> PO <sub>4</sub> , 42 mM HEPES, 11 mM glucose, adjust pH to 7.05
Chloroquine	25 mM chloroquine diphosphate in ddH <sub>2</sub> O, sterile filtered
Polybrene	4 mg/ml polybrene in PBS, sterile filtered
Cytomix	10 mM potassium phosphate buffer (pH 7.6), 120 mM KCl, 5 mM MgCl <sub>2</sub> , 25 mM HEPES, 0.15 mM CaCl <sub>2</sub> , 2 mM EGTA (pH 7.6) in dH <sub>2</sub> O; adjust pH 7.6 with 1 N KOH, sterile filtered. Add fresh prior to electroporation: 5 mM glutathione, 2 mM ATP
Trypsin-EDTA	0.05% Trypsin-EDTA
DPBS/PBS	1x Dulbecco's phosphate buffered saline, without CaCl <sub>2</sub> and MgCl <sub>2</sub>
PEG	40% (w/v) polyethylene glycol (PEG) in PBS

### 5.3 Solvents and buffers

#### 5.3.1 Lysis buffer

**Table 5: Lysis buffer.**

Name	Components
NP-40 lysis buffer	150 mM NaCl, 50 mM Tris-HCl (pH 7.4), 1% Nonidet P-40 (NP-40) in dH <sub>2</sub> O. Add fresh: 1x protease inhibitor cocktail (PIC), 1 mM PMSF

### 5.3.2 SDS PAGE and western blotting

**Table 6: SDS PAGE and western blotting buffer.**

Name	Components
6x Laemmli	375 mM Tris-HCl (pH 6.8), 25.8% (v/v) glycerol, 12.3% (w/v) SDS, 600 µg/ml bromophenol blue, 6% (v/v) β-mercaptoethanol in dH <sub>2</sub> O
10x running buffer	3.02% (w/v) Tris base, 18.8% (w/v) glycine, 1% (w/v) SDS in dH <sub>2</sub> O
10x transfer buffer	3.03% (w/v) Tris base, 14.4% (w/v) glycine in dH <sub>2</sub> O
1x transfer buffer	10% (v/v) 10x transfer buffer, 20% (v/v) methanol in dH <sub>2</sub> O
20x TBS-T	200 mM Tris-HCl (pH 7.7), 3 M NaCl, 1% (v/v) Tween-20 in dH <sub>2</sub> O
Blocking buffer	5% (w/v) nonfat dried milk powder in 1x TBS-T
Ponceau S	0.1% (w/v) ponceau S in 5% acetic acid
<u>Polyacrylamide gel</u>	
Stacking gel	130 mM Tris (pH 6.8), 17% (v/v) acrylamide, 1% SDS, 1% APS, 0.2 % (v/v) TEMED in ddH <sub>2</sub> O
12% running gel	500 mM Tris (pH 8.8), 40% (v/v) acrylamide, 1% SDS, 1% APS, 0.16% (v/v) TEMED in ddH <sub>2</sub> O
10% running gel	375 mM Tris (pH 8.8), 33% (v/v) acrylamide, 1% SDS, 1% APS, 0.16% (v/v) TEMED in ddH <sub>2</sub> O

### 5.3.3 Agarose gel electrophoresis

**Table 7: Agarose gel electrophoresis.**

Name	Components
50x TAE buffer	2 M Tris base, 5.71% acetic acid, 50 mM EDTA (pH 8) in dH <sub>2</sub> O
Agarose gel	1–2% (w/v) agarose, 1 µg/ml ethidium bromide (EtBr) in 1x TAE

### 5.3.4 DNA and protein ladder

**Table 8: DNA and protein standards.**

Ladder	Application	Company
GeneRuler DNA Ladder Mix	DNA/agarose gel electrophoresis	Thermo Fisher Scientific, Darmstadt
PageRuler Prestained Protein Ladder	Protein/western blotting	Thermo Fisher Scientific, Darmstadt

### 5.3.5 LD isolation buffer

**Table 9: Buffer used for LD isolation.**

Name	Components
Sucrose buffer	0.25 M Sucrose, 1 mM EDTA (pH 8) in ddH <sub>2</sub> O. Add fresh: 1 mM DTT, 1x PIC
Potassium phosphate buffer	190 mM KH <sub>2</sub> PO <sub>4</sub> , 810 mM K <sub>2</sub> HPO <sub>4</sub> , adjust to pH 7.4
Isotonic potassium phosphate buffer	50 mM potassium phosphate buffer (pH 7.4), 100 mM KCl, 1 mM EDTA (pH 8) in ddH <sub>2</sub> O. Add fresh: 1 mM PMSF

### 5.3.6 LEAP assay buffer

**Table 10: LEAP assay buffer.**

Name	Components
LEAP lysis buffer	1.5 mM KCl, 2.5 mM MgCl <sub>2</sub> , 5 mM Tris-HCl (pH 7.4), 1% (w/v) sodium deoxycholate, 1% (v/v) Triton-X-100 in nuclease-free H <sub>2</sub> O
Sucrose stock solution	80 mM NaCl, 5 mM MgCl <sub>2</sub> , 20 mM Tris-HCl (pH 7.4), 47% (w/v) sucrose in nuclease-free H <sub>2</sub> O, sterile filtered (0.22 µm). Add fresh: 1 mM DTT, EDTA-free protease inhibitors
Sucrose dilution buffer	80 mM NaCl, 5 mM MgCl <sub>2</sub> , 20 mM Tris-HCl (pH 7.4) in nuclease-free H <sub>2</sub> O, sterile filtered (0.22 µm). Add fresh: 1 mM DTT, EDTA-free protease inhibitors

Directly before usage, the LEAP assay lysis buffer was either supplemented with a combination of 1 mM PMSF, 20 µg/ml leupeptin, 2 µg/ml antipain and 1 µg/ml pepstatin or 1X cOmplete protease inhibitor. Sucrose solutions were either supplemented with combination of 1 mM PMSF, 20 µg/ml leupeptin, 2 µg/ml antipain and 1 µg/ml pepstatin or 1X cOmplete protease inhibitor directly before usage. For all reactions and buffers, nuclease-free water was used.

### 5.3.7 Solutions for immunofluorescence staining and microscopy

**Table 11: Solutions used for microscopy.**

Name	Components
Blocking solution	5% bovine serum albumin (BSA), 1% fish skin gelatin, 50 mM Tris-HCl in PBS
Mowiol	12% (w/v) Mowiol 4-88, 0.2 M Tris-HCl (pH 8.5), 30% (v/v) glycerol
Triton-X-100	0.1% (v/v) Triton-X-100 in PBS
PFA	16% (w/v) paraformaldehyde in PBS

### 5.4 Inhibitors

**Table 12: Inhibitors used in this study**

Inhibitor	Stock concentration	Company
Abacavir (ABA)	10 mM in DMSO	
Antipain	1 mg/ml in sterile H <sub>2</sub> O	Sigma-Aldrich Chemie GmbH, Taufkirchen
cOmplete™, EDTA-free protease inhibitor cocktail	25x in nuclease-free H <sub>2</sub> O	Sigma-Aldrich Chemie GmbH, Taufkirchen
Leupeptin	1 mg/ml in sterile H <sub>2</sub> O	Sigma-Aldrich Chemie GmbH, Taufkirchen
Pepstatin A	1 mg/ml in ethanol	Biomol GmbH, Hamburg
Phenylmethylsulfonyl fluoride (PMSF)	100 mM in isopropanol	Sigma-Aldrich Chemie GmbH, Taufkirchen
Protease inhibitor cocktail	100x	Sigma-Aldrich Chemie GmbH, Taufkirchen
RNaseOut	40 U/μl	Thermo Fisher Scientific, Darmstadt

### 5.5 Enzymes

**Table 13: Restriction enzymes.**

Enzyme	Company
EcoRI	New England Biolabs GmbH, Frankfurt am Main
NheI	New England Biolabs GmbH, Frankfurt am Main
SspI	New England Biolabs GmbH, Frankfurt am Main
MluI	New England Biolabs GmbH, Frankfurt am Main

All restriction enzymes were used with the supplied buffers according to the manufacturer's instructions.

**Table 14: Other enzymes.**

<b>Enzyme</b>	<b>Company</b>
Alkaline phosphatase, calf intestine (CIP)	New England Biolabs GmbH, Frankfurt am Main
Phusion high-fidelity DNA polymerase	Thermo Fisher Scientific, Darmstadt
RNAse A	Thermo Fisher Scientific, Darmstadt
SuperScript III reverse transcriptase	Thermo Fisher Scientific, Darmstadt
T4 DNA ligase	Thermo Fisher Scientific, Darmstadt
Taq DNA polymerase	Thermo Fisher Scientific, Darmstadt
Mung bean nuclease	New England Biolabs GmbH, Frankfurt am Main
T4 DNA polymerase, LIC qualified	New England Biolabs GmbH, Frankfurt am Main

## 5.6 Kits

**Table 15: Commercial kits used in this study.**

<b>Kit</b>	<b>Company</b>
DC protein assay	Bio-Rad Laboratories GmbH München
DNA-free DNA removal kit (Ambion)	Thermo Fisher Scientific, Darmstadt
Maxima SYBR green qPCR master mix	Thermo Fisher Scientific, Darmstadt
Megascript T7 transcription kit	Thermo Fisher Scientific, Darmstadt
Dual-luciferase reporter assay system	Promega GmbH, Mannheim
NucleoBond XtraMaxi kit	Macherey-Nagel, Düren
NucleoSpin Gel and PCR clean-up kit	Macherey-Nagel, Düren
NucleoSpin Plasmid kit	Macherey-Nagel, Düren
Pierce Coomassie Plus (Bradford) assay reagent	Thermo Fisher Scientific, Darmstadt
<i>Renilla</i> luciferase assay system	Promega GmbH, Mannheim
QUANTI-Blue solution	Invivogen, Toulouse (France)

## 5.7 Plasmids

**Table 16: HCV Plasmids.**

Number	Name	Description	Source/Reference
pMO661	pBR322 JFH <sup>wt</sup>	HCV JFH1 <sup>wt</sup>	Eva Herker (Wakita et al., 2005)
pMO702	pBR322 Jc1 <sup>wt</sup>	HCV Jc1 <sup>wt</sup> (J6/JFH1 chimera)	Ralf Bartenschlager (Pietschmann et al., 2006)
HH183	pBR322 Jc1 <sup>p7-GLuc-2A-NS2</sup>	Jc1 strain expressing a secreted gaussia luciferase followed by a modified P2A ribosomal skipping site between p7 and NS2.	Cloning strategy described by (Marukian et al., 2008). Cloned by Anja Schöbel
pMO981	pBR322 Jc1 <sup>NS5AB-EGFP-BSD</sup>	Jc1 reporter with an EGFP and a blasticidin resistance in a duplicated NS5AB cleavage site.	Brian Webster (Webster et al., 2013)
pMO977	pBR322 Jc1 <sup>NS5AB-EGFP</sup>	Jc1 reporter encoding an EGFP in a duplicated NS5AB cleavage site.	Brian Webster (Webster et al., 2013)
pMO979	pBR322 Jc1 <sup>NS5AB-mKO2</sup>	Jc1 reporter encoding an mKO2 in a duplicated NS5AB cleavage site.	Brian Webster (Webster et al., 2013)
HH337	pBR322 Jc1ΔE1E2 <sup>NS5AB-FLuc</sup>	Jc1 replicon with partly deleted envelope proteins and a firefly luciferase in a duplicated NS5AB cleavage site	Susan Lassen
HH366	pBR322 Jc1ΔE1E2 <sup>NS5AB-EGFP</sup>	Jc1 replicon with partly deleted envelope proteins and an EGFP in a duplicated NS5AB cleavage site	this thesis
HH166	pUC Con1 replicon	HCV gt1b subgenomic replicon. Expresses NS3-NS5B and a neomycin resistance gene	James Ou (Choi et al., 2004)

**Table 17: Expression plasmids.**

Number	Name	Description	Source/Reference
HH96	pCDNA3.1	Eukaryotic expression vector. Used as empty control vector in this study	Thermo Fisher Scientific, Darmstadt
HH98	Trip-RFP-NLS-IPS	Reporter plasmid for detection of HCV infection <i>in vitro</i>	Charles M. Rice (Jones et al., 2010)

## Material

HH106	LeGO-iCer2	Lentiviral vector containing cerulean and an IRES	Boris Fehse (Weber et al., 2008)
HH158	pSicoR-MS1ΔU6	Lentiviral expression vector carrying an mCherry and an EF1α promoter. The U6 promoter was removed from the original pSicoR-MS1	pSicoR-MS1: Matt Spindler (Wissing et al., 2011); pSicoR-MS1ΔU6 : Anja Schöbel
HH245	LeGO-iCer2 FLAG-core	Lentiviral vector for expression of 3X FLAG-Core (gt2a); expresses cerulean from an IRES	Kathrin Rösch (Rosch et al., 2016)
HH283	pEF1alpha HA-L1ORF1p	Eukaryotic expression vector for expression of an HA-tagged LINE1 ORF1; backbone: pEF1alpha from E. Herker	Silke Wissing
HH292	pKS (+) LRE3-EF1-mEGFPi	Retrotransposition reporter plasmid. pBluescript KS+ contains an EF1α-driven LINE1 element (LRE3) with an EGFP retrotransposition indicator cassette under the control of a ubiquitin promoter. The EGFP is disrupted by an intron.	Silke Wissing (Wissing et al., 2011)
HH293	pKS (+) LRE3-EF1-mEGFPiΔintron	Transfection control for HH292. Same construct but without the intron in the EGFP.	Silke Wissing (Wissing et al., 2011)
HH309	LeGO-iCer2 NS5A-FLAG	Lentiviral vector for expression of NS5A-FLAG (gt2a); expresses cerulean from an IRES	Kathrin Rösch (Rosch et al., 2016)
HH377	pSicoR-MS1ΔU6 HA-L1ORF1p_2A_mCherry	Lentiviral vector for expression of HA-L1ORF1p followed by a 2A sequence and mCherry	this thesis
HH439	pSicoR-MS1ΔU6 HA-L1ORF1p (261-262 mut)_2A_mCherry	Lentiviral vector for expression of a putative HA-L1ORF1p RNA binding mutant followed by a 2A sequence and mCherry. RR residues at position 261-262 were mutated to AA.	this thesis
pMO155	pHR' EGFP	Lentiviral vector expressing an IRES-driven EGFP	(Herker et al., 2010)
pMO160	pHR' Core EGFP	Lentiviral vector for expression of HCV core (gt1b) and an IRES-driven EGFP	(Herker et al., 2010)
pMO778	pHR'-FLAG-Core IRES EGFP	Lentiviral vector for expression of FLAG-HCV core (gt1b) and an IRES-driven EGFP	Eva Herker
HH282	pCEP4-EGFP	Eukaryotic expression vector containing an EGFP and a hygromycin resistance gene	Thermo Fisher Scientific, Darmstadt

## Material

HH311	pDK101	Episomal eukaryotic expression vector (pCEP4) for expression of a full-length LINE1 (L1.3) containing a Neo <sup>R</sup> retrotransposition indicator cassette. ORF1 is tagged with a T7 epitope tag. The backbone contains a hygromycin resistance gene for selection	Gerald G Schumann (Kulpa and Moran, 2005)
HH316	pDK135	L1ORF2p reverse transcriptase inactive mutant of pDK101 (D702A).	Gerald G. Schumann (Kulpa and Moran, 2005)
pGL4.75	pGL4.75[hRluc/CMV]	Control plasmid for dual luciferase assay; expresses the <i>Renilla</i> luciferase	Promega GmbH, Mannheim
pMO86	pCMVΔR8.91	Lentiviral packaging vector	(Naldini et al., 1996)
pMO87	pMD.G	VSV-G envelope glycoprotein	(Naldini et al., 1996)
pHR <sup>+</sup> 319	pCDNA-TO FLAG-Core	Eukaryotic expression vector; contains HCV core (gt2a) with an N-terminal 3X FLAG under the control of a CMV promoter in a pCDNA-TO backbone	Holly Ramage (Ramage et al., 2015)
HH440	pSicoR-MS1ΔU6 SEAP_2A_EGFP	Lentiviral vector for expression of a secreted embryonic alkaline phosphatase (SEAP). Also contains EGFP as marker for transduction.	this thesis
HH436	pSicoR-MS1ΔU6 EGFP	Lentiviral vector expressing EGFP. pEGFP-C1 (Clontech) was used as template for EGFP PCR	this thesis
pMO827	pLIVE SEAP	Eukaryotic expression vector for expression of SEAP in mice	Mirus Bio LCC
pMO226	pEGFP-C1	Eukaryotic expression vector; contains an EGFP and an MCS	Clontech Laboratories / Takara Bio USA Inc.



## 5.8 Oligonucleotides

**Table 18: PCR primer to clone HA-L1ORF1p and the HA-L1ORF1p RR261-262AA mutant into pSicoR-MS1ΔU6.**

Description	Primer no	Sequence 5'–3'
HA-L1ORF1p sense	Primer 1	TGGATCCGCTAGCATGTACCCATACGAT
L1ORF1p AAA as	Primer 2	CTCTGCTGCGGCTTGTAGGGTTTCTGCCGA GAG
AAA sense	Primer 3	CAAGCCGCAGCAGAGTGGGGGCCAATATT C
HA-L1ORF1p 2A as	Primer 4	TCGACGTCTCCCGCAAGCTTAAGAAGGTCA AAATTCATTTTGGCATGATT
mCherry 2A sense	Primer 5	TGCGGGAGACGTCGAGTCCAACCCTGGGC CA GTGAGCAAGGGCGAG
EcoRI mCherry as	Primer 6	CTCGACGAATTCTTACTTGTACAG

**Table 19: PCR Primer to clone SEAP\_2A\_EGFP or EGFP into pSicoR-MS1ΔU6.**

Description	Primer no	Sequence 5'–3'
<u>pSicoRAU6 EGFP</u>		
LIC NheI EGFP sense		GTGACCGGCGCCTACGCTAGATGGTGAGC AAGGGCGAG
LIC EGFP EcoRI as		ATTAGGTCCCTCGACGAATTTTACTTGTAC AGCTCGTC
<u>pSicoR-MS1ΔU6_SEAP_2A_EGFP</u>		
NheI SEAP sense	Primer 7	TACGCTAGCATGCTGCTGCTGCTGCTGCT G
SEAP 2A as	Primer 8	TCGACGTCTCCCGCAAGCTTAAGAAGGTC AAAATT TGTCTGCTCGAAGCGGCC
2A EGFP sense	Primer 9	TGCGGGAGACGTCGAGTCCAACCCTGGGC CA GTGAGCAAGGGCGAG
EGFP EcoRI as	Primer 10	CTCGACGAATTCTTACTTGTACAGCTCGTC

**Table 20: qRT-PCR primer.**

Name	Sequence 5'–3'	Reference
L1ORF1p fw	TCAAAGGAAAGCCCATCAGACTA	(Wissing et al., 2012)
L1ORF1p rev	TTGGCCCCCACTCTCTTCT	
L1ORF2p fw	GAGAGGATGCGGAGAAATAGGA	(Daskalos et al., 2009)
L1ORF2p rev	GGATGGCTGGGTCAAATGGT	
JFH1 fw	CGGGAGAGCCATAGTGG	(Herker et al., 2010)
JFH1 rev	AGTACCACAAGGCCTTTTCG	
18S rRNA fw	GTAACCCGTTGAACCCCAT	
18S rRNA rev	CCATCCAATCGGTAGTAGCG	

**Table 21: LEAP primer.**

Name	Sequence 5'–3'	Reference
LINE1 LEAP	GCGAGCACAGAATTAATACGACT CACTATAGGTTTTTTTTTTTT	(Kulpa and Moran, 2006)
HCV + strand LEAP	GCGAGCACAGAATTAATACGACT CACTATAGGAAAAAAAAAAAAA	
LINE1 PCR (ORF2p- 3'UTR sense)	GTAACCTAACCTGCACAATGTGCAC ATGTACCCTAAA	
HCV + strand PCR	ACCAAGCTCAAACCTCACTCCATTG CCGG	
HCV – strand PCR 1	TACGGCACTCTCTGCAGTCATGC GGCTCAC	
HCV – strand PCR 2	ACATGATCTGCAGAGAGACCAGT TACGGCA	
3' $\beta$ -Actin PCR	GGAGGTGATAGCATTGCTTTTCGT G	(Kulpa and Moran, 2006)
linker PCR	GCGAGCACAGAATTAATACGACT	(Kulpa and Moran, 2006)

## 5.9 Antibodies and dyes

**Table 22: Primary antibodies.**

Antigen/clone	Species	Dilution	Company	Catalogue no
HA	rb	WB 1:1000 IF 1:100	Sigma-Aldrich Chemie GmbH, Taufkirchen	H6908-100UL
HA (Y-11)	gt	WB 1:500; 1:1000	Santa Cruz Biotechnology, Heidelberg	sc-805-G
NS5A (2F6/G11)	ms	WB 1:500; 1:1000	IBT-GmbH, Reutlingen	HCM-131-5
HCV Core (C7-50)	ms	WB 1:500; 1:250 IF: 1:50; 1:25	Santa Cruz Biotechnology, Heidelberg	sc-57800
Flag	rb	WB 1:1000	Sigma-Aldrich Chemie GmbH, Taufkirchen	F7425-.2MG
PLIN2	gp	WB 1:1000	PROGEN Biotechnik GmbH, Heidelberg	GP40
PLIN2	rb	WB 1:1000	Abcam, Cambrige (UK)	ab52355
L1ORF1p #984	rb	WB 1:2000	Gerald G. Schumann	
L1ORF2p (mAb chA1-L1)	ms	WB 1:500	Gerald G. Schumann	(De Luca et al., 2016)
PABPC1 (10E10)	ms	WB 1:250	Santa Cruz Biotechnology, Heidelberg	sc-32318
MOV-10 (B-3)	ms	WB 1:250; 1:100	Santa Cruz Biotechnology, Heidelberg	sc-515722
Tubulin (B 5-1-2)	ms	WB 1:2000	Sigma-Aldrich Chemie GmbH, Taufkirchen	T6074
T7 Tag	ms	WB 1:7500	Merck, Darmstadt	69522-3

**Table 23: Secondary antibodies.**

<b>Antibody</b>	<b>Dilution</b>	<b>Company</b>
Peroxidase-AffiniPure goat anti-mouse IgG (H+L)	WB 1:10,000	JacksonImmunoResearch Laboratories, Suffolk (UK)
Peroxidase-AffiniPure goat anti-rabbit IgG (H+L)	WB 1:10,000	JacksonImmunoResearch Laboratories, Suffolk (UK)
Peroxidase AffiniPure Goat Anti-Guinea Pig IgG (H+L)	WB 1:10,000	JacksonImmunoResearch Laboratories, Suffolk (UK)
Peroxidase-AffiniPure donkey anti-goat IgG (H+L)	WB 1:10,000	JacksonImmunoResearch Laboratories, Suffolk (UK)
Rabbit TrueBlot: Anti-Rabbit IgG HRP	WB 1:1,000	eBioscience
Mouse TrueBlot ULTRA: Anti-Mouse IgG HRP clone eB144	WB 1:2,000	Rockland antibodies and assays <i>via</i> Biomol GmbH, Hamburg
Alexa Fluor 555 donkey anti-mouse IgG (H+L)	IF 1:1,000	Thermo Fisher Scientific, Darmstadt
Alexa Fluor 647 Donkey anti-rabbit IgG (H+L)	IF 1:1,500	Thermo Fisher Scientific, Darmstadt

**Table 24: Fluorescent dyes.**

<b>Dye</b>	<b>Dilution</b>	<b>Company</b>
BODIPY493/503 (1 mg/ml)	IF 1:750	Thermo Fisher Scientific, Darmstadt
Hoechst (10 mg/ml)	IF 1:6,000	Sigma-Aldrich GmbH, Taufkirchen

**Table 25: Agarose beads.**

<b>Description</b>	<b>Quantity</b>	<b>Company</b>	<b>Catalogue no</b>
Anti-FLAG M2 affinity gel (ms)	IP: 30 µl/sample	Sigma-Aldrich Chemie GmbH, Taufkirchen	A2220-5ML
HA agarose (HA-7) (ms)	IP: 30µl/sample	Sigma-Aldrich Chemie GmbH, Taufkirchen	A2095-1ML

## 5.10 Consumables

**Table 26: Consumables.**

Name	Company
Adhesive PCR seal	Sarstedt AG & Co KG, Nümbrecht
Amersham Hyperfilm ECL	Geyer Th. GmbH & Co.KG, Renningen
Blunt-end cannula	Kleiser Medical GmbH, Messkirch
Needle	neoLab Migge GmbH, Heidelberg
Amersham Protran Premium	Geyer Th. GmbH & Co.KG, Renningen
Nitrocellulose membrane	
96 Fast PCR Plate half skirt	Sarstedt AG & Co KG, Nümbrecht
1.5 ml-reaction tubes RNase free	Sarstedt AG & Co KG, Nümbrecht
5 Prime Phase-Lock Tube	5Prime GmbH, Hilden
Biosphere Filter Tips, RNase free	Sarstedt AG & Co KG, Nümbrecht
Cryo-Tubes	Sarstedt AG & Co KG, Nümbrecht
Centrifuge tube, thinwall ultraclear	Beckman Coulter GmbH, Krefeld
15 ml- and 50 ml-tubes (conical)	Greiner GmbH, Frickenhausen
96-Well microtestplate conical bottom	Sarstedt AG & Co KG, Nümbrecht
Cell scraper	VWR International GmbH, Darmstadt
Cell culture dishes	Sarstedt AG & Co KG, Nümbrecht; Greiner GmbH, Frickenhausen
Cell culture flasks	Sarstedt AG & Co KG, Nümbrecht
Cell culture plates	Sarstedt AG & Co KG, Nümbrecht
Cellstar serological pipettes	Greiner GmbH, Frickenhausen
Combitips advanced (Eppendorf)	VWR International GmbH, Darmstadt
Cover slips	VWR International GmbH, Darmstadt
Electroporation cuvette 2 mm	VWR International GmbH, Darmstadt
Electroporation cuvette 4 mm	VWR International GmbH, Darmstadt
Luer-Lok syringe	BD Plastipak, Heidelberg
C-Chip disposable Neubauer counting chamber	VWR International GmbH, Darmstadt
Glass slides	VWR International GmbH, Darmstadt
Dounce homogenizer, 2 ml	Thermo Fisher Scientific, Darmstadt
Microtest plate	Sarstedt AG & Co KG, Nümbrecht
Nunc-Immuno MicroWell 96 well polystyrene plates (white)	Thermo Fisher Scientific, Darmstadt

PCR tubes	Sarstedt AG & Co KG, Nümbrecht
Pipette tips	VWR International GmbH, Darmstadt
SafeSeal 1.5 ml-reaction tube	Sarstedt AG & Co KG, Nümbrecht
SafeSeal 2 ml-reaction tube	Sarstedt AG & Co KG, Nümbrecht
Parafilm	Bemis, Oshkosh, USA
Rotilabo liquid-reservoirs	Roth GmbH + Co. KG, Karlsruhe
Steriflip 0.22 µm	Merck Millipore, Darmstadt
Sterile filter 0.22 µm	Thermo Fisher Scientific, Darmstadt
Sterile filter 0.45 µm	Thermo Fisher Scientific, Darmstadt
Syringe	neoLab GmbH, Heidelberg
Whatman paper	GE Healthcare, München

## 5.11 Chemicals

**Table 27: Chemicals.**

Chemical	Company
1,4-Dithiothreitol (DTT)	Thermo Fisher Scientific, Darmstadt
100x BSA (bovine serum albumin for restriction enzymes)	New England Biolabs GmbH, Frankfurt am Main
10x Mung bean nuclease buffer	New England Biolabs GmbH, Frankfurt am Main
10x NEBuffer (NEB)	New England Biolabs GmbH, Frankfurt am Main
10x T4-ligase buffer	Thermo Fisher Scientific, Darmstadt
10x Taq buffer - $\text{MgCl}_2$ + $(\text{NH}_4)_2\text{SO}_4$	Thermo Fisher Scientific, Darmstadt
25 mM $\text{MgCl}_2$ (PCR)	Thermo Fisher Scientific, Darmstadt
2-Propanol	AppliChem GmbH, Darmstadt
5x Phusion HF buffer	Thermo Fisher Scientific, Darmstadt
6x DNA loading dye	Thermo Fisher Scientific, Darmstadt
Acetic acid	AppliChem GmbH, Darmstadt
Acrylamide solution (30%) - Mix 37.5	AppliChem GmbH, Darmstadt
Adenosine triphosphate (ATP)	AppliChem GmbH, Darmstadt
Agar bacteriology grade	AppliChem GmbH, Darmstadt
Agarose basic	AppliChem GmbH, Darmstadt
Albumin from bovine serum	AppliChem GmbH, Darmstadt
Ammonium persulfate (APS)	AppliChem GmbH, Darmstadt
Ampicillin sodium salt	AppliChem GmbH, Darmstadt
Blasticidin S	Invivogen, Toulouse, France

Bromophenol blue	AppliChem GmbH, Darmstadt
Calcium chloride (CaCl <sub>2</sub> )	AppliChem GmbH, Darmstadt
Chloroform	AppliChem GmbH, Darmstadt
Chloroquine diphosphate	Sigma-Aldrich Chemie GmbH, Taufkirchen
Coelenterazin	Roth GmbH + Co. KG, Karlsruhe
D (+)-Glucose monohydrat	AppliChem GmbH, Darmstadt
Dimethyl sulfoxide (DMSO)	AppliChem GmbH, Darmstadt
Dimethyl sulfoxide (DMSO) for PCR	Thermo Fisher Scientific, Darmstadt
di-potassium hydrogen phosphate (K <sub>2</sub> HPO <sub>4</sub> )	AppliChem GmbH, Darmstadt
Disodium phosphate (Na <sub>2</sub> HPO <sub>4</sub> )	AppliChem GmbH, Darmstadt
dNTP Mix 10 mM	Thermo Fisher Scientific, Darmstadt
Dulbecco's modified eagle medium (high glucose) (Gibco)	Thermo Fisher Scientific, Darmstadt
Dulbecco's phosphate buffered saline (DPBS)	Sigma-Aldrich Chemie GmbH, Taufkirchen
ECL Lumi-Light western blotting substrate	Hoffmann-la Roche, Basel (Switzerland)
EDTA	AppliChem GmbH, Darmstadt
Ethanol	Geyer Th. GmbH & Co.KG, Renningen
Ethanol absolute (used for RNA isolation)	AppliChem GmbH, Darmstadt
Ethanol ROTIPURAN 99,8%	Roth GmbH + Co. KG, Karlsruhe
Ethidium bromide (EtBr)	AppliChem GmbH, Darmstadt
Fetal calf serum (FCS)	Biochrom AG, Berlin
Fishskin gelatine	AppliChem GmbH, Darmstadt
Fugene6 transfection reagent	Promega GmbH, Mannheim
G418 disulfate solution	AppliChem GmbH, Darmstadt
GlutaMAX 100x (Gibco)	Thermo Fisher Scientific, Darmstadt
Glutathione	AppliChem GmbH, Darmstadt
Glycerol anhydrous	AppliChem GmbH, Darmstadt
Glycine	AppliChem GmbH, Darmstadt
Glycogen RNA grade	Thermo Fisher Scientific, Darmstadt
HEPES	Sigma-Aldrich Chemie GmbH, Taufkirchen
Hydrogen chloride (HCl)	AppliChem GmbH, Darmstadt
hygromycin B Gold	Invivogen, Toulouse, France
Isopropanol (used for RNA isolation)	Sigma-Aldrich Chemie GmbH, Taufkirchen
Kanamycin sulfate	AppliChem GmbH, Darmstadt
Magnesium chloride (MgCl <sub>2</sub> )	AppliChem GmbH, Darmstadt

Methanol (MeOH)	AppliChem GmbH, Darmstadt
Mowiol 4-88	AppliChem GmbH, Darmstadt
Nonfat dried milk powder	AppliChem GmbH, Darmstadt
Nonidet P-40	AppliChem GmbH, Darmstadt
Nuclease-free water (Ambion)	Thermo Fisher Scientific, Darmstadt
OptiMEM (Gibco)	Thermo Fisher Scientific, Darmstadt
Paraformaldehyde (PFA)	AppliChem GmbH, Darmstadt
Penicillin/streptomycin 100x	Sigma-Aldrich Chemie GmbH, Taufkirchen
Phenol-chloroform-isoamyl alcohol (25:24:1 vol/vol/vol)	AppliChem GmbH, Darmstadt
Phenylmethylsulfonyl fluoride (PMSF)	AppliChem GmbH, Darmstadt
Polybrene (hexadimethrine bromide)	Sigma-Aldrich Chemie GmbH, Taufkirchen
Polyethylene glycol (PEG) - 8000	AppliChem GmbH, Darmstadt
Ponceau S	AppliChem GmbH, Darmstadt
Potassium chloride (KCl)	AppliChem GmbH, Darmstadt
Potassium dihydrogenphosphate (KH <sub>2</sub> PO <sub>4</sub> )	AppliChem GmbH, Darmstadt
Potassium hydroxide (KOH)	AppliChem GmbH, Darmstadt
Random hexamer primer	QIAGEN, Hilden
Recombinant protein G agarose	Thermo Fisher Scientific, Darmstadt
RNase Away	Roth GmbH + Co. KG, Karlsruhe
Sodium acetate (C <sub>2</sub> H <sub>3</sub> NaO <sub>2</sub> ) 3 M pH 5.2	AppliChem GmbH, Darmstadt
Sodium chloride (NaCl)	AppliChem GmbH, Darmstadt
Sodium deoxycholate	AppliChem GmbH, Darmstadt
Sodium dodecyl sulfate (SDS)	AppliChem GmbH, Darmstadt
Sodium hydroxide	AppliChem GmbH, Darmstadt
Sodium hypochlorite	Merck, Darmstadt
Sspl-buffer	New England Biolabs GmbH, Frankfurt am Main
Sucrose	AppliChem GmbH, Darmstadt
SuperSignal West Femto	Thermo Fisher Scientific, Darmstadt
TEMED (Tetramethylethylenediamine)	AppliChem GmbH, Darmstadt
TRI reagent	Sigma-Aldrich Chemie GmbH, Taufkirchen
Tris ultrapure (Tris-base)	AppliChem GmbH, Darmstadt
Triton X-100	AppliChem GmbH, Darmstadt
Trypan blue solution 0,4%	Thermo Fisher Scientific, Darmstadt
Trypsin/EDTA (0,05%/0,02% w/v) (Gibco)	Thermo Fisher Scientific, Darmstadt



Tryptone	AppliChem GmbH, Darmstadt
Tween 20	AppliChem GmbH, Darmstadt
Yeast extract	AppliChem GmbH, Darmstadt
β-Mercaptoethanol	AppliChem GmbH, Darmstadt

## 5.12 Devices

**Table 28: Devices and Equipment.**

Name	Company
Eppendorf Research plus pipettes	Eppendorf AG, Hamburg
Erlenmeyer flask 1000 ml	VWR International GmbH, Darmstadt
Glass flask	VWR International GmbH, Darmstadt
Beaker 50–4000 ml	VWR International GmbH, Darmstadt
Centrifuge bottles for Sorvall	Thermo Fisher Scientific, Darmstadt
Agarose casting stand	Bio-Rad Laboratories GmbH München
Agarose gel chamber comb	Bio-Rad Laboratories GmbH München
Centrifuge 5424R	Eppendorf AG, Hamburg
Centrifuge 5810R	Eppendorf AG, Hamburg
Centrifuge Multifuge 3 SR	Thermo Fisher Scientific, Darmstadt
Centrifuge Sorvall RC5C Plus	Thermo Fisher Scientific, Darmstadt
BD FACSCanto Flow Cytometer	BD Science, Heidelberg
BD LSR Fortessa flow cytometer	BD Bioscience, Heidelberg
GelDoc	Bio-Rad Laboratories GmbH München
Gene Pulser Xcell electroporation system	Bio-Rad Laboratories GmbH München
GeneAmp PCR system 9700	Applied Biosystems, Darmstadt
7500 fast real time PCR system	Applied Biosystems, Darmstadt
Hera freezer	Thermo Fisher Scientific, Darmstadt
HERAsafe incubator	Thermo Fisher Scientific, Darmstadt
Herasafe sterile bench	Thermo Fisher Scientific, Darmstadt
Infinite M200 plate reader	Tecan Group Ltd, Männedorf
Leica DMIL microscope	Leica Camera AG, Wetzlar
Magnetic stirrer heating plate IKA RH basic	IKA-Werke GmbH & CO. KG, Staufen
Innova 43 incubator	New Brunswick Scientific, Hamburg
Micro centrifuge	Roth GmbH + Co. KG, Karlsruhe
Mini Trans-Blot Module	Bio-Rad Laboratories GmbH München

Mini-PROTEAN Tetra Cell	Bio-Rad Laboratories GmbH München
Multipipette plus	Eppendorf AG, Hamburg
Nanodrop 1000 Spectrophotometer	Peqlab Biotechnologie GmbH, Erlangen
Neubauer Counting Chamber	Cellomics Technology, Halethopre (MD)
Nikon C2plus	Nikon, Düsseldorf
Pipette boy	VWR International GmbH, Darmstadt
PowerPac HC High-Current Power Supply	Bio-Rad Laboratories GmbH München
Analytical balance Extend ED224S	Sartorius AG, Göttingen
Scale PM4600 DeltaRange	Mettler Toledo, Gießen
X-Ray film processor Agfa Classic E.O.S.	Siemens AG, Erlangen
Thermomixer comfort	Eppendorf AG, Hamburg
UV Illuminator	VWR International GmbH, Darmstadt
Vortex-Genie 2	VWR International GmbH, Darmstadt
Water bath WBT-series	LTF Labortechnik, Wasserburg
Wide Mini Sub Cell GT	BioRad Laboratories GmbH München
Optima L-90K ultracentrifuge	Beckman Coulter GmbH, Krefeld
Optima XE-90 ultracentrifuge	Beckman Coulter GmbH, Krefeld
SW 60 Ti Swinging-Bucket Rotor with buckets	Beckman Coulter GmbH, Krefeld
SW 28 Swinging-Bucket Rotor with buckets	Beckman Coulter GmbH, Krefeld
Plan Apo VC 60x H Oil objective	Nikon, Düsseldorf
Sorvall SLA-3000 Super-Lite rotor	Thermo Fisher Scientific, Darmstadt
Heraeus UT 6200	Thermo Fisher Scientific, Darmstadt
Platform rocker	LTF Labortechnik, Wasserburg
Tube roller SRT1	Stuart Equipment, Staffordshire (UK)
Graduated cylinder 50–2000 ml	VWR International GmbH, Darmstadt
Glass culture vials Duran 16x160mm	VWR International GmbH, Darmstadt

## 5.13 Software

**Table 29: Software.**

Name	Company
7500 Software v2.3	AB Applied Biosystems, Darmstadt
BD FACSDiva 5.0.3	BD Bioscience, Heidelberg
BD FACSDiva 8.0.1	BD Bioscience, Heidelberg
Fiji/ ImageJ 1.48t	Wayne Resband, National Institutes of Health (USA)

FlowJo	Treestar Inc., Ashland (USA)
NIS-Elements Ar 4.3	Nikon, Düsseldorf
NIS-Element Viewer 4.2	Nikon, Düsseldorf
R Studio Version 1.1.453	R Studio Inc., Boston (USA)
Serial Cloner 2.6.1	Serial Basics
Microsoft Office	Microsoft

## 6 Methods

### 6.1 Molecular biological methods

#### 6.1.1 Cultivation of bacteria

The cultivation of transformed *E. coli* DH5 $\alpha$  was performed in LB media at 37 °C, 230 rpm in a shaking device or on LB agar plates at 37 °C. LB media and agar plates contained 100  $\mu$ g/ml ampicillin or 50  $\mu$ g/ml kanamycin for selection of successfully transformed clones.

#### 6.1.2 Plasmid isolation

Plasmids were isolated from bacterial overnight (o/n) cultures using commercial plasmid isolation kits following the manufacturer's instructions. For small-scale isolation, 3 ml cultures were incubated o/n, and plasmid DNA was isolated using the NucleoSpin plasmid kit. For large-scale isolation, a 3 ml starter culture was inoculated and transferred to 300-500 ml LB medium for o/n incubation. Plasmid DNA was isolated using the Nucleobond Xtra Maxi Kit and the pellet was resolved in TE-buffer. Plasmid purity and concentration was photometrically determined (NanoDrop).

#### 6.1.3 Glycerol stocks

Glycerol stocks were prepared by mixing bacteria suspension with 100% glycerol and stored at -80 °C.

#### 6.1.4 Cloning

##### 6.1.4.1 Polymerase chain reaction (PCR)

DNA fragments of interest were amplified *in vitro* using specific primers. Standard reactions and PCR conditions are equivalent to the conditions listed below (see 6.1.4.2, table 30). Annealing temperatures were adjusted according to the primers'  $T_m$ .

##### 6.1.4.2 Overlap extension PCR

The overlap extension PCR was used to construct a lentiviral expression vector for the overexpression of an HA-tagged L1ORF1p (wt) and to introduce the RR261-262AA mutation. Further, the insert for a lentiviral vector for SEAP expression was generated by overlap PCR. In a first step, conventional PCR reactions were performed with primer pairs carrying specific

overhangs to generate overlapping PCR fragments. Primers are listed in table 18 and 19. The reaction mixture and PCR conditions are listed below (table 30 and 31).

**Table 30: PCR reaction mix.**

Component	Volume	wt	RR261-262AA	SEAP
5x Phusion HF buffer	10µl			
10 mM dNTPs	1 µl			
DMSO	2 µl			
Primer sense (10µM)	2.5 µl	PCR I = primer 1+4	PCR I = primer 1+2	PCR I = primer 7+8
Primer as (10µM)	2.5 µl	PCR II = primer 5+6	PCR II = primer 3+4 PCR III = primer 5+6	PCR II = primer 9+10
Template	100 ng			
Phusion DNA polymerase	0.5 µl			
dH <sub>2</sub> O	ad 50 µl			

**Table 31: PCR conditions.**

Cycle step	Temperature	Time	Repeat
Initial Denaturation	98 °C	2 min	1x
Denaturation	98 °C	10 s	25x
Annealing	57 °C	30 s	
Extension	72 °C	45 s	
Final Extension	72 °C	10 min	1x
hold	4 °C	∞	

PCR products were loaded to a 1% or 1.5% agarose gel. Fragments of the correct size were excised and purified using the NucleoSpin Gel & PCR Clean-up Kit according to the manufacturer's instructions. In a third PCR reaction (overlap), overlapping PCR products are mixed to enable hybridization followed by amplification. Here, equimolar amounts of the initial PCR products were used. In a final PCR reaction using the outer sense and as primer, the overlap product was purified. The PCR reaction mixture and PCR conditions are listed below (table 32, 33 and 34).

**Table 32: Overlap PCR reaction mix.**

Component	Volume
5x Phusion HF buffer	10 µl
10 mM dNTPs	1 µl
DMSO	2 µl
Product PCR I	x µl
Product PCR II	x µl
Phusion DNA-Pol	0.5 µl
dH <sub>2</sub> O	Ad 45 µl

**Table 33: Overlap PCR conditions.**

Cycle step	Temperature	Time	Repeats
Initial Denaturation	98 °C	2 min	1x
Denaturation	98 °C	10 s	15x
Annealing	60 °C (wt, RR261-262AA) 55 °C (SEAP)	30 s	
Extension	72 °C	1:30 min	

2.5 µl of the outer sense and as primer (wt = primer 1 + primer 6; RR261-262AA = primer 1 + primer 4; SEAP = primer 7 + primer 10) were added to the overlap PCR and the purification was performed as described below. For generation of the RR261-262AA mutant, a second overlap PCR was performed merging the product of the first overlap (PCR I + PCR II) with PCR product III. For purification, primer 1 and primer 6 were used.

**Table 34: Purification PCR conditions.**

Cycle step	Temperature	Time	Repeats
Initial Denaturation	98 °C	2 min	1x
Denaturation	98 °C	10 s	20x
Annealing	60 °C (wt, RR261-262AA) 55 °C (SEAP)	30 s	
Extension	72 °C	1:30 min	
Final Extension	72 °C	10 min	1x
hold	4 °C	∞	

PCR products were analyzed on a 1% agarose gel. Fragments of the correct size were excised and purified using the NucleoSpin Gel & PCR Clean-up Kit according to the manufacturer's instructions.

#### 6.1.4.3 Restriction endonuclease digestion

In order to insert the amplified PCR product into a vector backbone, restriction endonuclease digestion of the respective plasmid and insert was performed to create compatible overhangs. Cloning into the lentiviral vector pSicoR-MS1ΔU6 (HH158) used in this study was carried out using the NheI and EcoRI restriction sites. The protocol is listed below (table 35).

**Table 35: Restriction digest**

Component	Insert	Vector
DNA	0.1-0.5 µg	3 µg
10x NEB 1	2 µl	2 µl
10X BSA	2 µl	2 µl
NheI	0.5 µl	0.5 µl
EcoRI	0.5 µl	0.5 µl
dH <sub>2</sub> O	ad 20 µl	ad 20 µl

Digestion with EcoRI and NheI was performed for a minimum of 2 hours at 37 °C. For all other restriction digests performed in this study, buffer conditions for specific enzymes were selected according to the manufacturer's instructions. To avoid re-ligation of the vector, the vector was dephosphorylated for 20 minutes at 37 °C by adding 1 µl CIP to the vector digestion mixture. Successful digestion of the vector was analyzed on a 1% agarose gel. Fragments of the correct size were excised and purified using the NucleoSpin Gel & PCR Clean-up Kit according to the manufacturer's instructions. The digested insert was purified according to the instructions for the PCR clean up.

#### 6.1.4.4 Ligation

Vector DNA and insert were ligated as described in table 36. A ligation mixture without the insert served as negative control. Ligation was performed by incubating the mixture in a PCR cycler for 20 s at 28 °C followed by 20 s at 4 °C with a total of 50 repeats.

**Table 36: Ligation mixture.**

Component	Volume
Vector	10-50 ng
Insert	3:1 molar ratio over vector
10x T4-ligase buffer	1 µl
T4-ligase	0.5 µl
dH <sub>2</sub> O	ad 10 µl

#### 6.1.4.5 Ligation independent cloning

In addition to ligation, DNA fragments can be inserted into plasmids with complementary overhangs by ligation independent cloning (LIC). Here, the purified digested vector (without CIP treatment) and the respective insert were digested with the T4 DNA polymerase as described in table 37. Mixtures were incubated for 30 minutes at 22 °C followed by 20 minutes at 75 °C.

**Table 37: LIC mixture.**

Component	Insert	Vector
DNA	50 ng	50 ng
10x NEB 2.1	2 µl	2 µl
100 mM DTT	1 µl	1 µl
T4 DNA polymerase (LIC-qualified)	0.4 µl	0.4 µl
dH <sub>2</sub> O	ad 20 µl	ad 20 µl

For annealing, 2 µl vector and 4 µl or 6 µl insert were mixed and incubated for 30 s at 70 °C followed by 5 minutes at room temperature (rt) prior to transformation.

#### 6.1.4.6 Bacterial transformation

For transformation, 5 µl ligation mixture were added to 30-50 µl competent *E. coli* DH5α and incubated on ice for 30 minutes. In case of plasmid retransformation, 100 ng DNA were used. Heatshock was performed for 20 seconds at 42 °C, followed by 2 minutes incubation on ice. 250 µl pre-warmed LB medium (without antibiotics) was added to the bacteria and the suspension was either incubated at 37 °C, 350 rcf for up to 30 minutes before plating or

directly plated on selective LB agar plates. Colonies were grown o/n at 37 °C. For determination of successful cloning, few clones were picked, transferred to small-scale cultures and plasmid DNA was isolated and analyzed by restriction digestion. Correct insertion was confirmed by sequencing.

#### 6.1.4.7 Sequencing

Plasmids were sequenced at the GATC Biotech AG, Konstanz.

#### 6.1.5 Phenol-chloroform extraction

Plasmid samples or restriction mixtures were filled up with nuclease-free water to a total volume of 100 µl and transferred to a 5 Prime Phase Lock Gel Heavy tube (2 ml) for phenol-chloroform extraction. After addition of one volume phenol:chloroform:isoamylalcohol, the sample was mixed vigorously by inverting and centrifuged for 15 minutes, 12,000 x *g*, rt. One volume of chloroform was added, the sample was mixed vigorously by inverting and centrifuged for 5 minutes, 12,000 x *g*, rt. The aqueous phase was transferred into a fresh RNase free 1.5 ml tube and supplemented with 1/10 volume 3 M sodium acetate and 2.5 volumes 99% pure ethanol. Precipitation of the DNA was performed for 20 minutes at 12,000 x *g*, 4 °C. The supernatant was removed, and the pellet was washed with 500 µl 75% ethanol for 15 minutes at 12,000 x *g*, 4 °C. The supernatant was discarded, the pellet was air dried for up to 10 minutes at rt and resolved in nuclease-free water.

#### 6.1.6 HCV RNA *in vitro* transcription

To generate HCV RNA, HCV encoding plasmids were linearized and used as template for *in vitro* transcription. 16 µg plasmid DNA were digested with either SspI or MluI as described in 6.1.4.3 for 1 hour up to overnight. In case of MluI digestion, Mung bean nuclease treatment was performed for 30 minutes at 30 °C to remove single strand overhangs. The mixture is described in table 38.

**Table 38: Mung bean nuclease treatment.**

Component	Volume
Linearized DNA	19 µl
10x Mung bean buffer	3 µl
Mung bean nuclease	1.3 µl
dH <sub>2</sub> O	ad 30 µl

Linearization was confirmed on a 1% agarose gel and the linearized plasmid was purified via phenol-chloroform extraction under RNase-free conditions.



*In vitro* transcription of HCV RNA was performed using the MEGAscript T7 transcription kit following the manufacturer's protocol. Integrity of the RNA was analyzed on a 1% agarose gel and 10 µg aliquots were stored at -80 °C.

## **6.2 Cell culture techniques**

### **6.2.1 Cell culture**

All used cell lines were cultured in DMEM at 37 °C, 5% CO<sub>2</sub> and 95% relative humidity. Cells were passaged every 2-3 days at 80-90% confluence. After removing the medium, the cells were washed once with PBS and incubated with Trypsin/EDTA at 37 °C until detachment. Cells were resuspended in fresh DMEM and a part was transferred into a new cell culture flask for culture (split ratio 1:3–1:10, depending on confluency and growth rate). If needed, cells were counted using a Neubauer counting chamber.

### **6.2.2 Thawing and freezing of eukaryotic cells**

Frozen cells were thawed in a 37 °C water bath and transferred to 10 ml DMEM in a T75 cell culture flask. Medium was changed the following day to remove dead cells. For freezing, cells of a confluent T175 flask were washed with PBS, trypsinized, resuspended in DMEM and transferred to a 50 ml tube. After centrifugation for 5 minutes, 200 x g, rt, the pellet was resuspended in freezing media with a cell count of approximately 3x10<sup>6</sup>/ml. The cell suspension was split to cryovials with 1 ml per vial and cooled down in a cell freezing container to ensure a stable freezing rate of -1 °C/minute at -80 °C. Cells were kept at -80 °C and placed in a liquid nitrogen tank for long-term storage.

### **6.2.3 Electroporation of cells with *in vitro* transcribed HCV RNA**

*In vitro* transcribed HCV RNA was transfected into Huh7.5 or Huh7.5.1 cells via electroporation. 4x10<sup>6</sup> cells per electroporation of 10 µg RNA were transferred into a 50 ml tube, pelleted by centrifugation (200 x g, 5 minutes, rt) and washed in 5 ml OptiMEM (200 x g, 5 minutes, rt). After the wash, the cells were resuspended in 400 µl cytomix supplemented with 8 µl 0.1 M ATP and 20 µl 0.1 M glutathione. The cell suspension was added to the RNA and transferred into a 4 mm cuvette. Electroporation was performed at 260 V and 950 µF in a GenePulser II electroporation device. Directly after electroporation, the cells were transferred into a T75 cell culture flask containing 10 ml DMEM. The medium was changed after 2 to 4 hours and cells transfected with full-length HCV RNA were transferred into a BSL3\*\* laboratory.

### **6.2.4 Generation of HCV stocks**

For the generation of viral stocks, Huh7.5 or Huh7.5.1 cells were electroporated with *in vitro* transcribed HCV RNA (see 6.2.3) and the supernatant was harvested at day 3 and day 5 post electroporation. Naïve Huh7.5 or Huh7.5.1 cells seeded in a T175 cell culture flask were infected with the supernatant of electroporated cells and cultured for up to 8 days. During this

period the supernatant was harvested twice, and the cells were split at least once to support viral spread. To remove cell debris, the collected medium was centrifuged for 5 minutes at  $290 \times g$ , rt before it was pooled. Aliquots of 5 or 10 ml were stored at  $-20\text{ }^{\circ}\text{C}$  or  $-80\text{ }^{\circ}\text{C}$ . To generate higher concentrated viral stocks, precipitation with polyethylene glycol (PEG) was performed. Briefly, supernatants were filtered using a  $0.22\text{ }\mu\text{m}$  steriflip and mixed with 10% PEG (v/v; final concentration) in a 50 ml tube. The virus was incubated o/n at  $4\text{ }^{\circ}\text{C}$  and precipitation was performed the following day for 45–60 minutes at  $4\text{ }^{\circ}\text{C}$ ,  $1200 \times g$ . The pellet was resuspended in DMEM and aliquots were stored at  $-80\text{ }^{\circ}\text{C}$ .

### 6.2.5 Titration of HCV stocks ( $\text{TCID}_{50}$ )

To determine the titer of HCV stocks, Huh7.5-RFP-NLS-IPS reporter cells (Jones et al., 2010) were infected with a serial dilution from  $1:10^0$ – $1:10^6$  for non-concentrated or  $1:10^1$ – $1:10^7$  for concentrated virus. Therefore, cells were seeded at a density of  $6\text{--}8 \times 10^3/\text{well}$  in a 96 well plate. One day post seeding, six wells per dilution were infected and incubated for 3 days. After fixation with 2% PFA for 1 hour at  $4\text{ }^{\circ}\text{C}$ , the positive wells per dilution were determined on the basis of infected foci and the  $\text{TCID}_{50}$  was calculated using the Reed and Muench calculator described by Lindenbach *et al.* (Lindenbach, 2009).

### 6.2.6 Production of lentiviral pseudoparticles and lentiviral transduction

For production of lentiviral pseudoparticles,  $5 \times 10^6$  HEK 293T cells were seeded per 150 mm cell culture dish and transfected by calcium phosphate precipitation the following day. The transfection mixture is described in table 39.

**Table 39: Lentivirus transfection mix.**

Component	Quantity
Transfer plasmid	20 $\mu\text{g}$
Packaging plasmid	15 $\mu\text{g}$
Envelope plasmid	6 $\mu\text{g}$
2.5 M $\text{CaCl}_2$	50 $\mu\text{l}$
sterile $\text{H}_2\text{O}$	ad 500 $\mu\text{l}$

First, plasmids were mixed with sterile water before  $\text{CaCl}_2$  was added. Afterwards, the DNA- $\text{CaCl}_2$  mixture was slowly added to 500  $\mu\text{l}$  2x HBS in a 15 ml tube under constant air bubbling and incubated at rt for 15–20 minutes. Meanwhile, the media of the HEK 293T cells was changed to 15 ml DMEM supplemented with 25  $\mu\text{M}$  chloroquine. The transfection mix was carefully dropped to the media. After 6–8 hours, the media was changed to 20 ml fresh DMEM. Three days post transfection, the supernatant was collected in a 50 ml tube and centrifuged for 5 minutes at  $290 \times g$ , rt to remove cell debris. After filtration through a  $0.22\text{ }\mu\text{m}$

or 0.45  $\mu\text{m}$  sterile filter unit, the virus was either directly aliquoted or concentrated *via* ultracentrifugation at 12,2000  $\times g$ , 4  $^{\circ}\text{C}$ . Concentrated virus was resuspended in approximately 1 ml DMEM, aliquoted, and stored at -80  $^{\circ}\text{C}$ . Lentivirus titration was performed on Huh7 or Huh7.5 cells. Here,  $5 \times 10^4$  cells/well were seeded in a 12 well plate and transduced with 2–50  $\mu\text{l}$  of concentrated virus or 50–750  $\mu\text{l}$  of unconcentrated viral stock in DMEM containing 4  $\mu\text{g/ml}$  polybrene. Cells were fixed 3 days post transduction and transduction efficiency was determined by flow cytometry (see 6.2.8). All lentivirus transductions in this study were performed in DMEM + 4  $\mu\text{g/ml}$  polybrene.

### **6.2.7 Transfection of Huh7 and Huh7.5 cells using FuGENE**

Huh7 and Huh7.5 cells were transiently transfected with plasmids of interest using FuGENE according to the manufacturer's instructions. For all transfections, a FuGENE:DNA ratio of 3:1 was used. One day post transfection, media was changed to fresh DMEM.

### **6.2.8 Flow cytometry**

For flow cytometry analysis, cells were washed once with PBS, trypsinized, and transferred to a 1.5 ml tube. After centrifugation for 3–5 minutes at 160  $\times g$ , rt, the supernatant was aspirated, and the pellet was fixed in 2% PFA for at least 30–60 minutes at 4  $^{\circ}\text{C}$ . Flow cytometry was performed on a BD LSRFortessa or a BD Canto and data was analyzed with Flowjo.

### **6.2.9 LINE1 retrotransposition reporter assay**

To determine the LINE1 retrotransposition frequency, an EGFP-based reporter assay was used, allowing the analysis of LINE1 activity by flow cytometry.

#### **6.2.9.1 LINE1 retrotransposition in ABA-treated Huh7.5 cells**

To assess the functionality of the LINE1 retrotransposition reporter assay, the percentage of EGFP-positive cells was determined in cells treated with the nucleoside analog reverse-transcriptase inhibitor (NRTI) abacavir (ABA). Huh7.5 cells were seeded in 6 well plates at a density of  $1.2 \times 10^5$  or  $1.5 \times 10^5$  cells/well and transfected with 1–1.5  $\mu\text{g}$  of the LINE1 retrotransposition reporter plasmid (HH292). Transfection was performed in technical triplicates for each individual experiment. The next day, treatment with 10  $\mu\text{M}$  ABA or 0.1% DMSO as vehicle control was started and renewed every other day. Cells were fixed in 2% PFA at 6 days post transfection and analyzed by flow cytometry. Untransfected cells served as negative control.

#### **6.2.9.2 LINE1 retrotransposition in HCV-infected Huh7.5 cells**

Huh7.5 cells were infected with a Jc1<sup>NS5AB-mKO2</sup> reporter strain (MOI 0.004) and seeded in 6 well plates at a density of  $1.2 \times 10^5$  cells/well the following day. Uninfected cells were treated equally. Two days post infection, infected or uninfected cells were transfected with 1  $\mu\text{g}$  of

the LINE1 retrotransposition reporter plasmid (HH292) or the transfection control (HH293) using FuGENE. Transfection was performed in triplicates for each individual experiment. Untransfected cells served as negative controls. One day post transfection, media was changed to fresh DMEM and cells were fixed in 2% PFA for flow cytometry at 6 days post transfection, 8 days post infection. Equally, cells were transfected at 7 days post infection and fixed 6 days later to determine LINE1 retrotransposition at 13 days post infection. Samples were analyzed at the BD LSRFortessa. A minimum of  $3.2 \times 10^5$  cells for day 8 and  $4 \times 10^4$  cells for 13 days post infection was recorded for each sample.

#### **6.2.10 Immunofluorescence and LD staining for confocal microscopy**

Huh7 cells were infected with either Jc1<sup>wt</sup> or JFH1<sup>wt</sup> and seeded onto glass cover slips at a density of  $8 \times 10^4$  cells/6 well at 6 days post infection. The following day, cells were transiently transfected with 0.6  $\mu$ g HA-L1ORF1p overexpression plasmid (HH283). Uninfected cells were treated equally. For analysis of HA-L1ORF1p localization in presence of HCV core overexpression, Huh7 cells were co-transfected with the HA-L1ORF1p overexpression plasmid and an HCV core expression plasmid (pHR319) (0.3  $\mu$ g each). Two days post transfection, cells were washed once with PBS and fixed in 4% PFA for 1 hour at 4 °C. Cells were washed 3x with PBS/10 mM glycine followed by permeabilization with 0.1% Triton-X-100 in PBS for 5 minutes at rt. After 3 subsequent washing steps in PBS/10 mM glycine, cells were blocked in 5% BSA/1% fish skin gelatin (blocking solution) for minimum 30 minutes at rt. Cells were washed again (3x) followed by incubation with the respective primary antibody, diluted in blocking solution, o/n at 4°C. After three washing steps, secondary antibody and Hoechst staining was performed for 45–60 minutes at rt in the dark. Samples were washed again, and LDs were stained with BODIPY493/503 in PBS/10 mM glycine for 45–60 minutes in the dark at rt. Cover slips were washed once in ddH<sub>2</sub>O, embedded in Mowiol and stored in the dark until analysis. Microscopy was performed on a Nikon C2+ confocal laser scanning microscope (CLSM) using a 60x violet corrected oil objective with a NA of 1.4. For colocalization analysis, a region of interest (ROI) was manually drawn around transfected cells and the Manders' colocalization coefficient and the Pearson's correlation coefficient were calculated using the Coloc2 function of Fiji (Schindelin et al., 2012).

#### **6.2.11 LD Isolation**

For LD isolation, approximately  $5 \times 10^6$  cells were seeded to 150 mm cell culture dishes 2–3 days prior to harvest. Cells were washed once with cold PBS, scraped in cold PBS and transferred to a 50 ml tube, followed by centrifugation for 5 minutes at 200 x g, 4 °C. The supernatant was discarded and pellets were kept on ice until resuspension in 1 ml of sucrose buffer supplemented with protease inhibitor cocktail. Cells were lysed mechanically in a Dounce homogenizer for 5 to 10 minutes and efficient lysis was confirmed by trypan blue staining. The lysates were transferred to a 1.5 or 2 ml tube and centrifuged for 10 minutes at

1,000 x g, 4 °C to remove the nuclei. Post-nuclear fractions were transferred to SW 60 ultracentrifuge tubes and overlaid with isotonic potassium phosphate buffer supplemented with PMSF. 80 µl of the post-nuclear supernatant were kept as input control. LDs were isolated by ultracentrifugation for 2 hours at 100,000 x g, 4 °C in an SW 60 rotor and transferred to a new 1.5 ml tube using a syringe with a bent blunted cannula. A subsequent centrifugation step to concentrate the LD fraction was performed at 18,000 x g, 4° C for 10 minutes. The underlying buffer volume was reduced with a needle, and LDs and input lysates were stored at -20 °C or -80 °C until further analysis.

### 6.2.12 RNP isolation and LINE1 element amplification protocol (LEAP)

To investigate the L1ORF2p *in vitro* activity, LINE1 RNPs were isolated and the LINE1 element amplification protocol (LEAP) was performed as described with some modifications (Kopera et al., 2016; Kulpa and Moran, 2006).

#### 6.2.12.1 Transfection of Huh7 cells and RNP isolation

2x10<sup>6</sup> Huh7 cells were seeded in 150 mm cell culture dishes and transfected with 20 µg of a plasmid for overexpression of a RC-competent LINE1 (pDK101) or an RT mutant (pDK135) the following day. Two dishes per plasmid were transfected and media was changed one day post transfection. Three days post transfection, cells were selected with DMEM + 200 µg/ml hygromycin B for 4–6 days. Cells were washed once with PBS and once with DMEM and infection was carried out by adding 5x10<sup>5</sup> Jc1<sup>NS5AB-EGFP</sup>-infected Huh7 cells to the selected cell colonies. As a control, uninfected Huh7 cells were added to the second set of transfected cells. Selective pressure to remove untransfected cells was again applied after 3–4 days for a minimum of 5 days. Untransfected HCV-infected and uninfected cells were seeded in 150 mm cell culture dishes 3 days prior to harvest to serve as negative control. For RNP isolation, cells were washed once with cold PBS, scraped in 5 ml cold PBS and transferred to a 50 ml tube. After centrifugation for 5 minutes at 3,000 x g, 4 °C, the PBS was aspirated and the pellet was stored at -80 °C. Pellets were lysed in LEAP assay lysis buffer supplemented with EDTA-free protease inhibitors described in 5.3.6 for a minimum of 1 hour on ice. Lysates were centrifuged for 10 minutes at 3,000 x g, 4 °C to remove cell debris and transferred to a fresh 1.5 ml tube. 50–80 µl lysate were kept as input control. RNPs were isolated by ultracentrifugation on a sucrose cushion. 0.7 ml 17% sucrose was overlaid with 3.4 ml 8.5 % sucrose in a SW 60 ultracentrifugation tube; both solutions were supplemented with EDTA-free protease inhibitors. The lysate was loaded onto the sucrose and centrifugation was performed for 2 hours at 168,000 x g, 4 °C in an SW 60 rotor. After centrifugation, the sucrose was discarded and the remaining pellet was resuspended in 50 µl nuclease-free water supplemented with EDTA-free protease inhibitors. Protein concentration was determined using the DC protein assay. 20 µg RNPs were resolved in TRI reagent and RNA was isolated as described in 6.4. Further, lysates and isolated RNPs were mixed with 6x Laemmli and analyzed by western blotting for overexpression of LINE1. To conserve

L1ORF2p enzyme function, the RNP fractions were mixed 1:1 with 100% glycerol, frozen in dry ice, and stored at -80°C.

### 6.2.12.2 LEAP assay

To determine L1ORF2p reverse transcriptase activity *in vitro*, the LINE1 element amplification protocol described by Kulpa and Moran was used (Kulpa and Moran, 2006). The reaction mixture is shown in table 40. The LEAP reaction was performed for 1 hour at 37 °C. The LEAP primer contains a linker sequence that can be used for subsequent PCR analysis (table 20). As a control for the RT reaction, cDNA synthesis on isolated RNP RNA was performed as described in 6.5 using 0.5 µg RNA and the LEAP primer instead of the random hexamer primer.

**Table 40: LEAP reaction.**

Component	Quantity
RNPs	0.75 µg
Tris-HCl (pH 7.6)	50 mM
KCl	50 mM
25 mM MgCl <sub>2</sub>	5 mM
Tween 20	0.05%
DTT	10 mM
dNTPs	0.2 mM
RNAseOUT	20 U
LEAP primer	0.4 µM
Nuclease-free H <sub>2</sub> O	ad 50 µl

Following the LEAP reaction, a PCR using a linker primer and a specific primer to the target was performed for detection and amplification of cDNA (table 20). The PCR mixture is listed in table 41. PCR conditions are shown below (table 42).

**Table 41: LEAP PCR mixture.**

Component	Quantity
LEAP cDNA	2.5–3 $\mu$ l
or RT control cDNA	0.5 $\mu$ l
10x Taq Buffer - $\text{MgCl}_2$ + $(\text{NH}_4)_2\text{SO}_4$	5 $\mu$ l
25 mM $\text{MgCl}_2$	2 $\mu$ l
DMSO	2 $\mu$ l
10 mM dNTPs	1 $\mu$ l
Linker PCR primer	2 $\mu$ l
Target specific primer	2 $\mu$ l
Taq polymerase	0.5 $\mu$ l
Nuclease-free $\text{H}_2\text{O}$	ad 50 $\mu$ l

**Table 42: LEAP PCR conditions.**

Cycle step	Temperature	Time	Repeats
Initial Denaturation	94 °C	3 min	1x
Denaturation	94 °C	30 s	35x
Annealing	56 °C	30 s	
Extension	72 °C	40 s	
Final extension	72 °C	7 min	1x
hold	4 °C	$\infty$	

35  $\mu$ l of the PCR product was analyzed by agarose gel electrophoresis on a 2% agarose gel.

## 6.3 Biochemical methods

### 6.3.1 Cell lysates

Cell lysates for protein analysis were prepared in NP-40 lysis buffer with or without 1% sodium deoxycholate supplemented with protease inhibitor cocktail. Alternatively, the LEAP assay lysis buffer was used. Briefly, cells were washed once with PBS, resuspended in lysis buffer and incubated for a minimum of 30–60 minutes on ice. To remove cell debris, lysates were centrifuged for 15–20 minutes at 18,000  $\times g$ , 4 °C and transferred to a fresh 1.5 ml tube. Protein concentration was determined using the DC protein assay according to the manufacturer's instructions. Samples were stored at -20 °C or -80 °C until analysis by SDS-PAGE and western blotting.

### 6.3.2 SDS-PAGE and western blot analysis

Separation of proteins from cell lysates or LD fractions was performed by discontinuous SDS-polyacrylamide electrophoresis (SDS-PAGE). Samples were mixed with 6x Laemmli (Laemmli, 1970), denatured at 95 °C for 5 minutes and loaded to a 10% or 12% acrylamide gel. As a marker of molecular weight, a prestained protein standard was used. Electrophoresis was performed at 200 V until the dye front reached the end of the gel. For detection of proteins by specific antibodies, western blotting was performed. Proteins were transferred to a nitrocellulose membrane in a tank blot system for 90–120 minutes at 80 V under constant cooling. Ponceau S staining of the membrane was performed to confirm protein transfer. Afterwards, the membrane was blocked in blocking solution (5% skim milk in 1x TBS-T) for a minimum of 35 minutes at rt. Incubation with the respective primary antibody was performed o/n at 4 °C or 1 hour at rt on a rotation device. Next, the membrane was washed in 1x TBS-T for at least 30 minutes with 3x buffer exchange, followed by incubation with the respective secondary HRP-coupled antibody for 1 hour at rt. After a second wash in 1x TBS-T (3x buffer exchange), the membrane was incubated with ECL Lumi-Light or the more sensitive SuperSignal West Femto Chemiluminescent Substrate to specifically detect proteins by chemiluminescence.

### 6.3.3 Co-immunoprecipitation

For co-immunoprecipitation experiments of HA-L1ORF1p,  $4 \times 10^6$  HCV-infected or uninfected Huh7.5 cells were seeded to 100 mm cell culture dishes and transfected with 10 µg HA-L1ORF1p overexpression plasmid (HH283). Untransfected HCV-infected cells served as background control. Two days post transfection, cells were washed once with cold PBS and lysed in 500–700 µl NP-40 lysis buffer supplemented with 1x PIC. Viruses in lysates were inactivated for 1 hour on ice, centrifuged for 15 minutes at  $18,000 \times g$ , 4 °C to remove cell debris and the supernatant was transferred to a fresh 1.5 ml tube. Protein concentration was determined with the DC protein assay according to the manufacturer's instructions.

#### 6.3.3.1 Co-immunoprecipitation to determine HCV RNA copies in HA-L1ORF1p-precipitated samples

In order to determine the enrichment of HCV RNA in HA-L1ORF1p-precipitated samples, 100 U/ml RNaseOUT were added to the NP-40 lysis buffer to prevent RNA degradation. For HA-specific co-immunoprecipitation, HA-agarose beads were prepared by 3–4 times wash in NP-40 lysis buffer for 2 minutes at  $211 \times g$ , 4 °C. 30 µl HA-agarose were added to 1 mg protein in 1 ml total volume and incubated for 60 minutes up to 2 hours at 4 °C in an overhead rotator. Beads were washed 4 times in NP-40 lysis buffer (2 minutes,  $211 \times g$ , 4 °C) and the last wash was split to two 1.5 ml tubes. For RNA isolation, either 1/2 or 2/3 of the beads were resuspended in 500 µl or 1 ml TRI reagent. Total RNA was isolated and HCV copy numbers were determined by qRT-PCR (see 6.4–6.6). Note that in 3 of 6 experiments, DNase



treatment was not performed. Residual beads were resuspended in Laemmli buffer, incubated for 5 minutes at 95°C and analyzed by SDS-PAGE and western blotting.

#### **6.3.3.2 Co-immunoprecipitation with RNase A treatment to investigate RNA dependent interactions**

Two samples of the same lysate were prepared, each containing 700 µg protein in a total volume of 1200 µl. To reduce unspecific binding, samples of one individual experiment were pre-cleared with 35 µl recombinant protein G agarose for 30 minutes at 4 °C in an overhead rotator. Prior to co-immunoprecipitation, one sample was treated with 100 µg/ml RNase A, whereas 100 U/ml RNaseOUT were added to the other sample. After incubation for 45–60 minutes at 4 °C in an overhead rotator, 150 µl of each sample were transferred to a fresh 1.5 ml tube and resuspended in 500 µl TRI reagent for RNA isolation. Total RNA was isolated, subjected to DNase treatment, and successful RNase digestion was analyzed by agarose gel electrophoresis on a 1% agarose gel. For HA-specific co-immunoprecipitation, HA-agarose beads were prepared as described above and 30 µl HA-agarose were added to the lysates. Co-immunoprecipitation was performed for 1 hour at 4 °C in an overhead rotator. Beads were washed 4 times in NP-40 lysis buffer (2 minutes, 211 x g, 4 °C), resuspended in 3x Laemmli buffer and analyzed by SDS-PAGE and western blotting.

#### **6.3.3.3 Co-immunoprecipitation of FLAG-tagged viral proteins with RNase A treatment to investigate RNA dependent interactions**

For individual expression of FLAG-tagged HCV core or NS5A, 1–1.5x10<sup>6</sup> Huh7.5 cells were seeded to 100 mm dishes, transduced with lentiviral particles and lysed in NP-40 lysis buffer 3 days post transduction. Empty vector transduced cells served as control. Sample preparation and RNase A treatment were performed as described above. For FLAG-specific co-immunoprecipitation, FLAG-agarose beads were prepared as described and 30 µl FLAG-agarose were added to the lysates. Co-immunoprecipitation was performed for 1 hour at 4 °C, rotating. Beads were washed 4 times in NP-40 lysis buffer (2 minutes, 211 x g, 4 °C), resuspended in 3x Laemmli buffer and analyzed by SDS-PAGE and western blotting. Total RNA was isolated, subjected to DNase treatment and successful RNase digestion was analyzed by agarose gel electrophoresis on a 1% agarose gel.

### **6.4 RNA isolation**

RNA was isolated from cell lysates or co-immunoprecipitated samples using 500 µl to 1 ml TRI reagent per sample. 200 µl chloroform per ml TRI reagent were added, samples were shaken vigorously by hand for 15 seconds and incubated for 2–3 minutes at rt. After centrifugation for 15 minutes at 12,000 x g, 4 °C, the upper aqueous phase was transferred to a new 1.5 ml tube. As a carrier for RNA precipitation, 10–20 µg glycogen were added to samples in which low RNA yield was expected, prior to adding 500 µl isopropanol. Samples were inverted and incubated at rt for 10 minutes followed by precipitation for 10 minutes at

12,000 x g, 4 °C. The supernatant was discarded, and the RNA pellet was washed with 1 ml 75% ethanol at 7,500–8,000 x g, 5 minutes at 4 °C. The pellet was air dried for minimum 5 minutes at rt, resolved in 10 µl nuclease-free water and treated with DNaseI according to the manufacturer's protocol for 20–30 minutes at 37 °C. After DNase inactivation, samples were centrifuged for 1 minute at 15,000 x g, rt and transferred to a fresh 1.5 ml tube. RNA concentration was measured photometrically and samples were stored at -80 °C.

## 6.5 cDNA synthesis

Reverse transcription of RNA into cDNA was performed using the Superscript III reverse transcriptase. The two-step reaction is listed in table 43. For cDNA synthesis from co-precipitated samples, equal volumes of isolated RNA were used. cDNA was stored at -20 °C.

**Table 43: cDNA synthesis mixture.**

Components	Quantity	Time and temperature
RNA	0.4–1 µg / 9 µl	5 min at 65 °C
10 mM dNTPs	1 µl	
Random hexamer primer (1:10)	1 µl	
Nuclease-free H <sub>2</sub> O	ad 14 µl	
5x first-strand buffer	4 µl	5 min at 25 °C
100 mM DTT	1 µl	60 min at 50 °C
RNAseOUT	0.5 µl	15 min at 70 °C
Superscript III	0.5 µl	

## 6.6 Quantitative real time PCR (qRT-PCR)

qRT-PCR was performed using the Maxima SYBR green master mix in a 7500 HTFast Real-time PCR cycler. The PCR mixture is listed in table 44. A master mix of all components was prepared and mixed with the cDNA in a 96 well plate. Samples were measured in triplicates. qRT-PCR conditions are listed in table 45.

**Table 44: qRT-PCR mix.**

Components	Volume
cDNA	1 µl
2x Maxima SYBR green	10 µl
ROX (5 µM)	0.04 µl
qPCR primer mix	0.6 µl
Nuclease-free H <sub>2</sub> O	8.34 µl

**Table 45: qRT-PCR conditions.**

Temperature	Time	Repeats
95 °C	10 min	1x
95 °C	15 s	40x
60 °C	1 min	
95 °C	15 s	1x
60 °C	1 min	1x

### 6.6.1 HCV standard for qRT-PCR

1 µg of *in vitro* transcribed HCV RNA was reversely transcribed to prepare an HCV cDNA standard for qRT-PCR. A serial dilution of 1:10<sup>1</sup>-1:10<sup>8</sup> was prepared and 1 µl of each dilution was used for qRT-PCR, corresponding to 100000-0.01 pg HCV RNA per reaction.

## 6.7 Luciferase assays to analyze HCV replication in LINE1-overexpressing cells

### 6.7.1 HCV RNA replication in HA-L1ORF1p-overexpressing cells

4x10<sup>6</sup> Huh7.5 cells were electroporated with Jc1ΔE1E2<sup>NS5AB-FLuc</sup> RNA as described in 6.2.3. In parallel, 250 ng of the pGL4.75 renilla luciferase expression plasmid were co-electroporated as transfection control (of note, the renilla luciferase activity was not included in data analysis). Cells were resuspended in 26 ml DMEM and seeded in 12 well plates with 1 ml/well (~1.5x10<sup>5</sup> cells/well). Untransfected cells were seeded as control. Four hours post electroporation, cells were transduced with lentiviruses for HA-L1ORF1p overexpression or empty vector control in triplicates. In parallel, the electroporation control cells were lysed. Therefore, cells were washed once with PBS, 150 µl 1x passive lysis buffer per well were added and plates were stored at -20 °C. Medium of the lentivirus-transduced cells was changed the next day. Cells were lysed at 3 and 5 days post electroporation and samples were stored at -20 °C until analysis. For lysis, the plates were thawed and incubated for 30 minutes at rt, shaking. Samples were resuspended equally, transferred into a v-bottom 96 well plate and centrifuged for 2 minutes at 290 x g, rt to remove cell debris. The lysates were transferred to a new 96 well plate and kept on ice or stored at -20 °C. Luciferase activity (relative light units, RLU) was measured on a Tecan multi well plate reader using the Dual-Luciferase reporter assay system according to the manufacturer's instructions. Protein concentrations of the respective samples were measured in triplicates using the Pierce Coomassie Plus (Bradford) assay reagent. 5 µl sample were mixed with 150 µl Coomassie Reagent, incubated at rt for 10 minutes and absorbance was measured at 595 nm.

In a second approach, Huh7.5 cells were transduced for overexpression of HA-L1ORF1p or empty vector control and electroporated at 3 days post transduction. Here,  $2 \times 10^6$  cells per condition were resuspended in 200  $\mu$ l cytomix supplemented with 4  $\mu$ l ATP and 10  $\mu$ l glutathione and co-electroporated with 5  $\mu$ g RNA and 125 ng pGL4.75 in a 2 mm cuvette. Cells were resuspended in 13 ml medium and the experiment was performed as described above.

### 6.7.2 HCV replication in LINE1-overexpressing cells

In order to provide an internal control for cell viability, Huh7 cells used in this assay were first transduced with lentiviral particles for expression of a secreted embryonic alkaline phosphatase (SEAP) or an EGFP control. To introduce LINE1 overexpression, either of a RC-competent element or the RT mutant,  $3 \times 10^4$  Huh7 cells were seeded in 12 well plates and transfected with 250 ng of the respective plasmids or an empty vector the following day. Transfection was performed in duplicates. Three days post transfection, transfected cells were selected in DMEM + 200  $\mu$ g/ml hygromycin B for 8 days, followed by infection with equal volumes of a Jc1<sup>p7-GLuc-2A-NS2</sup> reporter virus. To remove the virus, cells were washed once with PBS and 500  $\mu$ l of DMEM + 200  $\mu$ g/ml hygromycin B per well were added. The supernatant was harvested every second day for a period of 14 days and replaced by 500  $\mu$ l fresh DMEM + 200  $\mu$ g/ml hygromycin B. At day 14, cells were washed once with PBS, lysed in 80  $\mu$ l LEAP assay lysis buffer, and protein concentration was determined using the DC protein assay. Collected supernatants were stored at -20 °C and prior to lysis, 200  $\mu$ l of supernatant was transferred to a v-bottom 96 well plate and centrifuged for 3 minutes at 500 x g, rt to remove cell debris. For determination of gaussia luciferase activity, supernatant was mixed 1:1 with 2x renilla luciferase lysis buffer and incubated for 1 hour at rt. 10  $\mu$ l of the lysed sample were transferred to a white 96 well plate, 50  $\mu$ l of 10  $\mu$ M coelenterazine (diluted in PBS) were injected per well and gaussia luciferase activity was measured using a Tecan multi well plate reader. Samples were measured in duplicates. The overexpression of LINE1 was analyzed by western blotting.

### 6.8 Secreted embryonic alkaline phosphatase (SEAP) assay

Secreted embryonic alkaline phosphatase (SEAP) activity was measured using the QUANTI-Blue Assay according to the manufacturer's protocol with some minor modifications. Briefly, infectious cell culture supernatants were inactivated with a final concentration of 1% Triton-X-100 for 1 hour at rt. 180  $\mu$ l of the prepared QUANTI-Blue solution were pipetted to a 96 well plate and 20  $\mu$ l sample were added. Duplicates were prepared for each sample. The assay was incubated for 30 minutes at 37 °C and absorbance was measured at 620 nm.

## **6.9 Statistical analysis**

Statistical analysis of not normalized data was performed using the two-sample t-test with Welch's correction. Normalized data was analyzed using the one sample t-test. Statistics were performed with R studio or Microsoft Excel.

## 7 References

- Adams JW, Kaufman RE, Kretschmer PJ, Harrison M, and Nienhuis AW. 1980. A family of long reiterated DNA sequences, one copy of which is next to the human beta globin gene. *Nucleic Acids Res.* 8:6113-6128.
- Adinolfi LE, Gambardella M, Andreana A, Tripodi MF, Utili R, and Ruggiero G. 2001. Steatosis accelerates the progression of liver damage of chronic hepatitis C patients and correlates with specific HCV genotype and visceral obesity. *Hepatology.* 33:1358-1364.
- Aisyah DN, Shallcross L, Hully AJ, O'Brien A, and Hayward A. 2018. Assessing hepatitis C spontaneous clearance and understanding associated factors-A systematic review and meta-analysis. *J. Viral Hepat.* 25:680-698.
- Ait-Goughoulte M, Kanda T, Meyer K, Ryerse JS, Ray RB, and Ray R. 2008. Hepatitis C virus genotype 1a growth and induction of autophagy. *J. Virol.* 82:2241-2249.
- Alisch RS, Garcia-Perez JL, Muotri AR, Gage FH, and Moran JV. 2006. Unconventional translation of mammalian LINE-1 retrotransposons. *Genes Dev.* 20:210-224.
- Andre P, Komurian-Pradel F, Deforges S, Perret M, Berland JL, Sodoyer M, Pol S, Brechot C, Paranhos-Baccala G, and Lotteau V. 2002. Characterization of low- and very-low-density hepatitis C virus RNA-containing particles. *J. Virol.* 76:6919-6928.
- Angus AG, Dalrymple D, Boulant S, McGivern DR, Clayton RF, Scott MJ, Adair R, Graham S, Owsianka AM, Targett-Adams P, Li K, Wakita T, McLauchlan J, Lemon SM, and Patel AH. 2010. Requirement of cellular DDX3 for hepatitis C virus replication is unrelated to its interaction with the viral core protein. *J. Gen. Virol.* 91:122-132.
- Antelo M, Balaguer F, Shia J, Shen Y, Hur K, Moreira L, Cuatrecasas M, Bujanda L, Giraldez MD, Takahashi M, Cabanne A, Barugel ME, Arnold M, Roca EL, Andreu M, Castellvi-Bel S, Llor X, Jover R, Castells A, Boland CR, and Goel A. 2012. A high degree of LINE-1 hypomethylation is a unique feature of early-onset colorectal cancer. *PLoS One.* 7:e45357.
- Appel N, Zayas M, Miller S, Krijnse-Locker J, Schaller T, Friebe P, Kallis S, Engel U, and Bartenschlager R. 2008. Essential role of domain III of nonstructural protein 5A for hepatitis C virus infectious particle assembly. *PLoS Pathog.* 4:e1000035.
- Ariumi Y. 2016. Guardian of the Human Genome: Host Defense Mechanisms against LINE-1 Retrotransposition. *Front Chem.* 4:28.
- Ariumi Y, Kuroki M, Abe K, Dansako H, Ikeda M, Wakita T, and Kato N. 2007. DDX3 DEAD-box RNA helicase is required for hepatitis C virus RNA replication. *J. Virol.* 81:13922-13926.
- Ariumi Y, Kuroki M, Kushima Y, Osugi K, Hijikata M, Maki M, Ikeda M, and Kato N. 2011a. Hepatitis C virus hijacks P-body and stress granule components around lipid droplets. *J. Virol.* 85:6882-6892.
- Ariumi Y, Kuroki M, Maki M, Ikeda M, Dansako H, Wakita T, and Kato N. 2011b. The ESCRT system is required for hepatitis C virus production. *PLoS One.* 6:e14517.
- Babushok DV, and Kazazian HH, Jr. 2007. Progress in understanding the biology of the human mutagen LINE-1. *Hum. Mutat.* 28:527-539.
- Babushok DV, Ostertag EM, Courtney CE, Choi JM, and Kazazian HH, Jr. 2006. L1 integration in a transgenic mouse model. *Genome Res.* 16:240-250.
- Badr CE, Hewett JW, Breakefield XO, and Tannous BA. 2007. A highly sensitive assay for monitoring the secretory pathway and ER stress. *PLoS One.* 2:e571.
- Baillie JK, Barnett MW, Upton KR, Gerhardt DJ, Richmond TA, De Sapio F, Brennan PM, Rizzu P, Smith S, Fell M, Talbot RT, Gustincich S, Freeman TC, Mattick JS, Hume DA, Heutink P, Carninci P, Jeddloh JA, and Faulkner GJ. 2011. Somatic retrotransposition alters the genetic landscape of the human brain. *Nature.* 479:534-537.
- Bandiera S, Billie Bian C, Hoshida Y, Baumert TF, and Zeisel MB. 2016. Chronic hepatitis C virus infection and pathogenesis of hepatocellular carcinoma. *Curr. Opin. Virol.* 20:99-105.

- Bannert N, and Kurth R. 2006. The evolutionary dynamics of human endogenous retroviral families. *Annu Rev Genomics Hum Genet.* 7:149-173.
- Barouch-Bentov R, Neveu G, Xiao F, Beer M, Bekerman E, Schor S, Campbell J, Boonyaratanakornkit J, Lindenbach B, Lu A, Jacob Y, and Einav S. 2016. Hepatitis C Virus Proteins Interact with the Endosomal Sorting Complex Required for Transport (ESCRT) Machinery via Ubiquitination To Facilitate Viral Envelopment. *MBio.* 7.
- Barth H, Schafer C, Adah MI, Zhang F, Linhardt RJ, Toyoda H, Kinoshita-Toyoda A, Toida T, Van Kuppevelt TH, Depla E, Von Weizsacker F, Blum HE, and Baumert TF. 2003. Cellular binding of hepatitis C virus envelope glycoprotein E2 requires cell surface heparan sulfate. *J. Biol. Chem.* 278:41003-41012.
- Barth H, Schnober EK, Zhang F, Linhardt RJ, Depla E, Boson B, Cosset FL, Patel AH, Blum HE, and Baumert TF. 2006. Viral and cellular determinants of the hepatitis C virus envelope-heparan sulfate interaction. *J. Virol.* 80:10579-10590.
- Bartosch B, Bukh J, Meunier JC, Granier C, Engle RE, Blackwelder WC, Emerson SU, Cosset FL, and Purcell RH. 2003. In vitro assay for neutralizing antibody to hepatitis C virus: evidence for broadly conserved neutralization epitopes. *Proc. Natl. Acad. Sci. U. S. A.* 100:14199-14204.
- Batzler MA, and Deininger PL. 2002. Alu repeats and human genomic diversity. *Nat. Rev. Genet.* 3:370-379.
- Beck CR, Collier P, Macfarlane C, Malig M, Kidd JM, Eichler EE, Badge RM, and Moran JV. 2010. LINE-1 retrotransposition activity in human genomes. *Cell.* 141:1159-1170.
- Beck CR, Garcia-Perez JL, Badge RM, and Moran JV. 2011. LINE-1 elements in structural variation and disease. *Annu Rev Genomics Hum Genet.* 12:187-215.
- Blanchard E, Belouzard S, Goueslain L, Wakita T, Dubuisson J, Wychowski C, and Rouille Y. 2006. Hepatitis C virus entry depends on clathrin-mediated endocytosis. *J. Virol.* 80:6964-6972.
- Bleykasten-Grosshans C, Friedrich A, and Schacherer J. 2013. Genome-wide analysis of intraspecific transposon diversity in yeast. *BMC Genomics.* 14:399.
- Blight KJ, McKeating JA, and Rice CM. 2002. Highly permissive cell lines for subgenomic and genomic hepatitis C virus RNA replication. *J. Virol.* 76:13001-13014.
- Blond JL, Lavillette D, Cheynet V, Bouton O, Oriol G, Chapel-Fernandes S, Mandrand B, Mallet F, and Cosset FL. 2000. An envelope glycoprotein of the human endogenous retrovirus HERV-W is expressed in the human placenta and fuses cells expressing the type D mammalian retrovirus receptor. *J. Virol.* 74:3321-3329.
- Boeke JD, Garfinkel DJ, Styles CA, and Fink GR. 1985. Ty elements transpose through an RNA intermediate. *Cell.* 40:491-500.
- Bogerd HP, Wiegand HL, Hulme AE, Garcia-Perez JL, O'Shea KS, Moran JV, and Cullen BR. 2006. Cellular inhibitors of long interspersed element 1 and Alu retrotransposition. *Proc. Natl. Acad. Sci. U. S. A.* 103:8780-8785.
- Boulant S, Montserret R, Hope RG, Ratnier M, Targett-Adams P, Lavergne JP, Penin F, and McLauchlan J. 2006. Structural determinants that target the hepatitis C virus core protein to lipid droplets. *J. Biol. Chem.* 281:22236-22247.
- Boulant S, Vanbelle C, Ebel C, Penin F, and Lavergne JP. 2005. Hepatitis C virus core protein is a dimeric alpha-helical protein exhibiting membrane protein features. *J. Virol.* 79:11353-11365.
- Brass V, Berke JM, Montserret R, Blum HE, Penin F, and Moradpour D. 2008. Structural determinants for membrane association and dynamic organization of the hepatitis C virus NS3-4A complex. *Proc. Natl. Acad. Sci. U. S. A.* 105:14545-14550.
- Brass V, Bieck E, Montserret R, Wolk B, Hellings JA, Blum HE, Penin F, and Moradpour D. 2002. An amino-terminal amphipathic alpha-helix mediates membrane association of the hepatitis C virus nonstructural protein 5A. *J. Biol. Chem.* 277:8130-8139.
- Brazzoli M, Bianchi A, Filippini S, Weiner A, Zhu Q, Pizza M, and Crotta S. 2008. CD81 is a central regulator of cellular events required for hepatitis C virus infection of human hepatocytes. *J. Virol.* 82:8316-8329.

- Bressanelli S, Tomei L, Roussel A, Incitti I, Vitale RL, Mathieu M, De Francesco R, and Rey FA. 1999. Crystal structure of the RNA-dependent RNA polymerase of hepatitis C virus. *Proc. Natl. Acad. Sci. U. S. A.* 96:13034-13039.
- Briese T, de la Torre JC, Lewis A, Ludwig H, and Lipkin WI. 1992. Borna disease virus, a negative-strand RNA virus, transcribes in the nucleus of infected cells. *Proc. Natl. Acad. Sci. U. S. A.* 89:11486-11489.
- Britten RJ, and Kohne DE. 1968. Repeated sequences in DNA. Hundreds of thousands of copies of DNA sequences have been incorporated into the genomes of higher organisms. *Science.* 161:529-540.
- Brouha B, Schustak J, Badge RM, Lutz-Prigge S, Farley AH, Moran JV, and Kazazian HH, Jr. 2003. Hot L1s account for the bulk of retrotransposition in the human population. *Proc. Natl. Acad. Sci. U. S. A.* 100:5280-5285.
- Bukh J, Purcell RH, and Miller RH. 1994. Sequence analysis of the core gene of 14 hepatitis C virus genotypes. *Proc. Natl. Acad. Sci. U. S. A.* 91:8239-8243.
- Callahan KE, Hickman AB, Jones CE, Ghirlando R, and Furano AV. 2012. Polymerization and nucleic acid-binding properties of human L1 ORF1 protein. *Nucleic Acids Res.* 40:813-827.
- Camus G, Herker E, Modi AA, Haas JT, Ramage HR, Farese RV, Jr., and Ott M. 2013. Diacylglycerol acyltransferase-1 localizes hepatitis C virus NS5A protein to lipid droplets and enhances NS5A interaction with the viral capsid core. *J. Biol. Chem.* 288:9915-9923.
- Carrere-Kremer S, Montpellier-Pala C, Cocquerel L, Wychowski C, Penin F, and Dubuisson J. 2002. Subcellular localization and topology of the p7 polypeptide of hepatitis C virus. *J. Virol.* 76:3720-3730.
- Castro-Diaz N, Ecco G, Coluccio A, Kapopoulou A, Yazdanpanah B, Friedli M, Duc J, Jang SM, Turelli P, and Trono D. 2014. Evolutionally dynamic L1 regulation in embryonic stem cells. *Genes Dev.* 28:1397-1409.
- Catanese MT, Uryu K, Kopp M, Edwards TJ, Andrus L, Rice WJ, Silvestry M, Kuhn RJ, and Rice CM. 2013. Ultrastructural analysis of hepatitis C virus particles. *Proc. Natl. Acad. Sci. U. S. A.* 110:9505-9510.
- Chalitchagorn K, Shuangshoti S, Hourpai N, Kongruttanachok N, Tangkijvanich P, Thong-ngam D, Voravud N, Sriuranpong V, and Mutirangura A. 2004. Distinctive pattern of LINE-1 methylation level in normal tissues and the association with carcinogenesis. *Oncogene.* 23:8841-8846.
- Chang KS, Jiang J, Cai Z, and Luo G. 2007. Human apolipoprotein e is required for infectivity and production of hepatitis C virus in cell culture. *J. Virol.* 81:13783-13793.
- Chatel-Chaix L, Germain MA, Motorina A, Bonneil E, Thibault P, Baril M, and Lamarre D. 2013. A host YB-1 ribonucleoprotein complex is hijacked by hepatitis C virus for the control of NS3-dependent particle production. *J. Virol.* 87:11704-11720.
- Chatel-Chaix L, Melancon P, Racine ME, Baril M, and Lamarre D. 2011. Y-box-binding protein 1 interacts with hepatitis C virus NS3/4A and influences the equilibrium between viral RNA replication and infectious particle production. *J. Virol.* 85:11022-11037.
- Chen L, Borozan I, Feld J, Sun J, Tannis LL, Coltescu C, Heathcote J, Edwards AM, and McGilvray ID. 2005. Hepatic gene expression discriminates responders and nonresponders in treatment of chronic hepatitis C viral infection. *Gastroenterology.* 128:1437-1444.
- Choi J, Hwang SY, and Ahn K. 2018. Interplay between RNASEH2 and MOV10 controls LINE-1 retrotransposition. *Nucleic Acids Res.* 46:1912-1926.
- Choi J, Lee KJ, Zheng Y, Yamaga AK, Lai MM, and Ou JH. 2004. Reactive oxygen species suppress hepatitis C virus RNA replication in human hepatoma cells. *Hepatology.* 39:81-89.
- Choo QL, Kuo G, Weiner AJ, Overby LR, Bradley DW, and Houghton M. 1989. Isolation of a cDNA clone derived from a blood-borne non-A, non-B viral hepatitis genome. *Science.* 244:359-362.



- Christensen SM, and Eickbush TH. 2005. R2 target-primed reverse transcription: ordered cleavage and polymerization steps by protein subunits asymmetrically bound to the target DNA. *Mol. Cell. Biol.* 25:6617-6628.
- Clarke D, Griffin S, Beales L, Gelais CS, Burgess S, Harris M, and Rowlands D. 2006. Evidence for the formation of a heptameric ion channel complex by the hepatitis C virus p7 protein in vitro. *J. Biol. Chem.* 281:37057-37068.
- Cocquerel L, Meunier JC, Pillez A, Wychowski C, and Dubuisson J. 1998. A retention signal necessary and sufficient for endoplasmic reticulum localization maps to the transmembrane domain of hepatitis C virus glycoprotein E2. *J. Virol.* 72:2183-2191.
- Cook PR, Jones CE, and Furano AV. 2015. Phosphorylation of ORF1p is required for L1 retrotransposition. *Proc. Natl. Acad. Sci. U. S. A.* 112:4298-4303.
- Cordaux R, and Batzer MA. 2009. The impact of retrotransposons on human genome evolution. *Nat. Rev. Genet.* 10:691-703.
- Cordaux R, Hedges DJ, Herke SW, and Batzer MA. 2006. Estimating the retrotransposition rate of human Alu elements. *Gene.* 373:134-137.
- Corless L, Crump CM, Griffin SD, and Harris M. 2010. Vps4 and the ESCRT-III complex are required for the release of infectious hepatitis C virus particles. *J. Gen. Virol.* 91:362-372.
- Cost GJ, and Boeke JD. 1998. Targeting of human retrotransposon integration is directed by the specificity of the L1 endonuclease for regions of unusual DNA structure. *Biochemistry.* 37:18081-18093.
- Cost GJ, Feng Q, Jacquier A, and Boeke JD. 2002. Human L1 element target-primed reverse transcription in vitro. *EMBO J.* 21:5899-5910.
- Coufal NG, Garcia-Perez JL, Peng GE, Yeo GW, Mu Y, Lovci MT, Morell M, O'Shea KS, Moran JV, and Gage FH. 2009. L1 retrotransposition in human neural progenitor cells. *Nature.* 460:1127-1131.
- Counihan NA, Rawlinson SM, and Lindenbach BD. 2011. Trafficking of hepatitis C virus core protein during virus particle assembly. *PLoS Pathog.* 7:e1002302.
- Cristofari G, Ivanyi-Nagy R, Gabus C, Boulant S, Lavergne JP, Penin F, and Darlix JL. 2004. The hepatitis C virus Core protein is a potent nucleic acid chaperone that directs dimerization of the viral (+) strand RNA in vitro. *Nucleic Acids Res.* 32:2623-2631.
- Da Costa D, Turek M, Felmlee DJ, Girardi E, Pfeffer S, Long G, Bartenschlager R, Zeisel MB, and Baumert TF. 2012. Reconstitution of the entire hepatitis C virus life cycle in nonhepatic cells. *J. Virol.* 86:11919-11925.
- Dao Thi VL, Granier C, Zeisel MB, Guerin M, Mancip J, Granio O, Penin F, Lavillette D, Bartenschlager R, Baumert TF, Cosset FL, and Dreux M. 2012. Characterization of hepatitis C virus particle subpopulations reveals multiple usage of the scavenger receptor BI for entry steps. *J. Biol. Chem.* 287:31242-31257.
- Daskalos A, Nikolaidis G, Xinarianos G, Savvari P, Cassidy A, Zakopoulou R, Kotsinas A, Gorgoulis V, Field JK, and Liloglou T. 2009. Hypomethylation of retrotransposable elements correlates with genomic instability in non-small cell lung cancer. *Int. J. Cancer.* 124:81-87.
- de Koning AP, Gu W, Castoe TA, Batzer MA, and Pollock DD. 2011. Repetitive elements may comprise over two-thirds of the human genome. *PLoS Genet.* 7:e1002384.
- De Luca C, Guadagni F, Sinibaldi-Vallebona P, Sentinelli S, Gallucci M, Hoffmann A, Schumann GG, Spadafora C, and Sciamanna I. 2016. Enhanced expression of LINE-1-encoded ORF2 protein in early stages of colon and prostate transformation. *Oncotarget.* 7:4048-4061.
- Deininger PL, Batzer MA, Hutchison CA, 3rd, and Edgell MH. 1992. Master genes in mammalian repetitive DNA amplification. *Trends Genet.* 8:307-311.
- Deleersnyder V, Pillez A, Wychowski C, Blight K, Xu J, Hahn YS, Rice CM, and Dubuisson J. 1997. Formation of native hepatitis C virus glycoprotein complexes. *J. Virol.* 71:697-704.
- Denli AM, Narvaiza I, Kerman BE, Pena M, Benner C, Marchetto MC, Diedrich JK, Aslanian A, Ma J, Moresco JJ, Moore L, Hunter T, Saghatelian A, and Gage FH. 2015.

- Primate-specific ORF0 contributes to retrotransposon-mediated diversity. *Cell*. 163:583-593.
- Dewannieux M, Blaise S, and Heidmann T. 2005. Identification of a functional envelope protein from the HERV-K family of human endogenous retroviruses. *J. Virol.* 79:15573-15577.
- Dewannieux M, Esnault C, and Heidmann T. 2003. LINE-mediated retrotransposition of marked Alu sequences. *Nat. Genet.* 35:41-48.
- Dmitriev SE, Andreev DE, Terenin IM, Olovnikov IA, Prassolov VS, Merrick WC, and Shatsky IN. 2007. Efficient translation initiation directed by the 900-nucleotide-long and GC-rich 5' untranslated region of the human retrotransposon LINE-1 mRNA is strictly cap dependent rather than internal ribosome entry site mediated. *Mol. Cell. Biol.* 27:4685-4697.
- Dombroski BA, Feng Q, Mathias SL, Sassaman DM, Scott AF, Kazazian HH, Jr., and Boeke JD. 1994. An in vivo assay for the reverse transcriptase of human retrotransposon L1 in *Saccharomyces cerevisiae*. *Mol. Cell. Biol.* 14:4485-4492.
- Dombroski BA, Mathias SL, Nanthakumar E, Scott AF, and Kazazian HH, Jr. 1991. Isolation of an active human transposable element. *Science*. 254:1805-1808.
- Doucet AJ, Hulme AE, Sahinovic E, Kulpa DA, Moldovan JB, Kopera HC, Athanikar JN, Hasnaoui M, Bucheton A, Moran JV, and Gilbert N. 2010. Characterization of LINE-1 ribonucleoprotein particles. *PLoS Genet.* 6.
- Doucet AJ, Wilusz JE, Miyoshi T, Liu Y, and Moran JV. 2015. A 3' Poly(A) Tract Is Required for LINE-1 Retrotransposition. *Mol. Cell.* 60:728-741.
- Dreux M, Gastaminza P, Wieland SF, and Chisari FV. 2009. The autophagy machinery is required to initiate hepatitis C virus replication. *Proc. Natl. Acad. Sci. U. S. A.* 106:14046-14051.
- DuBridge RB, Tang P, Hsia HC, Leong PM, Miller JH, and Calos MP. 1987. Analysis of mutation in human cells by using an Epstein-Barr virus shuttle system. *Mol. Cell. Biol.* 7:379-387.
- Dunn KW, Kamocka MM, and McDonald JH. 2011. A practical guide to evaluating colocalization in biological microscopy. *Am. J. Physiol. Cell Physiol.* 300:C723-742.
- EASL. 2018. EASL Recommendations on Treatment of Hepatitis C 2018. *J. Hepatol.* 69:461-511.
- Egger D, Wolk B, Gosert R, Bianchi L, Blum HE, Moradpour D, and Bienz K. 2002. Expression of hepatitis C virus proteins induces distinct membrane alterations including a candidate viral replication complex. *J. Virol.* 76:5974-5984.
- Erwin JA, Marchetto MC, and Gage FH. 2014. Mobile DNA elements in the generation of diversity and complexity in the brain. *Nat. Rev. Neurosci.* 15:497-506.
- Esnault C, Maestre J, and Heidmann T. 2000. Human LINE retrotransposons generate processed pseudogenes. *Nat. Genet.* 24:363-367.
- Ewing AD, and Kazazian HH, Jr. 2010. High-throughput sequencing reveals extensive variation in human-specific L1 content in individual human genomes. *Genome Res.* 20:1262-1270.
- Failla C, Tomei L, and De Francesco R. 1994. Both NS3 and NS4A are required for proteolytic processing of hepatitis C virus nonstructural proteins. *J. Virol.* 68:3753-3760.
- Fan Z, Yang QR, Twu JS, and Sherker AH. 1999. Specific in vitro association between the hepatitis C viral genome and core protein. *J. Med. Virol.* 59:131-134.
- Farese RV, Jr., and Walther TC. 2009. Lipid droplets finally get a little R-E-S-P-E-C-T. *Cell*. 139:855-860.
- Feng Q, Moran JV, Kazazian HH, Jr., and Boeke JD. 1996. Human L1 retrotransposon encodes a conserved endonuclease required for retrotransposition. *Cell*. 87:905-916.
- Feschotte C, and Pritham EJ. 2007. DNA transposons and the evolution of eukaryotic genomes. *Annu. Rev. Genet.* 41:331-368.
- Finnegan DJ. 1989. Eukaryotic transposable elements and genome evolution. *Trends Genet.* 5:103-107.
- Finnegan DJ. 1992. Transposable elements. *Curr. Opin. Genet. Dev.* 2:861-867.

- Florl AR, Lower R, Schmitz-Drager BJ, and Schulz WA. 1999. DNA methylation and expression of LINE-1 and HERV-K provirus sequences in urothelial and renal cell carcinomas. *Br. J. Cancer*. 80:1312-1321.
- Florl AR, Steinhoff C, Muller M, Seifert HH, Hader C, Engers R, Ackermann R, and Schulz WA. 2004. Coordinate hypermethylation at specific genes in prostate carcinoma precedes LINE-1 hypomethylation. *Br. J. Cancer*. 91:985-994.
- Freeman JD, Goodchild NL, and Mager DL. 1994. A modified indicator gene for selection of retrotransposition events in mammalian cells. *BioTechniques*. 17:46, 48-49, 52.
- Friebe P, and Bartenschlager R. 2002. Genetic analysis of sequences in the 3' nontranslated region of hepatitis C virus that are important for RNA replication. *J. Virol.* 76:5326-5338.
- Friebe P, Boudet J, Simorre JP, and Bartenschlager R. 2005. Kissing-loop interaction in the 3' end of the hepatitis C virus genome essential for RNA replication. *J. Virol.* 79:380-392.
- Friedli M, Turelli P, Kapopoulou A, Rauwel B, Castro-Diaz N, Rowe HM, Ecco G, Unzu C, Planet E, Lombardo A, Mangeat B, Wildhaber BE, Naldini L, and Trono D. 2014. Loss of transcriptional control over endogenous retroelements during reprogramming to pluripotency. *Genome Res*. 24:1251-1259.
- Fuhrman SA, Deininger PL, LaPorte P, Friedmann T, and Geiduschek EP. 1981. Analysis of transcription of the human Alu family ubiquitous repeating element by eukaryotic RNA polymerase III. *Nucleic Acids Res*. 9:6439-6456.
- Ganguly A, Dunbar T, Chen P, Godmilow L, and Ganguly T. 2003. Exon skipping caused by an intronic insertion of a young Alu Yb9 element leads to severe hemophilia A. *Hum. Genet.* 113:348-352.
- Gao XD, Qu JH, Chang XJ, Lu YY, Bai WL, Wang H, Xu ZX, An LJ, Wang CP, Zeng Z, and Yang YP. 2014. Hypomethylation of long interspersed nuclear element-1 promoter is associated with poor outcomes for curative resected hepatocellular carcinoma. *Liver Int.* 34:136-146.
- Garcia-Mediavilla MV, Sanchez-Campos S, Gonzalez-Perez P, Gomez-Gonzalo M, Majano PL, Lopez-Cabrera M, Clemente G, Garcia-Monzon C, and Gonzalez-Gallego J. 2005. Differential contribution of hepatitis C virus NS5A and core proteins to the induction of oxidative and nitrosative stress in human hepatocyte-derived cells. *J. Hepatol.* 43:606-613.
- Garcia-Perez JL, Marchetto MC, Muotri AR, Coufal NG, Gage FH, O'Shea KS, and Moran JV. 2007. LINE-1 retrotransposition in human embryonic stem cells. *Hum. Mol. Genet.* 16:1569-1577.
- Gardner MJ, Hall N, Fung E, White O, Berriman M, Hyman RW, Carlton JM, Pain A, Nelson KE, Bowman S, Paulsen IT, James K, Eisen JA, Rutherford K, Salzberg SL, Craig A, Kyes S, Chan MS, Nene V, Shallom SJ, Suh B, Peterson J, Angiuoli S, Pertea M, Allen J, Selengut J, Haft D, Mather MW, Vaidya AB, Martin DM, Fairlamb AH, Fraunholz MJ, Roos DS, Ralph SA, McFadden GI, Cummings LM, Subramanian GM, Mungall C, Venter JC, Carucci DJ, Hoffman SL, Newbold C, Davis RW, Fraser CM, and Barrell B. 2002. Genome sequence of the human malaria parasite *Plasmodium falciparum*. *Nature*. 419:498-511.
- Gastaminza P, Cheng G, Wieland S, Zhong J, Liao W, and Chisari FV. 2008. Cellular determinants of hepatitis C virus assembly, maturation, degradation, and secretion. *J. Virol.* 82:2120-2129.
- Gastaminza P, Dryden KA, Boyd B, Wood MR, Law M, Yeager M, and Chisari FV. 2010. Ultrastructural and biophysical characterization of hepatitis C virus particles produced in cell culture. *J. Virol.* 84:10999-11009.
- Gastaminza P, Kapadia SB, and Chisari FV. 2006. Differential biophysical properties of infectious intracellular and secreted hepatitis C virus particles. *J. Virol.* 80:11074-11081.
- Ge D, Fellay J, Thompson AJ, Simon JS, Shianna KV, Urban TJ, Heinzen EL, Qiu P, Bertelsen AH, Muir AJ, Sulkowski M, McHutchison JG, and Goldstein DB. 2009.

- Genetic variation in IL28B predicts hepatitis C treatment-induced viral clearance. *Nature*. 461:399-401.
- Germi R, Crance JM, Garin D, Guimet J, Lortat-Jacob H, Ruigrok RW, Zarski JP, and Drouet E. 2002. Cellular glycosaminoglycans and low density lipoprotein receptor are involved in hepatitis C virus adsorption. *J. Med. Virol.* 68:206-215.
- Giorgi G, Marcantonio P, and Del Re B. 2011. LINE-1 retrotransposition in human neuroblastoma cells is affected by oxidative stress. *Cell Tissue Res.* 346:383-391.
- Goodier JL, Cheung LE, and Kazazian HH, Jr. 2012. MOV10 RNA helicase is a potent inhibitor of retrotransposition in cells. *PLoS Genet.* 8:e1002941.
- Goodier JL, Cheung LE, and Kazazian HH, Jr. 2013. Mapping the LINE1 ORF1 protein interactome reveals associated inhibitors of human retrotransposition. *Nucleic Acids Res.* 41:7401-7419.
- Goodier JL, and Kazazian HH, Jr. 2008. Retrotransposons revisited: the restraint and rehabilitation of parasites. *Cell.* 135:23-35.
- Goodier JL, Ostertag EM, Engleka KA, Seleme MC, and Kazazian HH, Jr. 2004. A potential role for the nucleolus in L1 retrotransposition. *Hum. Mol. Genet.* 13:1041-1048.
- Goodier JL, Pereira GC, Cheung LE, Rose RJ, and Kazazian HH, Jr. 2015. The Broad-Spectrum Antiviral Protein ZAP Restricts Human Retrotransposition. *PLoS Genet.* 11:e1005252.
- Goodier JL, Zhang L, Vetter MR, and Kazazian HH, Jr. 2007. LINE-1 ORF1 protein localizes in stress granules with other RNA-binding proteins, including components of RNA interference RNA-induced silencing complex. *Mol. Cell. Biol.* 27:6469-6483.
- Gosert R, Egger D, Lohmann V, Bartenschlager R, Blum HE, Bienz K, and Moradpour D. 2003. Identification of the hepatitis C virus RNA replication complex in Huh-7 cells harboring subgenomic replicons. *J. Virol.* 77:5487-5492.
- Gouttenoire J, Castet V, Montserret R, Arora N, Raussens V, Ruyschaert JM, Diesis E, Blum HE, Penin F, and Moradpour D. 2009. Identification of a novel determinant for membrane association in hepatitis C virus nonstructural protein 4B. *J. Virol.* 83:6257-6268.
- Gower E, Estes C, Blach S, Razavi-Shearer K, and Razavi H. 2014. Global epidemiology and genotype distribution of the hepatitis C virus infection. *J. Hepatol.* 61:S45-57.
- Grakoui A, Wychowski C, Lin C, Feinstone SM, and Rice CM. 1993. Expression and identification of hepatitis C virus polyprotein cleavage products. *J. Virol.* 67:1385-1395.
- Green PM, Bagnall RD, Waseem NH, and Giannelli F. 2008. Haemophilia A mutations in the UK: results of screening one-third of the population. *Br. J. Haematol.* 143:115-128.
- Grimaldi G, Skowronski J, and Singer MF. 1984. Defining the beginning and end of KpnI family segments. *EMBO J.* 3:1753-1759.
- Guo H, Chitiprolu M, Gagnon D, Meng L, Perez-Iratxeta C, Lagace D, and Gibbings D. 2014. Autophagy supports genomic stability by degrading retrotransposon RNA. *Nat Commun.* 5:5276.
- Hajarizadeh B, Grebely J, and Dore GJ. 2013. Epidemiology and natural history of HCV infection. *Nat Rev Gastroenterol Hepatol.* 10:553-562.
- Hamdorf M, Idica A, Zisoulis DG, Gamelin L, Martin C, Sanders KJ, and Pedersen IM. 2015. miR-128 represses L1 retrotransposition by binding directly to L1 RNA. *Nat. Struct. Mol. Biol.* 22:824-831.
- Hancks DC, Goodier JL, Mandal PK, Cheung LE, and Kazazian HH, Jr. 2011. Retrotransposition of marked SVA elements by human L1s in cultured cells. *Hum. Mol. Genet.* 20:3386-3400.
- Hancks DC, and Kazazian HH, Jr. 2016. Roles for retrotransposon insertions in human disease. *Mob DNA.* 7:9.
- Harris C, Herker E, Farese RV, Jr., and Ott M. 2011. Hepatitis C virus core protein decreases lipid droplet turnover: a mechanism for core-induced steatosis. *J. Biol. Chem.* 286:42615-42625.

- Harris HJ, Davis C, Mullins JG, Hu K, Goodall M, Farquhar MJ, Mee CJ, McCaffrey K, Young S, Drummer H, Balfe P, and McKeating JA. 2010. Claudin association with CD81 defines hepatitis C virus entry. *J. Biol. Chem.* 285:21092-21102.
- Hata K, and Sakaki Y. 1997. Identification of critical CpG sites for repression of L1 transcription by DNA methylation. *Gene.* 189:227-234.
- Heidmann T, Heidmann O, and Nicolas JF. 1988. An indicator gene to demonstrate intracellular transposition of defective retroviruses. *Proc. Natl. Acad. Sci. U. S. A.* 85:2219-2223.
- Henne WM, Buchkovich NJ, and Emr SD. 2011. The ESCRT pathway. *Dev. Cell.* 21:77-91.
- Heras SR, Macias S, Plass M, Fernandez N, Cano D, Eyraas E, Garcia-Perez JL, and Caceres JF. 2013. The Microprocessor controls the activity of mammalian retrotransposons. *Nat. Struct. Mol. Biol.* 20:1173-1181.
- Herker E, Harris C, Hernandez C, Carpentier A, Kaehlcke K, Rosenberg AR, Farese RV, Jr., and Ott M. 2010. Efficient hepatitis C virus particle formation requires diacylglycerol acyltransferase-1. *Nat. Med.* 16:1295-1298.
- Herker E, and Ott M. 2012. Emerging role of lipid droplets in host/pathogen interactions. *J. Biol. Chem.* 287:2280-2287.
- Herrmann A, Wittmann S, Thomas D, Shepard CN, Kim B, Ferreiros N, and Gramberg T. 2018. The SAMHD1-mediated block of LINE-1 retroelements is regulated by phosphorylation. *Mob DNA.* 9:11.
- Hofmann S, Krajewski M, Scherer C, Scholz V, Mordhorst V, Truschow P, Schobel A, Reimer R, Schwudke D, and Herker E. 2018. Complex lipid metabolic remodeling is required for efficient hepatitis C virus replication. *Biochim. Biophys. Acta.* 1863:1041-1056.
- Hohjoh H, and Singer MF. 1996. Cytoplasmic ribonucleoprotein complexes containing human LINE-1 protein and RNA. *EMBO J.* 15:630-639.
- Hohjoh H, and Singer MF. 1997. Ribonuclease and high salt sensitivity of the ribonucleoprotein complex formed by the human LINE-1 retrotransposon. *J. Mol. Biol.* 271:7-12.
- Hollis GF, Hieter PA, McBride OW, Swan D, and Leder P. 1982. Processed genes: a dispersed human immunoglobulin gene bearing evidence of RNA-type processing. *Nature.* 296:321-325.
- Holmes SE, Dombroski BA, Krebs CM, Boehm CD, and Kazazian HH, Jr. 1994. A new retrotransposable human L1 element from the LRE2 locus on chromosome 1q produces a chimaeric insertion. *Nat. Genet.* 7:143-148.
- Holmes SE, Singer MF, and Swergold GD. 1992. Studies on p40, the leucine zipper motif-containing protein encoded by the first open reading frame of an active human LINE-1 transposable element. *J. Biol. Chem.* 267:19765-19768.
- Honda T. 2016. Links between Human LINE-1 Retrotransposons and Hepatitis Virus-Related Hepatocellular Carcinoma. *Front Chem.* 4:21.
- Horie M, Honda T, Suzuki Y, Kobayashi Y, Daito T, Oshida T, Ikuta K, Jern P, Gojobori T, Coffin JM, and Tomonaga K. 2010. Endogenous non-retroviral RNA virus elements in mammalian genomes. *Nature.* 463:84-87.
- Horn AV, Celic I, Dong C, Martirosyan I, and Han JS. 2017. A conserved role for the ESCRT membrane budding complex in LINE retrotransposition. *PLoS Genet.* 13:e1006837.
- Houck CM, Rinehart FP, and Schmid CW. 1979. A ubiquitous family of repeated DNA sequences in the human genome. *J. Mol. Biol.* 132:289-306.
- Hu S, Li J, Xu F, Mei S, Le Duff Y, Yin L, Pang X, Cen S, Jin Q, Liang C, and Guo F. 2015. SAMHD1 Inhibits LINE-1 Retrotransposition by Promoting Stress Granule Formation. *PLoS Genet.* 11:e1005367.
- Huang CR, Schneider AM, Lu Y, Niranjan T, Shen P, Robinson MA, Steranka JP, Valle D, Civin CI, Wang T, Wheelan SJ, Ji H, Boeke JD, and Burns KH. 2010. Mobile interspersed repeats are major structural variants in the human genome. *Cell.* 141:1171-1182.
- Huang H, Kang R, Wang J, Luo G, Yang W, and Zhao Z. 2013. Hepatitis C virus inhibits AKT-tuberous sclerosis complex (TSC), the mechanistic target of rapamycin (MTOR)

- pathway, through endoplasmic reticulum stress to induce autophagy. *Autophagy*. 9:175-195.
- Huang L, Hwang J, Sharma SD, Hargittai MR, Chen Y, Arnold JJ, Raney KD, and Cameron CE. 2005. Hepatitis C virus nonstructural protein 5A (NS5A) is an RNA-binding protein. *J. Biol. Chem.* 280:36417-36428.
- ICTV. 2017. Virus Taxonomy 2017.
- Ivanov AV, Smirnova OA, Ivanova ON, Masalova OV, Kochetkov SN, and Isaguliantz MG. 2011. Hepatitis C virus proteins activate NRF2/ARE pathway by distinct ROS-dependent and independent mechanisms in HUH7 cells. *PLoS One*. 6:e24957.
- Ivanyi-Nagy R, Kanevsky I, Gabus C, Lavergne JP, Ficheux D, Penin F, Fosse P, and Darlix JL. 2006. Analysis of hepatitis C virus RNA dimerization and core-RNA interactions. *Nucleic Acids Res.* 34:2618-2633.
- Jacobs JM, Diamond DL, Chan EY, Gritsenko MA, Qian W, Stastna M, Baas T, Camp DG, 2nd, Carithers RL, Jr., Smith RD, and Katze MG. 2005. Proteome analysis of liver cells expressing a full-length hepatitis C virus (HCV) replicon and biopsy specimens of posttransplantation liver from HCV-infected patients. *J. Virol.* 79:7558-7569.
- Jangra RK, Yi M, and Lemon SM. 2010. DDX6 (Rck/p54) is required for efficient hepatitis C virus replication but not for internal ribosome entry site-directed translation. *J. Virol.* 84:6810-6824.
- Jiang J, Cun W, Wu X, Shi Q, Tang H, and Luo G. 2012. Hepatitis C virus attachment mediated by apolipoprotein E binding to cell surface heparan sulfate. *J. Virol.* 86:7256-7267.
- Jirasko V, Montserret R, Lee JY, Gouttenoire J, Moradpour D, Penin F, and Bartenschlager R. 2010. Structural and functional studies of nonstructural protein 2 of the hepatitis C virus reveal its key role as organizer of virion assembly. *PLoS Pathog.* 6:e1001233.
- Jones CT, Catanese MT, Law LM, Khetani SR, Syder AJ, Ploss A, Oh TS, Schoggins JW, MacDonald MR, Bhatia SN, and Rice CM. 2010. Real-time imaging of hepatitis C virus infection using a fluorescent cell-based reporter system. *Nat. Biotechnol.* 28:167-171.
- Jones CT, Murray CL, Eastman DK, Tassello J, and Rice CM. 2007. Hepatitis C virus p7 and NS2 proteins are essential for production of infectious virus. *J. Virol.* 81:8374-8383.
- Jones DM, Patel AH, Targett-Adams P, and McLauchlan J. 2009. The hepatitis C virus NS4B protein can trans-complement viral RNA replication and modulates production of infectious virus. *J. Virol.* 83:2163-2177.
- Jones RB, Song H, Xu Y, Garrison KE, Buzdin AA, Anwar N, Hunter DV, Mujib S, Mihajlovic V, Martin E, Lee E, Kuciak M, Raposo RA, Bozorgzad A, Meiklejohn DA, Ndhlovu LC, Nixon DF, and Ostrowski MA. 2013. LINE-1 retrotransposable element DNA accumulates in HIV-1-infected cells. *J. Virol.* 87:13307-13320.
- Jopling CL, Schutz S, and Sarnow P. 2008. Position-dependent function for a tandem microRNA miR-122-binding site located in the hepatitis C virus RNA genome. *Cell Host Microbe*. 4:77-85.
- Jopling CL, Yi M, Lancaster AM, Lemon SM, and Sarnow P. 2005. Modulation of hepatitis C virus RNA abundance by a liver-specific MicroRNA. *Science*. 309:1577-1581.
- Jurka J. 1997. Sequence patterns indicate an enzymatic involvement in integration of mammalian retroposons. *Proc. Natl. Acad. Sci. U. S. A.* 94:1872-1877.
- Jurka J, Zietkiewicz E, and Labuda D. 1995. Ubiquitous mammalian-wide interspersed repeats (MIRs) are molecular fossils from the mesozoic era. *Nucleic Acids Res.* 23:170-175.
- Kammerer RA, Kostrewa D, Progiass P, Honnappa S, Avila D, Lustig A, Winkler FK, Pieters J, and Steinmetz MO. 2005. A conserved trimerization motif controls the topology of short coiled coils. *Proc. Natl. Acad. Sci. U. S. A.* 102:13891-13896.
- Kannan RP, Hensley LL, Evers LE, Lemon SM, and McGivern DR. 2011. Hepatitis C virus infection causes cell cycle arrest at the level of initiation of mitosis. *J. Virol.* 85:7989-8001.

- Kano H, Godoy I, Courtney C, Vetter MR, Gerton GL, Ostertag EM, and Kazazian HH, Jr. 2009. L1 retrotransposition occurs mainly in embryogenesis and creates somatic mosaicism. *Genes Dev.* 23:1303-1312.
- Kapitonov VV, and Jurka J. 2008. A universal classification of eukaryotic transposable elements implemented in Repbase. *Nat. Rev. Genet.* 9:411-412; author reply 414.
- Kawano K, Doucet AJ, Ueno M, Kariya R, An W, Marzetta F, Kuroki M, Turelli P, Sukegawa S, Okada S, Strebel K, Trono D, and Ariumi Y. 2018. HIV-1 Vpr and p21 restrict LINE-1 mobility. *Nucleic Acids Res.* 46:8454-8470.
- Kazazian HH, Jr. 1999. An estimated frequency of endogenous insertional mutations in humans. *Nat. Genet.* 22:130.
- Kazazian HH, Jr. 2004. Mobile elements: drivers of genome evolution. *Science.* 303:1626-1632.
- Kazazian HH, Jr., Wong C, Youssoufian H, Scott AF, Phillips DG, and Antonarakis SE. 1988. Haemophilia A resulting from de novo insertion of L1 sequences represents a novel mechanism for mutation in man. *Nature.* 332:164-166.
- Keum SJ, Park SM, Park JH, Jung JH, Shin EJ, and Jang SK. 2012. The specific infectivity of hepatitis C virus changes through its life cycle. *Virology.* 433:462-470.
- Khazina E, Truffault V, Buttner R, Schmidt S, Coles M, and Weichenrieder O. 2011. Trimeric structure and flexibility of the L1ORF1 protein in human L1 retrotransposition. *Nat. Struct. Mol. Biol.* 18:1006-1014.
- Khazina E, and Weichenrieder O. 2009. Non-LTR retrotransposons encode noncanonical RRM domains in their first open reading frame. *Proc. Natl. Acad. Sci. U. S. A.* 106:731-736.
- Khazina E, and Weichenrieder O. 2018. Human LINE-1 retrotransposition requires a metastable coiled coil and a positively charged N-terminus in L1ORF1p. *Elife.* 7.
- Klawitter S, Fuchs NV, Upton KR, Munoz-Lopez M, Shukla R, Wang J, Garcia-Canadas M, Lopez-Ruiz C, Gerhardt DJ, Sebe A, Grabundzija I, Merkert S, Gerdes P, Pulgarin JA, Bock A, Held U, Witthuhn A, Haase A, Sarkadi B, Lower J, Wolvetang EJ, Martin U, Ivics Z, Izsvak Z, Garcia-Perez JL, Faulkner GJ, and Schumann GG. 2016. Reprogramming triggers endogenous L1 and Alu retrotransposition in human induced pluripotent stem cells. *Nat Commun.* 7:10286.
- Klein KC, Dellos SR, and Lingappa JR. 2005. Identification of residues in the hepatitis C virus core protein that are critical for capsid assembly in a cell-free system. *J. Virol.* 79:6814-6826.
- Kopera HC, Flasch DA, Nakamura M, Miyoshi T, Doucet AJ, and Moran JV. 2016. LEAP: L1 Element Amplification Protocol. *Methods Mol. Biol.* 1400:339-355.
- Kowalski MP, and Krude T. 2015. Functional roles of non-coding Y RNAs. *Int. J. Biochem. Cell Biol.* 66:20-29.
- Kubo S, Seleme MC, Soifer HS, Perez JL, Moran JV, Kazazian HH, Jr., and Kasahara N. 2006. L1 retrotransposition in nondividing and primary human somatic cells. *Proc. Natl. Acad. Sci. U. S. A.* 103:8036-8041.
- Kulpa DA, and Moran JV. 2005. Ribonucleoprotein particle formation is necessary but not sufficient for LINE-1 retrotransposition. *Hum. Mol. Genet.* 14:3237-3248.
- Kulpa DA, and Moran JV. 2006. Cis-preferential LINE-1 reverse transcriptase activity in ribonucleoprotein particles. *Nat. Struct. Mol. Biol.* 13:655-660.
- Kunst F, Ogasawara N, Moszer I, Albertini AM, Alloni G, Azevedo V, Bertero MG, Bessieres P, Bolotin A, Borchert S, Borriss R, Boursier L, Brans A, Braun M, Brignell SC, Bron S, Brouillet S, Bruschi CV, Caldwell B, Capuano V, Carter NM, Choi SK, Cordani JJ, Connerton IF, Cummings NJ, Daniel RA, Denziot F, Devine KM, Dusterhoft A, Ehrlich SD, Emmerson PT, Entian KD, Errington J, Fabret C, Ferrari E, Foulger D, Fritz C, Fujita M, Fujita Y, Fuma S, Galizzi A, Galleron N, Ghim SY, Glaser P, Goffeau A, Golightly EJ, Grandi G, Guiseppi G, Guy BJ, Haga K, Haiech J, Harwood CR, Henaut A, Hilbert H, Holsappel S, Hosono S, Hullo MF, Itaya M, Jones L, Joris B, Karamata D, Kasahara Y, Klaerr-Blanchard M, Klein C, Kobayashi Y, Koetter P, Koningstein G, Krogh S, Kumano M, Kurita K, Lapidus A, Lardinois S, Lauber J, Lazarevic V, Lee SM, Levine A, Liu H, Masuda S, Mauel C, Medigue C, Medina N, Mellado RP, Mizuno

- M, Moestl D, Nakai S, Noback M, Noone D, O'Reilly M, Ogawa K, Ogiwara A, Oudega B, Park SH, Parro V, Pohl TM, Portelle D, Porwollik S, Prescott AM, Presecan E, Pujic P, Purnelle B, et al. 1997. The complete genome sequence of the gram-positive bacterium *Bacillus subtilis*. *Nature*. 390:249-256.
- Laemmli UK. 1970. Cleavage of structural proteins during the assembly of the head of bacteriophage T4. *Nature*. 227:680-685.
- Lander ES, Linton LM, Birren B, Nusbaum C, Zody MC, Baldwin J, Devon K, Dewar K, Doyle M, FitzHugh W, Funke R, Gage D, Harris K, Heaford A, Howland J, Kann L, Lehoczky J, LeVine R, McEwan P, McKernan K, Meldrim J, Mesirov JP, Miranda C, Morris W, Naylor J, Raymond C, Rosetti M, Santos R, Sheridan A, Sougnez C, Stange-Thomann Y, Stojanovic N, Subramanian A, Wyman D, Rogers J, Sulston J, Ainscough R, Beck S, Bentley D, Burton J, Clee C, Carter N, Coulson A, Deadman R, Deloukas P, Dunham A, Dunham I, Durbin R, French L, Grafham D, Gregory S, Hubbard T, Humphray S, Hunt A, Jones M, Lloyd C, McMurray A, Matthews L, Mercer S, Milne S, Mullikin JC, Mungall A, Plumb R, Ross M, Shownkeen R, Sims S, Waterston RH, Wilson RK, Hillier LW, McPherson JD, Marra MA, Mardis ER, Fulton LA, Chinwalla AT, Pepin KH, Gish WR, Chissoe SL, Wendl MC, Delehaunty KD, Miner TL, Delehaunty A, Kramer JB, Cook LL, Fulton RS, Johnson DL, Minx PJ, Clifton SW, Hawkins T, Branscomb E, Predki P, Richardson P, Wenning S, Slezak T, Doggett N, Cheng JF, Olsen A, Lucas S, Elkin C, Uberbacher E, Frazier M, et al. 2001. Initial sequencing and analysis of the human genome. *Nature*. 409:860-921.
- Lange CM, Bellecave P, Dao Thi VL, Tran HT, Penin F, Moradpour D, and Gouttenoire J. 2014. Determinants for membrane association of the hepatitis C virus NS2 protease domain. *J. Virol.* 88:6519-6523.
- Laricchia KM, Zdravljec S, Cook DE, and Andersen EC. 2017. Natural Variation in the Distribution and Abundance of Transposable Elements Across the *Caenorhabditis elegans* Species. *Mol. Biol. Evol.* 34:2187-2202.
- Lau CC, Sun T, Ching AK, He M, Li JW, Wong AM, Co NN, Chan AW, Li PS, Lung RW, Tong JH, Lai PB, Chan HL, To KF, Chan TF, and Wong N. 2014. Viral-human chimeric transcript predisposes risk to liver cancer development and progression. *Cancer Cell*. 25:335-349.
- Lehmann M, Meyer MF, Monazahian M, Tillmann HL, Manns MP, and Wedemeyer H. 2004. High rate of spontaneous clearance of acute hepatitis C virus genotype 3 infection. *J. Med. Virol.* 73:387-391.
- Lesburg CA, Cable MB, Ferrari E, Hong Z, Mannarino AF, and Weber PC. 1999. Crystal structure of the RNA-dependent RNA polymerase from hepatitis C virus reveals a fully encircled active site. *Nat. Struct. Biol.* 6:937-943.
- Li K, Chen Z, Kato N, Gale M, Jr., and Lemon SM. 2005a. Distinct poly(I-C) and virus-activated signaling pathways leading to interferon-beta production in hepatocytes. *J. Biol. Chem.* 280:16739-16747.
- Li K, Foy E, Ferreón JC, Nakamura M, Ferreón AC, Ikeda M, Ray SC, Gale M, Jr., and Lemon SM. 2005b. Immune evasion by hepatitis C virus NS3/4A protease-mediated cleavage of the Toll-like receptor 3 adaptor protein TRIF. *Proc. Natl. Acad. Sci. U. S. A.* 102:2992-2997.
- Li Q, Pene V, Krishnamurthy S, Cha H, and Liang TJ. 2013a. Hepatitis C virus infection activates an innate pathway involving IKK-alpha in lipogenesis and viral assembly. *Nat. Med.* 19:722-729.
- Li X, Zhang J, Jia R, Cheng V, Xu X, Qiao W, Guo F, Liang C, and Cen S. 2013b. The MOV10 helicase inhibits LINE-1 mobility. *J. Biol. Chem.* 288:21148-21160.
- Li XD, Sun L, Seth RB, Pineda G, and Chen ZJ. 2005c. Hepatitis C virus protease NS3/4A cleaves mitochondrial antiviral signaling protein off the mitochondria to evade innate immunity. *Proc. Natl. Acad. Sci. U. S. A.* 102:17717-17722.
- Lim YS, Ngo HT, Lee J, Son K, Park EM, and Hwang SB. 2016. ADP-ribosylation Factor-related Protein 1 Interacts with NS5A and Regulates Hepatitis C Virus Propagation. *Sci. Rep.* 6:31211.



- Lindenbach BD. 2009. Measuring HCV infectivity produced in cell culture and in vivo. *Methods Mol. Biol.* 510:329-336.
- Lindenbach BD. 2013. Virion assembly and release. *Curr. Top. Microbiol. Immunol.* 369:199-218.
- Lindenbach BD, Meuleman P, Ploss A, Vanwolleghem T, Syder AJ, McKeating JA, Lanford RE, Feinstone SM, Major ME, Leroux-Roels G, and Rice CM. 2006. Cell culture-grown hepatitis C virus is infectious in vivo and can be recultured in vitro. *Proc. Natl. Acad. Sci. U. S. A.* 103:3805-3809.
- Lindenbach BD, and Rice CM. 2013. The ins and outs of hepatitis C virus entry and assembly. *Nat. Rev. Microbiol.* 11:688-700.
- Loeb DD, Padgett RW, Hardies SC, Shehee WR, Comer MB, Edgell MH, and Hutchison CA, 3rd. 1986. The sequence of a large L1Md element reveals a tandemly repeated 5' end and several features found in retrotransposons. *Mol. Cell. Biol.* 6:168-182.
- Lohmann V. 2013. Hepatitis C virus RNA replication. *Curr. Top. Microbiol. Immunol.* 369:167-198.
- Lohmann V, Korner F, Koch J, Herian U, Theilmann L, and Bartenschlager R. 1999. Replication of subgenomic hepatitis C virus RNAs in a hepatoma cell line. *Science.* 285:110-113.
- Lorenz IC, Marcotrigiano J, Dentzer TG, and Rice CM. 2006. Structure of the catalytic domain of the hepatitis C virus NS2-3 protease. *Nature.* 442:831-835.
- Lou YT, Chen CW, Fan YC, Chang WC, Lu CY, Wu IC, Hsu WH, Huang CW, and Wang JY. 2014. LINE-1 Methylation Status Correlates Significantly to Post-Therapeutic Recurrence in Stage III Colon Cancer Patients Receiving FOLFOX-4 Adjuvant Chemotherapy. *PLoS One.* 10:e0123973.
- Lower R, Lower J, Frank H, Harzmann R, and Kurth R. 1984. Human teratocarcinomas cultured in vitro produce unique retrovirus-like viruses. *J. Gen. Virol.* 65 ( Pt 5):887-898.
- Lower R, Lower J, and Kurth R. 1996. The viruses in all of us: characteristics and biological significance of human endogenous retrovirus sequences. *Proc. Natl. Acad. Sci. U. S. A.* 93:5177-5184.
- Luan DD, Korman MH, Jakubczak JL, and Eickbush TH. 1993. Reverse transcription of R2Bm RNA is primed by a nick at the chromosomal target site: a mechanism for non-LTR retrotransposition. *Cell.* 72:595-605.
- Luik P, Chew C, Aittoniemi J, Chang J, Wentworth P, Jr., Dwek RA, Biggin PC, Venien-Bryan C, and Zitzmann N. 2009. The 3-dimensional structure of a hepatitis C virus p7 ion channel by electron microscopy. *Proc. Natl. Acad. Sci. U. S. A.* 106:12712-12716.
- Lundin M, Monne M, Widell A, Von Heijne G, and Persson MA. 2003. Topology of the membrane-associated hepatitis C virus protein NS4B. *J. Virol.* 77:5428-5438.
- Lupberger J, Zeisel MB, Xiao F, Thumann C, Fofana I, Zona L, Davis C, Mee CJ, Turek M, Gorke S, Royer C, Fischer B, Zahid MN, Lavillette D, Fresquet J, Cosset FL, Rothenberg SM, Pietschmann T, Patel AH, Pessaux P, Doffoel M, Raffelsberger W, Poch O, McKeating JA, Brino L, and Baumert TF. 2011. EGFR and EphA2 are host factors for hepatitis C virus entry and possible targets for antiviral therapy. *Nat. Med.* 17:589-595.
- Lussignol M, Kopp M, Molloy K, Vizcay-Barrena G, Fleck RA, Dorner M, Bell KL, Chait BT, Rice CM, and Catanese MT. 2016. Proteomics of HCV virions reveals an essential role for the nucleoporin Nup98 in virus morphogenesis. *Proc. Natl. Acad. Sci. U. S. A.* 113:2484-2489.
- Macia A, Widmann TJ, Heras SR, Ayllon V, Sanchez L, Benkaddour-Boumzaouad M, Munoz-Lopez M, Rubio A, Amador-Cubero S, Blanco-Jimenez E, Garcia-Castro J, Menendez P, Ng P, Muotri AR, Goodier JL, and Garcia-Perez JL. 2017. Engineered LINE-1 retrotransposition in nondividing human neurons. *Genome Res.* 27:335-348.
- Maestre J, Tchenio T, Dhellin O, and Heidmann T. 1995. mRNA retroposition in human cells: processed pseudogene formation. *EMBO J.* 14:6333-6338.

- Majeau N, Gagne V, Boivin A, Bolduc M, Majeau JA, Ouellet D, and Leclerc D. 2004. The N-terminal half of the core protein of hepatitis C virus is sufficient for nucleocapsid formation. *J. Gen. Virol.* 85:971-981.
- Malik HS, Burke WD, and Eickbush TH. 1999. The age and evolution of non-LTR retrotransposable elements. *Mol. Biol. Evol.* 16:793-805.
- Manders EMM, Verbeek FJ, and Aten JA. 1993. Measurement of co-localization of objects in dual-colour confocal images. *J. Microsc.* 169:375-382.
- Manns MP, Wedemeyer H, and Cornberg M. 2006. Treating viral hepatitis C: efficacy, side effects, and complications. *Gut.* 55:1350-1359.
- Martin SL, and Bushman FD. 2001. Nucleic acid chaperone activity of the ORF1 protein from the mouse LINE-1 retrotransposon. *Mol. Cell. Biol.* 21:467-475.
- Martin SL, Cruceanu M, Branciforte D, Wai-Lun Li P, Kwok SC, Hodges RS, and Williams MC. 2005. LINE-1 retrotransposition requires the nucleic acid chaperone activity of the ORF1 protein. *J. Mol. Biol.* 348:549-561.
- Marukian S, Jones CT, Andrus L, Evans MJ, Ritola KD, Charles ED, Rice CM, and Dustin LB. 2008. Cell culture-produced hepatitis C virus does not infect peripheral blood mononuclear cells. *Hepatology.* 48:1843-1850.
- Masaki T, Suzuki R, Murakami K, Aizaki H, Ishii K, Murayama A, Date T, Matsuura Y, Miyamura T, Wakita T, and Suzuki T. 2008. Interaction of hepatitis C virus nonstructural protein 5A with core protein is critical for the production of infectious virus particles. *J. Virol.* 82:7964-7976.
- Mathias SL, Scott AF, Kazazian HH, Jr., Boeke JD, and Gabriel A. 1991. Reverse transcriptase encoded by a human transposable element. *Science.* 254:1808-1810.
- Mayer J, and Meese E. 2005. Human endogenous retroviruses in the primate lineage and their influence on host genomes. *Cytogenet. Genome Res.* 110:448-456.
- McClintock B. 1950. The origin and behavior of mutable loci in maize. *Proc. Natl. Acad. Sci. U. S. A.* 36:344-355.
- McLauchlan J. 2000. Properties of the hepatitis C virus core protein: a structural protein that modulates cellular processes. *J. Viral Hepat.* 7:2-14.
- McLauchlan J, Lemberg MK, Hope G, and Martoglio B. 2002. Intramembrane proteolysis promotes trafficking of hepatitis C virus core protein to lipid droplets. *EMBO J.* 21:3980-3988.
- McMillan JP, and Singer MF. 1993. Translation of the human LINE-1 element, L1Hs. *Proc. Natl. Acad. Sci. U. S. A.* 90:11533-11537.
- Medstrand P, van de Lagemaat LN, and Mager DL. 2002. Retroelement distributions in the human genome: variations associated with age and proximity to genes. *Genome Res.* 12:1483-1495.
- Meertens L, Bertaux C, and Dragic T. 2006. Hepatitis C virus entry requires a critical postinternalization step and delivery to early endosomes via clathrin-coated vesicles. *J. Virol.* 80:11571-11578.
- Menzel N, Fischl W, Hueging K, Bankwitz D, Frentzen A, Haid S, Gentzsch J, Kaderali L, Bartenschlager R, and Pietschmann T. 2012. MAP-kinase regulated cytosolic phospholipase A2 activity is essential for production of infectious hepatitis C virus particles. *PLoS Pathog.* 8:e1002829.
- Messina JP, Humphreys I, Flaxman A, Brown A, Cooke GS, Pybus OG, and Barnes E. 2015. Global distribution and prevalence of hepatitis C virus genotypes. *Hepatology.* 61:77-87.
- Meylan E, Curran J, Hofmann K, Moradpour D, Binder M, Bartenschlager R, and Tschopp J. 2005. Cardif is an adaptor protein in the RIG-I antiviral pathway and is targeted by hepatitis C virus. *Nature.* 437:1167-1172.
- Mi S, Lee X, Li X, Veldman GM, Finnerty H, Racie L, LaVallie E, Tang XY, Edouard P, Howes S, Keith JC, Jr., and McCoy JM. 2000. Syncytin is a captive retroviral envelope protein involved in human placental morphogenesis. *Nature.* 403:785-789.
- Miki Y, Nishisho I, Horii A, Miyoshi Y, Utsunomiya J, Kinzler KW, Vogelstein B, and Nakamura Y. 1992. Disruption of the APC gene by a retrotransposal insertion of L1 sequence in a colon cancer. *Cancer Res.* 52:643-645.

- Mills RE, Bennett EA, Iskow RC, and Devine SE. 2007. Which transposable elements are active in the human genome? *Trends Genet.* 23:183-191.
- Mine M, Chen JM, Brivet M, Desguerre I, Marchant D, de Lonlay P, Bernard A, Ferec C, Abitbol M, Ricquier D, and Marsac C. 2007. A large genomic deletion in the PDHX gene caused by the retrotranspositional insertion of a full-length LINE-1 element. *Hum. Mutat.* 28:137-142.
- Mita P, Wudzinska A, Sun X, Andrade J, Nayak S, Kahler DJ, Badri S, LaCava J, Ueberheide B, Yun CY, Fenyo D, and Boeke JD. 2018. LINE-1 protein localization and functional dynamics during the cell cycle. *Elife.* 7.
- Miyanari Y, Atsuzawa K, Usuda N, Watashi K, Hishiki T, Zayas M, Bartenschlager R, Wakita T, Hijikata M, and Shimotohno K. 2007. The lipid droplet is an important organelle for hepatitis C virus production. *Nat. Cell Biol.* 9:1089-1097.
- Mizui T, Yamashina S, Tanida I, Takei Y, Ueno T, Sakamoto N, Ikejima K, Kitamura T, Enomoto N, Sakai T, Kominami E, and Watanabe S. 2010. Inhibition of hepatitis C virus replication by chloroquine targeting virus-associated autophagy. *J. Gastroenterol.* 45:195-203.
- Moldovan JB, and Moran JV. 2015. The Zinc-Finger Antiviral Protein ZAP Inhibits LINE and Alu Retrotransposition. *PLoS Genet.* 11:e1005121.
- Monot C, Kuciak M, Viollet S, Mir AA, Gabus C, Darlix JL, and Cristofari G. 2013. The specificity and flexibility of I1 reverse transcription priming at imperfect T-tracts. *PLoS Genet.* 9:e1003499.
- Moradpour D, Brass V, Bieck E, Friebe P, Gosert R, Blum HE, Bartenschlager R, Penin F, and Lohmann V. 2004. Membrane association of the RNA-dependent RNA polymerase is essential for hepatitis C virus RNA replication. *J. Virol.* 78:13278-13284.
- Moradpour D, and Penin F. 2013. Hepatitis C virus proteins: from structure to function. *Curr. Top. Microbiol. Immunol.* 369:113-142.
- Moradpour D, Penin F, and Rice CM. 2007. Replication of hepatitis C virus. *Nat. Rev. Microbiol.* 5:453-463.
- Moran JV, DeBerardinis RJ, and Kazazian HH, Jr. 1999. Exon shuffling by L1 retrotransposition. *Science.* 283:1530-1534.
- Moran JV, Holmes SE, Naas TP, DeBerardinis RJ, Boeke JD, and Kazazian HH, Jr. 1996. High frequency retrotransposition in cultured mammalian cells. *Cell.* 87:917-927.
- Morikawa K, Lange CM, Gouttenoire J, Meylan E, Brass V, Penin F, and Moradpour D. 2011. Nonstructural protein 3-4A: the Swiss army knife of hepatitis C virus. *J. Viral Hepat.* 18:305-315.
- Moriya K, Fujie H, Shintani Y, Yotsuyanagi H, Tsutsumi T, Ishibashi K, Matsuura Y, Kimura S, Miyamura T, and Koike K. 1998. The core protein of hepatitis C virus induces hepatocellular carcinoma in transgenic mice. *Nat. Med.* 4:1065-1067.
- Moriya K, Nakagawa K, Santa T, Shintani Y, Fujie H, Miyoshi H, Tsutsumi T, Miyazawa T, Ishibashi K, Horie T, Imai K, Todoroki T, Kimura S, and Koike K. 2001. Oxidative stress in the absence of inflammation in a mouse model for hepatitis C virus-associated hepatocarcinogenesis. *Cancer Res.* 61:4365-4370.
- Moriya K, Yotsuyanagi H, Shintani Y, Fujie H, Ishibashi K, Matsuura Y, Miyamura T, and Koike K. 1997. Hepatitis C virus core protein induces hepatic steatosis in transgenic mice. *J. Gen. Virol.* 78 ( Pt 7):1527-1531.
- Muckenfuss H, Hamdorf M, Held U, Perkovic M, Lower J, Cichutek K, Flory E, Schumann GG, and Munk C. 2006. APOBEC3 proteins inhibit human LINE-1 retrotransposition. *J. Biol. Chem.* 281:22161-22172.
- Murphy DG, Willems B, Deschenes M, Hilzenrat N, Mousseau R, and Sabbah S. 2007. Use of sequence analysis of the NS5B region for routine genotyping of hepatitis C virus with reference to C/E1 and 5' untranslated region sequences. *J. Clin. Microbiol.* 45:1102-1112.
- Nakabayashi H, Taketa K, Miyano K, Yamane T, and Sato J. 1982. Growth of human hepatoma cells lines with differentiated functions in chemically defined medium. *Cancer Res.* 42:3858-3863.

- Naldini L, Blomer U, Gallay P, Ory D, Mulligan R, Gage FH, Verma IM, and Trono D. 1996. In vivo gene delivery and stable transduction of nondividing cells by a lentiviral vector. *Science*. 272:263-267.
- Neufeldt CJ, Cortese M, Acosta EG, and Bartenschlager R. 2018. Rewiring cellular networks by members of the Flaviviridae family. *Nat. Rev. Microbiol.* 16:125-142.
- Nielsen SU, Bassendine MF, Burt AD, Martin C, Pumeekochchai W, and Toms GL. 2006. Association between hepatitis C virus and very-low-density lipoprotein (VLDL)/LDL analyzed in iodixanol density gradients. *J. Virol.* 80:2418-2428.
- Nielsen SU, Bassendine MF, Martin C, Lowther D, Purcell PJ, King BJ, Neely D, and Toms GL. 2008. Characterization of hepatitis C RNA-containing particles from human liver by density and size. *J. Gen. Virol.* 89:2507-2517.
- Okubo M, Horinishi A, Saito M, Ebara T, Endo Y, Kaku K, Murase T, and Eto M. 2007. A novel complex deletion-insertion mutation mediated by Alu repetitive elements leads to lipoprotein lipase deficiency. *Mol. Genet. Metab.* 92:229-233.
- Okuda M, Li K, Beard MR, Showalter LA, Scholle F, Lemon SM, and Weinman SA. 2002. Mitochondrial injury, oxidative stress, and antioxidant gene expression are induced by hepatitis C virus core protein. *Gastroenterology*. 122:366-375.
- Ono M, Kawakami M, and Takezawa T. 1987. A novel human nonviral retroposon derived from an endogenous retrovirus. *Nucleic Acids Res.* 15:8725-8737.
- Op De Beeck A, Montserret R, Duvet S, Cocquerel L, Cacan R, Barberot B, Le Maire M, Penin F, and Dubuisson J. 2000. The transmembrane domains of hepatitis C virus envelope glycoproteins E1 and E2 play a major role in heterodimerization. *J. Biol. Chem.* 275:31428-31437.
- Op De Beeck A, Voisset C, Bartosch B, Ciczora Y, Cocquerel L, Keck Z, Fong S, Cosset FL, and Dubuisson J. 2004. Characterization of functional hepatitis C virus envelope glycoproteins. *J. Virol.* 78:2994-3002.
- Orecchini E, Doria M, Antonioni A, Galardi S, Ciafre SA, Frassinelli L, Mancone C, Montaldo C, Tripodi M, and Michienzi A. 2017. ADAR1 restricts LINE-1 retrotransposition. *Nucleic Acids Res.* 45:155-168.
- Ostertag EM, DeBerardinis RJ, Goodier JL, Zhang Y, Yang N, Gerton GL, and Kazazian HH, Jr. 2002. A mouse model of human L1 retrotransposition. *Nat. Genet.* 32:655-660.
- Ostertag EM, Goodier JL, Zhang Y, and Kazazian HH, Jr. 2003. SVA elements are nonautonomous retrotransposons that cause disease in humans. *Am. J. Hum. Genet.* 73:1444-1451.
- Ostertag EM, and Kazazian HH, Jr. 2001. Biology of mammalian L1 retrotransposons. *Annu. Rev. Genet.* 35:501-538.
- Ostertag EM, Prak ET, DeBerardinis RJ, Moran JV, and Kazazian HH, Jr. 2000. Determination of L1 retrotransposition kinetics in cultured cells. *Nucleic Acids Res.* 28:1418-1423.
- Pace JK, 2nd, and Feschotte C. 2007. The evolutionary history of human DNA transposons: evidence for intense activity in the primate lineage. *Genome Res.* 17:422-432.
- Paek KY, Kim CS, Park SM, Kim JH, and Jang SK. 2008. RNA-binding protein hnRNP D modulates internal ribosome entry site-dependent translation of hepatitis C virus RNA. *J. Virol.* 82:12082-12093.
- Paoletta G, Lucero MA, Murphy MH, and Baralle FE. 1983. The Alu family repeat promoter has a tRNA-like bipartite structure. *EMBO J.* 2:691-696.
- Patchesung M, Boonla C, Amnattrakul P, Dissayabutra T, Mutirangura A, and Tosukhowong P. 2012. Long interspersed nuclear element-1 hypomethylation and oxidative stress: correlation and bladder cancer diagnostic potential. *PLoS One*. 7:e37009.
- Paul D, Hoppe S, Saher G, Krijnse-Locker J, and Bartenschlager R. 2013. Morphological and biochemical characterization of the membranous hepatitis C virus replication compartment. *J. Virol.* 87:10612-10627.
- Penin F, Brass V, Appel N, Ramboarina S, Montserret R, Ficheux D, Blum HE, Bartenschlager R, and Moradpour D. 2004. Structure and function of the membrane anchor domain of hepatitis C virus nonstructural protein 5A. *J. Biol. Chem.* 279:40835-40843.

- Perlemuter G, Sabile A, Letteron P, Vona G, Topilco A, Chretien Y, Koike K, Pessayre D, Chapman J, Barba G, and Brechot C. 2002. Hepatitis C virus core protein inhibits microsomal triglyceride transfer protein activity and very low density lipoprotein secretion: a model of viral-related steatosis. *FASEB J.* 16:185-194.
- Pietschmann T, Kaul A, Koutsoudakis G, Shavinskaya A, Kallis S, Steinmann E, Abid K, Negro F, Dreux M, Cosset FL, and Bartenschlager R. 2006. Construction and characterization of infectious intragenotypic and intergenotypic hepatitis C virus chimeras. *Proc. Natl. Acad. Sci. U. S. A.* 103:7408-7413.
- Ploss A, Evans MJ, Gaysinskaya VA, Panis M, You H, de Jong YP, and Rice CM. 2009. Human occludin is a hepatitis C virus entry factor required for infection of mouse cells. *Nature.* 457:882-886.
- Poenisch M, Metz P, Blankenburg H, Ruggieri A, Lee JY, Rupp D, Rebhan I, Diederich K, Kaderali L, Domingues FS, Albrecht M, Lohmann V, Erfle H, and Bartenschlager R. 2015. Identification of HNRNPK as regulator of hepatitis C virus particle production. *PLoS Pathog.* 11:e1004573.
- Popescu CI, Callens N, Trinel D, Roingeard P, Moradpour D, Descamps V, Duverlie G, Penin F, Heliot L, Rouille Y, and Dubuisson J. 2011. NS2 protein of hepatitis C virus interacts with structural and non-structural proteins towards virus assembly. *PLoS Pathog.* 7:e1001278.
- Powdrill MH, Tchesnokov EP, Kozak RA, Russell RS, Martin R, Svarovskaia ES, Mo H, Kouyos RD, and Gotte M. 2011. Contribution of a mutational bias in hepatitis C virus replication to the genetic barrier in the development of drug resistance. *Proc. Natl. Acad. Sci. U. S. A.* 108:20509-20513.
- Qian Y, Mancini-DiNardo D, Judkins T, Cox HC, Brown K, Elias M, Singh N, Daniels C, Holladay J, Coffee B, Bowles KR, and Roa BB. 2017. Identification of pathogenic retrotransposon insertions in cancer predisposition genes. *Cancer Genet.* 216-217:159-169.
- Raiz J, Damert A, Chira S, Held U, Klawitter S, Hamdorf M, Lower J, Stratling WH, Lower R, and Schumann GG. 2012. The non-autonomous retrotransposon SVA is trans-mobilized by the human LINE-1 protein machinery. *Nucleic Acids Res.* 40:1666-1683.
- Ramage HR, Kumar GR, Verschueren E, Johnson JR, Von Dollen J, Johnson T, Newton B, Shah P, Horner J, Krogan NJ, and Ott M. 2015. A combined proteomics/genomics approach links hepatitis C virus infection with nonsense-mediated mRNA decay. *Mol. Cell.* 57:329-340.
- Randall G, Panis M, Cooper JD, Tellinghuisen TL, Sukhodolets KE, Pfeffer S, Landthaler M, Landgraf P, Kan S, Lindenbach BD, Chien M, Weir DB, Russo JJ, Ju J, Brownstein MJ, Sheridan R, Sander C, Zavolan M, Tuschl T, and Rice CM. 2007. Cellular cofactors affecting hepatitis C virus infection and replication. *Proc. Natl. Acad. Sci. U. S. A.* 104:12884-12889.
- Reiss S, Rebhan I, Backes P, Romero-Brey I, Erfle H, Matula P, Kaderali L, Poenisch M, Blankenburg H, Hiet MS, Longerich T, Diehl S, Ramirez F, Balla T, Rohr K, Kaul A, Buhler S, Pepperkok R, Lengauer T, Albrecht M, Eils R, Schirmacher P, Lohmann V, and Bartenschlager R. 2011. Recruitment and activation of a lipid kinase by hepatitis C virus NS5A is essential for integrity of the membranous replication compartment. *Cell Host & Microbe.* 9:32-45.
- Rodic N, Sharma R, Sharma R, Zampella J, Dai L, Taylor MS, Hruban RH, Iacobuzio-Donahue CA, Maitra A, Torbenson MS, Goggins M, Shih Ie M, Duffield AS, Montgomery EA, Gabrielson E, Netto GJ, Lotan TL, De Marzo AM, Westra W, Binder ZA, Orr BA, Gallia GL, Eberhart CG, Boeke JD, Harris CR, and Burns KH. 2014. Long interspersed element-1 protein expression is a hallmark of many human cancers. *Am. J. Pathol.* 184:1280-1286.
- Rohrer J, Minegishi Y, Richter D, Eguiguren J, and Conley ME. 1999. Unusual mutations in Btk: an insertion, a duplication, an inversion, and four large deletions. *Clin. Immunol.* 90:28-37.

- Roingeard P, Hourieux C, Blanchard E, and Prensier G. 2008. Hepatitis C virus budding at lipid droplet-associated ER membrane visualized by 3D electron microscopy. *Histochem. Cell Biol.* 130:561-566.
- Romero-Brey I, Merz A, Chiramel A, Lee JY, Chlanda P, Haselman U, Santarella-Mellwig R, Habermann A, Hoppe S, Kallis S, Walther P, Antony C, Krijnse-Locker J, and Bartenschlager R. 2012. Three-dimensional architecture and biogenesis of membrane structures associated with hepatitis C virus replication. *PLoS Pathog.* 8:e1003056.
- Rosch K, Kwiatkowski M, Hofmann S, Schobel A, Gruttner C, Wurlitzer M, Schluter H, and Herker E. 2016. Quantitative Lipid Droplet Proteome Analysis Identifies Annexin A3 as a Cofactor for HCV Particle Production. *Cell Rep.* 16:3219-3231.
- Sainz B, Jr., Barretto N, Martin DN, Hiraga N, Imamura M, Hussain S, Marsh KA, Yu X, Chayama K, Alrefai WA, and Uprichard SL. 2012. Identification of the Niemann-Pick C1-like 1 cholesterol absorption receptor as a new hepatitis C virus entry factor. *Nat. Med.* 18:281-285.
- Santolini E, Migliaccio G, and La Monica N. 1994. Biosynthesis and biochemical properties of the hepatitis C virus core protein. *J. Virol.* 68:3631-3641.
- Sassaman DM, Dombroski BA, Moran JV, Kimberland ML, Naas TP, DeBerardinis RJ, Gabriel A, Swergold GD, and Kazazian HH, Jr. 1997. Many human L1 elements are capable of retrotransposition. *Nat. Genet.* 16:37-43.
- Scarselli E, Ansuini H, Cerino R, Roccasecca RM, Acali S, Filocamo G, Traboni C, Nicosia A, Cortese R, and Vitelli A. 2002. The human scavenger receptor class B type I is a novel candidate receptor for the hepatitis C virus. *EMBO J.* 21:5017-5025.
- Schindelin J, Arganda-Carreras I, Frise E, Kaynig V, Longair M, Pietzsch T, Preibisch S, Rueden C, Saalfeld S, Schmid B, Tinevez JY, White DJ, Hartenstein V, Eliceiri K, Tomancak P, and Cardona A. 2012. Fiji: an open-source platform for biological-image analysis. *Nat. Methods.* 9:676-682.
- Schmidt-Mende J, Bieck E, Hugle T, Penin F, Rice CM, Blum HE, and Moradpour D. 2001. Determinants for membrane association of the hepatitis C virus RNA-dependent RNA polymerase. *J. Biol. Chem.* 276:44052-44063.
- Schneider AM, Schmidt S, Jonas S, Vollmer B, Khazina E, and Weichenrieder O. 2013. Structure and properties of the esterase from non-LTR retrotransposons suggest a role for lipids in retrotransposition. *Nucleic Acids Res.* 41:10563-10572.
- Schobel A, Rosch K, and Herker E. 2018. Functional innate immunity restricts Hepatitis C Virus infection in induced pluripotent stem cell-derived hepatocytes. *Sci. Rep.* 8:3893.
- Sciamanna I, Landriscina M, Pittoggi C, Quirino M, Mearelli C, Beraldi R, Mattei E, Serafino A, Cassano A, Sinibaldi-Vallebona P, Garaci E, Barone C, and Spadafora C. 2005. Inhibition of endogenous reverse transcriptase antagonizes human tumor growth. *Oncogene.* 24:3923-3931.
- Scott AF, Schmeckpeper BJ, Abdelrazik M, Comey CT, O'Hara B, Rossiter JP, Cooley T, Heath P, Smith KD, and Margolet L. 1987. Origin of the human L1 elements: proposed progenitor genes deduced from a consensus DNA sequence. *Genomics.* 1:113-125.
- Sedano CD, and Samow P. 2014. Hepatitis C virus subverts liver-specific miR-122 to protect the viral genome from exoribonuclease Xrn2. *Cell Host Microbe.* 16:257-264.
- Shavinskaya A, Boulant S, Penin F, McLauchlan J, and Bartenschlager R. 2007. The lipid droplet binding domain of hepatitis C virus core protein is a major determinant for efficient virus assembly. *J. Biol. Chem.* 282:37158-37169.
- Shen L, Wu LC, Sanlioglu S, Chen R, Mendoza AR, Dangel AW, Carroll MC, Zipf WB, and Yu CY. 1994. Structure and genetics of the partially duplicated gene RP located immediately upstream of the complement C4A and the C4B genes in the HLA class III region. Molecular cloning, exon-intron structure, composite retroposon, and breakpoint of gene duplication. *J. Biol. Chem.* 269:8466-8476.
- Shi X, Seluanov A, and Gorbunova V. 2007. Cell divisions are required for L1 retrotransposition. *Mol. Cell. Biol.* 27:1264-1270.

- Shimoike T, Mimori S, Tani H, Matsuura Y, and Miyamura T. 1999. Interaction of hepatitis C virus core protein with viral sense RNA and suppression of its translation. *J. Virol.* 73:9718-9725.
- Shukla R, Upton KR, Munoz-Lopez M, Gerhardt DJ, Fisher ME, Nguyen T, Brennan PM, Baillie JK, Collino A, Ghisletti S, Sinha S, Iannelli F, Radaelli E, Dos Santos A, Rapoud D, Guettier C, Samuel D, Natoli G, Carninci P, Ciccarelli FD, Garcia-Perez JL, Faivre J, and Faulkner GJ. 2013. Endogenous retrotransposition activates oncogenic pathways in hepatocellular carcinoma. *Cell.* 153:101-111.
- Simmonds P, Bukh J, Combet C, Deleage G, Enomoto N, Feinstone S, Halfon P, Inchauspe G, Kuiken C, Maertens G, Mizokami M, Murphy DG, Okamoto H, Pawlotsky JM, Penin F, Sablon E, Shin IT, Stuyver LJ, Thiel HJ, Viazov S, Weiner AJ, and Widell A. 2005. Consensus proposals for a unified system of nomenclature of hepatitis C virus genotypes. *Hepatology.* 42:962-973.
- Singer MF. 1982. SINEs and LINEs: highly repeated short and long interspersed sequences in mammalian genomes. *Cell.* 28:433-434.
- Sir D, Chen WL, Choi J, Wakita T, Yen TS, and Ou JH. 2008. Induction of incomplete autophagic response by hepatitis C virus via the unfolded protein response. *Hepatology.* 48:1054-1061.
- Smit AF, and Riggs AD. 1995. MIRs are classic, tRNA-derived SINEs that amplified before the mammalian radiation. *Nucleic Acids Res.* 23:98-102.
- Smit AF, and Riggs AD. 1996. Tiggers and DNA transposon fossils in the human genome. *Proc. Natl. Acad. Sci. U. S. A.* 93:1443-1448.
- Smit AF, Toth G, Riggs AD, and Jurka J. 1995. Ancestral, mammalian-wide subfamilies of LINE-1 repetitive sequences. *J. Mol. Biol.* 246:401-417.
- Smith DB, Bukh J, Kuiken C, Muerhoff AS, Rice CM, Stapleton JT, and Simmonds P. 2014. Expanded classification of hepatitis C virus into 7 genotypes and 67 subtypes: updated criteria and genotype assignment web resource. *Hepatology.* 59:318-327.
- Soifer HS, Zaragoza A, Peyvan M, Behlke MA, and Rossi JJ. 2005. A potential role for RNA interference in controlling the activity of the human LINE-1 retrotransposon. *Nucleic Acids Res.* 33:846-856.
- Sokolowski M, Chynces M, deHaro D, Christian CM, and Belancio VP. 2017. Truncated ORF1 proteins can suppress LINE-1 retrotransposition in trans. *Nucleic Acids Res.* 45:5294-5308.
- Sotero-Caio CG, Platt RN, 2nd, Suh A, and Ray DA. 2017. Evolution and Diversity of Transposable Elements in Vertebrate Genomes. *Genome Biol. Evol.* 9:161-177.
- Sourisseau M, Michta ML, Zony C, Israelow B, Hopcraft SE, Narbus CM, Parra Martin A, and Evans MJ. 2013. Temporal analysis of hepatitis C virus cell entry with occludin directed blocking antibodies. *PLoS Pathog.* 9:e1003244.
- Speek M. 2001. Antisense promoter of human L1 retrotransposon drives transcription of adjacent cellular genes. *Mol. Cell. Biol.* 21:1973-1985.
- Steinmann E, and Pietschmann T. 2010. Hepatitis C virus p7-a viroporin crucial for virus assembly and an emerging target for antiviral therapy. *Viruses.* 2:2078-2095.
- Stenglein MD, and Harris RS. 2006. APOBEC3B and APOBEC3F inhibit L1 retrotransposition by a DNA deamination-independent mechanism. *J. Biol. Chem.* 281:16837-16841.
- Stoeck IK, Lee JY, Tabata K, Romero-Brey I, Paul D, Schult P, Lohmann V, Kaderali L, and Bartenschlager R. 2018. Hepatitis C Virus Replication Depends on Endosomal Cholesterol Homeostasis. *J. Virol.* 92.
- Sukarova E, Dimovski AJ, Tchacarova P, Petkov GH, and Efremov GD. 2001. An Alu insert as the cause of a severe form of hemophilia A. *Acta Haematol.* 106:126-129.
- Sumpter R, Jr., Loo YM, Foy E, Li K, Yoneyama M, Fujita T, Lemon SM, and Gale M, Jr. 2005. Regulating intracellular antiviral defense and permissiveness to hepatitis C virus RNA replication through a cellular RNA helicase, RIG-I. *J. Virol.* 79:2689-2699.
- Suppiah V, Moldovan M, Ahlenstiel G, Berg T, Weltman M, Abate ML, Bassendine M, Spengler U, Dore GJ, Powell E, Riordan S, Sheridan D, Smedile A, Fragomeli V, Muller T, Bahlo M, Stewart GJ, Booth DR, and George J. 2009. IL28B is associated

- with response to chronic hepatitis C interferon-alpha and ribavirin therapy. *Nat. Genet.* 41:1100-1104.
- Swergold GD. 1990. Identification, characterization, and cell specificity of a human LINE-1 promoter. *Mol. Cell. Biol.* 10:6718-6729.
- Szak ST, Pickeral OK, Makalowski W, Boguski MS, Landsman D, and Boeke JD. 2002. Molecular archeology of L1 insertions in the human genome. *Genome Biol.* 3:research0052.
- Tanaka N, Moriya K, Kiyosawa K, Koike K, Gonzalez FJ, and Aoyama T. 2008. PPARalpha activation is essential for HCV core protein-induced hepatic steatosis and hepatocellular carcinoma in mice. *J. Clin. Invest.* 118:683-694.
- Tanaka Y, Nishida N, Sugiyama M, Kurosaki M, Matsuura K, Sakamoto N, Nakagawa M, Korenaga M, Hino K, Hige S, Ito Y, Mita E, Tanaka E, Mochida S, Murawaki Y, Honda M, Sakai A, Hiasa Y, Nishiguchi S, Koike A, Sakaida I, Imamura M, Ito K, Yano K, Masaki N, Sugauchi F, Izumi N, Tokunaga K, and Mizokami M. 2009. Genome-wide association of IL28B with response to pegylated interferon-alpha and ribavirin therapy for chronic hepatitis C. *Nat. Genet.* 41:1105-1109.
- Targett-Adams P, Hope G, Boulant S, and McLauchlan J. 2008. Maturation of hepatitis C virus core protein by signal peptide peptidase is required for virus production. *J. Biol. Chem.* 283:16850-16859.
- Tauchi-Sato K, Ozeki S, Houjou T, Taguchi R, and Fujimoto T. 2002. The surface of lipid droplets is a phospholipid monolayer with a unique Fatty Acid composition. *J. Biol. Chem.* 277:44507-44512.
- Taylor MS, LaCava J, Mita P, Molloy KR, Huang CR, Li D, Adney EM, Jiang H, Burns KH, Chait BT, Rout MP, Boeke JD, and Dai L. 2013. Affinity proteomics reveals human host factors implicated in discrete stages of LINE-1 retrotransposition. *Cell.* 155:1034-1048.
- Tellinghuisen TL, Marcotrigiano J, Gorbalenya AE, and Rice CM. 2004. The NS5A protein of hepatitis C virus is a zinc metalloprotein. *J. Biol. Chem.* 279:48576-48587.
- Tellinghuisen TL, Marcotrigiano J, and Rice CM. 2005. Structure of the zinc-binding domain of an essential component of the hepatitis C virus replicase. *Nature.* 435:374-379.
- Teugels E, De Brakeleer S, Goelen G, Lissens W, Sermijn E, and De Greve J. 2005. De novo Alu element insertions targeted to a sequence common to the BRCA1 and BRCA2 genes. *Hum. Mutat.* 26:284.
- Thayer RE, Singer MF, and Fanning TG. 1993. Undermethylation of specific LINE-1 sequences in human cells producing a LINE-1-encoded protein. *Gene.* 133:273-277.
- Thein HH, Yi Q, Dore GJ, and Krahn MD. 2008. Estimation of stage-specific fibrosis progression rates in chronic hepatitis C virus infection: a meta-analysis and meta-regression. *Hepatology.* 48:418-431.
- Thursz M, and Fontanet A. 2014. HCV transmission in industrialized countries and resource-constrained areas. *Nat Rev Gastroenterol Hepatol.* 11:28-35.
- Timpe JM, Stamataki Z, Jennings A, Hu K, Farquhar MJ, Harris HJ, Schwarz A, Desombere I, Roels GL, Balfe P, and McKeating JA. 2008. Hepatitis C virus cell-cell transmission in hepatoma cells in the presence of neutralizing antibodies. *Hepatology.* 47:17-24.
- Trinchet JC, Ganne-Carrie N, Nahon P, N'Kontchou G, and Beaugrand M. 2007. Hepatocellular carcinoma in patients with hepatitis C virus-related chronic liver disease. *World J. Gastroenterol.* 13:2455-2460.
- Tscherne DM, Jones CT, Evans MJ, Lindenbach BD, McKeating JA, and Rice CM. 2006. Time- and temperature-dependent activation of hepatitis C virus for low-pH-triggered entry. *J. Virol.* 80:1734-1741.
- Udaka T, Okamoto N, Aramaki M, Torii C, Kosaki R, Hosokai N, Hayakawa T, Takahata N, Takahashi T, and Kosaki K. 2007. An Alu retrotransposition-mediated deletion of CHD7 in a patient with CHARGE syndrome. *Am. J. Med. Genet. A.* 143A:721-726.
- Ullu E, and Tschudi C. 1984. Alu sequences are processed 7SL RNA genes. *Nature.* 312:171-172.
- UNECE. 2017. GHS. In Globally Harmonized System of Classification and Labelling of Chemicals (GHS). Vol. Seventh Revised Edition.



- van den Hurk JA, Meij IC, Seleme MC, Kano H, Nikopoulos K, Hoefsloot LH, Sistermans EA, de Wijs IJ, Mukhopadhyay A, Plomp AS, de Jong PT, Kazazian HH, and Cremers FP. 2007. L1 retrotransposition can occur early in human embryonic development. *Hum. Mol. Genet.* 16:1587-1592.
- Van Meter M, Kashyap M, Rezazadeh S, Geneva AJ, Morello TD, Seluanov A, and Gorbunova V. 2014. SIRT6 represses LINE1 retrotransposons by ribosylating KAP1 but this repression fails with stress and age. *Nat Commun.* 5:5011.
- Vieyres G, Thomas X, Descamps V, Duverlie G, Patel AH, and Dubuisson J. 2010. Characterization of the envelope glycoproteins associated with infectious hepatitis C virus. *J. Virol.* 84:10159-10168.
- Voisset C, and Dubuisson J. 2004. Functional hepatitis C virus envelope glycoproteins. *Biol. Cell.* 96:413-420.
- Wakita T, Pietschmann T, Kato T, Date T, Miyamoto M, Zhao Z, Murthy K, Habermann A, Krausslich HG, Mizokami M, Bartenschlager R, and Liang TJ. 2005. Production of infectious hepatitis C virus in tissue culture from a cloned viral genome. *Nat. Med.* 11:791-796.
- Wallace MR, Andersen LB, Saulino AM, Gregory PE, Glover TW, and Collins FS. 1991. A de novo Alu insertion results in neurofibromatosis type 1. *Nature.* 353:864-866.
- Wallace NA, Belancio VP, and Deininger PL. 2008. L1 mobile element expression causes multiple types of toxicity. *Gene.* 419:75-81.
- Walters KA, Syder AJ, Lederer SL, Diamond DL, Paeper B, Rice CM, and Katze MG. 2009. Genomic analysis reveals a potential role for cell cycle perturbation in HCV-mediated apoptosis of cultured hepatocytes. *PLoS Pathog.* 5:e1000269.
- Walther TC, and Farese RV, Jr. 2012. Lipid droplets and cellular lipid metabolism. *Annu. Rev. Biochem.* 81:687-714.
- Wang C, Sarnow P, and Siddiqui A. 1993. Translation of human hepatitis C virus RNA in cultured cells is mediated by an internal ribosome-binding mechanism. *J. Virol.* 67:3338-3344.
- Wang H, Perry JW, Lauring AS, Neddermann P, De Francesco R, and Tai AW. 2014. Oxysterol-binding protein is a phosphatidylinositol 4-kinase effector required for HCV replication membrane integrity and cholesterol trafficking. *Gastroenterology.* 146:1373-1385 e1371-1311.
- Wang H, Xing J, Grover D, Hedges DJ, Han K, Walker JA, and Batzer MA. 2005. SVA elements: a hominid-specific retroposon family. *J. Mol. Biol.* 354:994-1007.
- Wang L, Kim JY, Liu HM, Lai MMC, and Ou JJ. 2017. HCV-induced autophagosomes are generated via homotypic fusion of phagophores that mediate HCV RNA replication. *PLoS Pathog.* 13:e1006609.
- Wang L, Tian Y, and Ou JH. 2015. HCV induces the expression of Rubicon and UVRAG to temporally regulate the maturation of autophagosomes and viral replication. *PLoS Pathog.* 11:e1004764.
- Wang N, Liang Y, Devaraj S, Wang J, Lemon SM, and Li K. 2009. Toll-like receptor 3 mediates establishment of an antiviral state against hepatitis C virus in hepatoma cells. *J. Virol.* 83:9824-9834.
- Waterston RH, Lindblad-Toh K, Birney E, Rogers J, Abril JF, Agarwal P, Agarwala R, Ainscough R, Alexandersson M, An P, Antonarakis SE, Attwood J, Baertsch R, Bailey J, Barlow K, Beck S, Berry E, Birren B, Bloom T, Bork P, Botcherby M, Bray N, Brent MR, Brown DG, Brown SD, Bult C, Burton J, Butler J, Campbell RD, Carninci P, Cawley S, Chiaromonte F, Chinwalla AT, Church DM, Clamp M, Clee C, Collins FS, Cook LL, Copley RR, Coulson A, Couronne O, Cuff J, Curwen V, Cutts T, Daly M, David R, Davies J, Delehaunty KD, Deri J, Dermitzakis ET, Dewey C, Dickens NJ, Diekhans M, Dodge S, Dubchak I, Dunn DM, Eddy SR, Elnitski L, Emes RD, Eswara P, Eyraas E, Felsenfeld A, Fewell GA, Flicek P, Foley K, Frankel WN, Fulton LA, Fulton RS, Furey TS, Gage D, Gibbs RA, Glusman G, Gnerre S, Goldman N, Goodstadt L, Grafham D, Graves TA, Green ED, Gregory S, Guigo R, Guyer M, Hardison RC, Haussler D, Hayashizaki Y, Hillier LW, Hinrichs A, Hlavina W, Holzer T, Hsu F, Hua A, Hubbard T, Hunt A, Jackson I, Jaffe DB, Johnson LS, Jones M, Jones

- TA, Joy A, Kamal M, Karlsson EK, et al. 2002. Initial sequencing and comparative analysis of the mouse genome. *Nature*. 420:520-562.
- Weber K, Bartsch U, Stocking C, and Fehse B. 2008. A multicolor panel of novel lentiviral "gene ontology" (LeGO) vectors for functional gene analysis. *Mol. Ther.* 16:698-706.
- Webster B, Ott M, and Greene WC. 2013. Evasion of superinfection exclusion and elimination of primary viral RNA by an adapted strain of hepatitis C virus. *J. Virol.* 87:13354-13369.
- Webster DP, Klenerman P, and Dusheiko GM. 2015. Hepatitis C. *Lancet*. 385:1124-1135.
- Wei W, Gilbert N, Ooi SL, Lawler JF, Ostertag EM, Kazazian HH, Boeke JD, and Moran JV. 2001. Human L1 retrotransposition: cis preference versus trans complementation. *Mol. Cell. Biol.* 21:1429-1439.
- Weinlich S, Huttelmaier S, Schierhorn A, Behrens SE, Ostareck-Lederer A, and Ostareck DH. 2009. IGF2BP1 enhances HCV IRES-mediated translation initiation via the 3'UTR. *RNA*. 15:1528-1542.
- WHO. 2017. Global hepatitis report.
- Whongsiri P, Pimratana C, Wijitsettakul U, Jindatip D, Sanpavat A, Schulz WA, Hoffmann MJ, Goering W, and Boonla C. 2018. LINE-1 ORF1 Protein Is Up-regulated by Reactive Oxygen Species and Associated with Bladder Urothelial Carcinoma Progression. *Cancer Genomics Proteomics*. 15:143-151.
- Wicker T, Sabot F, Hua-Van A, Bennetzen JL, Capi P, Chalhub B, Flavell A, Leroy P, Morgante M, Panaud O, Paux E, SanMiguel P, and Schulman AH. 2007. A unified classification system for eukaryotic transposable elements. *Nat. Rev. Genet.* 8:973-982.
- Wildschutte JH, Williams ZH, Montesion M, Subramanian RP, Kidd JM, and Coffin JM. 2016. Discovery of unfixed endogenous retrovirus insertions in diverse human populations. *Proc. Natl. Acad. Sci. U. S. A.* 113:E2326-2334.
- Will CL, and Luhrmann R. 2011. Spliceosome structure and function. *Cold Spring Harb. Perspect. Biol.* 3.
- Willems L, and Gillet NA. 2015. APOBEC3 Interference during Replication of Viral Genomes. *Viruses*. 7:2999-3018.
- Wimmer K, Callens T, Wernstedt A, and Messiaen L. 2011. The NF1 gene contains hotspots for L1 endonuclease-dependent de novo insertion. *PLoS Genet.* 7:e1002371.
- Wissing S, Montano M, Garcia-Perez JL, Moran JV, and Greene WC. 2011. Endogenous APOBEC3B restricts LINE-1 retrotransposition in transformed cells and human embryonic stem cells. *J. Biol. Chem.* 286:36427-36437.
- Wissing S, Munoz-Lopez M, Macia A, Yang Z, Montano M, Collins W, Garcia-Perez JL, Moran JV, and Greene WC. 2012. Reprogramming somatic cells into iPS cells activates LINE-1 retroelement mobility. *Hum. Mol. Genet.* 21:208-218.
- Xie Y, Mates L, Ivics Z, Izsvak Z, Martin SL, and An W. 2013. Cell division promotes efficient retrotransposition in a stable L1 reporter cell line. *Mob DNA*. 4:10.
- Xing J, Zhang Y, Han K, Salem AH, Sen SK, Huff CD, Zhou Q, Kirkness EF, Levy S, Batzer MA, and Jorde LB. 2009. Mobile elements create structural variation: analysis of a complete human genome. *Genome Res*. 19:1516-1526.
- Yamaga AK, and Ou JH. 2002. Membrane topology of the hepatitis C virus NS2 protein. *J. Biol. Chem.* 277:33228-33234.
- Yang N, and Kazazian HH, Jr. 2006. L1 retrotransposition is suppressed by endogenously encoded small interfering RNAs in human cultured cells. *Nat. Struct. Mol. Biol.* 13:763-771.
- Yi M, and Lemon SM. 2003. 3' nontranslated RNA signals required for replication of hepatitis C virus RNA. *J. Virol.* 77:3557-3568.
- Zemer R, Kitay Cohen Y, Naftaly T, and Klein A. 2008. Presence of hepatitis C virus DNA sequences in the DNA of infected patients. *Eur. J. Clin. Invest.* 38:845-848.
- Zhang Z, Harrison PM, Liu Y, and Gerstein M. 2003. Millions of years of evolution preserved: a comprehensive catalog of the processed pseudogenes in the human genome. *Genome Res*. 13:2541-2558.

- Zhao K, Du J, Han X, Goodier JL, Li P, Zhou X, Wei W, Evans SL, Li L, Zhang W, Cheung LE, Wang G, Kazazian HH, Jr., and Yu XF. 2013. Modulation of LINE-1 and Alu/SVA retrotransposition by Aicardi-Goutieres syndrome-related SAMHD1. *Cell Rep.* 4:1108-1115.
- Zhong J, Gastaminza P, Cheng G, Kapadia S, Kato T, Burton DR, Wieland SF, Uprichard SL, Wakita T, and Chisari FV. 2005. Robust hepatitis C virus infection in vitro. *Proc. Natl. Acad. Sci. U.S.A.* 102:9294-9299.
- Zhu C, Utsunomiya T, Ikemoto T, Yamada S, Morine Y, Imura S, Arakawa Y, Takasu C, Ishikawa D, Imoto I, and Shimada M. 2014. Hypomethylation of long interspersed nuclear element-1 (LINE-1) is associated with poor prognosis via activation of c-MET in hepatocellular carcinoma. *Ann. Surg. Oncol.* 21 Suppl 4:S729-735.
- Zibbell JE, Asher AK, Patel RC, Kupronis B, Iqbal K, Ward JW, and Holtzman D. 2018. Increases in Acute Hepatitis C Virus Infection Related to a Growing Opioid Epidemic and Associated Injection Drug Use, United States, 2004 to 2014. *Am. J. Public Health.* 108:175-181.
- Zona L, Lupberger J, Sidahmed-Adrar N, Thumann C, Harris HJ, Barnes A, Florentin J, Tawar RG, Xiao F, Turek M, Durand SC, Duong FH, Heim MH, Cosset FL, Hirsch I, Samuel D, Brino L, Zeisel MB, Le Naour F, McKeating JA, and Baumert TF. 2013. HRas signal transduction promotes hepatitis C virus cell entry by triggering assembly of the host tetraspanin receptor complex. *Cell Host Microbe.* 13:302-313.

## 8 Appendix

### 8.1 List of figures










Figure 1: Global prevalence of HCV genotypes 1-6.....	13
Figure 2: Morphology of the HCV particle.....	14
Figure 3: The HCV life cycle.....	15
Figure 4: HCV entry.....	16
Figure 5: HCV genome and viral proteins.....	18
Figure 6: Assembly and maturation of HCV particles.....	23
Figure 7: Abundance of retroelements in the human genome.....	26
Figure 8: Transposable elements in the human genome.....	27
Figure 9: Schematic representation of LINE1 and its encoded proteins L1ORF1p and L1ORF2p.....	31
Figure 10: LINE1 retrotransposition cycle.....	35
Figure 11: LINE1 mRNA and protein levels increase in HCV-infected cells.....	42
Figure 12: HCV infection induces the recruitment of L1ORF1p to lipid-rich fractions.....	44
Figure 13: Re-localization of L1ORF1p to LDs in HCV-infected cells.....	47
Figure 14: HCV RNA replication does not induce L1ORF1p-enrichment at LDs.....	48
Figure 15: HCV core re-localizes L1ORF1p to LDs.....	50
Figure 16: Expression of HCV core is sufficient to re-localize L1ORF1p to LDs.....	52
Figure 17: Comparison of LD-associated proteins and L1ORF1p interactors.....	54
Figure 18: RNA-dependent interaction between HA-L1ORF1p and HCV core.....	55
Figure 19: Endogenous L1ORF1p interacts with HCV core but not NS5A.....	56
Figure 20: Re-localization of L1ORF1p to LDs is partially dependent on its RNA-binding capacity.....	57
Figure 21: HCV RNA is enriched in co-IP fractions of HA-L1ORF1p.....	58
Figure 22: Presence of HCV RNA in LINE1 RNPs.....	60
Figure 23: L1ORF2p does not initiate reverse transcription from the HCV 3' UTR.....	62
Figure 24: Pre-established HA-L1ORF1p overexpression does not affect HCV RNA replication.....	63
Figure 25: HCV RNA replication is not altered by HA-L1ORF1p overexpression.....	64
Figure 26: Effect of LINE1 overexpression on HCV replication.....	66
Figure 27: HCV infection decreases LINE1 retrotransposition frequency.....	68
Figure 28: Interplay of LINE1 and HCV.....	79

### 8.2 List of tables




















Table 1: Single-gene diseases caused by LINE1 retrotransposition.....	38
Table 2: Bacterial strains.....	80
Table 3: Media for bacterial culture.....	80
Table 4: Cell culture media, buffers, and supplements.....	81
Table 5: Lysis buffer.....	81
Table 6: SDS PAGE and western blotting buffer.....	82
Table 7: Agarose gel electrophoresis.....	82
Table 8: DNA and protein standards.....	82
Table 9: Buffer used for LD isolation.....	83
Table 10: LEAP assay buffer.....	83
Table 11: Solutions used for microscopy.....	84
Table 12: Inhibitors used in this study.....	84
Table 13: Restriction enzymes.....	84
Table 14: Other enzymes.....	85

Table 15: Commercial kits used in this study.....	85
Table 16: HCV Plasmids. ....	86
Table 17: Expression plasmids.....	86
Table 18: PCR primer to clone HA-L1ORF1p and the HA-L1ORF1p RR261-262AA mutant into pSicoR-MS1ΔU6.....	89
Table 19: PCR Primer to clone SEAP_2A_EGFP or EGFP into pSicoR-MS1ΔU6.....	89
Table 20: qRT-PCR primer.....	90
Table 21: LEAP primer. ....	90
Table 22: Primary antibodies.....	91
Table 23: Secondary antibodies. ....	92
Table 24: Fluorescent dyes. ....	92
Table 25: Agarose beads. ....	92
Table 26: Consumables.....	93
Table 27: Chemicals.....	94
Table 28: Devices and Equipment.....	97
Table 29: Software. ....	98
Table 30: PCR reaction mix.....	100
Table 31: PCR conditions.....	100
Table 32: Overlap PCR reaction mix. ....	101
Table 33: Overlap PCR conditions.....	101
Table 34: Purification PCR conditions. ....	101
Table 35: Restriction digest.....	102
Table 36: Ligation mixture. ....	103
Table 37: LIC mixture.....	103
Table 38: Mung bean nuclease treatment.....	104
Table 39: Lentivirus transfection mix. ....	106
Table 40: LEAP reaction.....	110
Table 41: LEAP PCR mixture.....	111
Table 42: LEAP PCR conditions.....	111
Table 43: cDNA synthesis mixture.....	114
Table 44: qRT-PCR mix. ....	114
Table 45: qRT-PCR conditions.....	115










## 8.4 Toxicity of chemicals

Chemical	GHS pictogram	hazard statements	hazard	GHS precautionary statements
1,4-Dithiothreitol (DTT)		H302, H315, H319		P302+P350, P305+P351+P338
2-Mercaptoethanol		H301+H331, H310, H315, H317, H318, H373, H410		P273, P280, P302+P352, P304+P341, P305+P351+P338
2-Propanol		H225, H319, H336		P210, P233, P305+P351+P338
Acetic acid		H226, H314		P280, P308+P310, P301+P330+P331, P303+P361+P353, P305+P351+P338, P313
Acrylamide solution (30%) - Mix 37.5		H301, H312+H332, H315-H317, H319-H340, H350-H361f, H372		P201, P280, P302+P352, P305+P351+P338
Ammonium persulfate (APS)		H272, H302, H315, H317, H319, H334, H335		P220, P261, P280, P305+P351+P338, P342+P311
Ampicillin		H317, H334		P261, P280, P342+P311
Blasticidin S		H300, H301		P264, P270, P301+P310, P330, P405, P501
Calciumchloride (CaCl <sub>2</sub> )		H319		P264, P280, P305+P351+P338, P337+P313

# Appendix












Chloroform	 	H302, H315, H319, H331, H351, H361d, H372	P260, P280, P301+P312, P305+P351+P338, P405-P50
Chloroquine diphosphate		H302	
DNase I Buffer (10x)		H316	P332 + P313
DNase Inactivation Reagent	 	H315, H335, H318	P280, P305 + P351 + P338
EDTA	 	H319, H332, H373	P260, P261, P271, P304+P340, P305+P351+P338, P312
ELU buffer (NucleoBond Xtra Kit)	 	H226, H319	P210, P233, P280, P05+P351+P338, P337+P313, P403+P235
EQU, WASH buffer (NucleoBond Xtra Kit)		H226	P210, P233, P403+P235
Ethanol	 	H226, H319	P210, P233, P280, P305+P351+P338
Ethidiumbromide (EtBr)	 	H302, H330, H341	P281, P302+P352, P304+P340, P305+P351+P338, P309, P310
Guanidine hydrochloride 36–50% (A3 buffer NucleoSpin Plasmid)		H302, H319	P264, P280sh, P301+312, P330
Hoechst		H302, H315, H319	P280, P305+P351+P338, P313
Hydrochloric acid (HCl)	 	H290, H335, H314	P280, P301+P330+P331, P305+P351+P338, P308+P310

# Appendix

















Hygromycin B Gold		H301 + H311, H318, H330, H334	P264, P280, P284, P301+P310, P302+P352, P304+P340, P305+P351+P338
Kanamycin sulfate		H360	P201, P308+P313
LYS buffer (NucleoBond Xtra)		H315, H319	P234, P280, P302+P352, P05+P351+P338, P332+P313, P337+P313, P390, P406
Methanol (MeOH)		H225, H301+H311+H331, H370	P210, P233, P280, P302+P352, P309, P310, P501
Nonidet-P40		H302, H318, H411	P280, P301+P312, P305+P351+P338
Paraformaldehyde (PFA)		H228, H302, H315, H317, H319, H335, H351	P210, P241, P280, P305+P351+P338, P405, P501
Passive Lysis Buffer 5x		H360	P201, P202, P280, P308+P313, P405, P501
Phenol-Chloroform-Isoamyl alcohol (25:24:1 vol/vol/vol)		H301+H311+H331, H314, H341, H351, H361d, H372, H411	P280b, P301+P330+P331, P305+P351+P338, P309+P311
Phenylmethylsulfonyl fluoride (PMSF)		H301, H314	P280, P305+P351+P338, P310











# Appendix

Pierce Coomassie Plus (Bradford) Assay Reagent (contains phosphoric acid and methanol)		H314, H318, H371	P303 + P361 + P353, P305 + P351 + P338, P304 + P340, P310, P280, P260
Polybrene (Hexadimethrinbromid)		H302	
Potassium hydroxide (KOH)		H290, H302, H314	P280, P301+P330+P331, P305+P351+P338
QUANTI-Blue buffer		H319	P305 + P351 + P338
Renilla Luciferase Assay Substrate		H225	
Renilla Luciferase Assay Lysis Buffer 5x		H351, H360, H412	P201, P202, P280 P273, P308+P313, P405
RNAse A, lyophilized (NucleoBond Xtra)		H317, H334	P261, P280, P302+P352, P304+P340, P333+P313, P342+P311, P363
RNAse Away		H315, H319	
Sodium azide		H300, H310, H400, H410	P260, P280, P301+310, P501
Sodium deoxycholate		H302, H315, H319	P261
Sodium dodecyl sulfate (SDS)		H228, H302+H332, H315, H318, H335, H412	P210, P280, P302+P352, P304+P341, P305+P351+P338

## Appendix

Sodium hydroxide		H290, H314	P280, P301+P330+P331, P305+P351+P338
Sodium hypochlorite	 	H314, H400, EUH031	P280, P301+P330+P331, P305+P351+P338, P308+P310
Stop &Glo Substrate		H225	P243, P280, P241, P303+P361+P353, P370+P378, P403+P235
TEMED (Tetramethylethylenediamine)	  	H225, H302+H332, H314	P210, P233, P280, P301+P330+P331, P305+P351+P338
TRI Reagent / Trizol	   	H301+ H311+ H331, H314, H341, H373, H411	P201, P261, P280, P301+P310+P330, P303+P361+P353, P305+P351+P338
Tris ultrapure (Tris-base)		H315, H319	P302+P352, P305+P351+P338
Triton X-100	  	H302, H318, H411	P273, P280, P305+P351+P338, P310
Trypan blue solution 0.4%		H350	P201, P308+P313

## GHS pictogram guide

	<b>Harmful</b>	Identifies chemicals with the following hazards: skin sensitizer, irritant, acute toxicity (harmful), narcotic effects, respiratory tract infection, hazardous ozone layer
	<b>Toxic</b>	Identifies acutely toxic substances (fatal or toxic in case of oral, dermal or inhalative exposure)
	<b>Health Hazard</b>	Identifies chemicals with the following hazards: carcinogen, mutagen, reproductive toxicity, respiratory sensitizer, target organ toxicity, aspiration toxicity.
	<b>Environmental Hazard</b>	Identifies chemicals with acute or chronic toxicity for aquatic environments
	<b>Corrosive</b>	Identifies chemicals with the following hazards: eye damage, skin corrosion, corrosive to metals
	<b>Explosive</b>	Identifies unstable explosives, self-reactive substances and mixtures, organic peroxides
	<b>Flammable</b>	Identifies flammable agents, pyrophorics, self-reactive and self-heating substances and mixtures, substances emitting flammable gases in context with water, organic peroxides
	<b>Oxidizing</b>	Identifies oxidizing agents

## GHS hazard statements (UNECE, 2017)

<b>Code</b>	<b>Hazard Statement</b>
H200	Unstable explosive.
H201	Explosive; mass explosion hazard.
H202	Explosive; severe projection hazard.
H203	Explosive; fire, blast or projection hazard.
H204	Fire or projection hazard.
H205	May mass explode in fire
H220	Extremely flammable gas.
H221	Flammable gas.
H222	Extremely flammable aerosol.
H223	Flammable aerosol.
H224	Extremely flammable liquid and vapour.
H225	Highly flammable liquid and vapour.

H226	Flammable liquid and vapour.
H227	Combustible liquid.
H228	Flammable solid.
H240	Heating may cause explosion.
H241	Heating may cause fire or explosion.
H242	Heating may cause a fire.
H250	Catches fire spontaneously if exposed to air.
H251	Self-heating; may catch fire.
H252	Self-heating in large quantities; may catch fire.
H260	In contact with water releases flammable gases which may ignite spontaneously
H261	In contact with water releases flammable gas.
H270	May cause or intensify fire; oxidizer.
H271	May cause fire or explosion; strong oxidizer.
H272	May intensify fire; oxidizer.
H280	Contains gas under pressure; may explode if heated.
H281	Contains refrigerated gas; may cause cryogenic burns or injury.
H290	May be corrosive to metals.
H300	Fatal if swallowed.
H301	Toxic if swallowed.
H302	Harmful if swallowed.
H303	May be harmful if swallowed.
H304	May be fatal if swallowed and enters airways.
H305.	May be harmful if swallowed and enters airways
H310	Fatal in contact with skin.
H311	Toxic in contact with skin.
H312	Harmful in contact with skin.
H313	May be harmful in contact with skin.
H314	Causes severe skin burns and eye damage.
H315	Causes skin irritation.
H316	Causes mild skin irritation.
H317	May cause an allergic skin reaction.
H318	Causes serious eye damage.
H319	Causes serious eye irritation.
H320	Causes eye irritation.
H330	Fatal if inhaled.
H331	Toxic if inhaled.
H333	May be harmful if inhaled.
H334	H334 May cause allergy or asthma symptoms or breathing difficulties if inhaled.
H335	May cause respiratory irritation.

H336	May cause drowsiness or dizziness.
H340	May cause genetic defects.
H341	Suspected of causing genetic defects.
H350	May cause cancer.
H351	Suspected of causing cancer.
H360	May damage fertility or the unborn child.
H360F	May damage fertility
H360D	May damage the unborn child
H360FD	May damage fertility; May damage the unborn child
H360Fd	May damage fertility; Suspected of damaging the unborn child
H360Df	May damage the unborn child; Suspected of damaging fertility
H361	Suspected of damaging fertility or the unborn child.
H361f	Suspected of damaging fertility
H361d	Suspected of damaging the unborn child
H361fd	Suspected of damaging fertility; Suspected of damaging the unborn child
H362	May cause harm to breast-fed children.
H370	Causes damage to organs.
H371	May cause damage to organs.
H372	Causes damage to organs through prolonged or repeated exposure.
H373	May cause damage to organs through prolonged or repeated exposure.
H400	Very toxic to aquatic life.
H401	Toxic to aquatic life.
H402	Harmful to aquatic life.
H410	Very toxic to aquatic life with long lasting effects.
H411	Toxic to aquatic life with long lasting effects.
H412	Harmful to aquatic life with long lasting effects.
H413	May cause long lasting harmful effects to aquatic life.
H420	Harms public health and the environment by destroying ozone in the upper atmosphere

### **Combined H-Codes**

H300+H310	Fatal if swallowed or in contact with skin
H300+H330	Fatal if swallowed or if inhaled
H310+H330	Fatal in contact with skin or if inhaled
H300+H310+H330	Fatal if swallowed, in contact with skin or if inhaled
H301+H311	Toxic if swallowed or in contact with skin
H301+H331	Toxic if swallowed or if inhaled
H311+H331	Toxic in contact with skin or if inhaled.
H301+H311+H331	Toxic if swallowed, in contact with skin or if inhaled
H302+H312	Harmful if swallowed or in contact with skin

H302+H332	Harmful if swallowed or if inhaled
H312+H332	Harmful in contact with skin or if inhaled
H302+H312+H332	Harmful if swallowed, in contact with skin or if inhaled
H303+H313	May be harmful if swallowed or in contact with skin
H303+H333	May be harmful if swallowed or if inhaled
H313+H333	May be harmful in contact with skin or if inhaled
H303+H313+H333	May be harmful if swallowed, in contact with skin or if inhaled
H315+H320	Cause skin and eye irritation

### GHS precautionary statements

Code	Precautionary statement
P101	If medical advice is needed, have product container or label at hand.
P102	Keep out of reach of children.
P103	Read label before use
P201	Obtain special instructions before use.
P202	Do not handle until all safety precautions have been read and understood.
P210	Keep away from heat, hot surface, sparks, open flames and other ignition sources. - No smoking.
P211	Do not spray on an open flame or other ignition source.
P212	Avoid heating under confinement or reduction of the desensitized agent.
P220	Keep away from clothing and other combustible materials.
P221	Take any precaution to avoid mixing with combustibles/...
P222	Do not allow contact with air.
P223	Do not allow contact with water.
P230	Keep wetted with ...
P231	Handle under inert gas.
P232	Protect from moisture.
P233	Keep container tightly closed.
P234	Keep only in original container.
P235	Keep cool.
P240	Ground/bond container and receiving equipment.
P241	Use explosion-proof [electrical/ventilating/lighting/...] equipment.
P242	Use only non-sparking tools.
P243	Take precautionary measures against static discharge.
P244	Keep valves and fittings free from oil and grease.
P250	Do not subject to grinding/shock/friction/...
P251	Do not pierce or burn, even after use.
P260	Do not breathe dust/fume/gas/mist/vapors/spray.
P261	Avoid breathing dust/fume/gas/mist/vapors/spray.
P262	Do not get in eyes, on skin, or on clothing.

P263	Avoid contact during pregnancy/while nursing.
P264	Wash ... thoroughly after handling.
P270	Do not eat, drink or smoke when using this product.
P271	Use only outdoors or in a well-ventilated area.
P272	Contaminated work clothing should not be allowed out of the workplace.
P273	Avoid release to the environment.
P280	Wear protective gloves/protective clothing/eye protection/face protection.
P281	Use personal protective equipment as required.
P282	Wear cold insulating gloves/face shield/eye protection.
P283	Wear fire resistant or flame retardant clothing.
P284	[In case of inadequate ventilation] Wear respiratory protection.
P285	In case of inadequate ventilation wear respiratory protection.
P231+P232	Handle under inert gas/... Protect from moisture.
P235+P410	Keep cool. Protect from sunlight.
P301	IF SWALLOWED:
P302	IF ON SKIN:
P303	IF ON SKIN (or hair):
P304	IF INHALED:
P305	IF IN EYES:
P306	IF ON CLOTHING:
P307	IF exposed:
P308	IF exposed or concerned:
P309	IF exposed or if you feel unwell
P310	Immediately call a POISON CENTER or doctor/physician.
P311	Call a POISON CENTER or doctor/...
P312	Call a POISON CENTER or doctor/... if you feel unwell.
P313	Get medical advice/attention.
P314	Get medical advice/attention if you feel unwell.
P315	Get immediate medical advice/attention.
P320	Specific treatment is urgent (see ... on this label).
P321	Specific treatment (see ... on this label).
P322	Specific measures (see ...on this label).
P330	Rinse mouth.
P331	Do NOT induce vomiting.
P332	IF SKIN irritation occurs:
P333	If skin irritation or rash occurs:
P334	Immerse in cool water [or wrap in wet bandages].
P335	Brush off loose particles from skin.
P336	Thaw frosted parts with lukewarm water. Do not rub affected area.
P337	If eye irritation persists:

P338	Remove contact lenses, if present and easy to do. Continue rinsing.
P340	Remove victim to fresh air and keep at rest in a position comfortable for breathing.
P341	If breathing is difficult, remove victim to fresh air and keep at rest in a position comfortable for breathing.
P342	If experiencing respiratory symptoms:
P350	Gently wash with plenty of soap and water.
P351	Rinse cautiously with water for several minutes.
P352	Wash with plenty of water/...
P353	Rinse skin with water [or shower].
P360	Rinse immediately contaminated clothing and skin with plenty of water before removing clothes.
P361	Take off immediately all contaminated clothing.
P362	Take off contaminated clothing.
P363	Wash contaminated clothing before reuse.
P364	And wash it before reuse.[Added in 2015 version]
P370	In case of fire:
P371	In case of major fire and large quantities:
P372	Explosion risk.
P373	DO NOT fight fire when fire reaches explosives.
P374	Fight fire with normal precautions from a reasonable distance.
P376	Stop leak if safe to do so.
P377	Leaking gas fire: Do not extinguish, unless leak can be stopped safely.
P378	Use ... to extinguish.
P380	Evacuate area.
P381	In case of leakage, eliminate all ignition sources.
P390	Absorb spillage to prevent material damage.
P391	Collect spillage.
P301+P310	IF SWALLOWED: Immediately call a POISON CENTER/doctor/...
P301+P312	IF SWALLOWED: call a POISON CENTER/doctor/... IF you feel unwell.
P301+P330+P331	IF SWALLOWED: Rinse mouth. Do NOT induce vomiting.
P302+P334	IF ON SKIN: Immerse in cool water [or wrap in wet bandages].
P302+P335+P334	Brush off loose particles from skin. Immerse in cool water [or wrap in wet bandages].
P302+P350	IF ON SKIN: Gently wash with plenty of soap and water.
P302+P352	IF ON SKIN: wash with plenty of water.
P303+P361+P353	IF ON SKIN (or hair): Take off Immediately all contaminated clothing. Rinse SKIN with water [or shower].
P304+P312	IF INHALED: Call a POISON CENTER/doctor/... if you feel unwell.
P304+P340	IF INHALED: Remove person to fresh air and keep comfortable for breathing.
P304+P341	IF INHALED: If breathing is difficult, remove victim to fresh air and keep at rest in a position comfortable for breathing.
P305+P351+P338	IF IN EYES: Rinse cautiously with water for several minutes. Remove contact



	lenses if present and easy to do - continue rinsing.
P306+P360	IF ON CLOTHING: Rinse Immediately contaminated CLOTHING and SKIN with plenty of water before removing clothes.
P307+P311	IF exposed: call a POISON CENTER or doctor/physician.
P308+P311	IF exposed or concerned: Call a POISON CENTER/doctor/...
P308+P313	IF exposed or concerned: Get medical advice/attention.
P309+P311	IF exposed or if you feel unwell: call a POISON CENTER or doctor/physician.
P332+P313	IF SKIN irritation occurs: Get medical advice/attention.
P333+P313	IF SKIN irritation or rash occurs: Get medical advice/attention.
P335+P334	Brush off loose particles from skin. Immerse in cool water/wrap in wet bandages.
P337+P313	IF eye irritation persists: Get medical advice/attention.
P342+P311	IF experiencing respiratory symptoms: Call a POISON CENTER/doctor/...
P361+P364	Take off immediately all contaminated clothing and wash it before reuse.
P362+P364	Take off contaminated clothing and wash it before reuse.
P370+P376	in case of fire: Stop leak if safe to do so.
P370+P378	In case of fire: Use ... to extinguish.
P370+P380	In case of fire: Evacuate area.
P370+P380+P375	In case of fire: Evacuate area. Fight fire remotely due to the risk of explosion.
P371+P380+P375	In case of major fire and large quantities: Evacuate area. Fight fire remotely due to the risk of explosion.
P401	Store in accordance with ...
P402	Store in a dry place.
P403	Store in a well-ventilated place.
P404	Store in a closed container.
P405	Store locked up.
P406	Store in corrosive resistant/... container with a resistant inner liner.
P407	Maintain air gap between stacks or pallets.
P410	Protect from sunlight.
P411	Store at temperatures not exceeding ... °C/...°F.
P412	Do not expose to temperatures exceeding 50 °C/ 122 °F.
P413	Store bulk masses greater than ... kg/...lbs at temperatures not exceeding ... °C/...°F.
P420	Store separately.
P422	Store contents under ...
P402+P404	Store in a dry place. Store in a closed container.
P403+P233	Store in a well-ventilated place. Keep container tightly closed.
P403+P235	Store in a well-ventilated place. Keep cool.
P410+P403	Protect from sunlight. Store in a well-ventilated place.
P410+P412	Protect from sunlight. Do not expose to temperatures exceeding 50 °C/122°F.
P411+P235	Store at temperatures not exceeding ... °C/...°F. Keep cool.
P501	Dispose of contents/container to ...

P502                      Refer to manufacturer or supplier for information on recovery or recycling

## **8.5 Danksagung**

Zuallererst möchte ich mich besonders bei Frau Prof. Dr. Eva Herker bedanken. Danke für dieses überaus spannende Thema und die Betreuung meiner Arbeit. Danke für die vielen Ratschläge und das Vertrauen, das es mir ermöglicht hat meine eigenen Ideen in das Projekt einfließen zu lassen.

Ebenso möchte ich mich bei Herrn Prof. Dr. Chris Meier für die Zweitbetreuung meiner Dissertation bedanken. Mein Dank gilt auch Herrn Prof. Dr. Wolfgang Maison und Herrn Prof. Dr. Wolfram Brune für die Begutachtung meiner Disputation.

Des Weiteren danke ich Herrn Prof. Dr. Gerald G. Schumann für die Zusammenarbeit; ohne diese wäre das Projekt nicht so weit gekommen.

Ein riesiges Dankeschön geht auch an alle Mitglieder und ehemaligen Mitglieder der AG76. Danke für all die wissenschaftlichen Diskussionen und auch für die nichtwissenschaftlichen Gespräche. Eure Unterstützung und das positive Arbeitsklima haben mich immer motiviert und wesentlich zum Gelingen dieser Arbeit beigetragen.

Meiner Familie möchte ich an dieser Stelle sagen: Danke für alles! Danke, dass ihr immer an mich geglaubt habt.

Danken möchte ich auch meinen Freunden. Was wäre ich ohne euch!

Basti, dir kann ich nicht genug danken! Aber ich mache es trotzdem. Danke für alles! Für deine Unterstützung, die Motivation und dafür, dass du immer das Positive siehst.

## 8.6 Correctness of the English Language

### **Bestätigung der Korrektheit der englischen Sprache**

#### ***Confirmation of the correctness of the English language***

Hiermit erkläre ich, Christopher Thomas Ford, geboren am 30. Juli 1990 in Edinburgh, Schottland, UK, dass die Dissertation von Anja Schöbel mit dem Titel „Interaction between the LINE1 Retrotransposon and the Hepatitis C Virus“ in einem korrekten Englisch verfasst wurde.

*I, Christopher Thomas Ford, born on July 30<sup>th</sup>, 1990 in Edinburgh, Scotland, United Kingdom, hereby declare that the thesis with the title "Interaction between the LINE1 Retrotransposon and the Hepatitis C Virus" written by Anja Schöbel is written in grammatically correct English.*

HH, 19.12.2018

Ort, Datum

*City, date*

Christopher Thomas Ford

Unterschrift

*signature*

### **8.7 Eidesstattliche Versicherung**

Hiermit versichere ich an Eides statt, die vorliegende Dissertation selbst verfasst und keine anderen als die angegebenen Hilfsmittel benutzt zu haben. Die eingereichte schriftliche Fassung entspricht der auf dem elektronischen Speichermedium. Ich versichere, dass diese Dissertation nicht in einem früheren Promotionsverfahren eingereicht wurde.

---

Datum, Unterschrift